THESIS FOR THE DEGREE OF DOCTOR OF PHILOSOPHY

On the Small Strain Stiffness of Some Scandinavian Soft Clays and Impact on Deep Excavations

Tara Wood

Department of Civil and Environmental Engineering
Division of GeoEngineering
CHALMERS UNIVERSITY OF TECHNOLOGY
Gothenburg, Sweden 2016

On the small strain stiffness of some Scandinavian soft clays and its impact on deep excavations

TARA WOOD
ISBN 978-91-7597-433-0

Doktorsavhandling vid Chalmers tekniska högskola
Ny serie nr 4114
ISSN 0346-718X

Department of Civil and Environmental Engineering
Division of GeoEngineering
Chalmers University of Technology
SE-412 96 Gothenburg
Sweden
Telephone + 46 (0)31 772 10 00
www.chalmers.se

Cover:
Bender element testing and suction measurement of quick glacio-marine clay block samples at Gårda River, Lödöse, May 2012.

Chalmers reproservice
Gothenburg, Sweden 2016

On the small strain stiffness of some Scandinavian soft clays and its impact on deep excavations

TARA WOOD
Department of Civil and Environmental Engineering
Division of GeoEngineering
Chalmers University of Technology

ABSTRACT

This thesis presents the results of a comprehensive study on the small strain stiffness of several Swedish clays and its tentative effect on the design of retaining structures. A combination of field measurement techniques, seismic dilatometer and surface seismics, are complemented with bender element testing of the retrieved samples. The overall trend in the data is that the values found for the small strain shear modulus are larger than currently recommended in the Swedish Transport Authority guidelines, TKGEO (2013) (based on empirical correlations). Furthermore, the results indicate that multichannel analysis of surface waves (MASW) works best for acquiring a 2D profile of the small strain shear modulus within the top 10 meters of the subsoil, inferred from shear wave velocities. The seismic dilatometer is more appropriate for larger depths providing higher accuracy at the expense of losing the 2D spatial information. Additionally, it was found that the best laboratory based procedure was to measure the shear wave velocity on carefully extracted and transported samples (minimal disturbance) which were stored < 2 days and brought back to *in situ* anisotropic stress level. The horizontal stress component was obtained from the *in situ* dilatometer measurements while the vertical stress component was obtained from direct measurement of density (sampling levels) and from an existing correlation based on shear wave velocity. For determination of effective *in situ* stresses pore pressure profiles based on the yearly average were used. Different sample quality assessment methods have been compared but it was found no one method could be used to identify the best quality samples. Using a multiple method approach this was possible.

Stiffness degradation with strain is significant for all the clays tested. Many empirical relations exist however these tend to relate to shear strain amplitude, rather than shear strain (relevant in deep excavations), thus agreement is generally poor. Laboratory determined stiffness degradation appears particularly sensitive to the sample timeline (disturbance and reconsolidation procedure). Finally, the influence of the small strain shear moduli on the design of excavations with embedded retaining walls is elaborated by means of simulations of a theoretical 10 m excavation. Not surprisingly, the higher stiffness leads to large differences in structural response and more realistic deformations in the far field. It would seem prudent to insist that for critical deep excavation projects where Finite Element Analysis is performed the consistency of the model parameters are demonstrated with element test simulations on high quality test data. In this way the suitability of the chosen parameter set can be demonstrated.

Keywords: Soft clay, small strain stiffness, degradation, seismic testing, sample quality.

"Unfortunately, soils are made by nature and not by man, and the products of nature are always complex"

Karl Terzaghi

ACKNOWLEDGMENTS

The research presented within this thesis has been funded by the Swedish Transport Administration under BIG (Better Interaction in Geotechnics), the Swedish Building, Development and Research fund (SBUF), NCC AB and Chalmers University of Technology. Additional support in terms of financing, time and/or expertise has also been provided by Jernhusen (the Owner of the Swedish Railway Stations), Apex Geotechnical Services Ireland (for assisting with surface wave field testing and sensitivity analyses of inversion process), University College Dublin, Ireland and Studio Prof. Marchetti A.r.l.

Particular acknowledgement is given to: Claes Alén of Chalmers Technical University and Lars Olof Dahlström of NCC AB for giving me the opportunity to embark on this research and Göran Sällfors of Chalmers Technical University for obtaining the initial funding. I would also like to thank Mike Long of University College Dublin for his interest and enthusiasm in helping organise the field surface wave testing in addition to sharing literature and contact information and Diego Marchetti of Studio Prof. Marchetti for his support in the use, operation and maintenance of the seismic dilatometer. Without their help and support I would not have been able to have included *in situ* measurements of small strain stiffness in this research.

I would also like to thank my supervisor Jelke Dijkstra for his unyielding support and insight within both interpretation of experimental results and their presentation, Prof. Minna Karstunen for her support and experience in finite element modelling of soft structured clays at both element level and in boundary value problems, Peter Hedborg, Aaro Pirhonen and Mona Pålsson for their help in laboratory testing and development of experimental and interpretation tools, Ingemar Forsgren for his help and perseverance in the field testing and piston sample extraction and to my colleagues and fellow researchers in the geotechnical division at Chalmers. I have cherished the support and knowledge we have shared over the years.

A number of people made sites available for field testing, Anders Hansson (TrV), Per Ekström (NCC), Karin Kullander (NCC), Jan Ekström (TrV), Anders Kullingsjö (Skanska), Per-Gunnar Larsson (Bohusgeo), Torgeir Haugen (NCC Norway). To them I am also very thankful. Without their help I would not have been able to study such a wide range of clays. In addition a number of extra hands made quick standard testing of piston samples from Site 1, 3 and 7 a possibility, namely Daniel Kallus, Andreas Berg, David Andersson, Robert Lanzky and David Palmkvist. Your efforts helped greatly in understanding the sample disturbance chain and its effect on small strain stiffness.

Finally I have to thank my family. For reminding me that life is rich and that there should always be balance. You have accepted me working through holidays, weekends and evenings over many years. To my husband, thank you for your support and guidance in the darkest hours. To my beautiful girls, thank you for letting me work when you really wanted to play, thank you for all your works of art, produced almost daily to help keep me motivated and show that you care. You are my greatest treasures.

TABLE OF CONTENTS

APPENDICES

LIST OF NOTATIONS

The main notations used in this dissertation are given below and are also described in the relevant section.

Roman letters

A	Activity
B_q	pore pressure parameter
c_v	coefficient of compressibility
e	void ratio
e_0	initial void ratio
D	damping
D_r	drainage path length
D_1	inner diameter of the piston sample cutting shoe
D_2	outer diameter of piston sample tube
D_3	inner diameter of the piston sample tube
E	Young's modulus
E_D	dilatometer modulus
E_u	undrained Young's modulus
E_0	small strain Young's modulus
E'_{50}	drained Youngs modulus at 50% of peak strength
$E_{u\,50}$	undrained triaxial stiffness at 50% of peak strength
E_{ur}	unloading – reloading Young's modulus
E_{50}^{ref}	deviatoric reference stiffness at 50% of peak strength
E_{ur}^{ref}	reference Young's modulus for unloading-reloading corresponding to p^{ref}
E_{oed}^{ref}	oedometer reference tangent stiffness modulus
f	frequency
G	shear modulus at a given strain
G_0	small strain shear modulus
G_{0BE}	small strain shear modulus derived from bender element testing
$G_{0\,empirical}$	empirically derived estimate of small strain shear modulus
$G_{0\,field}$	small strain shear modulus derived from *in situ* testing
G_{0hh}	small strain shear modulus for a horizontally propagating wave with horizontal particle movement
G_{0hv}	small strain shear modulus for a horizontally propagating wave with vertical particle movement
$G_{0\,lab}$	small strain shear modulus, samples consolidated to *in situ* stresses in the laboratory
$G_{0\,ref}$	reference small strain shear modulus
G_{0vh}	small strain shear modulus for a vertically propagating wave with horizontal particle movement
G_s	specific gravity
H_{be_R}	transfer function for the receiving bender element
H_{soil}	transfer function for the soil
I_D	material index
I_P	plasticity index
k	hydraulic conductivity
k_i	exponent dependent on I_P
K_B	small strain bulk modulus
K_D	horizontal stress index

K_0	coefficient of lateral earth pressure at rest
K_{0nc}	coefficient of lateral earth pressure at rest for normally consolidated state
$K´$	effective bulk modulus of soil
L	distance
L_L	Liquid limit
L_u	relative measure of disturbance in terms of residual effective stresses
m	power for stress-level dependency of stiffness
M	stress ratio at critical state
M_c	stress ratio at critical state in triaxial compression
M_{DMT}	drained vertical constrained modulus
M_e	stress ratio at critical state in triaxial extension
M_i	initial 'disturbed' modulus
M_L	post yield modulus
M_{reload}	oedometer modulus in reloading (after unloading)
M_0	pre-yield modulus (average value in unloading-reloading)
$p´$	mean effective stress
p_a	atmospheric pressure
$p_0´$	initial mean effective stress
p'_{ref}	normalised mean effective stress ($p´/p'_{VC}$)
p^{ref}	reference for stiffness (p^{ref}= 100 stress units used)
P	a constant in a given geological deposit and site
P_L	Plastic limit
p'_{VC}	mean reconsolidation stress ($(\sigma´_v+2.\sigma´_h)/3$ in triaxial stress space)
P_0	the pressures to inflate a membrane 0.05 mm (Dilatometer test)
P_1	the pressures to inflate a membrane 1.1 mm (Dilatometer test)
q	deviatoric stress ($q= \sigma´_v- \sigma´_h$ in triaxial stress space)
q_a	deviatoric stress at asympotote
q_f	deviatoric stress at failure
q_{ref}	normalised deviatoric stress (q/ p'_{VC})
q_t	cone tip resistance
R_d	number of wavelengths between the source and the receiver
R_f	failure ratio q_f/q_a,
R_p	magnitude of the disturbed zone at the top of the sampled soil
R_M	correction factor to dilatometer modulus to obtain drained vertical constrained modulus
S_t	sensitivity
Su	undrained shear strength
t_c	cutting shoe thickness
t	time
t_a	travel time
t_{cc}	travel time based on cross correlation
T_v	time factor
u_r	residual effective stress due to suction
u_0	*in situ* pore pressure
u_2	the magnitude of pore pressure measured just above the cone tip (CPT)
V_p	compression wave velocity
V_R	Raleigh wave velocity
V_S	shear wave velocity
$Vs_{average}$	average shear wave velocity determined wave with respect to vertical and horizontal components

Vs_{field}	shear wave velocity determined *in situ*
V_{Shh}	shear wave velocity, horizontal propagation and horizontal particle movement
V_{Shv}	shear wave velocity, horizontal wave propagation and vertical particle movement
V_{Svh}	shear wave velocity, vertical propagation and horizontal particle movement
V_{S0}	unconfined shear wave velocity (based on bender element testing without application of addition stresses, only residual effective stresses present)
V_{S0vh}	unconfined shear wave velocity for vertical propagation and horizontal particle movement
$V_{S\ remoulded}$	shear wave velocity of an unconfined remoulded intrinsic sample
Vs_{SDMT}	shear wave velocity determined using seismic dilatometer
V_0	initial volume of sample
W_L	Atterberg liquid limit
W_N	natural water content
W_P	plasticity limit
Y	a constant in a given geological deposit and site

Greek letters

α_0	initial value of anisotropy
α_d	deviatoric fabric tensor
α_c	cutting shoe tapper angle
γ'	unit weight
γ	shear strain
γ_r	threshold shear strain amplitude*
$\gamma_{0.7}$	shear strain at 30% degradation of small strain stiffness (G/G_0=0.7)
$\Delta e/e_0$	relative change in void ratio
ε	strain
ε_a	axial strain
ε_r	radial strain
ε_v	volumetric strain
ε_d	deviatoric strain
η	stress ratio
κ^*	modified swelling index
κ^*_{SS}	modified swelling index relevant to small strain stiffness region
λ	wavelength
λ^*	modified compression index
λ_i^*	intrinsic modified compression index
μ	empirical correlation parameter for undrained shear strength based on liquid limit
μ^*	modified creep index (SSC creep index)
ν_0	Poisson's ratio at small strain
ν'	Poisson's ratio
ξ	Absolute rate of destructuration
ξ_d	Relative rate of destructuration
ρ	soil density
σ'_c	apparent preconsolidation stress
σ'_h	horizontal effective stress
σ'_{ps}	residual effective stress in perfect sample
σ'_v	vertical effective stress

σ'_{vc}	vertical reconsolidation stress
σ'_{v0}	vertical *in situ* effective stress
τ	reference time
τ_v	uncorrected undrained field vane strength
τ_u	corrected field vane shear strength
τ_{max}	shear stress at failure
ϕ'	friction angle
ϕ'_{cv}	critical state friction angle
$\Phi(f)$	phase angle
$Ø_{outer}$	outer diameter of the piston sampler
χ_0	initial bonding
ω	rate of rotation
ω_d	rate of rotation due to deviator stress

Abbreviations

AR	Area ratio
BE	Bender element
BES	Bender element system
CAUE	Consolidated anisotropic undrained extension
CAUC	Consolidated anisotropic undrained compression
CH	Cross hole
CPT	Cone penetration test
CPTU	Piezometric cone penetration tests
CRS	Constant Rate of Strain
CSW	Continuous surface wave
CTH	Chalmers University of Technology
DH	Down hole
DIC	Digital image correlation
DMT	Dilatometer test
DVRT	Differential variable reluctance transducers
DSS	Direct simple shear
ERT	Electrical resistivity tomography
ESP	Effective stress path
FE	Finite element
FEA	Finite element analysis
FIR	Finite impulse response
FD	Frequency domain
FFT	Fast fourier transform
G	Glacial
GDS	Global Digital Systems
HS	Hardening soil
HS	hydrogen sulphide
HSs	Hardening soil small
ICR	Inside clearance
IL	Incremental loading
KGS	Kansas Geolgical Society
LVDT	Linear variable differential transducer
MASW	Multichannel analysis of surface waves
n-SAC	Non-associated creep model for Structured Anisotropic Clay
NC	Normal consolidated

NGI	Norwegian Geotechnical Institute
NTNU	Norwegian University of Science and Technology
OCR	Over Consolidation Ratio OCR=σ'_c/σ'_0
P-waves	Compression waves
PG	Post glacial
PI	Plasticity index
PSD	Partical sedimentation distribution
RC	Resonant column
RMS	Root mean square error
sbPMT	Self-boring pressuremeter test
S-waves	Shear waves
SASW	Spectral analysis of surface waves
SCPT	Seismic cone penetration test
SDMT	Marchetti seismic dilatometer
SGI	Swedish Geotechnical Institute
SGU	Swedish Geological Survey
SMT	Soil Mechanics Triangle
SP	Screw plate
SSP	Steel sheet pile wall
STII	Standard Swedish piston sampler
$STII_{slow}$	Standard Swedish piston sampler with slow extraction
$STII_{60}$	60 mm diameter sampler that is a wider version of the Swedish STII
TD	Time domain
UCD	University College Dublin

1 INTRODUCTION

1.1 Background

Soft structured clays occur in many parts of Sweden, particularly in areas with the greatest urbanisation (Stockholm, Göteborg). The cost of constructing foundations in these soils is relatively high in relation to the construction costs, SGI (1991). In addition one third of additional unplanned costs incurred due to construction errors are due to foundation performance (Sherwood, 2011). In order to reduce errors and ensure that the foundations are safely optimised over their full service life, we need to find more reliable prediction methods than have traditionally been used in Sweden. One way of doing this is to go back to the concept of the Soil Mechanics Triangle (SMT) introduced by Burland (1987) shown in Figure 1.1. Aspects of the soil mechanics triangle in relation to deep excavation in soft Swedish clays will be considered, with particular focus on the measurement and modelling of non-linear stiffness at small strains. The non-linearity of soil stiffness, the range of mobilised strains for different boundary value problems and the measurement range of different laboratory devices are illustrated in Figure 1.2.

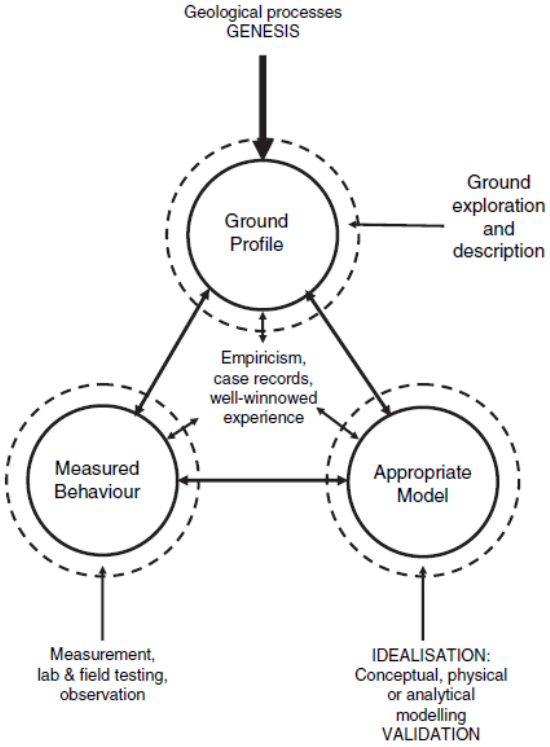

Figure 1.1 Soil mechanics triangle for geotechnical design, Burland (2012).

Soil properties at small strains are a research area that has become increasingly important over the past two decades. Interest has been driven both by the need to develop better predictions for high intensity redevelopment of urban areas, but also due to our increased understanding of soil-structure interaction and mobilisation of structural loads. Traditional limit equilibrium and limit analysis methods or empirical and semi-empirical approaches are not suitable for robust design in the serviceability limit state. In many cases the degree of restraint imposed by the retaining wall system will not allow for the full mobilisation of active and passive pressures. This means that

structural loads experienced by a retaining wall "in-service" is often the limiting design case in terms of structural loads, as shown by Potts (2003), Jardine *et al.* (1986), Jardine *et al.* (1991), Kullingsjö (2007) and Wood (2010). In addition, the predictions of deformation will most likely be inaccurate, which would have serious consequences in terms of risk management when using observational design methods and may lead to installation of unnecessary mitigation measures in the surrounding structures ahead of the planned works. Given these issues, the use of finite element analyses is becoming increasingly popular in the design of deep excavations. However, there are currently no constitutive models validated for Swedish soft structured clays for the strain range 10^{-5} to 0.1 at element level, let alone boundary value level where the method of implementation (pore pressure regime with time, influence of piles etc.), geometrical and ground profile simplifications can also have a significant impact on the predicted stresses and deformations.

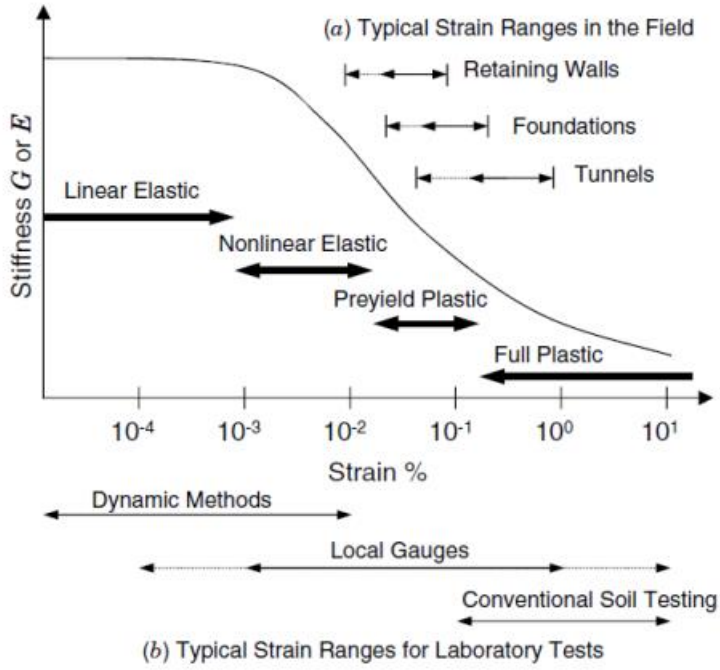

Figure 1.2 Reduction of stiffness with increasing strain and typical ranges of strains in laboratory and field applications, Mitchell & Soga (2005) after Atkinson & Sällfors (1991) and Mair (1993).

Most commonly, the small strain stiffness and its degradation with strain is described in terms of the shear modulus as this describes the behaviour under both drained and undrained conditions, however degradation can also be found in literature with respect to Young's modulus, E. It is also common to present normalised stiffness degradation curves in terms of G/G_0 where G is the current shear modulus at a given strain and G_0 is the initial stiffness at very small strains. The factors affecting small strain stiffness and its degradation with strain has been studied by numerous authors including: Hardin & Drnevich (1972), Dobry & Vucetic (1987), Andréasson (1979), Vucetic & Dobry (1988), Jamiolkowski (1994), Hight & Higgins (1994), Darendeli (2001), Benz (2007), Clayton (2011), Yimsiri & Soga (2011). Very few studies, however, exist for Swedish soft structured clays. The main factors identified in the literature affecting the stiffness under operational conditions and their relative influence are summarised in Table 1.1.

Small strain stiffness is commonly studied in the field and the laboratory, while stiffness degradation is most commonly studied using advanced laboratory tests. Disparities tend to exist between the field and laboratory behaviour relating to the sample disturbance and the methods of interpretation. In this thesis the small strain stiffness and the degradation of shear modulus of different Swedish soft clays in the very small (10^{-5}) to large (0.1) strain range will be studied.

Table 1.1 Factors affecting soil stiffness at small strains, adapted from Benz (2007).

Factor	G_0 of clays
Strain amplitude	V
Confining stress	V
Void ratio	V
Plasticity index (PI)	V
Over consolidation	L
Stress history (stress path)	R
Diagenesis (geological aging and cementation)	V
Strain history (strain path)	R
Rate of loading	R
Strain rate	R
No. of cycles	R
Effective material strength	L
Grain charateristics (size, shape)	L*
Degree of saturation	V
Dilatency	R
Structure and Fabric	R
Temperature	V

V=very important, R= relatively important and L= less important
* adapted from the original table by Hardin & Drnevich (1972)

1.2 Aims and objectives

The thesis aims to give a comprehensive overview of the small strain stiffness and its degradation for several Swedish clays using state-of-the-art *in situ* and laboratory techniques. The focus will be on acquiring a consistent data set and give recommendations for reliably obtaining these soil properties. Additionally, the new measurements will be evaluated the in context of existing guidelines and the implications of any differences highlighted. Finally, the implications of incorporating this measured small-strain stiffness in the analysis of retaining walls in soft soils will be demonstrated.

The objectives are the following:

- Perform a comprehensive field and laboratory study to acquire values for the small strain stiffness for several clays in Sweden.

- Perform a comprehensive laboratory study to measure the stiffness degradation for several relevant clays in Sweden.

- Characterisation of the sites studied in terms of geology, ground profile, stress history, hydrological profile.

- Based on the above, assess the impact of the newly determined small strain stiffness on the design of a deep excavation in soft clay.

2 ASSESSMENT OF SMALL STRAIN STIFFNESS

2.1 Introduction

Small strain stiffness refers to the material behaviour at small strains ($\varepsilon < 10^{-5}$), which is fully reversible: no plastic deformations are expected and the behaviour is considered to be 'elastic'. The range of strains to which 'elastic' behaviour is observed varies depending on, among other things on the material composition, the fabric and the stress-strain history (Hardin & Drnevich 1972). In this 'elastic' zone particles do not slide relative to other, and the stiffness will mainly depend on the contact stiffness, the packing of particles and the particle stiffness. To determine small strain shear moduli from field and laboratory tests, elasticity theory is used.

In the elastic domain compression waves (P-waves) and shear waves (S-waves) can be used to define various stiffness properties of soils. If both the S-wave velocity (V_S) and the P-wave (V_P) velocity are known, the Poisson's ratio (ν) of the material may also be derived. The equations for derivation of these properties are given below based on the assumption of the isotropic porous elasticity.

$$G_0 = \rho V_S^2 \qquad \text{Eq. 2-1}$$

where G_0 is the small strain shear modulus, ρ is the soil density and V_S is the shear wave velocity.

$$\nu = \frac{1 + 2\left(\frac{V_S}{V_P}\right)^2}{2 - 2\left(\frac{V_S}{V_P}\right)^2} \qquad \text{Eq. 2-2}$$

where ν is the Poisson's ratio, V_S is the shear wave velocity and V_P is the compression wave velocity.

$$E_0 = 2G_0(1 + \nu_0) \qquad \text{Eq. 2-3}$$

where E_0 is the small strain Young's modulus, ν_0 is the Poisson's ratio at small strains and

$$K_B = \frac{G_0}{3(1 - 2\nu_0)} \qquad \text{Eq. 2-4}$$

where K_B is the small strain bulk modulus.

It should be noted, however, that in a transverse isotropic medium, which is generally relevant for soft clays, the stiffness parameters both in the vertical and horizontal direction often need to be defined. As highlighted by Clayton (2011), a set of 5 parameters enables the full definition of stiffness in a cross-isotropic drained material. In the undrained case, this can be reduced to 3 parameters after Atkinson (1975). When determining the stiffness parameters for design both Burland (1989) and Clayton (2011) point out the need to critically review both the field and the laboratory derived stiffness. If *in situ* conditions change (stress, strain, chemical changes, etc.) the stiffness will change and derived stiffness may no longer be relevant to the case at hand.

Previous studies of the *in situ* small strain stiffness in Swedish soft clays are summarized in Table 2.1. One site, Vatthammar, is included even though it is typically silt with clayey varves. This site is included as the boundary between silty clay and clayey silt is not always identified in commercial projects as sedimentation tests are rarely performed. Of the 11 sites previously studied only 3 sites extend beyond 20 m depth and the vast majority of tests were conducted on soils from <10 m depth.

Table 2.1 Summary of previous small strain stiffness studies in Swedish soft soils

Site	Ground profile description	G_{0field} measurements to depth (m)			Av. G_{0lab}/ G_{0field}	$G_{0lab.}$ to depth (m)		G/ G_{0lab} depth (m)	G/ G_{0field} depth (m)
		CH	DH	SW		RC	BE		
Bäckebol II	Post glacial marine clay	9[1]	21[1,2]		0.8[1]	9[1]		6[1]	SP 6[1]
Bäckebol I	Post glacial marine clay	9[1]	9[1]		0.72[1]	10[1]			
Välen	Post glacial organic/ inorganic marine clay	9[1]	9[1,2]		0.54[1]	10[1]			
Tuve	Post glacial/ glacial marine clay		25[2]						
Munkedal	Post glacial/ glacial quick marine clay		26[2]						
Särö Road	Post glacial organic clay		8[2]						
Lilla Mellösa	Post glacial organic clay/inorganic clay		12[2]						
Skå Edeby	Post glacial/ glacial varved clay		11[2]						
Norrköping	Post glacial organic clay/ glacial varved clay		15.5[2]	10[3]					
Kristianstad	Post glacial organic clay/ sand/glacial varved clay silt layers			8[3]	0.41		8[3*]		
Vatthammar	Silt, clayey silt, silty clay varves		11.5[2]	12[2]					

CH= crosshole, DH= downhole, SW=surface wave, SP= screw plate RC=resonant column, BE=bender element, [1] Andréasson (1979), [2] Larsson and Mulabdic (1991), [3] Svensson (2001), * no details of tests are provided.

Not included above are the field measurements during excavation by Persson (2004), which presented measurements of initial volumetric stiffness and its degradation during unloading for which a hyperbolic function in terms of OCR is used. A variation of this formulation is found in the Swedish transport guidelines (TKGEO, 2013) for determination of stiffness degradation from unloading (excavation).

2.2 Field measurement of small strain stiffness

2.2.1 Introduction

The *in situ* methods for measuring the small strain shear modulus (G_0) are generally based on measuring the shear wave velocity (V_S), and subsequently relating it to the small strain shear modulus using Eq. 2-1. The soil density ρ used in Eq. 2-1 can be determined from samples extracted at the relevant levels, while V_S measurements are typically taken at 0.2 to 2 m intervals throughout the profile. Empirical determination of soil density using V_S measurements by Mayne (1999) appears to work well for the full range of soils and can be used to determine G_0 if the relationship has been validated, refer to Wood (2015).

Generally, three methods shown in Figure 2.1, can be distinguished (Clayton, 2011):

1. Surface wave measurement,
2. Vertical measurement of V_S below ground which can define V_{Svh} where "*vh*" stands for vertical wave propagation and horizontal particle movement.
3. Horizontal measurement of V_S below ground which can define V_S properties in two orientations V_{Shv} and V_{Shh}, depending on the orientation of the source and receivers, where "hv" is horizontal wave propagation with vertical particle movement and "hh" is horizontal propagation and horizontal particle movement.

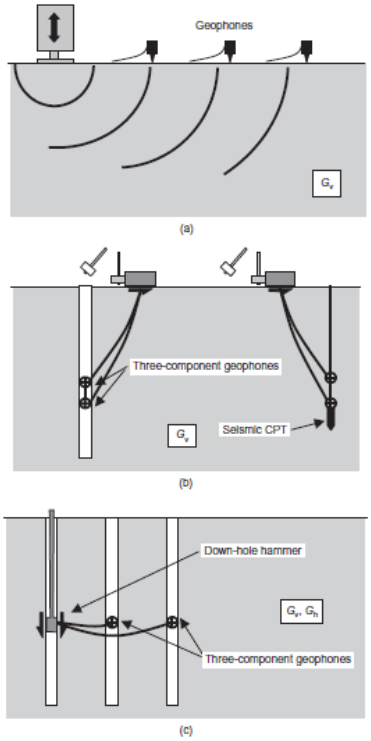

Figure 2.1 Seismic field measurement methods (a) surface wave (vibratory source), (b) down hole (hammer), (c) cross hole, Clayton (2011).

Below ground measurement (downhole & crosshole) tend to involve *direct* assessment of V_S. Alternatively, modern interpretation of surface wave measurements tends to involve *diffuse* analysis, where V_S is determined using inversion techniques. However surface wave refraction tests can also be interpreted directly.

2.2.2 **Surface measurement techniques**

Surface measurement techniques for measurement of the compression wave (P-wave) and the shear wave (S-wave) velocity have been in use for almost 100 years, Ismail *et al.* (2012). There are two common techniques, surface wave measurement using Raleigh waves, and seismic refraction analysis of body waves (shear or compression waves). These waves occur simultaneously, as indicated in Figure 2.2 (b) thus instrumentation and interpretation techniques are devised to reduce unwanted wave interference.

The test setup is essentially the same for both methods and requires a source or 'shot' (to produce waves), a medium (the ground) and a receiver (typically geophone array). For surface wave testing conducted in Sweden and Norway, the set-up typically consists of 24 geophones or more at 1 to 5 m spacing with 5-7 "shots" or excitations per measurement along different positions of the section to be investigated. The depth of penetration is typically ¼ of the length of the measurement section (along the ground). The shots can be produced by a hammer hitting a plate, but in order to ease interpretation, a vibration generator can be used. When increased penetration depth is required small explosive charges (Marek, 2010), or passive noise (Park & Miller 2008) can be used.

Originally interpretation of seismic refraction tests were based on Snell's law, as indicated in Figure 2.2 (a). This method of interpretation is of limited use for soft clays given the underlying assumption that layers become increasingly stiff with depth (normally dry crust present). Given such issues the method is generally only used for determining bedrock profiles and not soil properties, Marek (2010). However, more modern interpretation using inversion techniques appears to successful, at least in the determination of compression wave velocity Donohue *et al.* (2014), Malehmir *et al.* (2013) and appears particularly useful for multiscale approaches in collaboration with cone penetration tests, refer to Ghose & Goudswaard (2004).

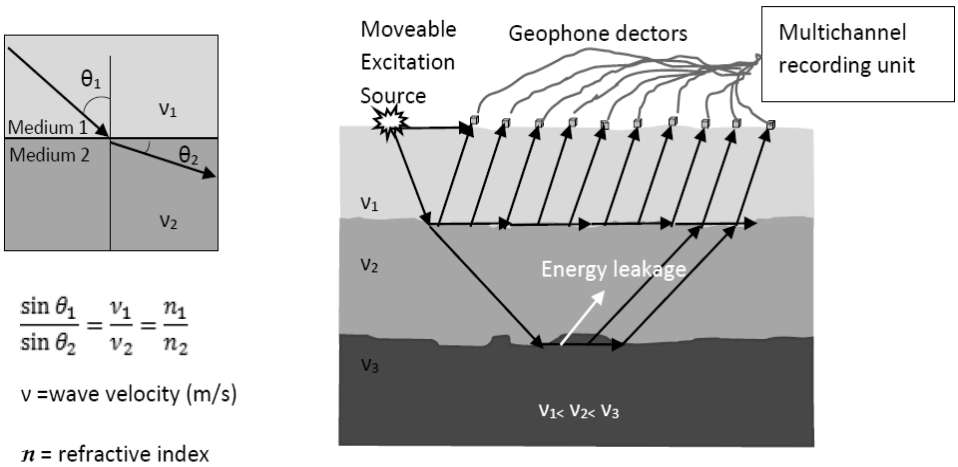

(a) (b)

Figure 2.2 (a) Concepts for direct interpretation of seismic refraction (b) surface wave test set-up and different waves produced in surface wave testing.

The first application of surface waves for geotechnical engineering purposes was by Jones (1958) who used a steady state Raleigh wave from a vibratory source, known as the Steady State Surface Wave technique. Another type of surface wave called the Love wave has also been used for determination of small strain stiffness in the field (Dorman & Ewing 1962), but use of Raleigh waves is most common.

The Raleigh wave consists of a propagating wave resulting from interfering P and S waves. Raleigh waves have an elliptical particle movement with its major axis perpendicular to the surface of the stratum. Early interpretation methods assumed the soil to be a homogenous elastic half space and that wave travel was non-dispersive. As highlighted by Svensson (2001) and Xia *et al*. (2002) in reality soil profiles are heterogeneous (layered) and dispersive (particularly in soft clays), observed by the decrease in width and height of the elliptical particle motion with depth (Russell, 2015). Raleigh waves with high frequency components are found closer to the surface, while low frequency components, which have longer wavelengths, penetrate deeper. It is therefore often advantageous to use a low frequency source in geotechnical applications to maximize the depth of penetration of the investigation.

The Raleigh wave velocity, V_R is very similar to the shear wave velocity, V_S. A relationship between the two has been defined by Richart *et al*. (1970) in terms of a constant (C) where V_R = C. V_S, C is dependent on Poisson's Ratio. The relationships of V_S, V_P and V_R with respect to Poisson's ratio are illustrated in Figure 2.3. With increased computational advances the steady state method developed into the Continuous Surface Wave (CSW) method (Tokimatsu *et al.* 1991, Butcher & Powell 1996, Clayton *et al.* 1995). The testing procedure required was relatively time consuming and expensive when compared to more modern surface wave methods described later in this section and use of a vibratory source often gave limited penetration depth. In addition problems of interpretation associated with removal of noise and interference from different modes of the Raleigh wave were also an outstanding issue.

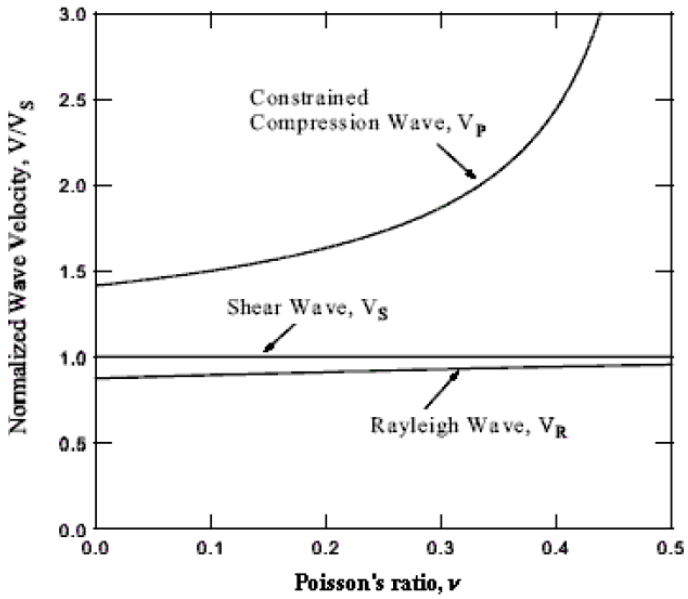

Figure 2.3 Comparison of compression wave velocity V_P, shear wave velocity, V_S and Rayleigh wave velocity V_R for varying Poisson's ratio in a linear elastic half space from Donohue (2005) after Richart et al. (1970).

A special type of Raleigh wave created is ground roll. Ground roll involves waves travelling along or near the ground surface and is used in Spectral Analysis of Surface Waves (SASW). The SASW method was first developed by Heisley (1982) and Stokoe & Nahazarian (1983) to study near surface shear wave velocity profiles. It is a diffuse method where V_s is not measured directly, but instead is found by comparison of measured response and an iterated "best fit" theoretical model (inversion). An illustration of the SASW method by Stokoe *et al.* (2004) is presented in Figure 2.4. In the field a coherence function is used to check the accuracy of the test, however, the interpretation tends to be conducted later. A complete field dispersion curve is built from different receiver separations (receiver separation increasing with increasing wavelength) and is presented in terms of surface wave phase velocity and wavelength (or frequency). From the phase difference the time difference, Δt, between two receivers can be determined provided the distance between the receivers is known. From this the Raleigh wave velocity V_R can be calculated for these wavelengths and consequently a shear wave velocity, V_S, and wavelength, λ, plot can also be calculated using the formulation by Richart *et al*. (1970).

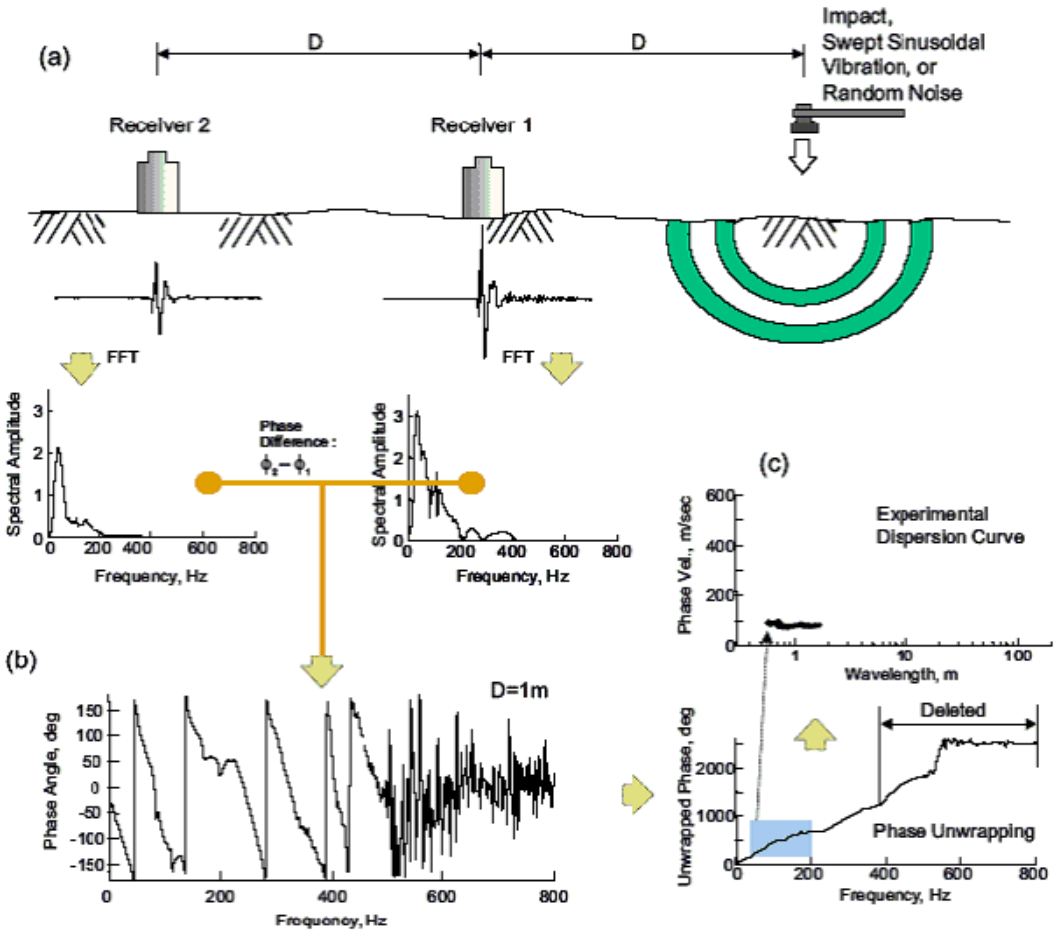

Figure 2.4 Illustration of the SASW method from Stokoe et al. (2004) (a) data acquisition and determination of wave frequency (spectral analysis) using a fast Fourier transform (FFT) to convert from time domain to frequency domain (b) determination of phase difference Ø(f) between two received signals as a function of frequency (or wavelength), (c) complete field dispersion curve built from signals at different receiver separations and conversion from phase angle to phase velocity.

In geotechnical engineering the shear wave velocity variation with depth is generally required, and this can only be determined by inversion or forward modelling. In the inversion process a theoretical model (earth model) is made where the elastic properties of the soil (V_S, V_P, v, γ) are defined. Iteration of these parameters is then used to find the best fit between the theoretical and experimental dispersion curve using a least squares approach. The number of layers affects the complexity of the stiffness matrix used to define the theoretical earth model and accuracy, Lai & Rix (1998) used a four layer system, which gave accuracy in terms of root mean square error (RMS) of around 6% in Swedish soils, Svensson (2001). In addition, errors and uncertainty in determination of V_S using SASW methods were highlighted by Svensson (2001) who compared three G_0 profiles from a Swedish clay moraine/limestone site determined by 3 different institutions (different setup and inversion methods) and found that the values for G_0 varied by up to a factor 3, with differences increasing with depth. Part of this difference may be related to difficulty in identifying the fundamental mode of the Raleigh wave arrival amongst background noise and higher order modes, see Xia *et al.* (2003), Luo *et al.* (2007), Donohue *et al.* (2004). Such issues can make interpretation impossible. There are also a number of practical problems associated with SASW testing such as the need for reconfiguration of the geophone positions, and multiple shots at each source position, which makes field testing time consuming, and therefore expensive.

The Multichannel Analysis of Surface Wave (MASW) method has been developed by the Kansas Geological Survey (KGS) over the last 16 years (Park *et al.* 1999, Xia *et al.* 2002 and Park & Miller 2008). The MASW test equipment is similar to the SASW method, but with a greater number of receivers. Both geophones and accelerometers can be used although geophones are generally preferred (more accurate). The MASW technique requires only one shot at each source position, and does not require repositioning of the geophones when testing a single profile. The position of the source is often offset from the geophone array although some shots can be carried out within the array to improve accuracy in soft soils, as shown by Donohue & Long (2008). The distance between the geophones, source excitation energy and the length of the geophone array determine the precision and penetration depth of the test. For soft clays KGS recommend the use of 4.5 *Hz* geophones. However work by Long & Donohue (2008) found no discernible difference in comparative tests performed with 10 *Hz* geophones, even in very soft Norwegian clay deposits. Systems with over 50 geophones have been utilized in practice, Xia *et al.* (2003) although MASW soft soil testing in Scandinavia has generally been achieved with good accuracy using 24 geophones at 1-2 m spacing, Donohue & Long (2008), Donohue *et al.* (2012). The use of combined active and passive sources is relatively new, and offers some potential advantages as this is often rich in both high and low frequency waves giving increased precision near surface, while also penetrating deeper into the profile. Testing with multiple linear geophone arrays can be used in a grid formation to transform multiple 2D V_S profiles into an approximate 3D profile.

Interpretation of MASW tests outlined by Miller *et al.* (1999) uses a frequency domain approach, very similar to the SASW procedure defined by Stokoe *et al.* (2004). Dispersion curves can be determined manually from the frequency record, Donohue (2005), however work at KGS has led to development of a commercially available automated software package (Surfseis) that can directly use the recorded wave fields of the shot gather (assembled signal data from all geophones in the array) to determine the field dispersion curve. The software is based on the work of Park *et al.* (1998), Miller *et*

al. (1999) and Xia *et al.* (2003). The properties of all types of wave (body and surface waves) are imaged through the wave field transformation process to give the dispersion image. From this image the measured dispersion curve is determined. Subsequently, the parameters of a theoretical earth model are optimised in a least squares approach to obtain V_S, V_P, soil density, γ' and Poisson's ratio, υ for the soil. The MASW interpretation of V_S within Surfseis has limited sensitivity of V_P and γ' so these are set as a constant, reducing computation effort (Xia *et al.* 1999). In Scandinavian soft clays this method has been widely used, Donohue (2005), Long & Donohue (2010), Donohue *et al.* (2004), Donohue *et al*. (2012), L'Heureux & Long (2015). Accuracy in Scandinavian soft clays is reported to be good, with root mean square error (RMS)<1.5, for 24 channel tests, Donohue *et al.* (2012), also the general fit of the final theoretical dispersion curve appears excellent when the inversion is conducted using Surfseis software. This fit is significantly better than SASW tests presented by Svensson (2001) on the Swedish clay sites where accuracy in terms of RMS was reported between 3 and 0.5 over the full frequency range.

It should be noted that the inversion technique applied is one of the greatest potential sources of error in both SASW and MASW techniques as shown by Ismail *et al*. (2012), Luo *et al*. (2007) and Xia *et al.* (2003). Stratification should be verified using field tests such as the Cone Penetration Test (CPT) or dilatometer test (DMT). In critical cases results should be compared to direct shear wave measurements (e.g. seismic CPT/DMT).

2.2.3 **Direct measurement methods**

Today the use of boreholes for downhole, uphole or cross-hole measurements (Figure 2.1(b) on the left hand side and (c)) are not commonly used. This is mainly due to practical issues such as ensuring verticality, the need for support fluid and/or casing, clamping of senders/receivers in the borehole, correct positioning of them and creation of a "shot" downhole. Dealing with these issues leads to significantly more expense and uncertainty in the interpretation. Instead, the use of a seismic probe with single (e.g. Campanella *et al.*, 1986, Larsson & Mulabdic, 1991) or multiple receivers (e.g. Marchetti *et al.*, 2008, Ghose, 2012) is more common. Penetration of the probe is achieved by pushing the devise into the ground using a standard CPT/DMT rig/truck as counter weight. Additional pull out screws can be required for deep penetration. This method is cost effective for the relatively shallow depths studied for geotechnical engineering (typically < 100m).

A single seismic probe with a mono axial geophone can be used to determine the vertical shear wave velocity (V_{Svh}) if the source is close to the probe at ground surface. Multiple probes or multi-directional geophones are required to determine the horizontal components of shear wave velocity, V_{Shh}. The use of multiple receivers/probes is superior in minimising interface effects at the surface of the probe as well as other potential issues with interpretation relating to comparison of different 'shots'. For soft clays it is often assumed for practical engineering purposes that small strain stiffness is isotropic thus $V_{Svh}= V_{Shh}= V_{Shv}$. Comparisons of direct measurements of V_{Svh} and V_{Shh} in Scandinavian soft clays by Andréasson (1979) and Donohue & Long (2010) suggest that differences are small but that $V_{Shh} \geq V_{Svh}$. The amplitude of the received waves reduces with increasing distance between the source and receiver thus shear strains tend also to reduce. This can be compensated for by applying additional energy to the source

excitation although some studies such as Larsson & Mulabdic (1991) suggest application of a correction factor for field V_S measurements, the determination of which lacks scientific rigour.

Different interpretation methods are used, depending on if single or multiple geophones are used. For all methods, the soil is assumed to be elastic and that waves produced from the shot travel in straight lines, in reality these are slightly curved. For single geophone systems the received signals from different depths (and 'shots') can be used to determine V_{Svh} by the time difference between the points of arrival of the initial shear wave for each shot/depth. Alternatively, two shots at the same depth but with reversed polarity can be used and the received signals stacked as shown Figure 2.5(a). The point of shear wave arrival or 'pick' varies from the point of first cross over (first deviation from x-axis), first peak, maximum peak, etc. Clearly the position of the 'pick' will affect the magnitude of V_S determined. There are a number of problems with both these methods. The received signals that are compared stem from different 'shots', and therefore, the initial excitation source is different and may not be directly comparable. The reflected compression waves can hide the point of shear wave arrival, and the change in shape of the travelling waves is often great due to both dispersion and attenuation. Yet the interpretation method assumes there is no change. The chosen 'pick' of the shear wave arrival is also subjective. The use of multiple probes as indicated in Figure 2.5(b) can mitigate some of these problems, particularly when the time difference *(*Δt*)* between the shear waves is determined using cross correlation techniques, refer to Marchetti *et al.* (2008). This removes the subjectivity of determining the picks and provides a fit to the initial part of the wave as oppose to a specific point on it.

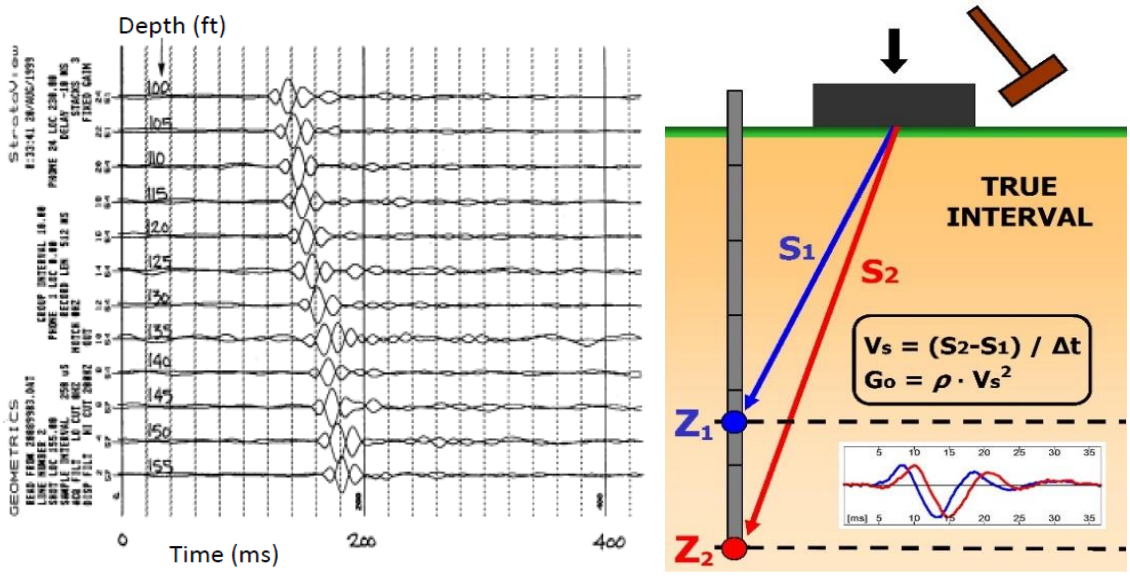

(a) (b)

Figure 2.5 (a) Typical down hole test single geophone test profile with a stacked trace of two shear waves with opposing polarization, Crice (2002) (b) test set up and interpretation using multiple geophones, Marchetti et al. (2008).

2.2.4 **Measurement of stiffness degradation**

In addition to the shear wave based techniques, other techniques to determine *in situ* small strain stiffness and its degradation include: dynamically loaded screw plate load

tests to capture damping (Andréasson 1979) and stiffness degradation with respect to strain amplitude; a self-boring pressuremeter test (sbPMT) to obtain stiffness degradation as function of strain magnitude (Jardine, 1992), and back analysis of monitoring data of geotechnical structures and/or the ground to guesstimate the stiffness response (e.g. Burland, 1989, Persson, 2004 & 2007, Clayton, 2011) with respect to stain magnitude. A problem with many of these techniques is that they require a number of idealisations and assumptions to be made.

The use of monitoring results from the ground/structures is also difficult due to the following issues:

- Lack of sufficient resolution (spatial and temporal) and accuracy to define total stress, pore pressures and displacements to allow full definition of the *in situ* state and its changes.
- Noise in monitoring results caused by nearby ongoing construction activities
- Resolution of measurement system
- Assumptions/idealisations made to allow interpretation

Attempts to measure the incremental total stress tensor *in situ* has been made in practice with "rosettes" of cells inclined at different orientations. Six cells are required for full definition, and this reduces to three for plain strain conditions. In Sweden measurement of total stress *in situ* has generally been limited to a single horizontal direction using hydraulic Glötz cells, Persson (2004), Johansson & Jendeby (1998), Smith (1989) and Kullingsjö (2007). Potential errors include the disturbance of soil around the cell, the changes in the boundary stresses due to insertion, the cell compliance, the stiffness compatibility and the interpretation (often assumes behaviour is elastic which is only true at small strains).

Of the approaches presented in this section the sbPMT is most attractive as it entails direct measurement of stiffness. Back-analysis of soil properties from measured displacements, loads, stresses etc. in the soil or geo-structure will always be hampered by crude measurements and complex boundary conditions.

Clearly empirical correlations for stiffness based on back calculation of field behaviour need to be used with extreme caution, and only for preliminary design purposes. Within deep excavations one such correlation, which is often used in Sweden, is the unloading moduli defined in the Swedish Transport design guidelines (TKGEO, 2013).

2.3 Laboratory methods

2.3.1 Introduction

Similarly to the field testing different laboratory testing methods can be used for determination of the dynamic and the static small strain stiffness. In the past emphasis was placed on the dynamic small strain stiffness and damping, determined using resonant column and torsional shear tests for a wide range of soils, with stiffness degradation defined in terms of strain amplitude; Hardin & Drnevich (1972), Andreasson (1979). Since the mid 1980's the measurement of shear wave velocity using bender elements and interpreted using elastic theory has gained popularity for determination of small strain stiffness, with its degradation defined in terms of shear or

axial strain determined from local displacement measurements, such as those described by Jardine *et al.* (1984) and Clayton *et al.* (1989).

There is often a discrepancy between the field and the laboratory determined small strain stiffness and its degradation, as shown by Andréasson (1979), Mitchell & Soga (1976), Long *et al.* (2003) and Persson (2004), with laboratory tests tending to give lower values. This discrepancy is caused by both sample disturbance and/or errors related to the interpretation (assumptions, idealisations etc.). Care with both is required, if stiffness representative of *in situ* conditions is to be determined in the laboratory.

2.3.2 **Resonant column and torsional shear tests**

Resonant column tests have been performed for more than half a century. In its simplest form the base of a sample is fixed and the top free to move, often within an ordinary triaxial apparatus. A wave is generated by a vibratory source and allowed to propagate. The frequency of the wave and its attenuation are used to obtain the modulus and damping properties of soils, as a function of vibratory strain amplitude, typically in the strain range 10^{-5} to 10^{-3}. The apparatus can also be used to study other influencing factors on small to medium strain stiffness, such as confining stress, void ratio, degree of saturation, time and temperature. The vibrational source may be vertical or torsional and is typically created using an electromagnet. In its more modern form a harmonic excitation force is applied with frequency, f, and response of the top of the sample monitored with accelerometers. The excitation frequency is changed until resonance is observed and this frequency recorded. The resonant frequency is normally defined as the frequency for which the displacement amplitude is 90 degrees out of phase with the input signal polarity. For vertical vibration (typically above 20 Hz) determination of shear modulus requires accurate assessment of specimen and vibration source inertia which can be difficult. An alternative method is torsional shear tests which are generally performed at lower frequencies (0.1 to 10 Hz) with displacements measured directly. Torsional shear tests are quasi-static tests that involve controlled rotation of the top platen. No inertia effects are present in the test, and the hysteresis loop is determined by measuring the torque-twist response of the sample. From this shear modulus, G, is determined and damping (D). Test set-ups have been devised that can perform both resonant column tests and torsional shear tests such as that presented by Stokoe *et al.* (1995).

The method of assessment of stiffness degradation from resonant column tests differs depending on the type of oscillation applied. However, all methods assume an isotropic linear elastic material with a cylindrical bar geometry for which the base is fixed. Resonant column tests have been used to investigate dynamic and static small strain stiffness behaviour for a wide range of soils such as the work presented by Hardin & Drnevich (1972), Drnevich *et al*. (1978), Dobry (1991), Dyvik & Madshus (1985), Clayton (2011) and Andréasson (1979). However, much of this research has been conducted on isotropically consolidated samples as pointed out by Stokoe *et al.* (1995). Today it is understood that isotropic loading does not give behaviour representative of anisotropic field conditions, and will affect both the shape and magnitude of stiffness degradation curves, refer also to Bjerrum (1973).

2.3.3 **Bender element tests**

Rather than measuring the dynamic response of a dynamically excited sample, the small strain stiffness can also be inferred from the shear wave velocity in the laboratory similar to direct measurement methods used in the field and discussed in Section 2.2.3. In the laboratory this requires generation and acquisition of mechanical waves using piezoelectric bender elements. A rigorous analysis of this type of testing is presented by Lee & Santamaria (2005).

Bender element (BE) tests were first conducted by Shirey & Hampton (1978). The magnitude of induced strains generated will vary depending on test conditions but are less than 10^{-5}, which often lies within the linear elastic part of stiffness response, Brignoli *et al.* (1996). Bender elements are used in pairs as source and receiver, and can comprise of series-series, parallel-series, or parallel-parallel pairs. Lee & Santamaria (2005) suggest that parallel-parallel systems have the least amount of signal disturbance caused by cross- talk, however comparative studies by Yamashita *et al.* (2009) concluded that results of bender element tests were not significantly affected by the choice of bender element pair but that parallel transmitters and series receivers were most commonly used. Bender elements can be used both to study compression (P) waves and shear (S) waves, but in soft clays with high water content the P-wave velocity, and the corresponding stiffness, is dominated by pore water, and thus does not reveal much information about clay behaviour.

Bender elements were first incorporated into standard triaxial test equipment by Dyvik & Madshus (1984) and were fully validated for soft Scandinavian clays by Dyvik & Olsen (1985) by comparison with resonant column tests on high quality samples. A typical bender element test uses a triaxial setup, e.g. Dyvik & Madshus (1985), Viggiani & Atkinson (1995), Brocanelli & Rinaldi (1998), Alvarado & Coop (2007), Landon (2007), Leong *et al.* (2009), Jovi$\hat{c}$ić *et al.* (1996) as indicated in Figure 2.6. Additional pairs can be added in the horizontal plane when the full range of cross-isotropic elastic parameters are required to give G_{0hh} and $G_{0\mathrm{hv}}$ as shown by Pennington *et al.* (1997), Lings *et al.* (2000), Callisto & Rampello (2002) and Clayton *et al.* (2004). Bender elements have also been incorporated into other sorts of laboratory test such as oedometer tests, Comina *et al.* (2008), resonant column tests (Dyvik & Madshus 1985), and simple shear apparatus (Kuwano *et al.* 1999). Measurement of shear wave velocity is often more difficult for these tests as discussed by Sánchez-Salinero *et al.* (1986) due to reflected waves, wave interference and damping, generally termed 'near field' effects. The influence this has on interpretation is discussed later in this section.

Test execution is relatively straightforward for soft clays, as good contact between the bender element device and the soil can be established and the signal dispersion is less significant than with sands (although attenuation is greater). Significant reduction of voltage amplitude occurs between transmission and arrival of the shear wave (up to 5000 times in soft clay based on Donohue, 2005), thus amplification of the received signal is normally required.

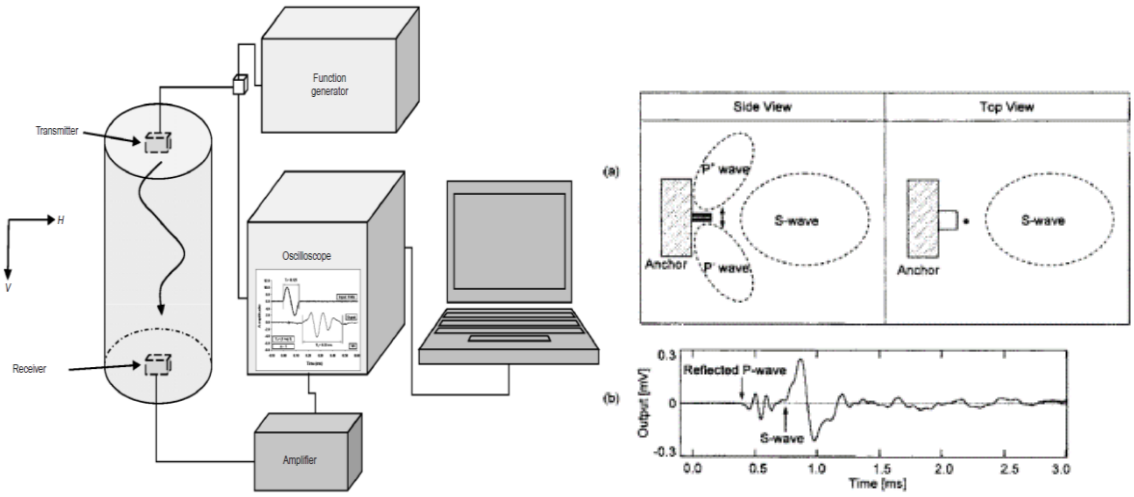

(a) (b)

Figure 2.6 (a)Typical test set up for measurement of G_{0vh}, Alvarado & Coop (2007) (b) Directivity of the bender element waves, in-plane shear wave and transverse P –waves and measured signal response indicating the position of P and S wave arrival, Lee & Santamaria (2005).

The choice of excitation frequency is a trade-off between attenuation of the signal at high frequencies, with only limited near field effects (less impact of traverse P waves on received signal), or a strong received signal at lower frequencies, but significant near field effects (significant impact of traverse P waves on received signal) as indicated in Figure 2.6 (b). The choice of waveform is often dictated by ease of detection of the 1st shear wave arrival, where less frequency components are often preferred (Viggiani & Atkinson, 1995, Clayton, 2011). This depends however on the method of interpretation, for example when comparing 1st and 2nd received signals, a broad range of frequencies in the input signal (typically a square or step wave) is preferred, as these give a richer received signal with larger amplitude (for the part of the wave where the frequency causes resonance) making interpretation easier (Lee & Santamaria 2005). Unfortunately, even the use of a single frequency input does not mean that the interpretation of the travel time (& wave velocity) between the transmitted and received signal is trivial. Several time domain (TD) and frequency domain (FD) interpretation methods have been introduced to determine the shear wave travel time (e.g. TD: first positive signal Dyvik & Madhus 1985, Brignoli *et al.* 1996, to first zero crossover, t_1 Kawaguchi 2001, Donohue 2005, Clayton 2011, to first positive peak, Persson 2004, Kullingsjö 2007, Clayton 2011, Yamashita *at al.* 2009, to second cross over (B') Lohani *et al.* 1999; FD: Viggani & Atkinson (1995); Brocanelli & Rinaldi (1998), Greening *et al.* (2003), Blewett *et al.* (1999) Greening & Nash (2004), Bonal (2012); FD cross-correlation: Viggani & Atkinson 1995, Moshin & Airey 2003, Yamashita *et al.* 2009, and signal matching Lee & Santamaria 2005, Wang *et al.* 2006). The validity of these methods is dependent on the combination of factors such as; soil type, signal type and bender element system (BES) and test setup (BES components and applied stresses etc.). These factors lead to different transfer functions (damping) within the BES, which is often ignored or simplified during interpretation, and is a major reason why so many different procedures and interpretation methods have evolved. The differences in the shear wave travel time can be significant, particularly at low frequencies.

The first interpretation methods of V_S from BE tests were based on time domain assessments involving the 'pick' the first shear wave arrival, similar to early direct field

assessment. These remain popular and appear to be widely used in practice. For this interpretation method the shear wave is assumed singular, non-dispersive, planar and the soil medium isotropic elastic, thus V_S can be determined from the distance travelled by wave between the transmitting and the receiving bender elements tips, if the travel time, t_a and travel distance L is known, or alternatively between the 1st and 2nd shear wave arrival at the receiving bender element. The assumptions infer that the shape and frequency of the transmitted signal does not change, which is particularly untrue when comparing the 1st shear wave arrival to the assumed input signal. Identification of the second shear wave arrival is often difficult due to attenuation of the signal, particularly in soft clays, thus the comparison of the 1st and 2nd shear wave arrival is not always possible. Consequently for these soils the 1st shear wave arrival is generally preferred. The preferred position of the 'pick' given by different authors is related to the significance of reflected P-waves, dispersion and damping observed in the received signals, which are specific to a given soil, BES and triaxial test procedure.

The masking of the arrival of a shear wave due to the presence of reflected P waves in the time domain has been studied by a number of authors, e.g. Sánchez-Salinero *et al.* (1986), Mancuso *et al.* (1989), Clayton *et al.* (2004), Lee & Santamaria (2005) and Rio (2006). Often the BES is chosen such that the impact of "near field" effects, which tends to mask the first shear wave arrival, are minimised by optimising the frequency of the applied signal so that the ratio (L/λ) is maximised (often referred to in literature as R_d), where L is the BE tip to tip distance and λ is the wavelength of the transmitted wave. R_d represents the number of wavelengths between the source and the receiver. The recommended values of R_d to avoid "near field" effects vary between 2 and 10, refer to Jovičić *et al.* (1996), Arroyo *et al.* (2006) and Brignoli *et al.* (1996). Other BES systems have combated this problem by increasing the length of the sample, as shown by Viggiani & Atkinson (1995) and Kawaguchi (2001), while Lee & Santamaria (2005) increased the width of the sample such that P-waves dissipated at the boundaries or arrived after the S-waves.

The difficulty in identification of the first wave arrival in the presence of "near field" effects is one of the reasons why peak to peak 'pick' for the measurement of shear wave travel is often found to be more reliable. Unfortunately, although less affected by reflected waves, the use of the peak to peak 'pick' can give values of V_S that are too low when the travelling wave is significantly affected by dispersion and distortion, Alvarado & Coop (2012), Wang *et al.* (2007). To this end Clayton (2011) makes as reasonable recommendation that V_S from both the first cross over and peak to peak 'pick' be determined and compared.

A more robust, yet simple, approach when compared to time domain analysis is use cross- correlation techniques. Cross-correlation can be done within the time domain, but is most commonly conducted within the frequency domain. While this method shares the assumptions of time domain interpretation, the subjectivity of the 'pick' is removed and a fit made over part of the signal and not a specific point, removing much of the subjectivity of defining the exact position of the 'picks'. A more rigorous approach using cross-correlation techniques is the comparison of the 1st and 2nd shear waves arrivals, as these signals are automatically more similar, and the uncertainty surrounding the transfer functions of the BES removed, refer to Santamaria & Fam (1997), Arulnathan *et al.* (1998), Lee & Santamaria (2005). Some issues remain, however, with regard to non-planar wave travel (Fonseca *et al.*, 2009) and attenuation (damping),

which can be large (Mohsin &Airey 2003, Arulnathan *et al.* 1998, Donohue 2005). In soft Norwegian clays Donohue (2005) found that the wave attenuation was so great that the 2nd or 3rd shear wave arrivals were rarely identifiable.

As discussed, the interpretation using the time domain and cross correlation ignores dispersion. There are a number of methods for determination of V_S within the frequency domain that have been put forward, which utilise the occurrence of wave dispersion instead of ignoring it. One of these is the phase-delay method, which is determined either by multiple tests of different frequency using continuous sine input waves (the π-point method) or using a continuous sine sweep signal. Sine wave input signals are chosen so that the distortion is limited. It is assumed that there is only a singular vibration mode, thus it should not be used where "near field" effects are significant (low values of R_d). In the π- point method a continuous sine wave input is applied, and the frequency is altered until the input and output signals are exactly in and out of phase (these are the harmonic frequencies of the system). The shear wave velocity can be determined using BE tests in a similar manner to spectral analysis of surface waves presented in Figure 2.4 referred to by Viggani & Atkinson (1995) as the Cross Power Spectrum Method. The method stems from Bodare & Massarsch (1984) for field testing of V_s. The method assumes that the group travel time for a given range of frequencies can be found by linearly interpolating the absolute cross-power spectrum phase diagram within that range, and has been used by numerous authors in bender element testing, see e.g. Brocanelli & Rinaldi (1998), Greening *et al.* (2003), and Blewett *et al.* (1999). An improvement of the π-method is the Frequency Spectral Analysis or Sweep method; see e.g. Greening (2003), Greening & Nash (2004). In this method a frequency sweep of continuous sine waves is input and the phase angle determined. This allows a more continuous plot of phase angle against frequency. At harmonic frequencies this plot should co-inside with values found using the π-point method, as shown by Greening & Nash (2004) and Fonseca *et al.* (2009). The sweep sine signal used by Greening & Nash (2004) covered a range of 0 to 20 kHz and was repeated for a few "shots". Although the method has been used by a number of other authors, e.g. Brocanelli & Rinaldi (1998), Blewett *et al.* (1999), there is a problem with this and π-point method, as both assume that wave travel is linear and that damping and other peripheral effects of the BE-soil system are negligible. Work by Camaco-Tauta *et al. (*2011) compared time-domain and frequency-domain methods, and assessed their validity based on the measurement of the propagation of shear waves using embedded accelerometers. This work suggested that the time-domain analysis gave reasonable results, whereas frequency domain analysis had a number of inconsistencies.

The impact of the BES component transfer functions on the overall dispersion, and damping of the system, has been studied by Wang *et al.* (2007) who compared the measured and the simulated receiver signals using the analytical solutions by Cruse & Rizzo (1968), which were the same as those used by Sánchez-Salinero *et al.* (1986) and Lee & Santamaria (2005) to study "near field" effects. The results suggest that the transfer function for the soil (H_{soil}) only causes a small distortion in front of the transmitted shear wave, seen by the dip before the positive part of the output signal. The rest of the simulated output is, however, significantly different to the measured output signal. If, however, the transfer function for the receiving bender element H_{be_R} is added to the analytical solution, the simulated output and measured output are in much better agreement. Some differences remain, which may be due to anisotropy of the medium and/or the lack of allowance for the transfer functions of peripheral electronics, the

bender element transmitter and the boundary effects causing additional wave interference, energy dissipation and visco-elastic effects that cause signal dispersion and damping.

In conclusion many of the direct experimental test regimes proposed in the literature strive for "non-subjective" determination of shear wave velocity, often requiring increasingly rigorous experimental and interpretation procedures. However the international study by Yamashita *et al.* (2009) did not find that more advanced methods performed better than simple time domain interpretation, provided R_d was high. The fact that more complex methods did not lead to more reliable determination of V_s may be due the fact that many of the more complex interpretation techniques still assume wave travel to be isotropic linear elastic, which can have a significant impact on interpretation of V_s even when measurement/interpretation techniques are applied that take account of end effects, dispersion and attenuation (damping). In fact Yamashita *et al.* (2009) presented recommendations in line with Clayton (2011) that the time domain picks for the first cross over and first peak to peak should be used for interpretation of V_S provided a high frequency sine wave is used. The difference in V_S between the two picks can then be used to identify if the initial part of the shear wave arrival is significantly affected by dispersion and or multimodal vibrations. This essentially gives a 'check' as to the validity of V_S determined using all linear interpretation methods (time domain, frequency domain and cross correlation). Confidence in this approach can also be gained considering the experimental results and numerical simulations presented by Wang *et al.* (2007) and Alvarado & Coop (2012) when R_d is high. When R_d is low (< 4) account must to be taken of both multimodal vibrations, and the BES component transfer functions to avoid significant errors in the interpretation of V_S, as discussed by Wang *et al.* (2007), Jovičić *et al*. (1996), Lee & Santamaria (2005), Sánchez-Salinero *et al.* (1986), Alvarado & Coop (2012), Bonal *et al.* (2013) and Santamaria & Fam (1997).

Diffuse interpretation of V_S using signal matching techniques that allow for damping and multimodal vibrations is an attractive way forward but due to the number of unknowns present requires a large test series to corroborate the final value of V_S, which makes this method computationally and experimentally intensive, especially when transfer functions can be expected to vary with soil type (and degree of sample disturbance), signal type, stress level and time for soft clays. The BE-soil interface may continuously change due to creep for example. However, the accuracy of this technique in the presence of "near field" effects was shown by Lee & Santamaria (2005) to be within 1%, which is clearly better than many of the methods discussed in this section even in the far field. It still assumes, however, that behaviour is isotropic elastic, which may be an issue for some soils. The experimental/interpretation intensity maybe justified for use of horizontal BE measurements in triaxial apparatus or other test situations, where R_d<4 is unavoidable, or when very dispersive behaviour is present (due to discontinuities for example). It is, however, clear from the literature that for soft clays the behaviour is generally less dispersive, providing "near field" effects are avoided (R_d>4), in which case time-domain and cross-correlation techniques should give reasonable results.

2.3.4 **Local instrumentation**

In addition to capturing the dynamic response through shear wave velocities the small strain stiffness can also be determined by measuring the displacement (when normalised: the strains) of a sample during testing. Local measurements with sensors directly attached to the sample prevent end effects, system compliance and geometrical distortion effects in the measurements, as discussed by Jardine *et al.* (1984) and presented in Figure 2.7.

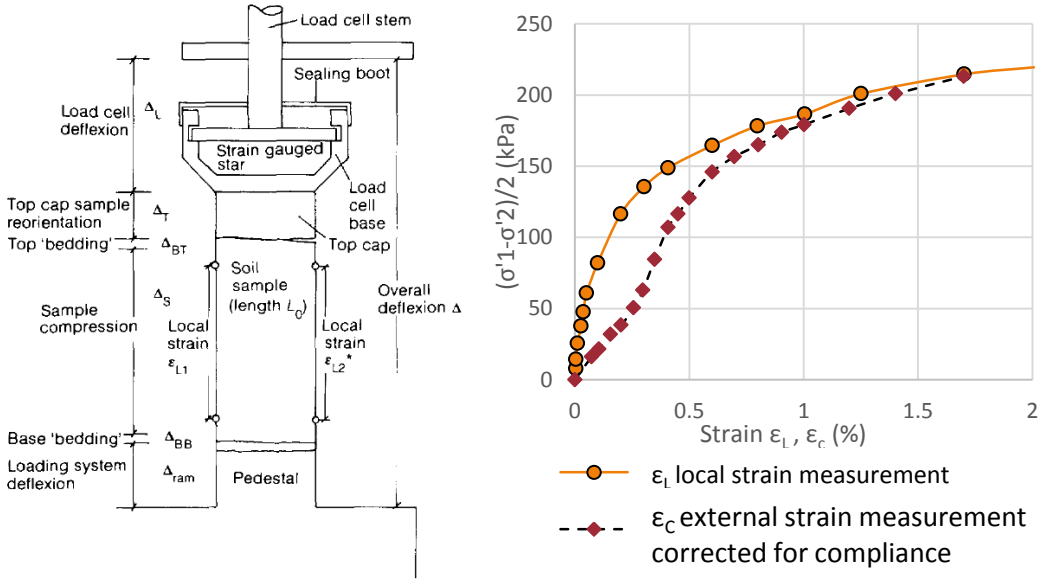

(a) (b)

Figure 2.7 (a) Sources of error in external axial strain measurement in standard triaxial apparatus (b) Comparison of local and external strain measurement of lightly over consolidated glacio-marine clay, reproduced from Jardine et al. (1984).

Several instruments that are able to sense very small displacements have been successfully applied, e.g. miniature inductive or resistive displacement transducers (Olsson 2013, Bhandari *et al.* 2012, Goto *et al.* 1991), Hall effect sensors (Clayton *et al.* 1989, Long *et al.* 2003) and electrolytic liquid levels (Burland & Symes 1982, Jardine *et al.* 1984). When combined with high quality data acquisition (>16 bit), regular calibration and proper mounting, the miniature inductive displacement transducers appear superior and trouble free.

For local strain testing of soft soils a measurement system with a large range and high resolution is required. In the devices discussed above, a larger range comes at the expense of accuracy of the measurement. For such soils it may be more prudent to use optical techniques that utilise of resolution digital imaging (cameras). Such a method is presented and validated for use in triaxial testing of sands by Bhandari *et al.* (2012) and shows very good agreement between small range LVDTs and displacements derived from digital image correlation (DIC) (difference < $4x10^{-6}$ m), which may be sufficiently accurate to provide the full stiffness degradation curve for soft Scandinavian clays.

2.4 Sample disturbance and assessment

2.4.1 Introduction

Sample disturbance and reconconsolidation procedures form part of the recent stress history of samples and have been shown to have significant influence on the small strain stiffness of soft clays, see e.g. Bjerrum (1973), Ladd & Foot (1974), Gens (1982), Kilpatrick & Khan (1984), Burland (1989), Jardine *et al.* (1991), Hight *et al*. (1992), Smith (1992), Clayton *et al.* (1992), Clayton *et al.* 1998, Santagata & Germaine (2002), Lunne *et al.* (2006), Landon (2007), Zapata-Medina *et al.* (2014). The changes that occur in samples of soft clay when removed from the ground for laboratory testing, and the influence this has on behaviour overall, has been studied by many authors. However, the focus is often placed on the sample extraction method, rather than differences in the sample disturbance chain.

Hight *et al.* (1992) postulated that sample disturbance modifies behaviour by altering the soil's initial bounding surface and behaviour within this surface. This tends to affect the yield stress (reducing the apparent pre-consolidation pressure), reduces the initial stiffness, increases the post yield stiffness and alters the undrained and the drained effective stress paths, and hence the peak strengths and strains at which this occurs. Sample disturbance is always present in laboratory samples, however, its severity will depend on the sample disturbance chain which is sensitive to soil plasticity (worse in low plasticity), stress history (worse for low OCR), level of structure (worse in highly structured clays), sampling method (and sampler geometry), laboratory extrusion and preparation procedures, storage time and test procedures (different stress paths, strain paths, reconsolidation time, etc.).

2.4.2 Sample disturbance chain

The problem of sample disturbance in soft Swedish clay samples has been identified for a long time. This is not surprising, given that Swedish clays are often only lightly or normally consolidated (low OCR), highly structured and in some areas are of low plasticity (Swedish East coast), which are factors found to give rise to the greatest disturbance in laboratory samples based on the work of Hvorslev (1949), Skempton & Sowa (1963), Bjerrum (1973), Hight *et al.* (1992). The method of removal of samples from the ground was identified very early in Sweden as a key factor in sample disturbance, and led to early development of a fixed piston sampler to combat this problem, Olsson (1925). The importance of minimising disturbance during sampling was also confirmed by Hvorslev (1949) who identified that the disturbance was related not only to the magnitude and complexity of changes in the effective stress experienced by the sample, but also with what speed these occurred. It was later found out, however, that while the effective stress changes can be a significant factor in sample disturbance, if the centreline strains experienced by the soil during sampling and extrusion are minimised and the sample is then anisotropically reconsolidated, behaviour representative of the field can be captured in clay samples (Skempton & Sowa, 1963, Santagata & Germaine, 2002, Hight & Leroueil, 2003). This was also shown analytically/numerically by Baligh *et al.* (1987), Clayton *et al.* (1998) and Doran *et al.* (2000). Such findings have led to continuous research and development of different sampling methods that minimise centreline strains in addition to investigations into the

influence of other parts of the disturbance chain (transportation, storage, extrusion, preparation and test procedures) some of which are summarised in Table 2.2.

Each part of the sample disturbance chain contributes to the behaviour observed in the laboratory. Disturbance occurring after removal of samples from the ground (described by Kallenius (1972) as secondary disturbance) is often dependent on the initial disturbance caused by penetration, cutting/pressing and extraction of samples as shown by Arman & McManis (1976). The need to minimise not only the sample disturbance, but also the secondary disturbance is also evident in the work of Drnevich & Massarsch (1979) who show that while the initial disturbance during sample removal from the ground is the largest single factor, however the culminated effect of secondary disturbance can be as large, and in some cases greater than the initial disturbance, which appears to be overlooked in much of the comparative work that exists in literature. It is, therefore, pertinent to remember that the sample disturbance chain has a significant effect on clay behaviour observed in the laboratory, and not just the sampling method.

The main changes in soft clay samples which cause disturbance are outlined below:

- Changes in mean effective stress, *p'*
- Mechanical damage to structure by shear or volumetric strains
    - Progressive destruction of cementing and aging effects
    - Introduction of discontinuities
    - Movement along existing fissures or discontinuities
- Water content redistribution post sampling and loss
- Gas dissolution
- Chemical and biological alteration during storage.

Unfortunately, the method shown to give least disturbance (block samples) is also the most expensive and time consuming to use, and can only be used to limited depths (<22 m). This is an issue for Swedish soft clays where samples are often required below this at depth and at lower cost. For this reason fixed piston samplers are favoured, more specifically the STII sampler which is illustrated in Appendix A2 together with the definition of the key sample tube geometry parameters used for tube samplers.

Experimental and analytical studies given in Table 2.2 identify the following key geometry parameters for minimisation of disturbance caused by tube samplers, whose use is often necessary given both economic and practical considerations for soft clay sampling:

- Low area ratio, $AR= (D_2^2-D_1^2)/(D_1)^2$ (reduce volume of displaced material)
- Minimise cutting shoe tapper angle, α_c ($\leq 5°$) (reduce peripheral and centreline strains)
- Low inside clearance $ICR=(D_3-D_1)/D_1$ (reduce volume of expansion)
- Minimise cutting shoe thickness , t (reduce peripheral and centreline strains)
- Large diameter sample D_3 (allows the removal of peripheral highly disturbed layer and reduces water content redistribution/softening)
- Low length to diameter ratio, L/D_3 (reduce need for inside clearance)
- High tube Ø/thickness ratio, D_2/t_c (reduce peripheral and centreline strains defined as B/t_c by Baligh ,1985 and Baligh, 1987)

Table 2.2 Research on sample disturbance in clays and relevance to small strain stiffness of soft Swedish soils (indicates numerical or analytical studies).

Disturbance chain	Published research	Relevence for this research
Sample method- general studies	Hvorslev (1949), Jakobson (1954), Skempton & Sowa (1963), Ladd & Lambe (1963), Rowe (1972), Hight *et al.* (1992), Ladd & De Groot (2003)	Minimising the changes in effective stress and strains experienced by the sample will give more representative behaviour of laboratory samples.
Sample method- Block (hand cut, Sherbrook, mini block)	La Rochelle & Lefebvre (1971), Holm & Holtz (1977), Arman & McManis (1976), Lefebvre & Poulin (1979), Clayton *et al.* (1992), Hight *et al.* (1992), Smith (1992), Lunne et al. (1997), Tanaka (2000), DeGroot *et al.* (2003), Lacasse *et al.* (2003), Landon *et al.* (2004), Poirier *et al.* (2005), Long (2006), Donahue & Long (2010), Karlsrud & Hermandex-Martinez (2013), Emdal *et al.* (2016), Karlsson *et al.* (2016)	Block samples represent the best possible samples for the study of small strain stiffness. Handcut samples are potentially best method but- limited depth and potential issues associated with base failure of excavation, Sherbrook & mini block samplers are a good alternative but expensive and time consuming- require rare specialised equipment & highly skilled operators.
Sample method- large diameter thin wall tube (Laval, SGI, etc.)	La Rochelle & Lefebvre (1971), La Rochelle *et al.* (1981), Larsson (1981), Hight *et al.* (1992), Smith (1992), Hight & Leroueil (2003), Löfroth (2012)	Expensive - rare specialised equipment & highly skilled operators, push in tube in an excavation possible –same issues as handcut block.
Sample method- tube samplers	Jakobson (1954), Kallstenius (1958), SCPS (1961), Berre (1969), Arman & Mcmanis (1976), Andresen & Kolstad (1979), Larsson (1981), Baligh *et al.* (1987), Budhu & Wu (1992), Leroueil & Tavenas (1993), Lunne *et al.* (1997), Clayton *et al.* (1998), Tanaka *et al.* (1996), Tanaka & Tanaka (1999), Lunne *et al.* (1999), Hight & Leroueil (2003), Landon *et al.* (2007), Low *et al.* (2010), Karlsson *et al.* (2016).	Different sized pistons require different transport, extrusion and trimming proceedures, disturbance related to key geometrical properties of tube identified in Appendix A2. The STII sampler used almost exclusively in Sweden (developed from the STI). Larger area ratios with sharp cutting angle and smaller inside clearance might be preferable
Handling and transport	Kallstenius (1972), Doran *et al.* (2000), Ladd & DeGroot (2003)	Minimise vibration and shocks - short transport routes with damping liners
Storage effects	Jakobsen (1954), Söderblom (1969), Kallstenius (1972), Söderblom (1974), Torrance (1976), Bozozuk (1976), Kilpatrick & Khan (1984), La Rochelle *et al.* (1986), Lessard & Mitchell (1985), Henriksson & Carlsten (1994), Heymann & Clayton (1999), Hight (2000), Hight & Leroueil (2003), L'Heureux & Kim (2013)	Differences shown in pore water distribution, pore water chemistry, index test properties and mechanical properties during storage- may affect design parameters and is most prominent in high sensitivity clays. Storage time should be limited although low disturbance samples appear to have a longer 'shelf life'.
Sample preparation (& temperature during testing)	Kallstenius (1972), Kimura & Saitch (1982), Magnusson *et al.* (1989), Atkinson *et al.* (1992), Tidefors (1987)	Huge variation in test results due to differences in laboratory procedure and conditions are observed- which will affect all soil parameters.
Method of reconsolidation	Bjerrum (1973), Ladd & Foot (1974), La Rochelle *et al.* (1976), Atkinson *et al.* (1990), Jardine *et al.* (1991), Smith (1992), Graham & Lau (1998)	Large influence on stiffness from samples consolidated using different stress paths, important that ESP lie well within the initial yield surface

2.4.3 **Assessment of sample disturbance**

Given the impact sample disturbance has on geotechnical parameters determined from laboratory tests, a number of methods have evolved, which attempt to classify the degree of this disturbance, referred to as sample quality assessment. These can be broadly split into two general categories, non-destructive tests and destructive tests. The use of non-destructive quality assessments gives the possibility of selecting only the best specimens for testing, which could save time and expense both in terms of the site investigations and the design of groundworks, refer to Lacasse *et al.* (2003). Destructive assessment relies on the interpretation of laboratory test results, and thus can be used to identify disturbed samples such that they can be removed from datasets used for determination of design parameters. Both qualitative and quantitative methods exist for non-destructive and destructive assessment, although quantitative methods are favoured as these remove subjectivity and potential bias in the selected design parameters.

Destructive methods

For soft lightly to normally consolidated clays the criteria defined by Lunne *et al.* (1997) is often adopted, which has evolved from the work of Andresen & Kolstad (1979). This method classifies the volume change in terms of a relative void ratio ($\Delta e/e_0$) as shown in Table 2.3. The method has been validated for a large range of clays from around the world, Lunne *et al*. (1997), Lunne *et al.* (2006), Landon *et al.* (2007), Donohue *et al*. (2010). In Sweden Larsson *et al.* (2007) defined an alternative quality assessment method based on Lunne *et al.* (1997) for Swedish clays. This method is occasionally used in Sweden where sample quality is defined in terms of the magnitude of volumetric strains occurring during reconsolidation to *in situ* stress and liquid limit. This should not, however, be confused with the SQD method (Terzaghi *et al.* 1996) which only takes account of volumetric strains. Both Lunne *et al.* (1997) and Larsson *et al.* (2007) have allowance for the initial state of the sample, which gives them significant advantages over the SQD method. However it is unclear what assumption is made within the Larsson *et al.* (2007) quality assessment for the magnitude of the specific gravity (*Gs*) which must have been assigned to convert the Lunne *et al.* (1997) criteria from void ratio change to a volumetric strain/water content based criterion. It is also unclear at what OCR the alternative procedure should be adopted for over consolidated clays (which uses 75% of the defined maximum volume change on the volume change/water content quality criteria graph) as such further validation may be required for use in over consolidated clays. Qualitative assessments based on the shape of test curves are commonly used in Swedish practice, however, such methods are highly objective and in many cases unreliable. Especially for the Swedish West Coast clays these are not recommended as they can be highly misleading.

Table 2.3 Clay sample quality assessment criteria for volume change during reconsolidation from Lunne et al. (1997).

OCR	$\Delta e/e_0$			
	very good to excellent	good to fair	Poor	Very poor
1-2	<0.04	0.04-0.07	0.07-0.14	>0.14
2-4	<0.03	0.03-0.05	0.05-0.1	>0.10
Quality	1	2	3	4

Alternative methods of sample quality assessment of soft clays from test results include the use of the initial modulus at yield in CRS tests, Karlsrud & Hernandez-Martinez (2014) or methods involving comparison of laboratory and field derived small strain stiffness, as discussed by Bjerrum (1973), Hight *et al.* (1992), and Hight & Leroueil (2003). Another variation of this method is the metastability index by Shibuya *et al.* (2000), which also involves laboratory and field determination of G_0, as well comparison with the intrinsic behaviour of reconstituted samples.

Non-destructive methods

Qualitative visual/tactile assessments of samples following extrusion should be conducted on all test specimens using the visual indicators described by Hvorslev (1949) and Burland (2001) (distortion of lamina, presence of discontinuities, presence of voids, colour, brittleness, presence of precipitates, moistness, etc.). Such an assessment relates not only to identification of mechanical damage, but also chemical, biological and water content changes, and can be very useful in identification of samples which are not suitable for testing. Radiography can be used to assess mechanical damage which has the added advantage that assessment can be conducted within the sample tube as shown by Hvorslev (1949), Ladd & DeGroot (2003) and L'Heureux *et al.* (2015). Other non-destructive quantitative assessment methods relate to suction measurement, shear wave velocity measurement and combined suction and shear wave velocity methods, which will be discussed in slightly more depth below.

Suction assessment methods work on the principle that matrix suction measurements (u_r) will give an indication of the residual effective stresses present within the sample. A sample with high residual effective stresses will have experienced less swelling (volume change), and hence should maintain more of its original structure (less centreline strains). This is however, provided the sample has remained fully saturated. Partially saturated samples will also give high suction values, and thus can give erroneous assessment of high quality, which is why some authors only recommend suctions as a complementary assessment method, Hight & Leroueil (2003), while others suggest a limited span where the best quality samples can be found, Tanaka *et al.* (1996). Suction based assessments were first used by Ladd & Lambe (1963) where a normalised suction (u_r/σ'_{ps}) was used for classification of quality, where σ'_{ps} is the residual effective stress in a hypothetical perfect sample (reduction in deviatoric and isotropic effective stress only due to unloading). Other assessment methods using normalisation of suction with effective vertical stresses include Tanaka *et al.* (1996). It should be noted, however, that the classification criteria given by different authors tends to be specific to a given soil and test method, thus may require recalibration for other soils, as discussed by Tanaka & Tanaka (2006).

The magnitude of suctions and the duration with which these can be maintained is dependent on the chemistry between the soil and the porewater, as well as the pore size and shape and the storage conditions. There are a number of both direct and indirect methods of measurement of matrix suction. A thorough evaluation of these methods can be found in Poirer *et al.* (2005), however, an overview is given in Table 2.4

In sample quality assessment, the use of high air entry probes (Ridley & Burland, 1993, Tanaka *et al*., 1996) and filter paper methods (Hamblin, 1981, Chandler & Gutierrez, 1986, Bulut *et al*,. 2001, Ridley *et al*., 2003, Donohue, 2005) appear to dominate in literature.

Table 2.4 Summary of suction measurement methods, adapted from Pan et al. (2010).

Method type	Method	Suction range (kPa)	Equilibrium time
Direct	axis-transition	0-1500	Hours
	tensiometer		Hours
	suction probe		Minutes
Indirect	Time domain reflectometry	0-1500	Hours
	Electrical conductivity sensor	50-1500	6-50 hours
	Thermal conductivity senor	0-1500	Hours-days
	In-contact filter paper	all	7-14 days

A non-destructive shear wave velocity based method for soft clay has been put forward by Landon *et al.* (2007), which compares shear wave velocity of unconfined samples to field measurement. This method was calibrated using Lunne *et al.* (1997) method as shown in Figure 2.8. The Landon *et al.* (2007) approach appears to be successful in classifying sample quality on the Norwegian Onsøy clay, which is similar to the soft glacio-marine clays found on the Swedish West coast.

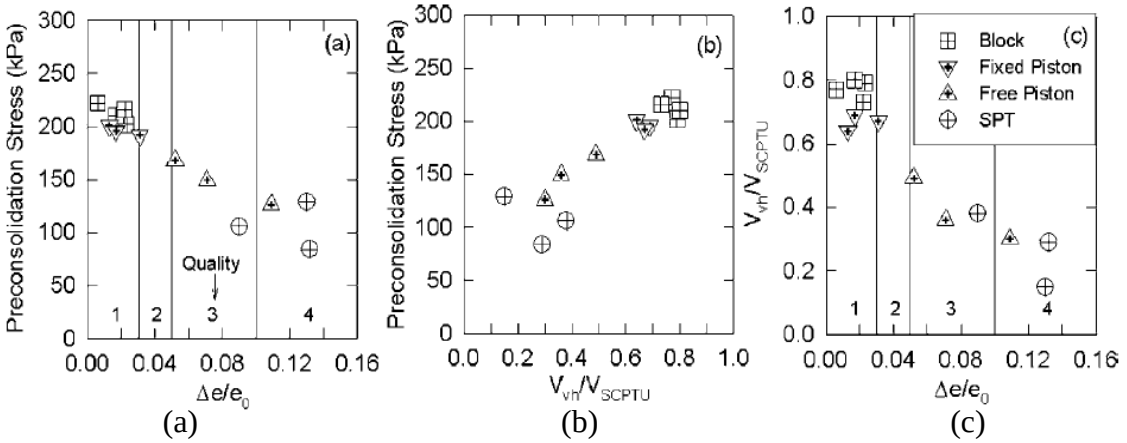

Figure 2.8 Sample quality comparisons (a) preconsolidation stress verses $\Delta e/e_0$; (b) preconsolidation stress verses V_{vh}/V_{SCPTU} and (c) V_{vh}/V_{SCPTU} (Landon et al. 2007).

Other seismic based methods include Hight (1998), which also compares field and laboratory (unconfined) shear wave velocities, but also includes allowance for the prevailing effective stresses in the sample at the time of shear wave velocity measurement (for the laboratory sample this is based on suction measurements at the time of test). Donohue & Long (2010) also defined a combined seismic/suction method for assessment of both on and offshore soft clay samples.

3 METHODOLOGY

3.1 Introduction to experimental work

This Chapter describes how field and laboratory testing was conducted for the study of small strain stiffness and it's degradation within this research project. Small strain stiffness G_0 is determined from the shear wave velocity, V_S, and soil density, ρ, as outlined in Eq. 2-1. The need for field measurements of V_S was two-fold; to understand the initial small strain stiffness *in situ* ($G_{0\ field}$), but also to compare this value with measurements taken in the laboratory when samples were consolidated to *in situ* stresses ($G_{0\ lab}$). A comparison of the two could then be used to provide an indication of how well laboratory values of G_0 represented *in situ* conditions and help verify the ability of the laboratory samples to truly describe behaviour in the field. Previous agreement between laboratory and field measurements in Swedish clays had been poor, as noted in Persson (2004), Andréasson (1979) and Svensson (2001) and indicated by the ratio $G_{0\ lab}$ / $G_{0\ field}$ shown in Table 2.1.

Considerable effort was spent in understanding the degree of disturbance in laboratory samples, and how this affects the ability of the laboratory results to describe field behaviour. Different methods of sample quality assessment methods were tested. In addition the effect of different parts of the sample disturbance chain on small strain stiffness was investigated from extraction to test execution in terms of V_S as indicated in Figure 3.1.

Figure 3.1 Sample time line from field to start of triaxial test.

3.2 General methodology for the determination of G_0

Experimental work carried out within this project consists of field and laboratory measurement of small strain stiffness, G_0, at *in situ* stresses while studies of the stiffness degradation are based only on laboratory measurement. In addition, the magnitude of G_0 in unconfined samples and the changes occurring through the sample timeline has been studied. For these samples there is no applied stress, but these samples have varying residual effective stress, dependent on the degree of excess pore pressure dissipation that has occurred. The sensitivity of clays to the changes in the initial state, the stress level, the stress path direction and the stress history, in addition to the impact of mode of shear and the strain magnitude on $G_{0\ lab}$ and G/G_0, has been investigated within a Bishop and Wesley type triaxial cell.

Multiple methods of parameter determination are used to minimise system bias. The measurement of the shear wave velocity was, therefore, determined using three different systems both in the field and laboratory. In the field one direct method with a seismic probe, one diffuse method using surface waves and one method which involved bender

element measurements on clay immediately after extraction (retaining maximum possible residual effective stresses in the sample) were adopted. Work by Donohue (2005) on Onsøy clay found that block samples tested in this way gave values of *Vs* very similar to those obtained using SCPT and MASW tests. For the measurement of stiffness degradation, two systems of local strain measurement were compared resulting in a preferred method for the study of stiffness degradation, G/G_0. Alternative methods of determining $G_{0\ lab}$, such as resonant column (RC) testing were not utilised given the findings of Long *et al.* (2003) and Andréasson (1979). However, within this study it was possible to corroborate the values of $G_{0\ lab}$ determined from BE tests using $G_{0\ field}$ measurements at all 12 sites studied.

The methods used to determine $G_{0\ field}$ within this project, and the directional component of shear wave velocity measured, are given below:

- Seismic probe: Marchetti seismic dilatometer (SDMT), V_{Svh}
- Multiple Analysis Surface Wave Method (MASW), $Vs_{average}$
- Unconfined BE testing $V_{Shh,}$ V_{Svh} conducted directly after extraction

For laboratory testing of small strain stiffness three different bender element systems (BES) were compared in a benchmarking exercise. In addition, the results from local strain measurements when the "elastic region" was captured could also be used, as summarised below:

- Commercial GDS BES system: confined and unconfined V_{Svh} and V_{Shh} in vertical and horizontal samples respectively.
- CTH developed BES system: unconfined V_{Svh} and V_{Shh} in vertical and horizontal samples.
- SGI BES system: Unconfined BE tests V_{Svh} (two configurations were used for benchmarking only)
- Direct measurement of G_0 using local strain measurements, G_{0vh} (only possible in tests where the "elastic region" was captured by the measurement system.

The process for determination of G_0 from V_S is similar for both field and laboratory tests, with the exception that the BE tests have additional components prior to generation of a physical wave, as indicated in Figure 3.2. Noise was present in received signals due to background vibrations. On site the main source of vibration was the diesel generator used to power the equipment and vehicular traffic, while in the laboratory the climate control system was a major source of noise. Following the recommendations of Lee & Santamaria (2006) signals were stacked to reduce noise and improve signal to noise ratio, as opposed to use of other methods such as additional filters or additional electronic amplification.

Once the received signal was acquired, post processing was necessary for interpretation of V_s, particularly where reflected/refracted waves were present. The steps in the general interpretation process are illustrated in Figure 3.3. The abbreviation FIR filter relates to

use of a finite impulse response filter, which is often used for phase sensitive filtering of signals. Both interpretation within the frequency domain and time domain has been carried out. Interpretation within the time domain relates to the picking of the arrival time of the shear wave. As discussed in Section 2.4.2, the interpretation of waves in the time and frequency domain is dependent on the transmission of the propagating shear wave remaining planar and elastic and that multiple modes of vibration are avoided.

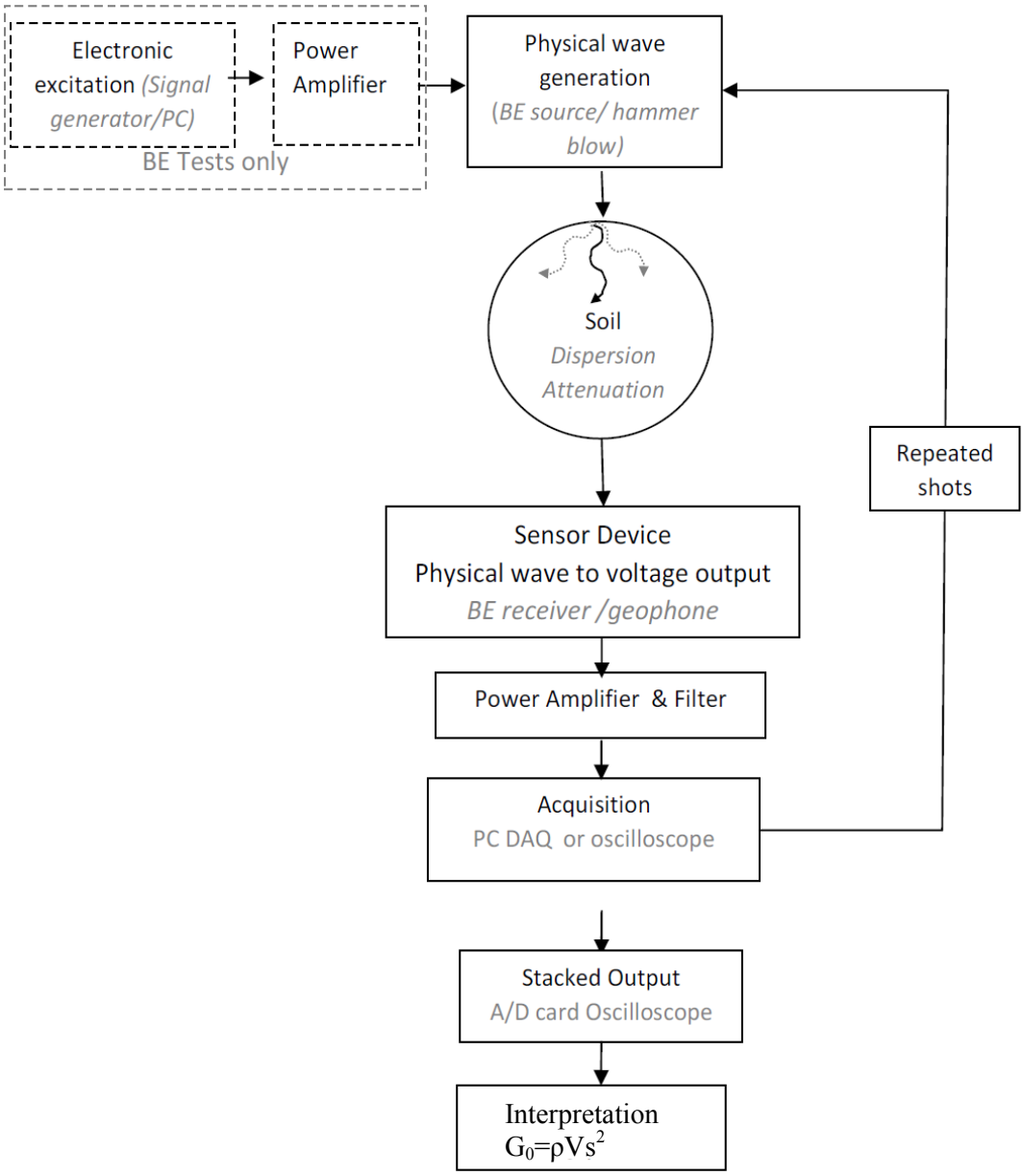

Figure 3.2 Generalised work flow for determination of G_0.

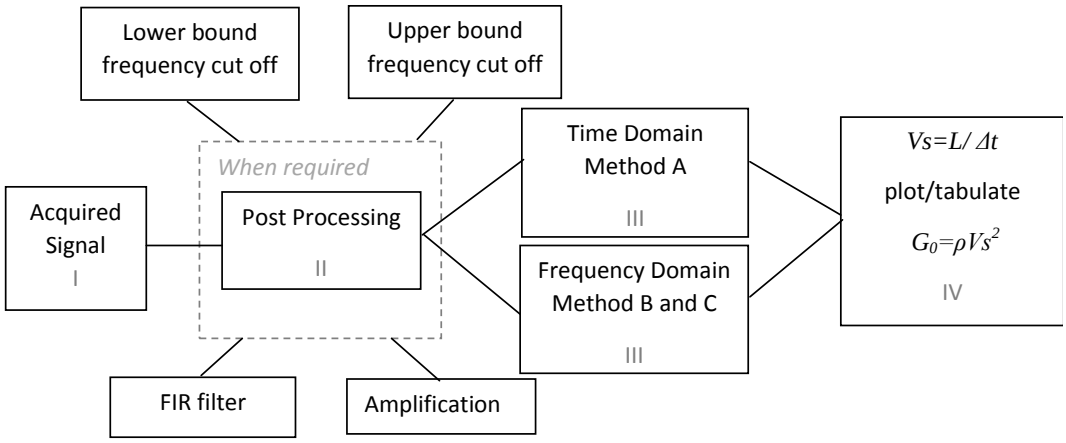

Figure 3.3 *Stages of interpretation of small stiffness.*

Method A relates to determination of shear wave travel time by picking specific points or 'picks' on the initial received wave and determining the time between the same points on the either the source signal or a 2nd received wave. The shear wave velocity is then determined using Eq. 2-1.

Method B relates to determination of shear wave travel time using cross correlation techniques discussed in Section 2.3.3. For details on cross correlation techniques within the frequency domain and mathematical formulations used refer to Oppenheim *et al.* (1989).

Method C relates the discrete determination of V_s using a phase delay analysis that utilizes dispersion of the signal instead of ignoring it. The phase angle $\Phi(f)$ is determined from the difference in phase between the input and output signal, referred to by Viggiani & Atkinson (1995) as the cross power spectrum, the basis of which was discussed in Section 2.2.2 and 2.3.3. In this case V_S refers to the group velocity.

In principle, the shear strains experienced by the soil can be assessed from the ratio of the particle velocity and the shear wave velocity. However, no measurement equipment capable of determining particle velocity independently was available for any of the seismic tests carried out. This, as well as that the complexity of the soil profiles and excitation source, has ruled out any elasto dynamic analysis of the wave propagation phenomena to derive the particle velocity theoretically. Hence, no calculation of the strain produced by different wave amplitudes has been determined within this work.

3.3 Field testing

3.3.1 Sampling methods and sample management procedures

Significant site investigation information was available at the 12 study sites which were used for an initial desk top study. This formed part of the ground profiling procedure used as shown in Figure 3.4 and was used for determination of sampling levels and reconsolidation stresses for laboratory tests. A number of different sampling methods

and sample preparation techniques were utilised, as outlined in Table 3.1 and illustrated in Figure 3.5.

In line with Swedish practice, almost all clay samples extracted for this research used the STII piston sampler with extraction procedures in accordance with Swedish standards (SGF, 2009), except where effects of alternative methods of sampling and transport were being investigated in which case details are given.

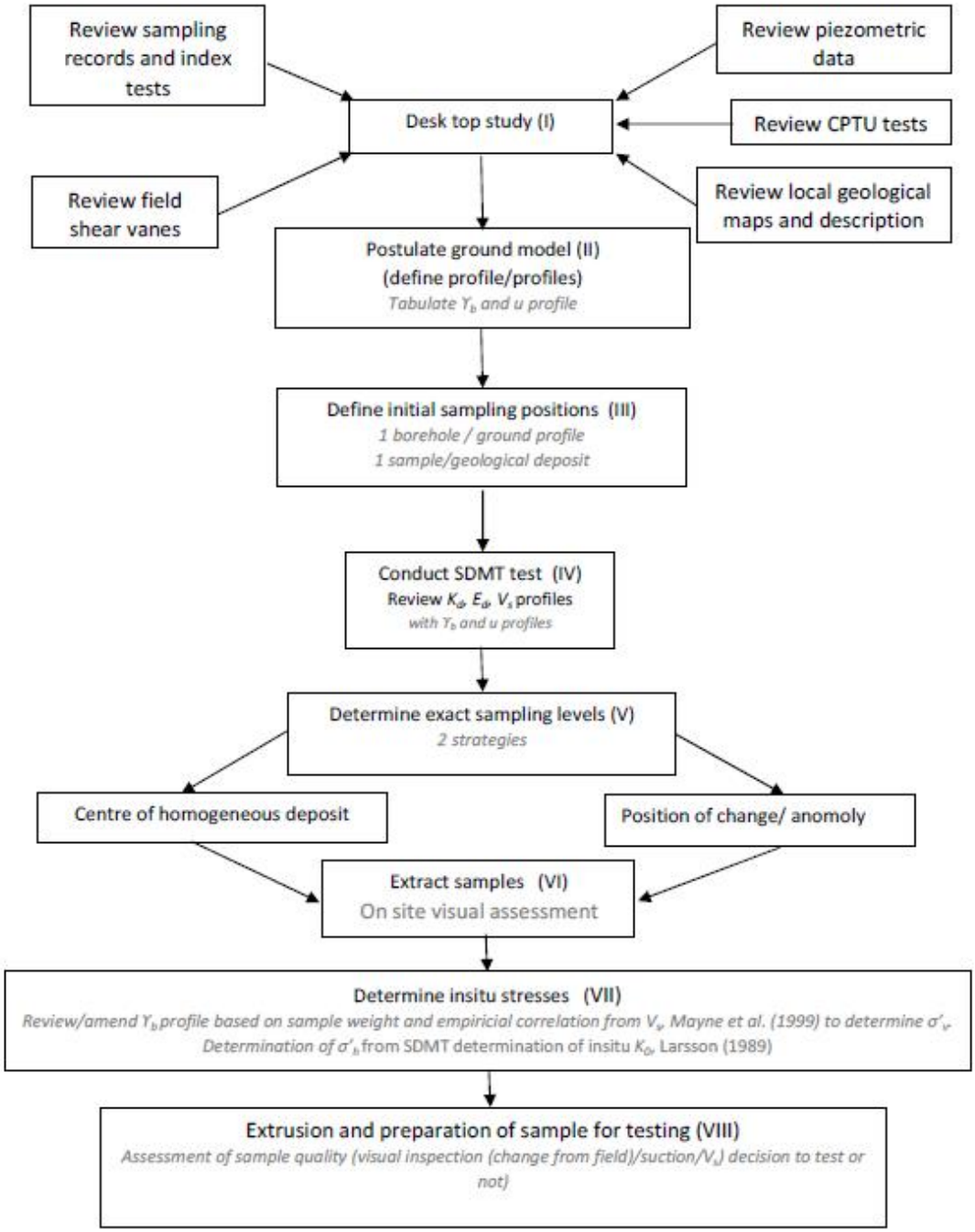

Figure 3.4 Workflow for determination of sampling levels and sample quality controls.

Table 3.1 Sampling and preparation methods for test specimens, refer to Figure 3.5 Figure 3.5for visualisation of equipment used for trimming.

Sample Origin/ stages	Sampling Description	Sample preparation methods used
STII	Standard 50 mm Ø STII Swedish fixed piston samples, equipment and sampling procedure in accordance with SGF Report 1:2009.	Jacked extrusion 50 mm Ø: trim ends with piano wire 38 mm Ø: trim sides with hand lathe or sample peeler and ends with piano wire
$STII_{slow}$	Standard 50 mm Ø STII Swedish fixed piston sampler, sampling according to SGF Report 1:2009 but with slow extraction: 0-2 m 5 mm/s 2-6 m 10 mm/s 6-8 m 20 mm/s 8-10 m 30 mm/s >10 m 40 mm/s	Jacked extrusion 50 mm samples: Trim ends with piano wire
$STII_{60}$	A 60 mm Ø widened version of the STII sampler commissioned by BohusGeo AB, refer to Lanzky & Palmkvist (2013). SGF Report 1:2009 procedure followed.	Jacked extrusion 50 mm Ø: trim sides with hand lathe or sample peeler and ends with piano wire
TW_{100}	100 mm Ø thin wall open sampler pushed slowly into clay at base of excavation	Sample released with piano wire then tube cut, sides trimmed to 50 mm Ø with hand lathe and sample peeler and ends trimmed with piano wire
Block	Hand cut block sample, trimmed and sealed on site prior to transport.	Removal of seal, cut to 70 mm square rectangular block with piano wire, trimmed to 50 mm Ø with hand lathe or sample peeler and ends trimmed with piano wire

(a) (b) (c)

Figure 3.5 Sample preparation (a) removal of confinement and initial cut of 70x70 mm block (b) trim Ø with piano wire and hand lathe (c) trim Ø with sample peeler.

Some test data presented in Appendix A8 is taken from the desk study, and includes tests on Sherbrook block samples and NGI 54 mm piston samples which are not presented in Table 3.1 (Site 12) as the specific details of preparation and storage conditions are unknown. However, the geometry of all tube samplers for which data is presented, including the NGI 54 mm piston sampler, can be found in Table 3.2 using the tube geometry factors defined by Hvorslev (1949) and discussed in Section 2.4.2. Also shown are the details of the Laval block sampler used by Larsson (1981) to show the similarities to the thin wall sampler used within this study. The magnitude of the disturbed zone at the top of the sample, R_p, for a Laval type sampler is based on drilling under bentonite slurry support in accordance with Britto & Kusakabe (1982), while R_p for piston samples is based on the samplers outer diameter when pushed down to the sampling depth where $R_p=2Ø_{outer}$ where $Ø_{outer}$ refers to the outer diameter of the piston sampler during insertion to the sampling level, and not the outer diameter of the piston during sampling.

All samples once removed from the ground where packed in purpose-built boxes and transported to the laboratory. During transportation, piston sample boxes were tied down in the boot of a works vehicle (typically pickup truck), except where specific transport vibration studies were conducted where a car was used. On arrival at the laboratory samples were stored in a climate controlled room at ≈100% humidity and ≈7°C. Different transport procedures outlined in Table 3.3 were used for block samples.

Table 3.2 Comparison of tube sample geometry used for sample extraction (refer to Section 2.4.2 and Appendix A2 for definition of sampler geometries)

Sampler	Ø D_1 (mm)	R_p (mm)	L/D_3	AR (%)	ICR (%)	D_2/t B/t	Tapper angle, α (°)
STII fixed piston	50	170	13.8	16.6	0.4	30	5°
$STII_{60}$ fixed piston	60.3	190	11.5	13.8	0.4	35.6	5°
NGI fixed piston	54	128	14.8	11.4	0.6	39.3	5°
Laval sampler	208	150	2.9	9.8	0	43.6	5°
Thin wall open tube	97	-	2.0	6.3	0	66.7	5°

Table 3.3 Details of block sample sealing and transport method (PU = pickup truck)

Block	Sealing method on site	Transport
Site 3: B1	Clingfilm and fixed steel and wooden plates	Placed in plastic container filled with Styrofoam and placed in PU on mattress
Site 8: B1[1]	50/50 Beeswax/paraffin mix and muslin layers 3 layers	Plastic container filled with straw and fixed to PU
Site 8: B2	50/50 Beeswax/paraffin mix and muslin layers 3 layers	Plastic container filled with straw and fixed to PU
Site 8: B3	50/50 Beeswax/paraffin mix and muslin layers 3 layers	Plastic container filled with straw and fixed to PU
Site 8: B4	3 layers of cling film	Placed on back seat of pickup truck
Site 8: B5	3 layers of cling film but confined on arrival at lab as[1]	Plastic container filled with bubble wrap and fixed to PU
Site 8: B6	3 layers of cling film confined on arrival at lab as[1]	Plastic container filled with straw wrap and placed on back seat of PU

3.3.2 **Diffuse measurement of G_0: Seismic surface wave testing**

Surface wave determination of V_S at two sites (Site 6 and 7) in collaboration with University College Dublin (UCD) and APEX Geoservices using MASW techniques were conducted specifically for this project. At a third site (approximately 8 km from Site 12) UCD and APEX Geoservices in collaboration with NGI and NTNU conducted MASW measurements at a geotechnical research site used to study the clays at Site 12. Two different profiles were conducted at each site. The steps in the MASW test procedure and analysis described by Miller *et al.* (1999) and Xia *et al.* (2003) were used refer to Section 2.2.2. The acquisition method was amended slightly for from Miller *et al.* (1999) as it was found by Donohue *et al.* (2012) that sufficient accuracy was obtained with larger geophone spacing and higher frequency devices. A summary of the acquisition parameters used for tests conducted for this work are presented in Table 3.4 and the work-flow diagram for test execution is given in Figure 3.6.

Table 3.4 Acquisition information for MASW tests (specific for this research), where N= no. of source positions, X1 = offset, dx =receiver spacing, XT = Total length of receiver spread.

Profile	N/X_1 (m)	d_x (m)	X_T (m)	Sensor (Hz)	Source (hammer)	Recording Time (ms)	Sampling Interval (ms)
S13, S14, S15, S16	5/1-20 and middle	2	46	10	5 kg	1000-2000	0.5

The work-flow for interpretation of the MASW tests is illustrated in Figure 3.7.with the output at key stages illustrated in Figure 3.8. The interpretation of data was mainly conducted at UCD in 2010 using the KGS Surfseis software, Version 2, however, the interpretation of one shot gather (central source at S14) was repeated by CTH/APEX Geoservices in 2015 using a later version of the Surfseis software (Version 3) to examine the sensitivity of the inversion process on V_S. The number of layers in the earth model used for inversion varied: UCD used an 8 layer model and CTH/APEX Geoservices used a 10 layer model. A visual illustration of these steps using the Surfseis software is given in Appendix A3.

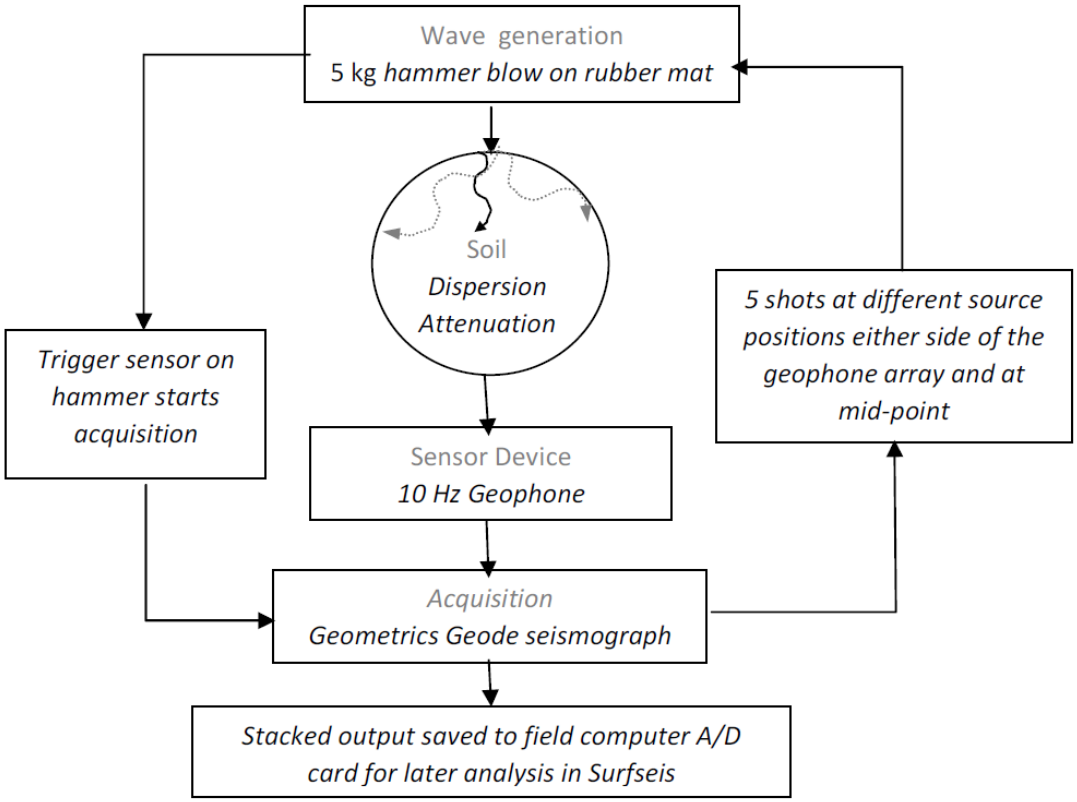

Figure 3.6 MASW field test work flow for acquisition of data.

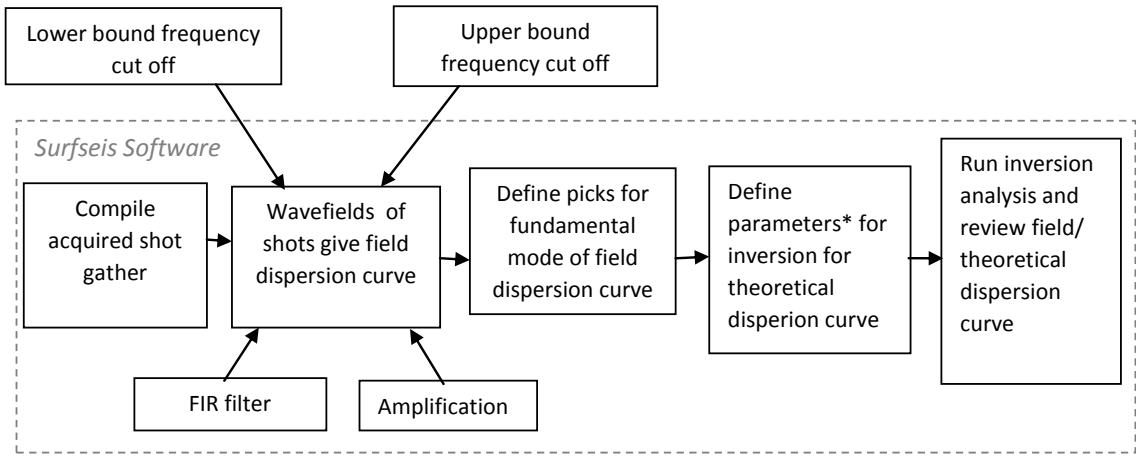

Figure 3.7 Post processing and analysis of MASW tests (Method C) for V_S using Surfseis software.

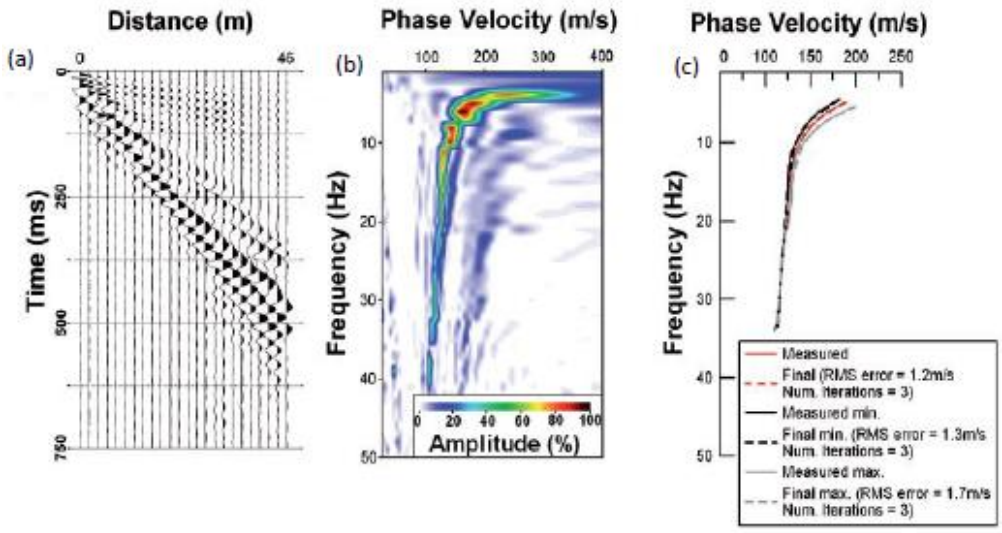

Figure 3.8 (a) Shot gather, (b) field dispersion image, (c) field and theoretical dispersion curves and accuracy, Root Mean Square (RMS) at Vestfossen using Surfseis software, Donohue et al. (2012).

The details of the inversion process used in the Surfseis analyses are as follows:

1. Initial estimate of theoretical dispersion curve by assuming the depth of penetration, z of a particular wave is a fraction of its wavelength, λ;

$$Z = \frac{\lambda}{n} \qquad \text{Eq. 3-1}$$

where n is a constant. The value of n was chosen to be 2 for the initial estimate.

2. Surface wave phase velocity V_R is converted to V_S using Figure 2.3

$$V_S = \frac{V_R}{C} \qquad \text{Eq. 3-2}$$

where C is a function of Poisson's ratio, v, which based on Richart *et al.* (1970) gives C=0.911 for v=0.2 and C=0.955 for v=0.5, thus incorrect approximation of v has minimal impact on V_S.

3. Initial earth model: an initial estimate of the profile must be made by defining the initial earth model in terms of:
    a. Number of soil layers (8 or 10)
    b. Thickness of each layer, increased exponentially automatically by Surfseis
    c. V_S of each layer evaluated by Surfseis based on picks of fundamental curve
    d. V_P of each layer evaluated by Surfseis based on V_s
    e. Density of each layer evaluated by Surfseis based on picks of fundamental curve.
4. Inversion with an iterative approach using a least-square technique, Xia *et al.* (1999). The stop criteria for the iteration is based on the specified allowable root mean square error (RMS) which was set to 2 m/s in the analyses conducted at UCD whereas the analyses done by CTH/APEX Geoservices used RMS values

of between 5 and 1 m/s to understand the impact this has on the inversion process.

5. A review of theoretical and field dispersion curves is made at the end of the Surfseis iteration as a final check. Only 1 to 3 iterations were required to give RMS values < 2 m/s in agreement with Donohue *et al.* (2012).

6. Transformation from 1D V_S to 2D V_S profile was not conducted within this work however if required this can be done within Surfseis, refer to Appendix A3.

7. Input V_S and soil density at mid-point of layer into Eq. 2-1.

The software assigns constant values of V_S, V_P and density in the layers therefore the accuracy of the V_S profile is affected by the thickness and number assigned. Sensitivity analyses by Xia *et al.* (1999) found that synthetic dispersion curves were dominated by V_S, thus only this is changed in the iteration process. Thinner layers are assigned closer to the ground surface as the largest change in V_S often occurs in this area. This means that the resolving power of the MASW data decreases with depth, Donohue *et al.* (2012). In the results presented in this work the value of V_S determined for each layer is related to its midpoint, in addition the final layer is discounted, as this extends to infinity in the inversion process.

3.3.3 **Direct measurement with down hole seismic probe (SDMT)**

Down-hole measurements of V_S conducted within this work were generally conducted using the Marchetti seismic dilatometer (SDMT) system adjacent to borehole sampling positions. At one site seismic cone penetrometer tests (SCPT) conducted by NGI and NTNU are used which were taken at a geotechnical research site (8 km away) set up to study the soils present at this site (Site 12). At one site (Site 4) two SDMT tests were carried out specifically to verify the repeatability of the tests. However, tests conducted at different sites, but in the same geological deposit, could also be used for this purpose provided the clays had the same stress history.

SDMT tests were conducted using a Geotech 504 boring rig in accordance with the recommendations of the International Society of Soil Mechanics and Geotechnical Engineering, ISSMGE Report TC16 (2001) (Marchetti *et al.* (2001) and Swedish Geotechnical Society recommendations described in SGF Report 1: 1996, Field handbook. For dilatometer tests care was taken to keep the expansion of the membrane at a constant rate, as work by Smith (1989) showed that rate of expansion can affect the P_0 and P_1 pressure measurements, where P_0 and P_1 relate to the pressures to inflate the membrane 0.05 mm and 1.1 mm, respectively. Calibration of the DMT blade was conducted both in the laboratory at 7°C, and in the field immediately before insertion, and following extraction. Very little variation of the calibration parameters was noted provided the temperature of the blade remained at around 7°C. The seismic probe used to determine *Vs* consists of a cylindrical probe placed above the DMT blade. The DMT blade and working principle is presented in Figure 3.9 (a) and (b) and the seismic probe in (c). This is similar to the arrangement described by Marchetti *et al.* (2008). Details of equipment and interpretation of the SCPT tests conducted near to Site 12 by NGI/NTNU can be found in Takke Eide (2015).

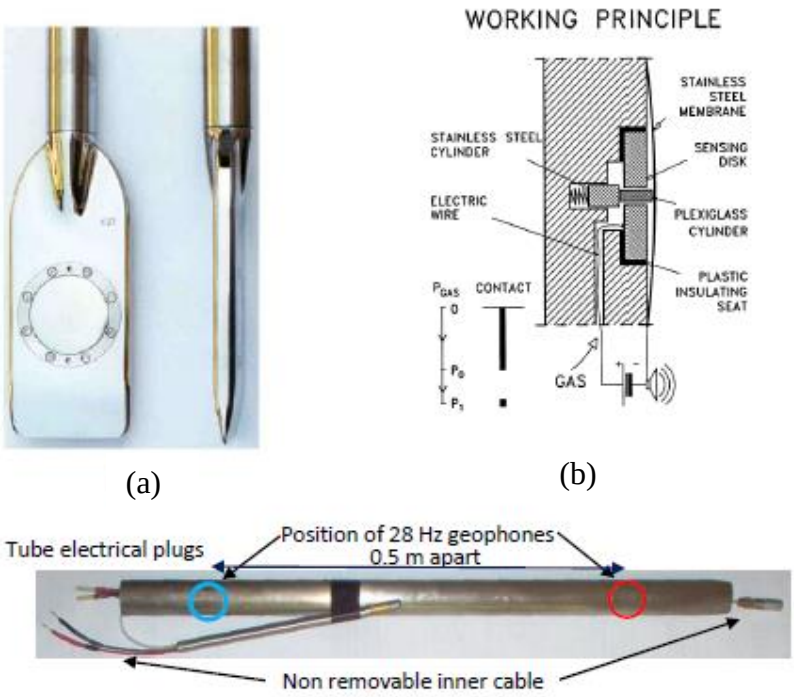

Figure 3.9 SDMT measurement device (a) DMT blade, (b) DMT working principle, (c) Seismic probe with position of geophones which attaches to the DMT blade, (a) and (b) are taken from Marchetti et al. (2001) while (c) is from Marchetti (2012).

The SDMT test work flow is described in Figure 3.10, with details of the parameters that must be defined given in Table 3.5, while an overview of the interpretation process is given in Figure 3.11. An illustrative step by step description is given in Appendix A4 using the SDMT Elab interpretation software. Control of signal acquisition and post-processing was conducted in the field using the SDMT Elab software on a standard PC computer.

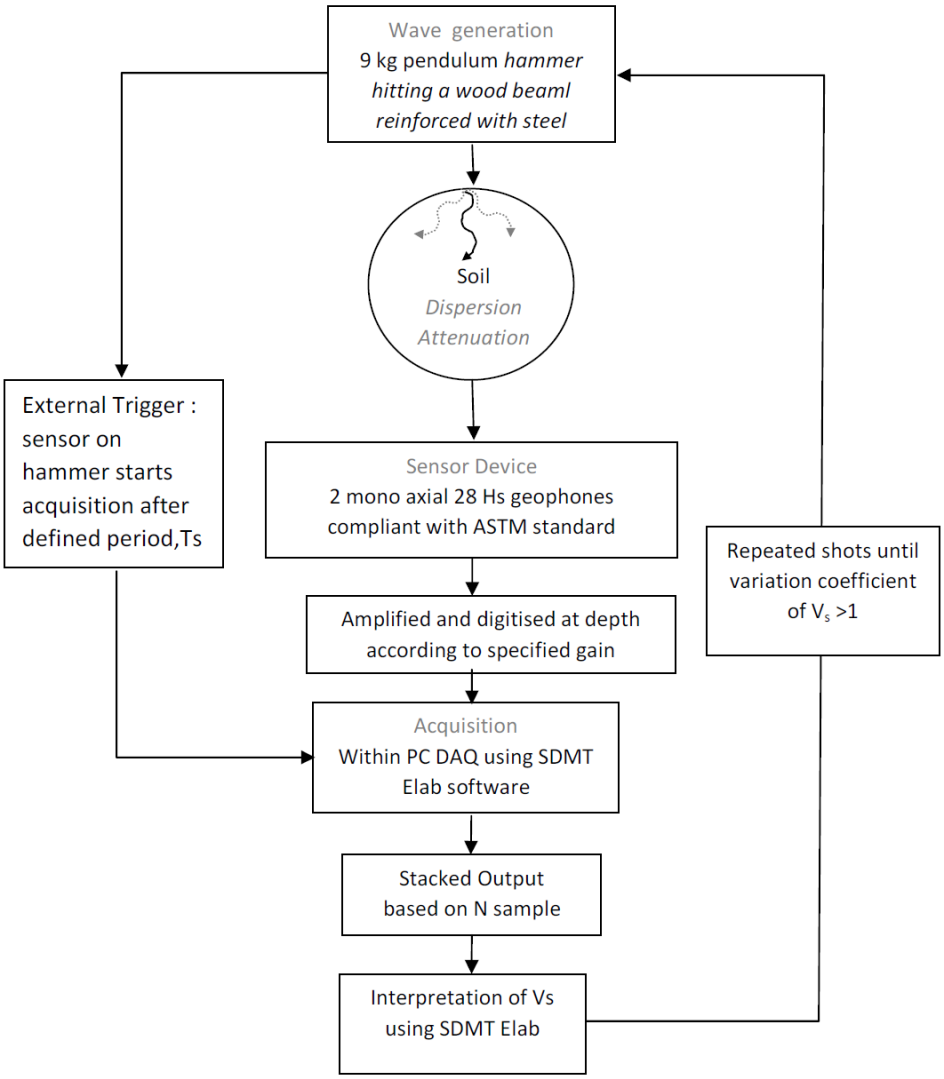

Figure 3.10 SDMT field test work flow for acquisition of data.

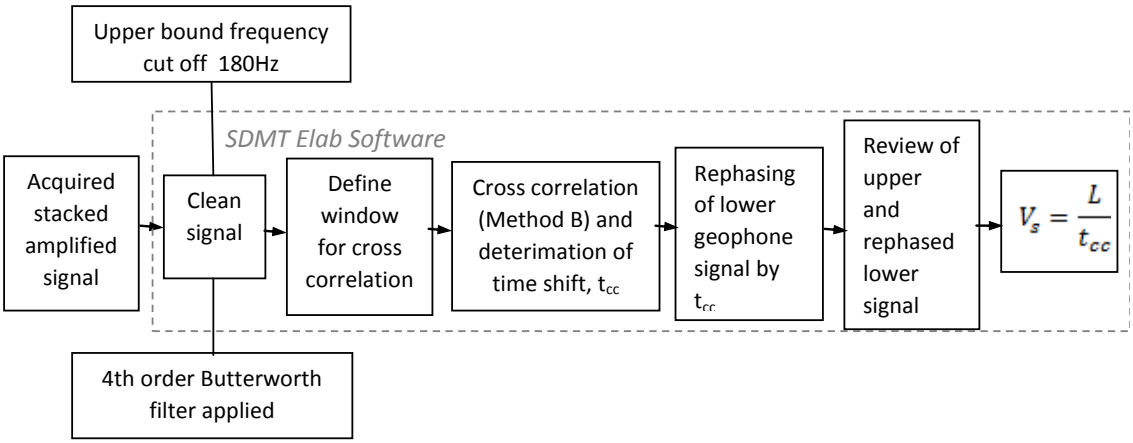

Figure 3.11 Post processing and analysis of SDMT tests (Method B) for V_S using SDMT Elab software (Note L= travel path of wave with respect to probe verticality and distance of source from probe between the geophones).

Table 3.5 Description of acquisition parameters to be defined in SDMT tests.

Parameters	Description
Z (DMT)	Depth of the tip of the blade, software automatically removes 0.5m when plotting the Vs_{SDMT} profiles (mid-point of sensors is 0.5 m above the tip of the blade)
Hammer Dist	Horizontal distance of SDMT blade from the energiser (must be noted to determine the wave travel path as illustrated in Figure 2.5)
Gain	Defines the amplification applied to the two acquired signals at depth. The gain required to interpret signals generally needs to be increased with increasing depth
T sample	Is the time of each sample, longer time results in lower quality data (lower sample rate). The combination of T sample and N_s should be sufficiently large that the full wave produced by the energiser is captured but small enough so that arrival of the wave at the first and second geophone can clearly be distinguished. T sample time was generally set between 50 and 150 μs (sampling rate between 20 000- 6 700 S/sec)
N sample	Number of samples recorded for each test. The number of samples can be chosen with data acquisition slowing with an increasing number of samples.
Trigger method	One of three methods can be chosen: the external trigger was found most reliable and used for the majority of testing • Auto trigger: automatic detection of wave based on sensitivity setting in the acquisition parameters • External trigger: trigger sensor attached to hammer frame, time delay parameter specified in the acquisition parameters to optimise sampling time so sampling doesn't start immediately • Intermediate trigger – sampling starts when the acquire button is pressed on the PC screen (before the hammer is energised)
Sensitivity	Used if auto trigger is selected, sets the sensitivity of the automatic trigger in the sensor, too low and the wave arrival will not activate the trigger, too high and the acquisition may start due to background noise
Time shift	Used when use of the external trigger is selected to delay the start of signal acquisition following triggering of the external trigger sensor. The time shift was increased with increasing depth below 5m in order to minimise the sample time and optimise signal acquisition quality

Good energy transfer between the hammer and the ground was achieved by placing the energizer slightly below ground level, and using the fork arms of the rig to provide down force. This procedure worked well even on frozen ground, provided fine (non-frozen) material was placed directly under the shear beam. This arrangement also meant the shear waves measured by the geophones were fairly vertical as the energiser (shear beam) was placed <400 mm horizontally from the probe. The impact of different drop heights was investigated, and found to have only a very small effect on the value of Vs_{SDMT}. However, it was easier to interpret tests at depth when using a larger drop height, as this increased the amplitude of the acquired signal thus reducing the amount of signal amplification required, thus the drop height was increased with depth.

Choice of trigger method and sensitivity setting for data acquisition

An external trigger was found to be the optimum trigger method. The auto trigger worked relatively well near surface, but failed to register the wave arrival at depth. When the sensitivity was increased, the device was triggered by the background noise or the compression waves travelling down the SDMT rods. Vibration in the rods could be removed by using a separate dead load to provide down force on the beam (pickup truck), however, this meant that the beam had to be placed further from the SDMT probe, which would reduce the verticality of the shear waves measured by the geophones. Thus, the external trigger with increasing time shift with depth was found to be the preferred method.

Post processing choices

Different filters available in the Elab software were tested but it was found that the choice of the filter had no impact on the V_S interpretation, as the raw signals obtained were already fairly clear. The clay had already filtered the transmitted waves, except near surface where the reflected compression waves were sometimes significant. In this situation, the upper cut-off frequency was reduced, to help remove some of the faster moving compression waves from the data.

The selection of the window to delimit the signal prior to cross correlation could be chosen manually, or using an automatic selection algorithm. This automatic selection algorithm prioritises the part of the signal with high amplitude and low frequency, which favours the part of the signal that represents shear wave arrival. Automatic selection worked well in the absence of significant background vibration. When significant background vibration was present, caused by either reflected compression waves following energisation, nearby building works (jack hammers) or heavy traffic, the automatic selection algorithm did not work well, thus the window was defined manually. A cross-correlation algorithm within the Elab software was used to determine the time shift between the upper and lower geophone signals, and was found to be very effective in providing a good match of the rephased lower signal, as indicated in Figure 3.12. G_0 was assessed at the midpoint between the geophones (0.5 m above the tip of the DMT blade) substituting $V_{S\ SMDT}$ and assessed density (measured laboratory values or empirical values using Mayne *et al.*, 1999) into Eq. 2-1.

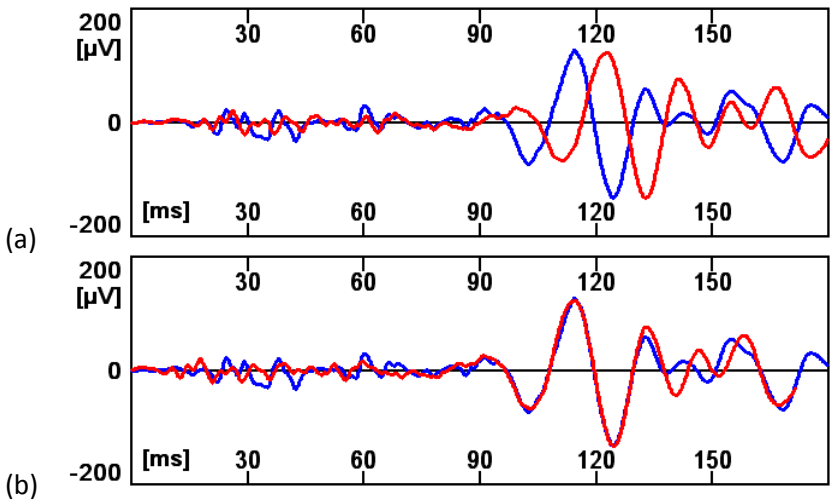

Figure 3.12 (a) Typical SDMT filtered geophone signals (b) Review of upper geophone signal and re-phased lower geophone signal following cross correlation.

3.3.4 **Other test methods used for characterization of soils**

All field testing was conducted using standard boring rigs. These tests include piezometric Cone Penetration Tests (CPTU) and field shear vane, a brief description follows.

Cone Penetration Tests

Cone penetration testing was conducted at all of the study sites using CPTU type cones. Details of the CPTU tests conducted are presented in Table 3.6. In Chapter 4 and 5 graphs are presented for CPTU test data in terms of tip resistance, q_t and pore pressure parameter B_q. These are necessary to enable use of the CPTU based classification of the sites suggested by Robertson (1990) and empirical assessment of V_S and G_0 by Long and Donohue (2010), presented in Appendix A1. The pore pressure parameter B_q is not commonly used in Sweden, and thus is defined in Eq. 3-3.

$$B_q = \frac{u_2 - u_0}{(q_t - \sigma_{v0})} \qquad \text{Eq. 3-3}$$

where σ_{v0} is the *in situ* total stress, q_t is the cone tip resistance (resistance from ground only) and u_2 is the magnitude of pore pressures measured just above the tip, and u_0 is the assessed pore pressures *in situ* at the time of test, refer to Larsson (2007) for details.

Table 3.6 Comparison of CPT test equipment and analysis used for data presented.

CPTU test details	Swedish CPTU tests	Norwegian CPTU tests
Equipment	SGF Report 1:1993 SS EN ISO22476-1:2012	Statens Vegvesen felthandbok 016:2006
CPTU procedure	SGF Report 1:1993 SS EN ISO22476-1:2012	Statens Vegvesen felthandbok 016:2006
Application class (Swedish classification)	1 (CPTA)	1
Cone angle	60°	60°
Cone diameter	35.7 mm	35.7 mm
Cone area	1000 mm^2	1000 mm^2
Filter stone placement	U_2 position (above cone)	U_2 position (above cone)
Filter fluid	Glycerine	Deaired water
Pre-boring	Yes-to below fill/dry crust	Yes-to below fill/dry crust
Penetration rate	2 cm/s	2 cm/s
Verticality measurement	Yes	Not indicated
Interpretation	Larsson (2007)	CPTUEXTRA-V3

Field Shear Vane Testing

The results of the field shear vane testing presented in this report have been carried out commercially or within other research projects (not conducted specifically for this research). The results are used in this report to define the sensitivity, S_{tv} to avoid issues relating to storage time, refer to Söderblom (1969), Kallstenius (1972), Henriksson & Carlsten (1994) and Åhnberg & Larsson (2012) where ever possible. Field vanes were also used to provide an estimation of the undrained shear stress *in situ*.

According to the Swedish practice τ_v is corrected for use in design, in order to give τ_u, the mobilised strength after failure and large strains as indicated Eq. 3-4. The value of μ is an empirical relationship based on liquid limit, W_L, refer to Eq. 3-5. In high plasticity inorganic clays this relationship, typically reduces τ_v by 15 to 25% while in low plasticity clays very little change occurs.

$$\tau_u = \mu \tau_v \qquad \text{Eq. 3-4}$$

where $\mu = \left(\frac{0.43}{W_L}\right) \geq 0.5$ Eq. 3-5 and τ_v is the uncorrected field shear vane strength

This correlation presented by Larsson *et al.* (2007) is used to correct both fall cone and shear vane test results however in some cases it was found that the correlation led to unlikely values of τ_u thus was not applied (primarily in the glacial Swedish west coast clays) and is discussed further within Section 4.7.

Dilatometer Testing

The seismic dilatometer used for field testing of V_S was also used for the ground characterisation and the estimation of basic soil properties. The tests were conducted in accordance with the recommendations of the International Society of Soil Mechanics and Geotechnical Engineering, ISSMGE Report TC16 by Marchetti *et al.* (2001) and the Swedish Geotechnical Society recommendations described in SGF Report 1: 1996 Field handbook. For details refer to Marchetti *et al.* (2001). For dilatometer tests care was taken to keep the expansion of the membrane to a constant rate, as work by Smith (1989) showed that rate of expansion can affect the P_0 and P_1 pressure measurements in Swedish soft clays, refer to Eq. 3-6 for definition. Calibration of the DMT blade was carried out before and after testing (at 7°) to ensure pressure readings from field tests were reliable. Marchetti (1980) defines three 'intermediate' parameters from P_0 and P_1 that are used in correlations with other soil properties, defined as follows:

$$I_D = \frac{(P_1 - P_0)}{(P_0 - u_0)} \qquad \text{Eq. 3-6}$$

where I_D is material index, u_0 is the equilibrium pore pressure acting on the DMT blade, and P_0 and P_1 relate to the pressure required to inflate the membrane 0.05 mm and 1.1 mm, respectively.

$$K_D = \frac{(P_0 - u_0)}{\sigma'_{v0}} \qquad \text{Eq. 3-7}$$

where K_D is the horizontal stress index and σ'_{vo} is the *in situ* effective vertical stress.

$$E_D = 34.7(P_1 - P_0) \qquad \text{Eq. 3-8}$$

where E_D is called the dilatometer modulus.

In clays the 'intermediate' parameters are then used as follows:

- I_D is used for classification of soil type and density (together with E_D)
- K_D is used for determination of K_0, *OCR*, c_u and the drained vertical constrained modulus, M_{DMT} (together with E_D)
- E_D is used in determination of the density *(*together with $I_{D)}$ and M_{DMT} (together with $K_{D)}$

A re-evaluation of the SDMT results to determine basic soil properties in Swedish clays can be found in Wood (2015), which compares existing correlations of basic soil parameters to field and high quality laboratory data. Within this thesis the correlations that agreed best are used to help characterise the *in situ* soil conditions. SDMT data has been used to define:

- density in between the sampling levels based on V_S measurements using an empirical relationship defined by Mayne *et al.* (1999)
- K_0 in accordance with Larsson (1989)
- τ_u in accordance with Lunne *et al.* (1989)
- *OCR* in accordance with Chang (1991)

In many soils M_{DMT} defined by Marchetti (1980) has been found useful for providing predictions of settlement calculations where M_{DMT} is defined as:

$$M_{DMT} = R_M E_D \qquad \text{Eq. 3-9}$$

where for clays R_M is defined as: $R_M = 0.14 + 2.36 log K_D$ Eq. 3-10

For the Swedish clays tested within this thesis this correlation is poor. In order to give an indication of *in situ* confined modulus site specific correlations are therefore given based on E_D and K_D (through OCR determined using Chang, 1991) are presented in Section 4.7 and Appendix A8. These are not recommended for use in design, and should only be treated as an indication of the variation in *in situ* stiffness. The general correlation for the pre-yield modulus, M_0 (average reloading modulus after reconsolidation, unloading and then reloading) is shown in Eq. 3-11. This is not the initial 'disturbed' modulus, M_i, observed in standard CRS and IL stepwise oedometer tests. The general correlation for the post yield modulus, M_L used in this work is shown in Eq. 3-12.

$$M_0 = PE_D OCR \qquad \text{Eq. 3-11}$$

where P is constant in a given geological deposit and site, P=5 was a general fit.

$$M_L = \frac{E_D OCR}{Y} \qquad \text{Eq. 3-12}$$

where Y is a constant in a given geological deposit and site.

The value for Y was found to vary between 2 and 8 for soils with horizontal bedding (not applicable for samples that have been rotated during geological reworking).

3.4 Laboratory testing

3.4.1 Introduction

Laboratory testing conducted within this project was primarily aimed at the study of small strain stiffness behaviour of soft clays, and its degradation during undrained triaxial shearing. In general 100 mm high samples with diameter 50 mm have been used for testing. However for some tests 75 mm high samples with diameter 38 mm were tested (to study the effect of removing the outer zone of the clay on aged samples). Additional laboratory testing was, however, required to assist in characterisation and understanding of behaviour of the clays studied. In addition, efforts have been made to investigate the ability of some existing sample quality assessment methods to identify samples most representative of *in situ* conditions (low disturbance). This was not, however, the primary goal of this research, and was purely a means to assist in the evaluation of the representativeness of the laboratory samples in the small to medium strain range with respect to field conditions.

3.4.2 Triaxial equipment and loading procedures

The study of small strain stiffness under confining stress, and its degradation with strain was conducted within a Bishop and Wesley type triaxial cell manufactured by GDS instruments. This cell is specifically designed for stress path testing, as it enables control of the stresses directly on the sample. The triaxial tests were controlled using the GDS advanced digital control system, fully described in the GDS Advanced Digital Controller Handbook (2000).

Details of standard triaxial system

The volume and pressure control was performed using three identical controllers. The limitations of these controllers are summarized in Table 3.7, while details of the other transducers used within the standard system are given in Table 3.8. These devices were connected to a GDS 8 Channel 16 bit Serial Data Acquisition pad.

Table 3.7 Details of digital controller units (DCU) for automated control of cell pressure, back pressure and lower chamber pressure.

Standard Digital Control Unit	Detail standard unit
Accuracy of Pressure Measurement	Accurate to 0.75 kPa (<0.15% full range)
Accuracy of Volume Measurement	accuracy 0.25% measured value
Pressure Range (kPa)	500
Max volume (cm^3)	200
Resolution of Pressure Measurement (kPa)	0.25
Resolution of Volume Measurement (mm^3)	1

Table 3.8 Transducers attached to GDS 8 Channel serial acquisition pad as part of standard triaxial equipment for automated control using GDSlab software.

Standard Triaxial Transducer Type	Transducer Device	Range	Accuracy	Gain range GDS serial pad
Load cell	STALC9	0 – 0.5 kN	± 0.029 %	± 10 mV
Pore pressure	GDS 4B-C2.5	0-500 kPa	<0.1%	± 100 mV
Axial deformation	Penny and Giles linear displacement potentiometer	0-50 mm	± 0.25 %	± 1 V

Local strain measurement

Two types of local strain transducers have been used within this project to study stiffness degradation during triaxial undrained shearing tests: Differential Variable Reluctance Transducers (DVRT) and Hall effect transducers, details of these devices are given in Table 3.9. The data acquisition system used for both methods of strain measurement was a 16 bit 24 channel DAQ card in a standard PC. The performance of the Hall effect devices (horizontal and vertical) with soft soil samples was not satisfactory. The problems that arose with this device for local axial and local radial strains are discussed in Section 5.9.4 and within Appendix A6.

Table 3.9 Comparison of the local strain devices used within the project.

Advanced Displacement Transducers	Transducer Device	Body length (mm)	Stroke length (mm)	Accuracy	Resolution (strain*)
Local axial displacement	GDS Hall effect bi-polar slide by magnet	70	6 (± 3)	< ± 0.8 %	3.48 μm (2.4×10^{-4})
Local radial displacement	Calliper mounted GDS Hall effect bi-polar slide by magnet	50	6 (± 3)	< ± 0.8 %	3.48 μm (4.8×10^{-4})
Local radial displacement	CTH Calliper Microstrain SG-DVRT-8	50.5	8	± 0.1%	2 μm (4×10^{-5})

** assessed strain resolution for a typical 100 mm x 50 mm Ø triaxial sample*

For radial strain measurement a DVRT transducer was used for most tests. The device was attached to a carefully tuned spring connecter on a radial calliper that was positioned on the sample with very light contact, refer to Figure 3.13(a). This light contact ensured minimum impact of the device on the specimen. Attachment between the calliper and the sample was throughout the full cross section of the sample, except at the position of the spring, as indicated in Figure 3.13(b). This helped reduce errors associated with non-uniform radial strains.

(a) (b)

Figure 3.13 DVRT local radial strain measurement device (a) before triaxial testing (b) after triaxial testing (sample taken to 25% axial strain).

Reconsolidation and loading procedures

All triaxial tests conducted within this work were initially subjected to a small ramped isotropic stress, and were then anisotropically consolidated to *in situ* stresses. Vertical reconsolidation stresses were determined from the measured densities of laboratory samples. Pore pressures assumed were based on average long term piezometric measurements. Horizontal effective stresses were initially estimated using K_0 values, based on Schmidt (1966) shown in Eq. 3-13. This formulation is derived for K_0 in unloading. Many other formulations have been proposed for estimation of K_0, not less those given by Wroth (1965), Mayne & Kullhawy (1982), Meyerhof (1976) and Kullingsjö (2007). However within this work the method proposed by Schmidt (1966) worked well when compared to the *in situ* measurements of K_0 by Smith (1989), if the OCR value was determined from stepwise oedometer tests and the actual values of K_{0nc} (i.e. the K_0 corresponding to the normally consolidated state) were used (from K_0 triaxial tests). The values of K_0 empirically determined from SDMT also agreed well with Eq. 3-13 and the *in situ* measurements by Smith (1989), refer to Wood (2015). These values were, therefore, used in the assessment of the *in situ* mean effective stress (p') where SDMT test data was available. The value of K_{0nc} was determined from K_0 triaxial consolidation tests conducted both within this work and by Olsson (2013).

$$K_0 = K_{0nc} OCR^{\mu} \qquad \text{Eq. 3-13}$$

where μ is defined as: $\mu = 1.2 \sin \phi'_{CV}$ Eq. 3-14

and φ'_{CV} is the (drained) friction angle at critical state (constant volume).

The reconsolidation and triaxial loading procedures used are presented Table 3.10. Method 1 and 2 were used for reconsolidation of samples for standard triaxial tests. Method 1 involves reloading directly to the *in situ* stresses in accordance with recommendations by Bjerrum (1973), refer to Table 2.2. The SHANSEP method recommended by Ladd & Foot (1974) was not used due to the potential changes that would be incurred on soft soil samples. However, a variation of this method was used for some tests where just a small additional load (well within the initial state boundary surface) was applied and then removed, and is referred to as Method 2 herewith.

After reconsolidation some additional stress paths involving additional loading, unloading and, in some cases, reloading were applied to some specimens prior to shearing, as outlined in Table 3.10 (Method 3, 4 5). These tests these were used to simulate situations that might arise in the field during deep excavation works. Method 6 relates to K_0 triaxial tests used to define K_{0nc}. For all loading and unloading stages the speed of drained loading was adjusted so that the excess pore pressures were < 5 kPa. At the end of a stage, the next stage was not started until pore pressures had equalised and the back pressure ≈ measured pore pressure. During shearing the frequency of measurement was generally every 120 seconds, however, for some tests a frequency of measurement of 10 seconds was utilised.

Table 3.10 Reconsolidation and loading stages 1, 2, 3, 4, 5 and 6; U= undrained, D= drained, I= isotropic, R=linearly ramped with specified effective stress path (ESP), K_0=loading or unloading to specified σ'_{v0} with zero radial strain control, A= anisotropic.

Stage	Method 1	Method 2	Method 3	Method 4	Method 5	Method 6
1	D, I, R load to ≈⅕ σ'_{v0} but ≤ 20 kPa 2-4 hours	D, I, R load to ≈⅕ σ'_{v0} but ≤ 20 kPa 2-4 hours	D, I, R load to ≈⅕ σ'_{v0} but ≤ 20 kPa 2-4 hours	D, I, R load to ≈⅕ σ'_{v0} but ≤ 20 kPa 2-4 hours	D, I, R load to ≈⅕ σ'_{v0} but ≤ 20 kPa 2-4 hours	D, I, R load to ≈⅕ σ'_{v0} but ≤ 20 kPa 2-4 hours
2	D, A, R load to σ'_{v0}, σ'_{h0} 16-24 hours	D, A, R load to σ'_{v0}, σ'_{h0} 16-24 hours	D, A, R load to σ'_{v0}, σ'_{h0} 16-24 hours	D, A, R load to σ'_{v0}, σ'_{h0} 16-24 hours	D, A, R load to σ'_{v0}, σ'_{h0} 16-24 hours	D, A, R load to σ'_{v0}, σ'_{h0} 16-24 hours
3	U shearing at rate 0.06%/h 10-24 hours	D,A,R load to: σ'_{v0}+0.2(σ'_c- σ'_{v0}), σ'_{h0}+0.2K_0 (σ'_c- σ'_{v0})	D, A, R or K_0 unload to OCR 2 (Δu< 5kPa)	D, A, R or K_0 unload to OCR 2, 4 or 6 (Δu< 5kPa)	D, A, R load to 0.8 σ'_{vc}, 0.8σ'_{hc} (16-24 hours)	D, A, K_0 load to beyond σ'_c (Δu< 5kPa) (3-5 weeks)
4		D, R unload to σ'_{v0}, σ'_{h0} (2-4 hours)	D, A, R or K_0 reload to σ'_{v0}, σ'_{h0} (Δu< 5kPa)	U shearing at rate 0.06%/h (10-24 hours)	U shearing at rate 0.06%/h (10-24 hours)	U shearing at rate 0.06%/h (10-24 hours)
5		U shearing at rate 0.06%/h (10-24 hours)	D, A, R or K_0 unload to OCR 4 (Δu< 5kPa)			
6			D, A, R or K_0 reload to σ'_{v0}, σ'_{h0} (Δu< 5kPa)			
7			U shearing at rate 0.06%/h (10-24 hours)			

3.4.3 **Evaluation of soil moduli during undrained triaxial shearing**

Within this thesis the secant shear modulus is generally used to describe the stiffness of the clay specimen at a given strain during triaxial shearing, determined as shown in Figure 3.14 (a). The shear modulus for both drained and undrained shearing should be the same, given that pore water cannot carry shear. In some cases the undrained secant Young's modulus is used to describe stiffness degradation, as not all triaxial tests had local radial strain measurement. For this case the interpretation of undrained Young's modulus, E_u, assumes isotropic porous elasticity (even though soil stiffness is anisotropic), as only axial strain data was available as defined in Figure 3.14(b). Work by Kawaguchi *et al*. (2003) suggests, however, that this assumption is reasonable for clays within the small to medium strain range.

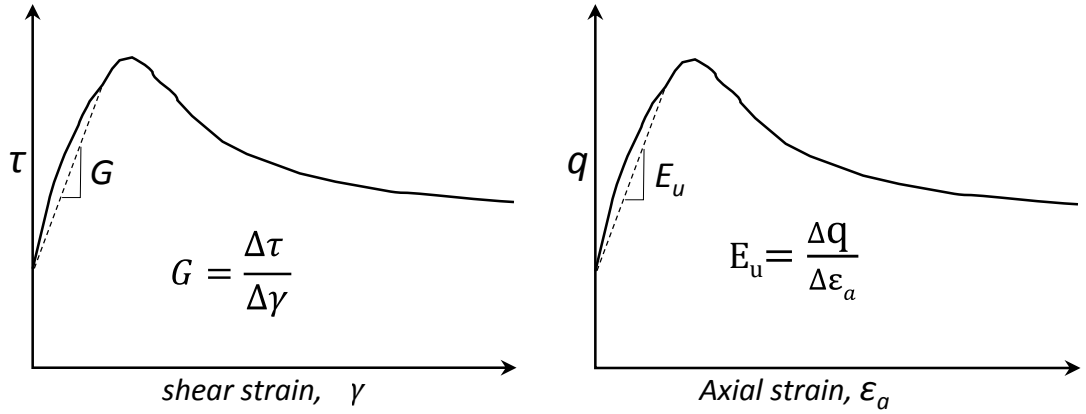

(a) (b)

Figure 3.14 Definition of soil moduli used to define stiffness degradation with strain (a) secant shear Modulus, G.

The shear strain was determined from:

$$\gamma = \varepsilon_a - \varepsilon_r \qquad \text{Eq. 3-15}$$

where ε_a was measured using either local radial strain gauges, or external axial displacement measurements, and ε_r was measured using local radial strain gauges.

Within this thesis the stiffness degradation during shear is described using normalisation, so that samples tested at different stresses can be compared. The shear modulus degradation is presented in terms of G/G_0 with respect to the shear strain, while the degradation in E_u is presented in terms of E_u/p'_{VC} where p'_{VC} is the mean effective stress at the start of shear, with respect to axial strain.

Potential errors in the G/G_0 ratio relate to the accuracy in the shear strain measurement and the stress measurement, which combine to give the accuracy of the shear modulus and accuracy of G_0. In order to formulate the positive limit of error bars for G/G_0, the errors leading to a maximum value of G and a minimum value of G_0 were calculated. For the negative error bars limit errors associated with minimum values of G and maximum values of G_0 were calculated. Based on the findings presented in Chapter 5, a standard error of ±10% of G_{0BE} was assumed for all tests. The accuracy of secant shear modulus (G) is highly dependent on the shear stress interval from the start of shearing.

As stated above, in this work triaxial shearing uses displacement control, with a standard rate of 0.01 mm/min. This means that for the softest clays the magnitude of the shear stress interval between data sampling points used to determine shear modulus was in some cases smaller that the potential error in the stress measurement alone. For these cases (very soft soils) the errors in the G/G_0 ratio were unreasonably large until strains of around $5x10^{-4}$. For the stiffest soils, the error in the G/G_0 ratio was low even for an initial data point taken after 120 seconds after the start of the undrained shearing.

Potential errors in the E_u/p'_{VC} ratio are similar to the G/G_0 ratio, if the error associated with G_0 is excluded. The additional error in E_u, due to the assumption of isotropic porous elasticity, is thought to be small based on the work Kawaguchi *et al.* (2003).

3.4.4 **Bender Element Testing**

Different BES interpretation methods and the corresponding challenges for determination of G_0 were discussed in Section 2.3.3. For the soils tested, the focus has been placed on using high quality fresh large clay specimens (≥100 mm) with high frequency Sine wave signal excitation to study G_0. In this situation R_d (L/λ) is maximized, and the group/phase velocity errors are minimized even in the presence of some multi-modal vibrations.

Poor quality clay specimens may require more sophisticated analyses, if reliable determination of G_0 is to be achieved, as the multimodal vibration and dispersion (group velocity errors) become more prolific in the high plasticity clays. However, given the already non-representative nature of poor quality samples with respect to the field, the efforts required to conduct more sophisticated analyses was judged unwarranted. Instead, such tests results were simply deemed unrepresentative. In general, the applicability of Method A, B or C interpretation (defined in Figure 3.3) was found to be good for good quality samples. The suitability of these interpretation methods was determined by studying the phase velocity of multiple points on the transmitted and received signal in the time domain, and by comparing these to the cross-correlation results. In addition, the initial shear wave arrival and the 2nd shear wave arrival were also compared, where possible. In high quality clay samples very little change in the phase velocity of the transmitted wave occurred, thus the interpretation using Method A and B yielded very similar values.

Bender element systems (BES) used

Four bender element (BE) test setups using three bender element systems (BES) have been used within this project. Initially all testing was to be done using a commercial BES system developed by GDS. It was found, however, that the flexibility of this system was insufficient for some areas of this research, due to the limited frequency range and the low sampling rate, which hampered the post-processing and the use of more sophisticated methods of analysis than Method A (picking points in time domain). In addition, it was not clear what type of signal conditioning was applied to the input/output signals. For this reason a purpose-built system was developed at CTH which had a greater frequency range, higher sampling speed (20 times greater) and full control over the signal conditioning and processing. This new CTH system was validated during a visit to the Swedish Geotechnical Institute where parallel unconfined tests were conducted on a block sample (approx. 70 mm x 70 mm by 50 mm) and a $STII_{slow}$ piston sample. During this visit, the BE tests were conducted using the CTH

system, GDS system, which both used GDS BE devices, and two SGI BE test setups (the later differing only in the mounting material of the BE devices which were manufactured by GEONOR). Details of the BE semiconductor devices used are given in Table 3.11. All confined testing was conducted using the GDS system, while both the GDS and the CTH system were used for testing on unconfined samples. These two systems are described in Figure 3.16 and Figure 3.17. The SGI BE test setups used for benchmarking are described in Appendix A5.

*Table 3.11 Details of bender element devices, * penetration into sample*

BE device	BE thickness (mm)	BE width (mm)	BE length (mm)	Source/ receiver type
GDS	1	10	10 (2)*	parallel: series
GEONOR	1	10	12 (4)*	parallel: series

The PC-based GDS/CTH BES systems use a data acquisition card to transmit and receive signals, removing the need for a separate function generator and oscilloscope. Transmission of the signal from the data card to the bender element is done using a PC interface. A comprehensive study by Schmalz *et al.* (2007) that compared bender element testing with traditional equipment (such as the SGI system), and PC-based versions in soft clay found that results agreed well (within 2.6%). This is similar to the findings of Greening *et al.* (2003) and Moshin *et al.* (2004), although the latter noted that although the interpreted values of V_s were similar, there was more noise in the PC-based system. Consequently, no significant differences between the BES results due to the signal generation and acquisition system alone were expected.

Bender element interpretation: Method A-Time Domain

The position of the "pick" used for time domain analysis was discussed in Section 2.3.3. The position of the "pick" used for assessment of the shear wave travel time and the changes in the shear wave while travelling through the sample are defined in Figure 3.15. The peak-peak (B-B') position was used for the final assessment of G_0, however, during testing the shear wave velocity at all 'pick' positions was assessed. If A-A' and B-B' differed significantly, the test was repeated with different frequencies. This was done to ensure that the correct first wave arrival was identified. Comparison of the travel times at the different picks (or corresponding V_S) were used to identify potential group/phase velocity errors and hence the reliability of the interpretation when using Method A, B and C.

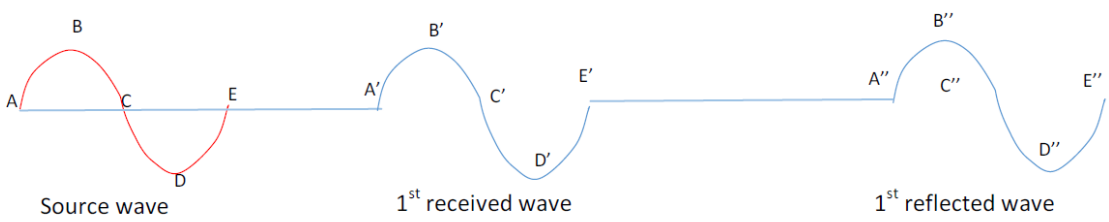

Figure 3.15 Travel time measurement positions on acquired signal during BE testing, A= Zero crossing, B= 1st +ve peak to peak, C=2nd zero crossing, D=1st –ve peak to peak, E= 3rd zero crossing.

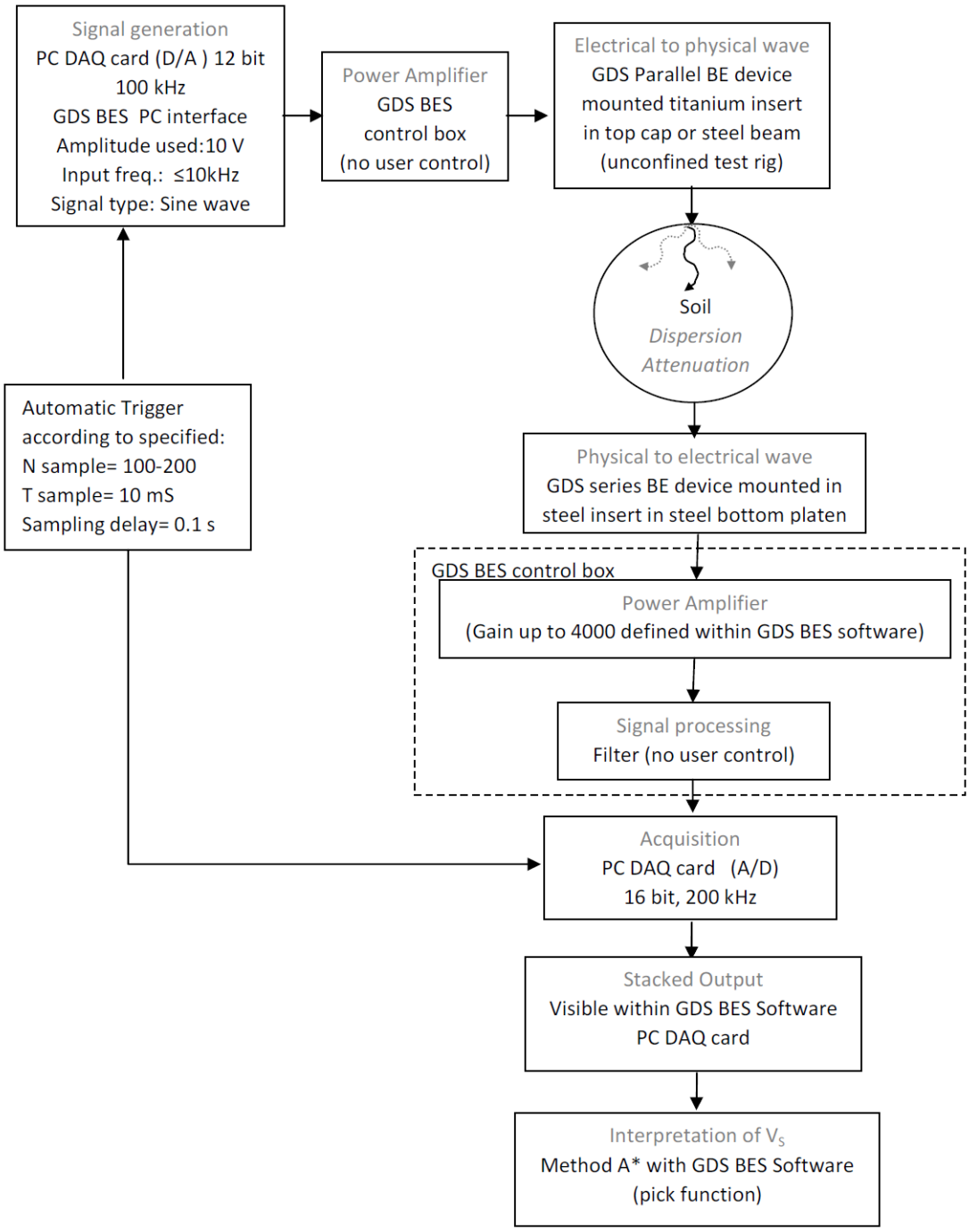

*Figure 3.16 GDS BES work flow for determination of G_0, *V_S interpretation possible using Method B and C by reanalysis of the stored output files, refer to Figure 3.3.*

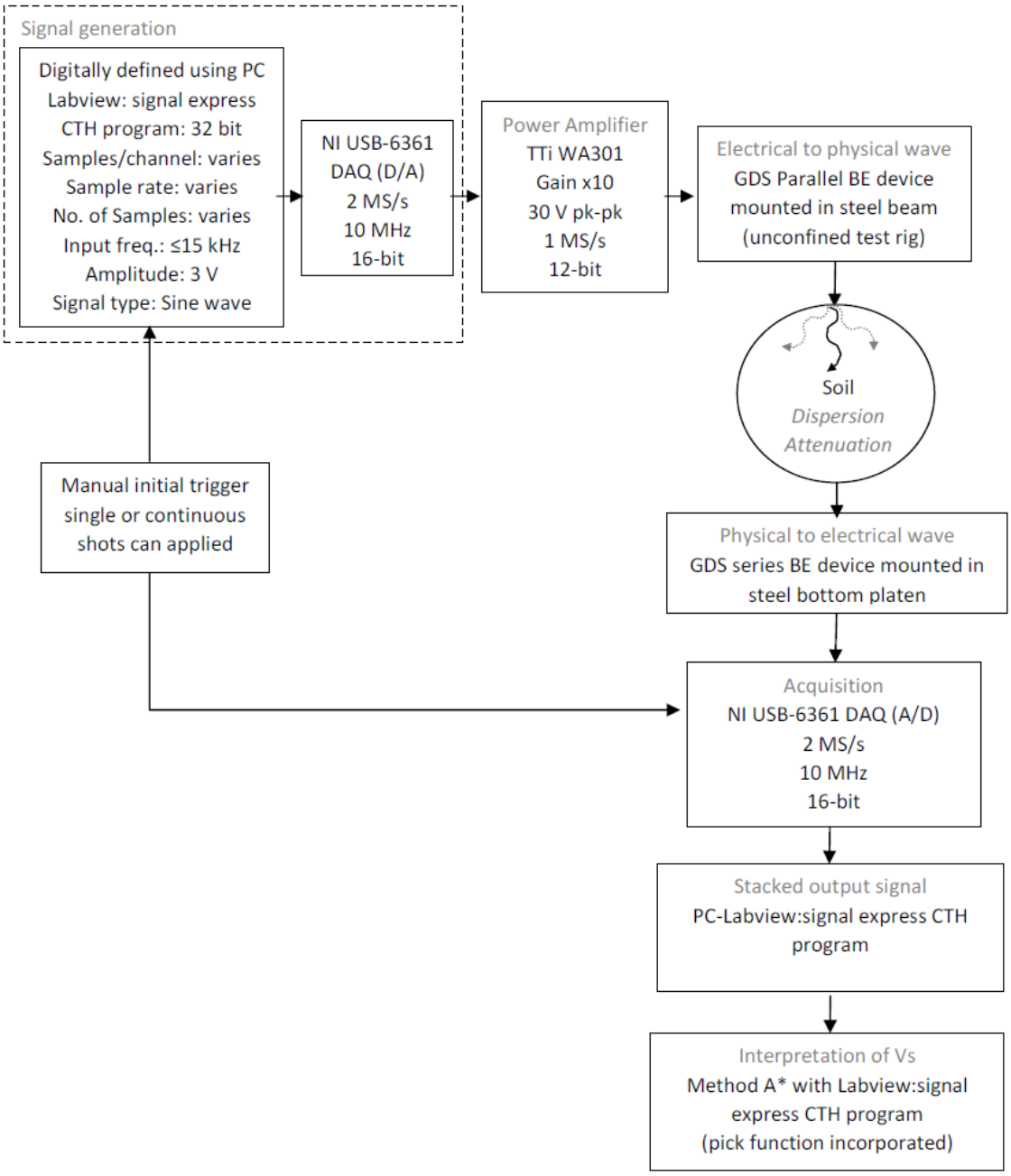

*Figure 3.17 CTH system work flow for determination of G_0, *V_S interpretation also possible using Method BB and BC by reanalysis of the stored output files, refer to Figure 3.3.*

Bender element interpretation: Method B-Frequency domain using cross-correlation

Method A is often seen as being very subjective, given the way in which the picks are selected. In order to help to remove this subjectivity, cross-correlation of the input and the output signals has been carried out on tests using the GDS and CTH BES. The correlation was carried out within a Matlab program developed at CTH, further referred to as Method B. An illustration of the cross-correlation output from this program is shown in Figure 3.18 (a) (solid line) using an output file directly from the GDS BES, without any additional processing (GDS output=dotted lines). This cross-correlation is performed on an unconfined field BE test on a block sample.

In many cases the received signals needed additional processing for the cross-correlation to work reliably. This is due to the fact that the cross-correlation correlates to the largest peak in the received wave. In many of the BE tests, the largest peak was not the first wave arrival, but slower superimposed waves caused by multimodal vibrations and dispersion. This error is evident in the received signal shown in Figure 3.18 (b), with the cross-correlation (solid line) giving estimations of V_S that are too low, if no additional postprocessing is carried out. In this example the error in V_S using the standard cross-correlation is around 24.5 m/s or 30%. However, if the acquired signal is subjected to additional postprocessing in accordance with Figure 3.3, using an additional FIR filter and a lower and upper bound frequency cut-off, then a more reasonable assessment of V_S could be made.

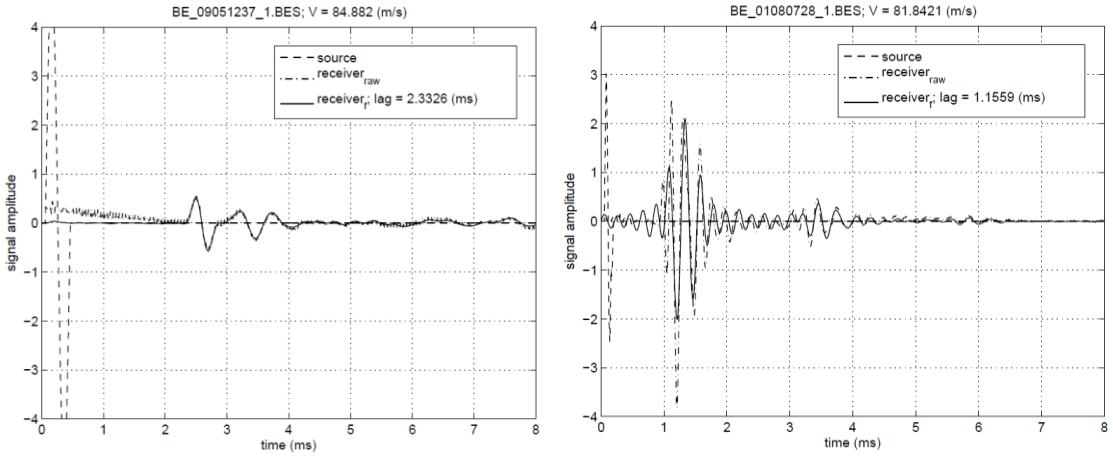

(a) (b)

Figure 3.18 Typical output from CTH cross correlation program (a) unconfined block sample, (b) confined STII piston sample at in situ stresses, the error in cross correlation when the 1st peak is not the maximum peak.

In very high quality samples both the received wave and multiple reflections could be observed, as seen in Figure 3.18 (b). In this situation, a cross correlation of the received wave and the 1st reflected wave could be used to determine V_S, without any influence from the BE transfer functions. For this analysis, the CTH cross-correlation program was amended by splitting the received signal, and conducting a standard cross-correlation. The cross-correlation worked well without the need for additional post-processing, due to the similarity in the shape of the signal from the first received waves and the reflected waves.

Bender element interpretation: Method C-Frequency Domain Spectral analysis

Method C was not used to determine V_S from BE tests directly within this work as no significant benefits were expected based on the literature review. However, as part of the post-sampling procedures, a spectral analysis of the received signal was conducted to identify the key frequencies present. This was then used to identify unwanted background frequencies, so that these could be removed, which then improved the accuracy/ease of interpretation using Method A and B.

Unconfined Bender Element Tests

Laboratory and field studies using bender elements (BE) were carried out on unconfined clay specimens; that is to say on samples without applied confining stress. Residual effective stresses were often present during these tests through suction, thus it would be inaccurate to say these specimens were unstressed. Unconfined shear wave velocity

measurements V_{SO} were used to track potential changes in clay specimens following extraction within the steps outlined in Figure 3.1. It was also hoped that these tests could be used to evaluate the non-destructive sample quality assessment methods proposed by Landon *et al*. (2007) and Donohue & Long (2008) for Swedish clays. The unconfined BE tests were generally conducted within a purpose- made test rig shown in Figure 3.19, although some tests were also conducted within the GDS BES when the top cap was in place, but prior to closing the cell. The unconfined test rig was built based on the equipment described by Landon (2007), but with small amendments, such as the addition of a suction probe holder, and the positioning groves for correct placement of STII piston samples.

(a) (b) (c)

Figure 3.19 Unconfined bender element testing of (a) Block sample in field (b) Block sample in the laboratory, (c) STII piston sample in the field.

Interpretation of the unconfined BE tests were generally carried out using Method A (multiple positions). However, in the presence of rigid side boundaries, such as testing specimens within the STII sample tube, the interpretation was in some cases difficult due to multimodal vibrations. A study on the impact of the rigidity of the specimen boundaries during BE testing was conducted by O'Donovan *et al.* (2015) who suggested that an increased boundary rigidity reduces the amplitude of the received signal significantly, and causes increased multimodal vibration. This appears to be confirmed by testing carried out within this study, particularly for samples which were stored over longer periods of time. To illustrate the influence of the sample tube on the received signal, the results of two unconfined BE tests tested with the sample within the sample tube are presented in Figure 3.20. In the test conducted immediately after extraction, it is not clear where the first arrival occurs due to the influence of reflected waves, while the BE test on day 15 had significantly reduced signal amplitude (increased damping) making the interpretation even more difficult. For this reason Method A was not used for interpretation of bounded unconfined tests. In these situations Method C was used to remove the high frequency components that related to reflected compression waves, and the resulting signal analysed using Method B. In many cases the BE unconfined tests were conducted in the sampling tube, and then again directly after removal from the tube, when the sample was installed in the triaxial cell. In this situation the unconfined test conducted in the triaxial GDS BES could be used to help identify the actual shear wave arrival time for the BE test conducted within the sample tube. When such a check was conducted on the 15 day sample, represented in Figure 3.20, the result from the GDS BES suggested that the second red ring encompasses the initial shear wave arrival. When testing the block samples with wax/paraffin remaining around the sample, no issues arose with the interpretation of the signal.

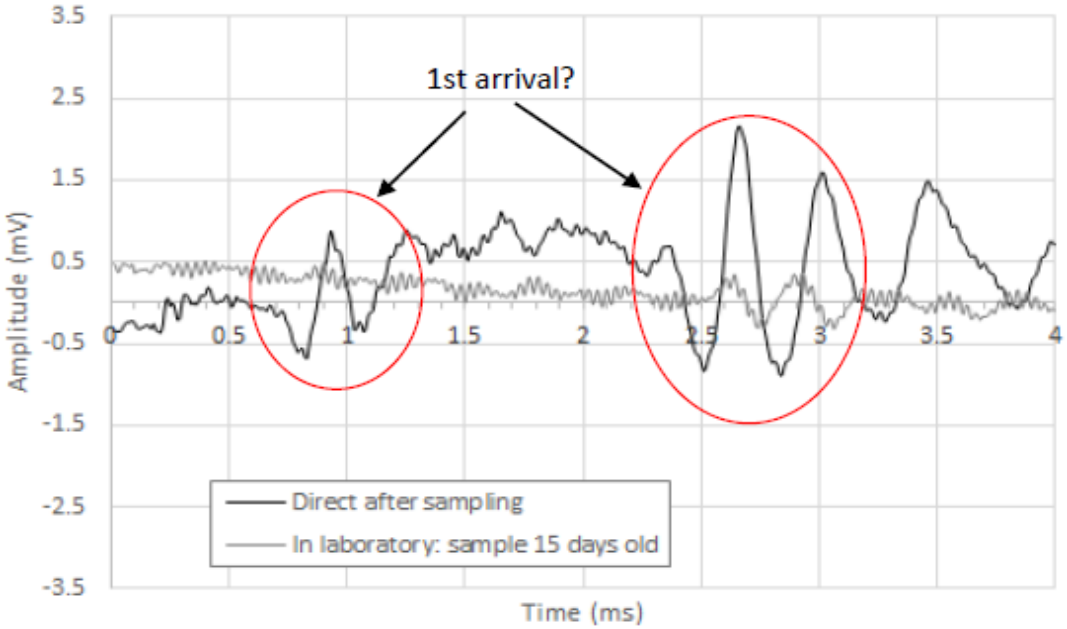

Figure 3.20 Unconfined BE tests within sample tube after sampling and 15 days later.

3.4.5 **Other laboratory tests**

The tests conducted to classify the soil as a whole included: constant rate of strain (CRS) oedometer tests, step wise incremental load (IL) oedometer tests, undrained direct simple shear (DSS) tests, specific density (G_s) tests, sedimentation tests (PSD), pore water chemistry analyses, organic content, index tests (P_L, L_L W_n, Υ_b, τ_{uc}), K_0 – consolidated triaxial undrained compression and extension tests (CAUE, CAUC), and the drained triaxial K_0 -tests to determine the value for K_{0NC}. For details of the test method and procedures involved for these tests, the reader is referred to the relevant European standard. It should be noted, however, that the interpretations of the CRS tests were done according to the method proposed by Sällfors (1975), despite being judged to be invalid in some instances. The interpretation of IL tests was done using the Casagrande method. In general, the results of IL tests were used as a basis for determination of the over consolidation ratio in field, due to the issues surrounding the Sällfors (1975) method relating to rate effects and basis of validation (depths ≤ 15 m).

Skempton activity number

The Skempton activity number is used in Chapter 4 and 5, as it is very useful in differentiating between clays sedimented in differing physiochemical environments. Soil activity is defined as the ratio of plasticity index (I_p), defined in Eq. 3-14, and the percentage of the clay sized particles < 2μm (% clay), as shown in Eq. 3-15.

$$I_P = W_L - W_P \qquad \text{Eq. 3-16}$$

where W_L is the liquid limit and W_P is the plastic limit

$$\text{Activity, } A = \frac{I_P}{\%\ \text{clay}} \qquad \text{Eq. 3-17}$$

3.4.6 **Studies of transport effects**

Some measurements of the vibration experienced by samples during transport have been conducted using multi-directional accelerometers placed on or in sample boxes, as indicated by Table 3.12 and Figure 3.21. This was done to see if the transportation method itself had a significant impact on the vibrations experienced by samples. Some measurements on the effect of transport on STII piston samples (post-glacial marine clay and post-glacial, marine organic silty clay) has been undertaken for samples that were properly packed in accordance with SGF Report 1:2009. The results of the comparative studies are discussed in Chapter 5 within the context of small strain stiffness (effect on V_S).

Table 3.12 Details of transportation method during vibration studies (clay types: PG= post glacial, G= glacial, GM=glacio-marine, M= marine, L= lacustrine)

Clay type	Sample method	Position of accelerometer; I= in sample tube embedded in play doe, O= taped to sample box and Transport method: CB=Car boot, PU= Fixed in pickup truck, M=box on mattress, sample box lining:transport time, type of driving			
		CBI: polystyrene: 45 min: town	CBI: foam 45 min town	CBMO: foam 45min: motorway & town	PUO: foam 45 min: motorway & town
PG: GM	$STII_{slow}$	X	X	X	X
PG:M	STII	X	X		
G:L	STII	X	X		

Figure 3.21 Sample transport boxes used in town driving vibration test lined with foam or polystyrene.

3.4.7 **Assessment of sample quality**

Different methods of sample quality assessments were discussed in Section 2.5.3. Within this work five different methods are compared, encompassing both destructive and non-destructive assessment methods. These are summarised in Table 3.13, together with the highest quality criteria for each method.

For triaxial tests the accuracy of the volume change measurement relates to the number of steps of the motor. The configuration of the GDS system was such that 1 step = 1 mm^3. As such the volume change, which was between 1500 to 9000 mm^3, gave an accuracy of the volume change measurement during reconsolidation $\Delta V/V_0$ within 0.05%. For CRS and IL oedometer tests the accuracy of the volume change was dependent on the external measurement gauges used, which were of similar accuracy to those described in Table 3.8. Determination of specific gravity, G_s used to determine $\Delta e/e_0$ was found to be sensitive to the amount of material used and the procedures followed. A large amount of soil was used, with tests repeated 3 times, and the average value used to define G_s to minimise errors. Due to both natural variation and the impact of sampling, the water contents, W_n, in samples also vary which effects the value of e_0 determined. For this reason water content, W_n, was determined from large samples in order to avoid some of the issues associated with local variations and was repeated before every laboratory test that was performed, such that any significant differences would be identified. As such, the accuracy of $\Delta e/e_0$ is thought to be good but it is difficult to define a specific accuracy.

Table 3.13 Summary of sample quality assessment methods used for soft clays (OCR< 2) (ND=none destructive, D=destructive assessment, refer to Section 2.4.3 for definition of symbols.

Method	Assessment type	Basis of assessment	Highest quality criteria (light OC clay)
Tanaka *et al.* (1990)	ND	Matrix suction measurement u_r relative to the *in situ* vertical effective stress	$\sigma'_{v0}/6 \geq u_r \leq \sigma'_{v0}/5$
Landon *et al.* (2007)	ND	Ratio of the unconfined shear wave velocity over the field shear wave velocity	$V_{S0}/V_{S\ field} \geq 0.6$
Donohue & Long (2010)	ND	Matrix suction relative to the *in situ* vertical effective stress, L_u & unconfined shear wave velocity relative to the intrinsic and the field shear wave velocity, L_{vs}	L_u[1] < 0.4 & L_{VS}[2] <0.65
Lunne *et al.* (1997)	D	Ratio of the pore volume change during reconsolidation, Δe, to initial void ratio e_0	$\Delta e/e_0 < 0.04$
Larsson *et al.* (2007)	D	Ratio of the volume change during reconsolidation, ΔV, to the initial volume V_0 and the liquid limit, W_L	Dependent on W_L between ε_{vol} 2.8-1.5 %

[1] L_u gives a relative measure of disturbance in terms of residual effective stresses defined as:

$$L_u = \frac{\chi\sigma'_{v0} - u_r}{\chi\sigma'_{v0}} \quad \text{Eq. 3-18}$$

where χ is defined as 0.2, by Donohue & Long (2010), and $\chi.\sigma'_{v0}$ represents the maximum suction an undisturbed fully saturated clay sample is able to withhold, and u_r is the measured suction of the sample. For a completed disturbed sample L_u is assumed to be zero.

[2] L_{vs} is defined as:

$$L_{VS} = \frac{V_{Sinsitu} - V_{S0}}{V_{Sinsitu} - V_{Sremoulded}} \quad \text{Eq. 3-19}$$

where $V_{S\ insitu}$ is the shear wave velocity determined in the field, V_{S0} is the shear wave velocity of the unconfined sample (no load applied) and $V_{S\ remoulded}$ is the shear wave velocity of an unconfined remoulded sample.

3.4.8 **Intrinsic sample preparation**

Reconstituted samples were prepared for three reasons;

1. To understand the influence of clay structure and pore water chemistry on G_0.
2. To determine the intrinsic value required as input for advanced numerical models that include de-structuring post-peak.
3. To enable the use of the sample quality assessment method proposed by Donohue & Long (2010).

When preparing reconstituted samples, the initial clay structure is fully erased by remoulding combined with the addition of water to form slurry. Burland (1990) suggested that water should be added to 125% of the liquid limit, however, for the high plasticity West Coast clays a water content of at least 150% liquid limit was required. Remoulding can be done by hand or within a mixer once all lumps are removed. It was found that remoulding by hand gave the best results as this erased the natural clay structure with minimum trapped air. Once all lumps were removed and the water was added any trapped air in the slurry was removed using a vacuum pump. Following this the de-aired slurry was carefully poured into the sedimentation tubes ensuring no entrapment of air. The sample was allowed to re-consolidate with a nominal load applied (3 kg although in one case an additional 1kg was applied after 2 days due to friction issues (gap between upper piston and slurry), until the reconstituted sample achieved a void ratio similar to the natural sample (if possible). The design of the sedimentation tubes was based on Mataic (2012) shown in Figure 3.22 (a). The consolidation was monitored based on movement of a central steel bar, refer to Figure 3.22 (b), and an example of one of the 7 reconstituted samples prepared is presented in Figure 3.22(c) following extrusion from the sedimentation tube.

The tests conducted on reconstituted samples included CRS and IL oedometer tests, triaxial tests and unconfined BE tests, and played a vital role in the understanding laboratory results for the natural samples and the impact of disturbance. These assessments fuelled changes in the sampling, transportation and storage of samples over the duration of the project, in order to obtain the best possible samples. The results were also used in the sample quality assessment method put forward by Donohue & Long

(2010) for soft clays, and included a study on the impact of the ionic strength of pore water during sedimentation on V_{S0}.

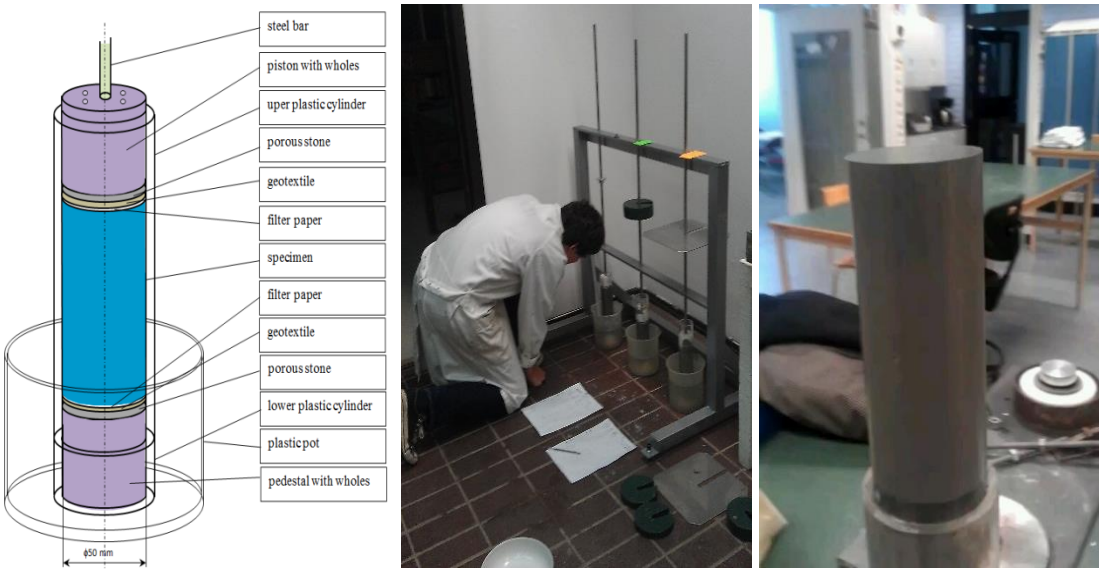

(a) (b) (c)

Figure 3.22 Preparation of reconstituted samples (a) schematic diagram of equipment used from Mataic (2012) (b) Initial reading of slurry height prior to re-sedimentation period (c) Extruded intrinsic sample following 3 months re-sedimentation.

4 MATERIALS STUDIED

4.1 Introduction

The depositional environment, digenesis and the geological and recent history are very important to the behaviour of clays. Deformation in particular is strongly influenced by the physiochemical environment during sedimentation and its effects in establishing a flocculated or dispersed clay structure, Bergsten (1991). As such there is merit in understanding the origin of the clays used in this research. High concentration ionic solutions (marine) during sedimentation cause clay particles to flocculate and form large dense clay aggregates which sediment together with silt to form an open structure, Figure 4.1(a), deposition in fresh water leads to smaller more porous aggregates and closer packing of the particles, Figure 4.1(b) and brackish water deposition lies somewhere between these two, Figure 4.1(c). The depositional environment, digenesis and the geological and recent stress history and typical soil properties for the sites studied are presented in this chapter.

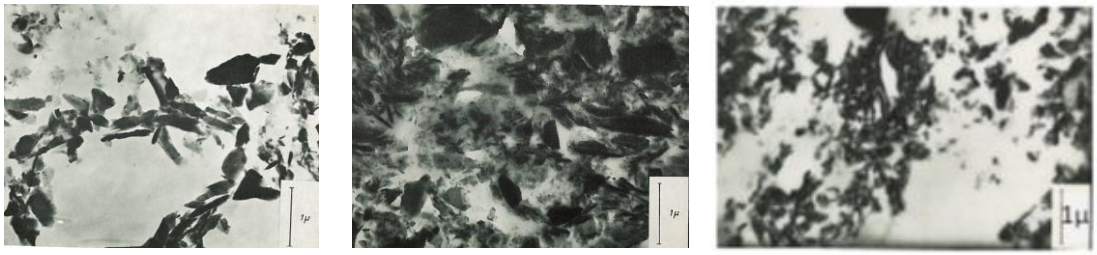

(a) (b) (c)

Figure 4.1 Swedish clay structure observed using electron microscopy (a) Quick marine clay South West coast (b) freshwater clay South East coast, c) Brackish water clay North East coast, Pusch (1966).

4.2 Location of sites

The sites investigated were chosen partly due to their varying stress history and geology, but also due to their accessibility. The locations of these sites are presented in Figure 4.2. The sites cover soils of varying composition, from organic clays to pure clays and clayey silts. The characteristic features of these soils vary from quick to low sensitivity, high to low plasticity, normally consolidated to over consolidated *in situ* stress states.

In Gothenburg six sites (Site 1 to 6) were chosen. These share similar geological histories and lie within 1 km of the Göta River, but do not necessarily share the same recent history. Gothenburg clays have been studied by a number of authors, such as; Torstensson (1973), Sällfors (1975), Andrésson (1979), Claesson (1998) and Olsson (2013), to name but a few. All six sites lay within the project boundaries of future deep excavation works (≥ 10m deep). Site 7, situated approximately 24 km north of Gothenburg at Nödinge, lies adjacent to the Göta River. This site shares similar geological history to the Gothenburg sites, but is less affected by human activity (less aging caused by land reclamation). This site was also used for the study of lime-cement strengthened embankments, refer to Alén *et al.* (2006) and Olsson *et al.* (2009). Further north by 20 km at Lödöse, Site 8 is found adjacent to a small river (Gårdaån) that is a

contributor to the Göta River. This site shares the same depositional environment as Sites 1 to 7, however, geological unloading has occurred. Geomorphology and artesian water conditions have also contributed to leaching, resulting in highly sensitive (quick) clay, the properties of which have also been studied by Söderblom (1969) at this site. Sites 9, 10 and 11 are all located in Uppsala. Unlike Gothenburg, these sites have quite different ground profiles due to the complexity of the quaternary geological history. Both marine and lacustrine clays of medium to low plasticity are found within these sites, in addition to some organic marine sediments. Site 12 is located on the Norwegian West Coast within the city of Trondheim. Marine/coastal deposition has been more influenced by wave activity and under water currents in this area giving lower plasticity, lower sensitivity marine clays/silts. However over part of the site leaching has given rise to highly sensitive (quick) sediments. Site characterization and discussion of deep foundation design solutions at this site can be found in Rönning *et al.* (2009) and Tørum *et al.* (2009).

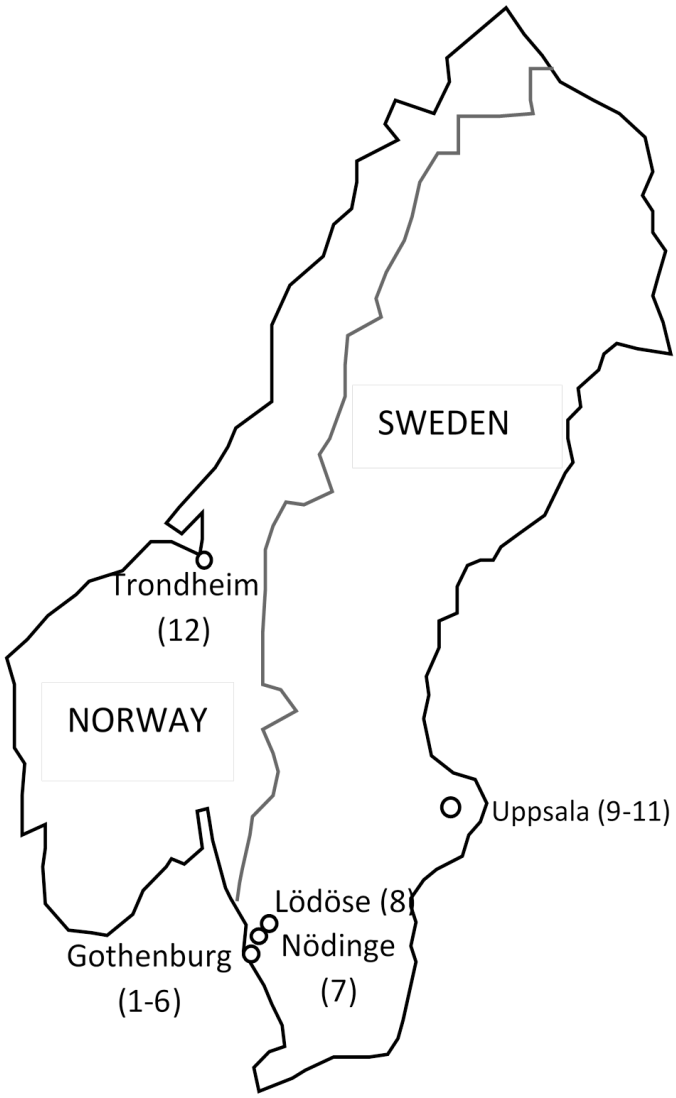

Figure 4.2 Location of Scandinavian sites studied and site reference number in (brackets).

4.3 Overview of geology

The clays studied are quaternary deposits from the Pleistocene (last period of glaciation) and Holocene epoch (current inter glacial period). Within the Holocene epoch there are further geological sub-divisions relating to varying climatic conditions, refer to Bergsten (1991) and Wohlforth *et al.* (1993). In this section focus is on the evolution of the physiochemical environment during deposition for the sites studied, as this has such a strong influence on the clay structure and thus its behaviour. Sediments originating directly from the glacial melt water, ice rafting etc. are referred to as glacial clays, and those formed by reworked glacial sediments are referred to as post glacial clays, Freden (1986). In this thesis the term marine/lacustrine relates to the ionic strength of water at the time of deposition. Much of the variation in the Swedish quaternary clays stems from the interplay between land uplift caused by the retreat of the Weichselian glacier and the rising sea levels and the influence this had on the physiochemical deposition environment. This uplift continues to this day at varying rates across Scandinavia.

The oldest clays studied were deposited during the late Weichselian period. At this time the West Coast of Sweden and Norway remained a marine environment, however, the Göta River valley was a major drainage channel for glacial melt water thus gave rise to glacio-marine clays (Sites 1 to 8). At the same time on the Swedish East Coast land uplift caused by deglaciation produced a freshwater lake known as the Baltic Ice Lake around 13000 to 11 600 BP, Jensen (1999).

The structure of the glacio-marine clays are heavily influenced by the ionic concentration of the seawater, sediment transport load (speed of accumulation), sea /fjord bed topography, landslide and erosion activity, ice rafting, distance to the ice front, depth of water and temperature (affecting biological activity). As shown by Suzuki and Matushi (2015) in concentrated ionic solutions rapid flocculation of clay particles occurs, forming dense silt sized particles and it is generally accepted that such particles were formed as glacial meltwater flowed into the sea through the Göta River valley giving the glacial Swedish West Coast clays a typical structure as indicated in Figure 4.1(a). In lower strength ionic solutions less silt was deposited within the clay matrix, but was often present in similar quantities, but instead as separate silt partings, refer to Stevens (1990) and Bergsten (1991). To illustrate the differences due to depositional environment glacio-marine clays from 45m and 55m are shown in Figure 4.3 (a) and (b). These samples have identical sedimentation curves but very different structure due to differences in the physiochemical environment at deposition where (a) has discrete silt partings while (b) has the same quantity of silt, however, in this case silt lies primarily within the clay matrix and not as discrete layers. Such differences give rise to varying robustness during sampling and storage, refer to Hvorslev (1949). Significant digenesis has occurred in these clays due to biological oxidation of organic matter resulting in the formation of hydrogen sulphide (*HS*), further biologically mediated reactions resulted in the formation of sulphur and sulphur compounds, which under these conditions reduced Fe(III) ions to Fe(II). These ions reacted with hydrogen sulphide to form iron sulphide minerals such as FeS and FeS_2 which can be identified by their dark grey or black colour. For details of these reactions refer to Cornwell and Morse (1987) and Stevens *et al.* (1987).

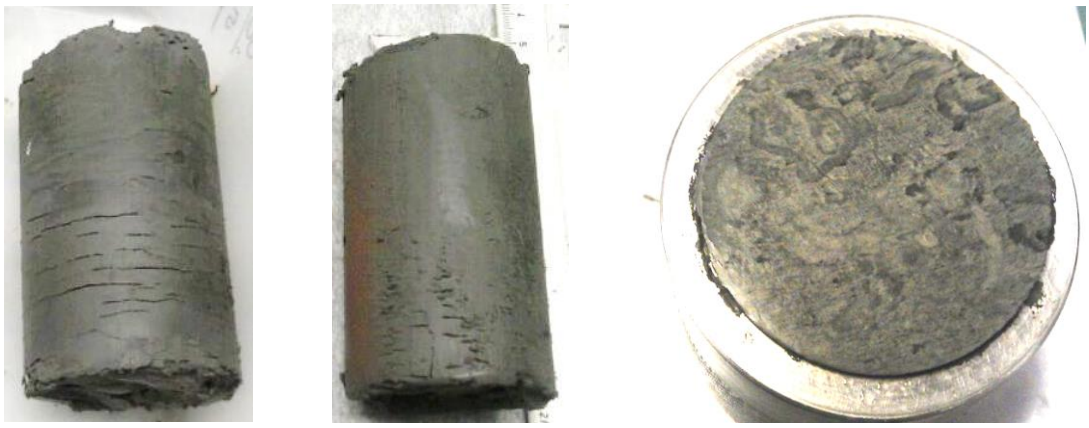

(a) (b) (c)

Figure 4.3 Gothenburg glacial clay: (a) 55m: silt partings every 5mm, (b) 45m: no silt partings evident (same amount present within clay matrix) (c) 27m: sulphide staining from digenesis.

The glacial soils deposited on the East Coast at this time (Figure 4.1 (b)) were also significantly affected by the variable sediment load and speed of meltwater flow, which affected the deposition environment leading to seasonal varves. The varves have very different thicknesses and constituent materials, as indicated by Figure 4.4 (a) and (b). Digenesis also occurred within these soils through the actions of biological activity of sulphate reducing bacteria and resulted in their brown/beige colour. Clays dominant in Fe (III) irons (Fe_2O_3) are typically reddish brown in colour, while clays dominant in Fe (II) irons (Fe0) are typically grey, Stevens *et al.* (1987).

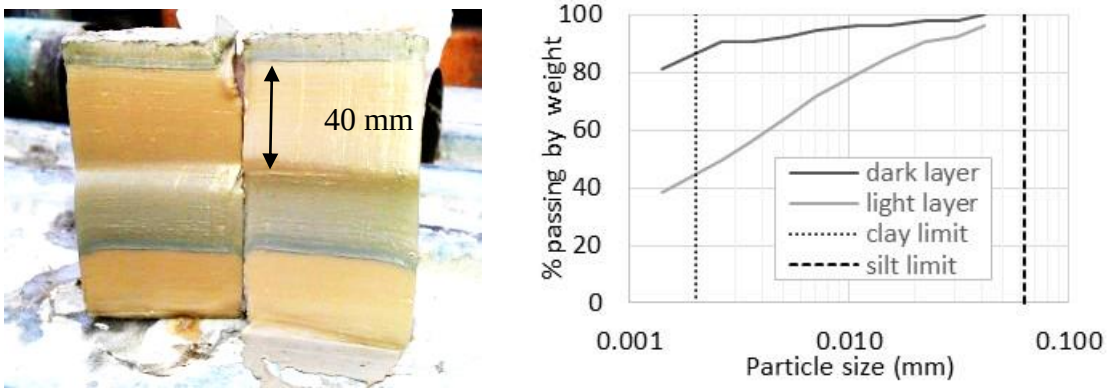

Figure 4.4 (a) Glacial lacustrine varved clay from Site 10, (b) Variation in sedimentation curves of light (brown) varves and dark (grey varves).

There are different schools of thought regarding the exact geological history of the East and West coast clays in Sweden. However, an appreciation is required given its impact on the ability of samples extracted to reproduce behaviour representative of field conditions. The following account is based on descriptions found in literature that appear to be consistent with findings during field testing and sampling within this work.

The first break through of the Baltic Ice Lake is thought to have occurred around 11,300 BP, Jensen *et al.* (1998) and marked the start of sedimentation of post glacial sediments. Under a short period, an area of the Baltic Ice Lake became a deep brackish deposition environment known as the Yoldia Sea until around 11 200 BP, and clay deposits from

this time can be found on the Swedish East Coast (and within the sites studied). The water level in the Baltic Ice Lake was higher than the surrounding sea, thus when the drainage occurred it was rapid and part of this fast moving meltwater was transported through the Göta River valley to the Swedish West Coast. Sand layers found at the boundary of the glacial and post glacial clays in the Göta region are reported by a number of sedimentary geologists, Stevens (1990), Persson (2014), to be evidence of drainage of the Baltic Ice Lake. However, these deposits may also have been formed from ice rafting or slope failures upstream, Bergsten (1991). Further land rise continued to lift the land mass out of the sea and in the east a new fresh water lake was formed around 10500 to 7800 BP, known as the Ancylus lake. During this time, significant reworking occurred in some of the lacustrine deposits on the East Coast, typified by the clay shown in Figure 4.5 as such these clays are highly variable and heterogenous. The area marked "undisturbed varves" in Figure 4.5(a) are clearly not undisturbed but appear to have maintained the original lacustrine varved structure, while other areas have been completely resedimented, in what was most likely a fairly rapid deposition environment given the presence of both sand and silt within this 50 mm diameter STII sample cross-section.

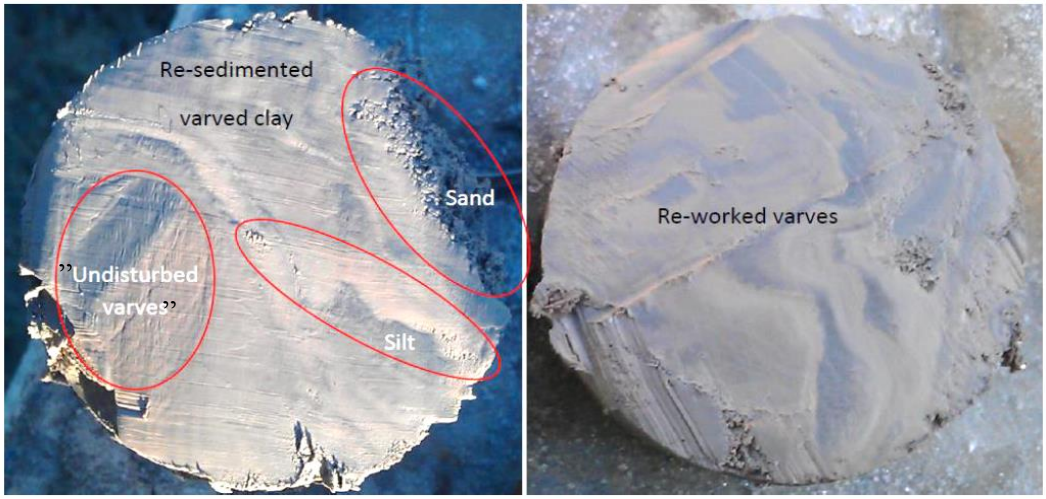

Figure 4.5 Reworked/resedimented glacial lacustrine varved clay, (Site 11).

The presence of the Ancylus Lake reduced sediment loads though the Göta River valley giving less sedimentation in the deep sounds (high ionic concentrations in deposition environment). From around 9000 BP an erosional estuarine environment occurred, giving higher energy depositional environments (more silt and flocculated clay structure) until around 5000 BP after which shallow water transitional conditions prevailed and marine muds were deposited in sheltered areas. The city of Gothenburg lifted out of the sea around 2000-3000 years ago, Klingberg *et al.* (2006) with further sedimentation limited to transitional marshland areas.

On the East Coast the Ancylus Lake area was reconnected to the North Sea, and sedimentation once again occurred in a salt water environment, SGU (2009). The transition phase of the Ancylus Lake to a marine environment is sometimes given the name the Mastogloia Sea, and refers to the period when connection to the Atlantic Ocean was not continuous. As sea levels rose, continuous connection was achieved and the Littorina Sea was formed. The land mass continued to lift reducing the size of the Litorina Sea, giving the Post Litoria Baltic Sea we know today at around 4000 BP. At

this time Site 10 had lifted out of the sea while Site 9 and 11 remained below sea level until between 1500 and 1000 years ago.

Digenesis driven by bacterial activity has also occurred in the post-glacial marine clays (East and West Coast). Given the slightly warmer climate, this activity was often more prolific resulting dark grey/black clays. In these deposits it was not uncommon to find larger pores visual to the eye, which may be indicative of pores which were gas filled prior to extraction (gas bubbles are commonly observed in standing water within deep excavations in these soils and observations of pockets of gas during sampling are not uncommon), in addition to other local anomalies such as shells, holes left from degraded marsh grass, marsh grass remnants and sand/silt filled vertical cracks (desiccation/tension cracks).

At Site 12 the glacial ice retreated from around 11000 to 9000 years ago, then returned but retreated again around 6000 years ago causing significant erosion, followed by estuarine deposition, the effects of which need to be considered when determining OCR/POP profiles. The shallow sediments at Site 12 relate to more recent post glacial wave-affected near shore deposition thus have higher silt and sand content while sediments below around 15 m relate to deep marine deposition (≈ 150 m).

4.4 Local geology, sampling observations and stress history

Göta River Valley Sites (Site 1 to 8)

The soft sediments in the Göta River valley have been geologically classified by numerous authors, however the work by Stevens (1990) (focus on sedimentary geology) and Bergsten (1991) (focus on nature of sedimentation environment) is amalgamated here to give a geological classification of the typical ground profile and is presented in Table 4.1. The extent of soft clay sediments below which moraine and crystalline rock resides varies, thus Zone 3a and/or Zone 3b clays are not present at some of the sites studied. In Gothenburg, further subdivision of some geological layers were made for the purposes of the ground profile, given the influence of erosional boundaries as these gave rise to changes in observed *in situ* behaviour, refer to Figure 4.7.

The detailed location of the Gothenburg city sites is presented in Figure 4.6. Sites 1, 2, 3 and 6 have clay deposits up to 115 m thick, while Site 4 and 5 have clays to around 42 m and 36 m respectively. Site 1 to 6 share similar stress history relating to loading from land reclamation works in the 1800's, which was typically achieved using dredged sediments from the Göta River. Site 4 has, however, experienced some unloading caused by excavation of a canal in the late 1800's, while Site 5 has also been subjected to significant unloading/reloading, associated with excavation of a dock which was later backfilled in 1934. Site 6 lies on the West Bank of the Göta River, however *in situ* profiling does not indicate significant variation to the other sites, which are located near the East Bank of the Göta River. In general fills above the clay did not exceed 2-3m, but were locally up to 7.5m thick (within the infilled dock at Site 5). The boundary between the dredged sediment fill and Zone 1A clays is often difficult to identify, given the similarity of these soils.

Table 4.1 Overview of the ground profile and sedimentation environment for Göta River valley clays (PG=post glacial, G= Glacial).

Strata	Age (years)	Deposition Environment	Elevation (±2m)
Made Ground	≈ 150	Fill placed on transitional marshland areas	≈ 2- 7.5m
PG Zone 1A clay	3000	Temperate climate deposition in brackish water-transitional environment	2 -5.5 m
PG Zone 1B clay	5 000	Erosional estuarine environment	5.5-8 m
PG Zone 1C clay	10 000	Cold conditions estuarine deposition	8-12 m
PG Zone 2D clay	10 600	Highly variable cold conditions, variable sediment and salt concentrations in estuarine deposition environment	12-21 m
G Zone 3aD clay	12 000	Artic conditions rapid sedimentation (very open structure)	21-42 m
G Zone 3bD clay	13 000	Artic conditions clay varves, deep water deposition (possibly inter stadia clays below 62m).	42 to ≤ 115 m

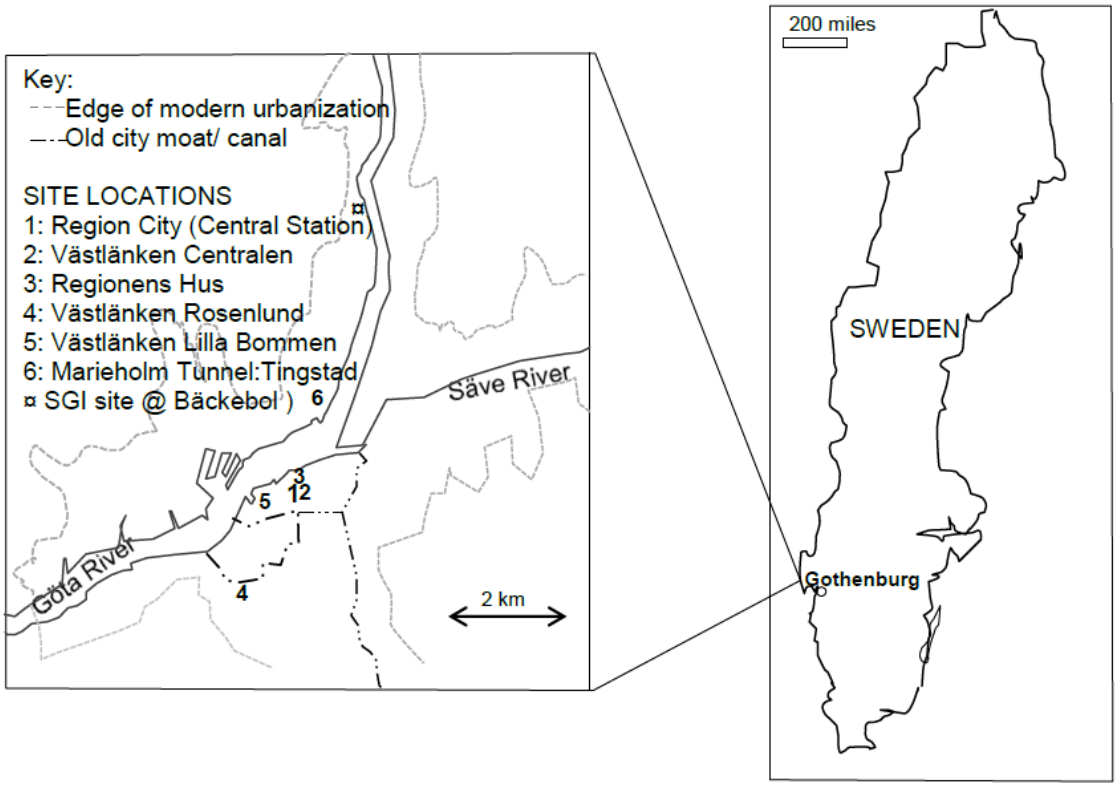

Figure 4.6 Location of sites within Gothenburg used within this study, the location of SGI Bäckebol Research Site, Larsson & Mulabdić (1991) is also marked ¤

Field measurements such as the cone penetration tests (CPT), the field vane tests, and the seismic dilatometer tests (SDMT) indicated mainly homogenous soils within Gothenburg as indicated in Figure 4.7. However, at the upper end of the profile (post-glacial clays) some differences are noted pertaining to recent stress history, particularly in SDMT profiles (V_S, K_D and E_D), refer to Wood (2015). Similarly, the clays at the bottom of the clay profiles included more sand and silt partings, associated with higher energy deposition. Given that the elevation of this boundary varies across Gothenburg, so does the level at which these more sandy- silty clays are found (which in field vanes tends to give lower values, refer to Figure 4.7 (longer rectangular data points).

During field work at Site 1, one of the 8 CPTU soundings could not penetrate further due to a frictional moraine at 58 m and when the CPT equipment was removed from the ground methane gas was released and continued to be released for around two months (100 m from sampling and SDMT positions). The presence of significant quantities of gas is normally associated with extensive bacterial activity in warmer climatic conditions, so there is a possibility that some of the sediments below this level originate from an earlier inter-glacial period. Other observations during piston sample extraction include thixotropy and significant discolouration of samples from grey to brown during storage. This discolouration was most prevalent at the extremities of the sample and along silt or sand partings as shown in Figure 4.8.

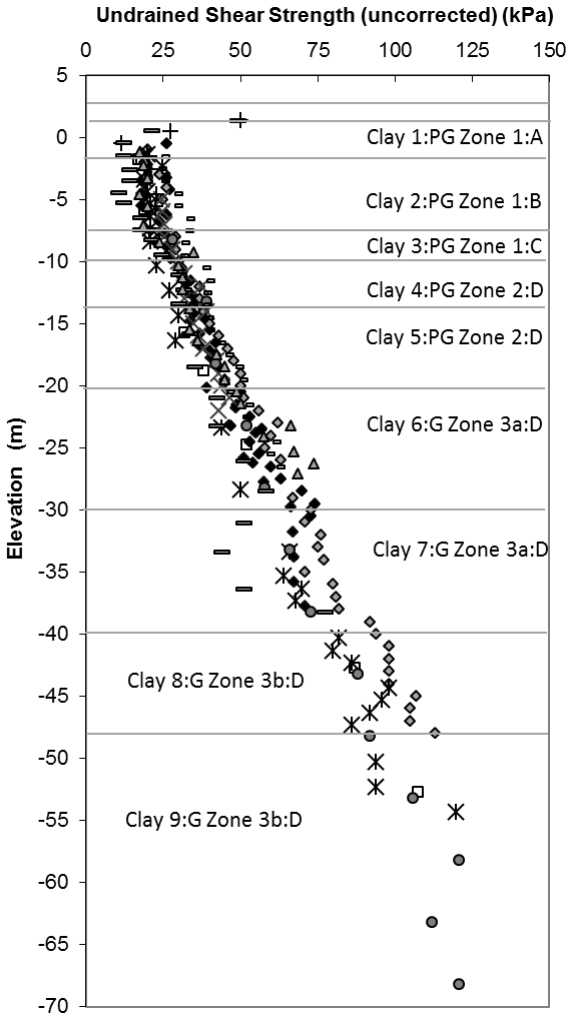

Figure 4.7 Generalised ground profile for Gothenburg (Sites 1 to 6), and uncorrected field vane profiles from around the city of Gothenburg (PG= post glacial, G=glacial).

(a) (b) (c)

Figure 4.8 Observed discolouration post sampling of Gothenburg clay samples (a) Zone 3b clay (55 m) sample age 30 days, (b) Zone 3a clay (27 m) sample age 160 day, (c) Zone 2 clay (18 m) sample age 150 days .

The location of testing at Site 7 is shown in Figure 4.9. Only natural sediments were encountered at the sampling position, however, the Banaväg Väst railway embankment adjacent to this site may have had some influence on these soils.

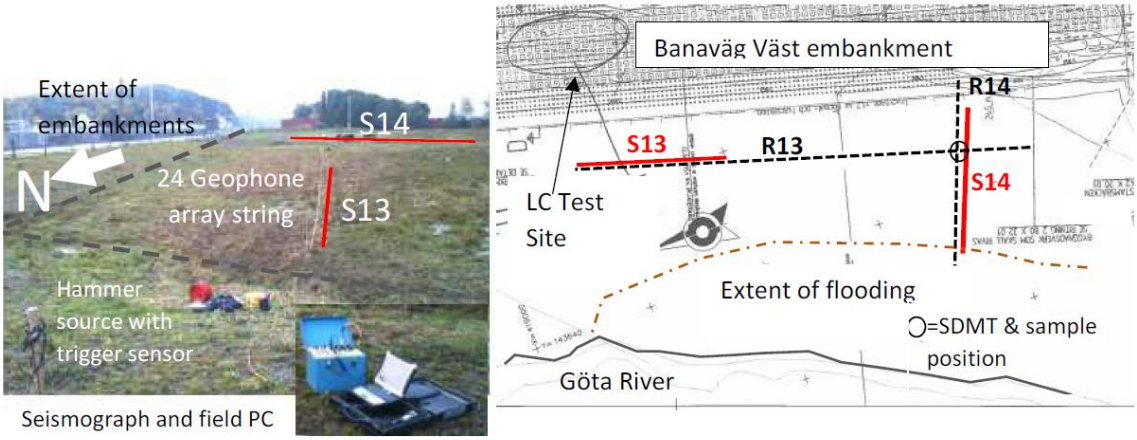

Figure 4.9 Location of Site 7 and position of field testing (S13 & S14 indicates location of MASW testing, R13 and R14 relate to position of ERT testing not included in this work),

Only post-glacial clays were observed to depths of around 20m, significantly greater depths of clay are described by Olsson *et al.* (2009) at this site. Similar to the Gothenburg clays thixotropy was observed immediately following extraction of samples (initially jellylike but stiffened within minutes) in addition to discolouration after storage, which at some levels occurred more rapidly than typically observed in Gothenburg, refer to Figure 4.10(c). This combined with the existence of large pores that may indicate that gas is present and would make samples more susceptible to disturbance. Of note was that the first borehole extracted in 2012 with 8 sample levels had to be discarded for the purposes of studying representative clay behaviour based on a visual assessment of samples. Apart from obvious mechanical damage in samples at 5

m and 17.5 m (cracks or partly filled sample tubes) these samples were also mouldy and discoloured when examined after 45 days. Clays from 2.5 m, 7.5 m, 12.5 m, 15 m and 20 m had no mould, but had significant salt precipitations at the top of the samples suggesting pore water migration and desaturation.

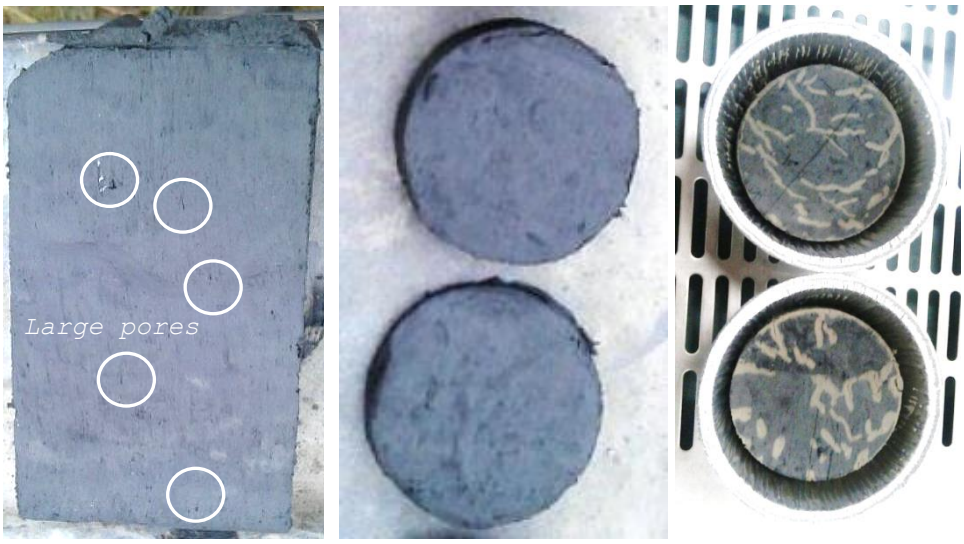

(a) (b) (c)

Figure 4.10 Site 7-17.5m (a) At extraction: vertical cross section from cutting shoe (b) At extraction: lower sample tube horizontal cross section (c) After transport and storage 48 hours- colour change from grey to brown along fissures.

Most of the sites studied were relatively flat. However Site 8 lies within a valley formed by erosion and numerous landslides, as indicated in Figure 4.11 (a) making the clays at this location naturally over-consolidated. Figure 4.11(b) indicates post glacial clays at the position of sampling (cream colour). At the depth studied (5.5 m) the clays are visually similar to the distal glacio- marine clays in Gothenburg found at 55 m depth, i.e. grey and black varves of similar size and colour, compare Figure 4.8 (a) to Figure 4.12 however they are thought to relate to early post glacial deposition even though glacial glacio marine clays are also indicated higher up the valley sides in Figure 4.11 (b) (orange colour) given grass present. Leaching has given rise to immeasurable sensitivities between 3 to 5.5 m depth at Site 8 (S_t> 391 to S_t>500) and is undoubtedly a major cause of landslide activity in the area, refer also to Söderblom (1969).

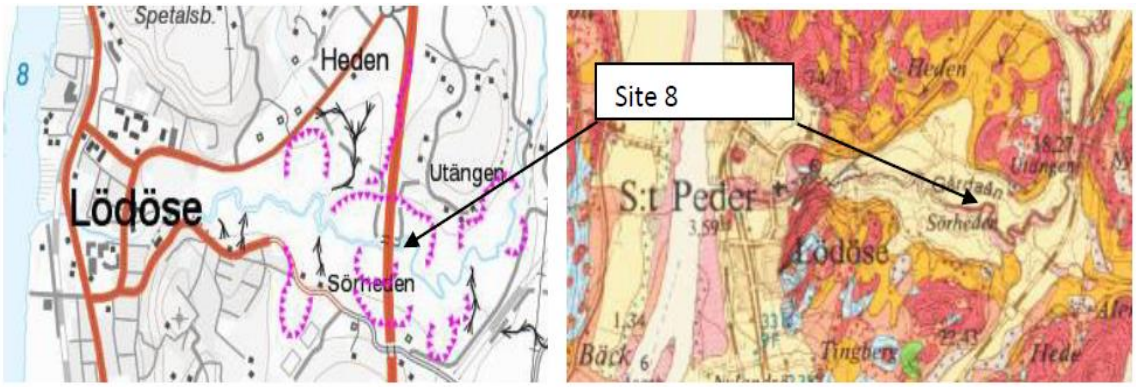

(a) (b)

Figure 4.11 (a) Documented landslide activity around Site 8 (b) Complex quaternary geology map in the area surrounding Site 8, SGU (2015).

Samples were taken during excavation works for re-routing the Gårda River. Macro-scale structure was observed in freshly excavated slopes in the field and oxidised sloping cracks were also noted at regular intervals within the top 1.5 m of the profile. It is thought this may be related to passive relaxation. A number of the block samples extracted had pre-existing shear planes within them, as indicated in Figure 4.12 (b). These shear planes had a shiny yet rough surface typical of solifluction planes, where the shininess stems from alignment of clay particles during small seasonal movements over long periods of time. Block 4 had extensive shear bands some of which were not shiny, and are therefore thought to relate to shear bands caused during transportation and or sampling. This block was unconfined during transportation and lay on the car seat, thus the block suffered significant deformation during transportation as indicated in Figure 4.12 (c) (block originally had straight edges prior to transport). Freshly cut slopes below 1.5 m indicate regular grey and black varves down to 5.5 m with no indication that these clays had been transported (landslide flow). However within 10 minutes of excavation the clay surface had oxidized to a beige colour. Discolouration was also noted in samples when storage time exceeded 30 days, found initially at the position of anomalies such as organic matter, pre-existing shear planes (helping identify them as seen in Figure 4.12 (b) and (c) and at the edges of the samples. The discolouration of samples tended to be initially light grey, but later changing to a beige colour. When preparing the test specimens, the parts of the block samples with oxidation and visible pre-existing shear bands were discarded.

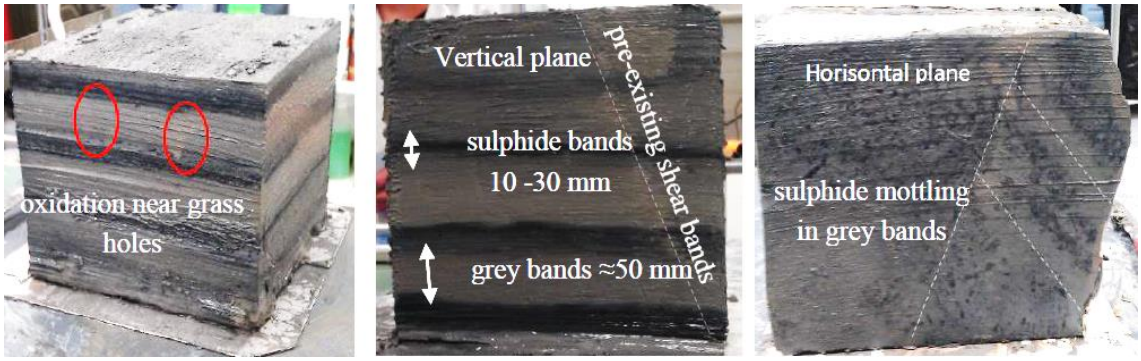

(a) (b) (c)

Figure 4.12 (a) Block 2 local visible oxidation after 36 days, (b) Block 2 magnitude of varves and oxidation along a pre-existing shear band in Block 2, (c) sulphide mottling and oxidation along pre-existing shear bands in Block 4.

Swedish East Coast-Uppsala sites (Site 9 to 11)

The locations of the sites in Uppsala are shown in Figure 4.13 together with the quaternary geology map of the area. All three sites are flat. Site 9 and 11 are at the same elevation, while Site 10 lies at a higher elevation (by 8 m). At all three sites the topography of the underlying crystalline bedrock and frictional glacial sediments varies which has contributed to varying geological profiles at the three sites. All three sites include glacial lacustrine reddish brown varved clays (as shown in Figure 4.4). However, these occur at different elevations with differing degrees of geological reworking. At Site 10 only the glacial lacustrine clays were observed, while at Site 9 and 11 the upper part of these sediments had been reworked before being overlain by post glacial marine deposits, refer to Figure 4.5. Samples extracted from Site 9 appear to capture a number of different clays relating to the evolution of the Baltic Sea as indicated in Table 4.2.

The recent stress history at Site 9 relates to placement of fill in the 1940's and dewatering of the underlying aquifer since the 1980's. Due to the influence of the dewatering, the sediments are lightly consolidated in the upper layers but tend to a normally consolidated state at the base (porewater pressures < hydrostatic conditions). Observations from sampling at this site include difficulty in extracting samples from the post Litoria Sea sediments (upper 5 m).

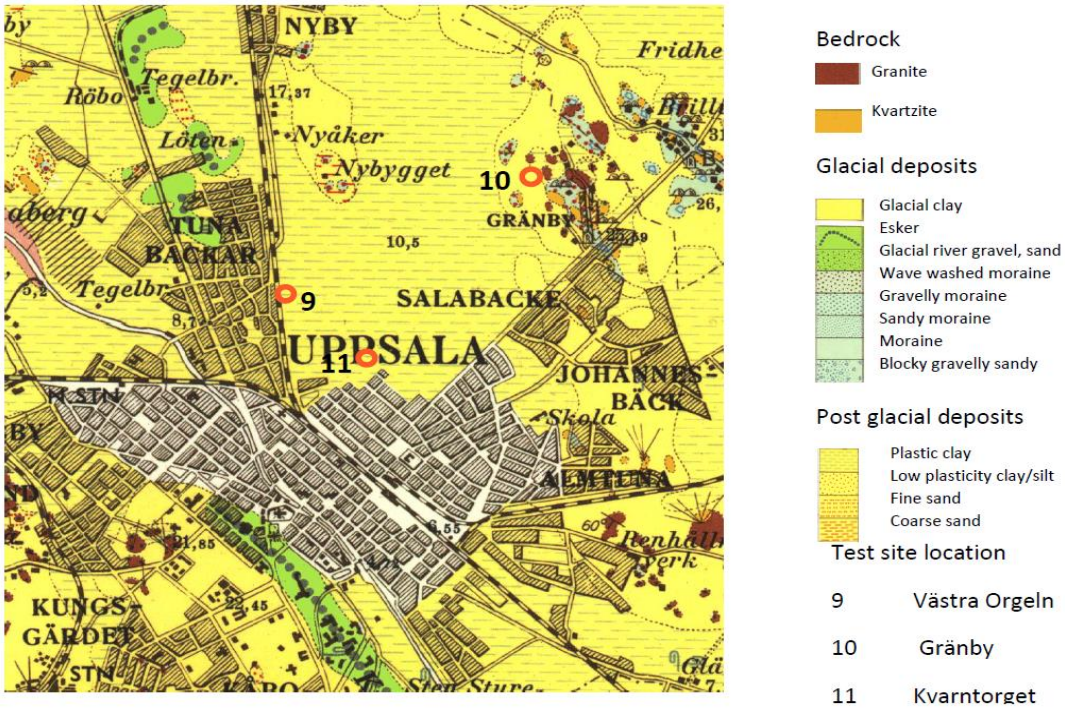

Figure 4.13 Quaternary deposits and site locations in Uppsala, adapted from SGU (1966).

*Table 4.2 Ground profile and interpretation of sedimentation environment for Site 9 * clays sampled within this project*

Ground Profile	Depth (m)	Interpretation of Sedimentation Environment
Fill	0 -1.5	Fill placed within the last 100 years
Black/dark grey gyjitig sulphide rich clayey Silt with shells*	1.5 -5	Shallow sedimentation in the Post Litorina Sea (similar to present day salinity)*
Black/dark grey sulphide rich clayey Silt with mussel shells (locally defined as sulphide Clay)*	5-11	Rapid marine sedimentation within the Litorina Sea (high ionic concentration)
Sulphide mottled grey Clay	11-14	Sedimentation in saline stratified, brackish water associated in the Mastoglica Sea
Grey clay with silt partings	14-18	Fresh water sedimentation in the Ancylus Lake
Grey varved clay*	18-21	Rapid fresh water sedimentation just before the break through of the Baltic Ice Lake
Reddish brown/grey varved clay with silt partings*	21-24	Fresh water sedimentation within the Baltic Ice Lake
Reddish brown/grey varved clay relocated by landslide activity (vertical varves)*	24-27	Fresh water sedimentation within the Baltic Ice Lake subject to reworking during deglaciation (rotated 90° vertical varves)
Reddish brown/grey varved clay with silt and sand partings	27-44	Fresh water sedimentation within the Baltic Ice Lake

Samples taken within the Litoria sediments (organic clayey silt) also had a strong smell of hydrogen sulphide, as well as numerous mussel shells, refer to Figure 4.14 (a). Like the samples from Nödinge, these samples oxidised quickly when stored at 7 °C and 100 % humidity, refer to Figure 4.14(b). Samples taken at the position of an "anomaly" in the SDMT profiles were reworked lacustrine sediments that were rotated approx. 90 °, refer to Figure 4.14(c).

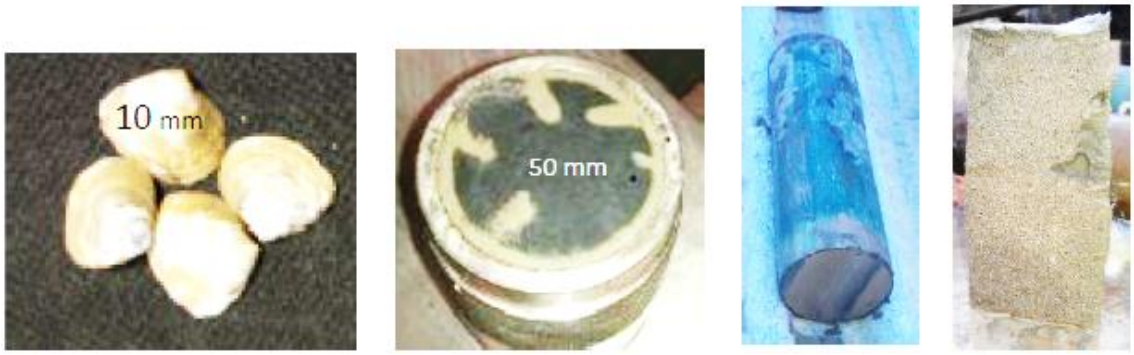

(a) (b) (c) (d)

Figure 4.14(a) Mussel shells from Site 9:9 m (b) Oxidation of samples from Site 9:9 m (c) Evidence of landslide activity Site 9: 25 m (d) Sand filled tension crack evident in samples at Site 10: 8m.

Site 10 is located at a sports field, which was previously used for agriculture, thus no loads had been applied through human activity. There is some evidence suggesting geological unloading, however similar to Site 9 dewatering of the underlying aquifer has caused the clays to alter from an over-consolidated state to a normally consolidated state at the base of the clay deposits. Previous ground water measurements at this site suggest that drawdown of the piezometric head has occurred since the mid 1980's. Below a desiccated 1.5 m thick dry crust, reddish brown-grey lacustrine clays were found to depths between 6 to 12 m and had similar colouring and stratification as Site 9 (final clay stratum in Table 4.2). Samples and field testing used in this study were conducted in the area with 12 m thick clay deposits. No evidence of landslide activity or sediment reworking was identified, however, a thin vertical sand filled crack was found at 10.5 m which was at least 0.5 m in length (present in all sampling tubes), which may be related to an erosion boundary. This site was above the sea level during deposition of the Post Litoria Sea sediments, and the deposits from the Litoria Sea appear to have been removed following its recession.

At Site 11 the geological sequence is similar to Table 4.2 except that each stratum is thinner and higher deposition energies have resulted in greater proportions of silt and sand in the lacustrine varved clay. The lacustrine clays were found at higher elevations than Site 9 (between 8 to 23 m below ground level). At a depth of 13.5m the glacial varved clays were significantly reworked with relatively speaking "undisturbed" varved clay clumps present within a matrix of re-sedimented silty slightly sandy clay as indicated in Figure 4.5. Field testing and sampling at this site was conducted within an existing building. This low rise building was founded on an end bearing precast concrete pile foundation; a void of around 60 mm was present between base slab and underlying fill, indicating that significant settlements had occurred since construction approximately 30 years earlier. No excess pore water pressures could be identified in piezometer measurements relating to loads applied, this is no doubt masked by the effects of drawdown associated with water extraction beneath the clay. The marine clays at Site 11 were much denser than those found at Site 9, indicative of a more

compact clay structure, and possibly brackish environment. The clay profile was lightly consolidated tending to normally consolidated at the base, similar to Site 9 and 10 due to dewatering of the lower aquifer.

Norwegian West Coast-Trondheim site (Site 12)

The extent of sediments from differing deposition environments found in Trondheim is indicated in Figure 4.15. The sampling locations BH809 (Site 12A) and BH823 (Site 12B) lie within the E6 cut-and-cover tunnel project: Trondheim-Størdal are also shown in these figures and lie close to the River Nidelva. The deepest profile, BH809, had clays of low to medium plasticity and low sensitivity while the sediments found at BH823 contained much more silt, most likely due to the proximity of the bedrock causing increased influence by base currents. The upper sediment deposits at BH823 are defined as clayey marine silt, while the lower deposits are defined as silty marine clays. Leaching of salts from these deposits has resulted in highly sensitive quick clay conditions, the approximate extent of which is indicated in Figure 4.15(b) marked in red. This boundary was determined based on resistivity testing and extensive sampling, but given the potential inaccuracies of resistivity testing should not be viewed as exact. Both profiles have been preloaded with fill associated with development of the harbour area, however, the field and laboratory tests suggest that over-consolidated conditions exist at the surface of the sediments, reducing to lightly over-consolidated conditions at depth. It is possible that the over-consolidation in the upper clay/silt profile has been caused by geological erosion and that the influence of placement of fill is small in comparison. Field seismic testing (SCPT and MASW) used within this report for Site 12 is taken from work by others at another research site (Tiller) approximately 8 km south of Site 12 but that lies within the same geological deposits and at a similar distance from the River Nidelva. The Tiller research site was set up to study the clays found within the E6 Trondheim- Størdal project. Both field and laboratory testing from Site 12 and the Tiller site were very similar given that they shared the same depositional environments and geological history.

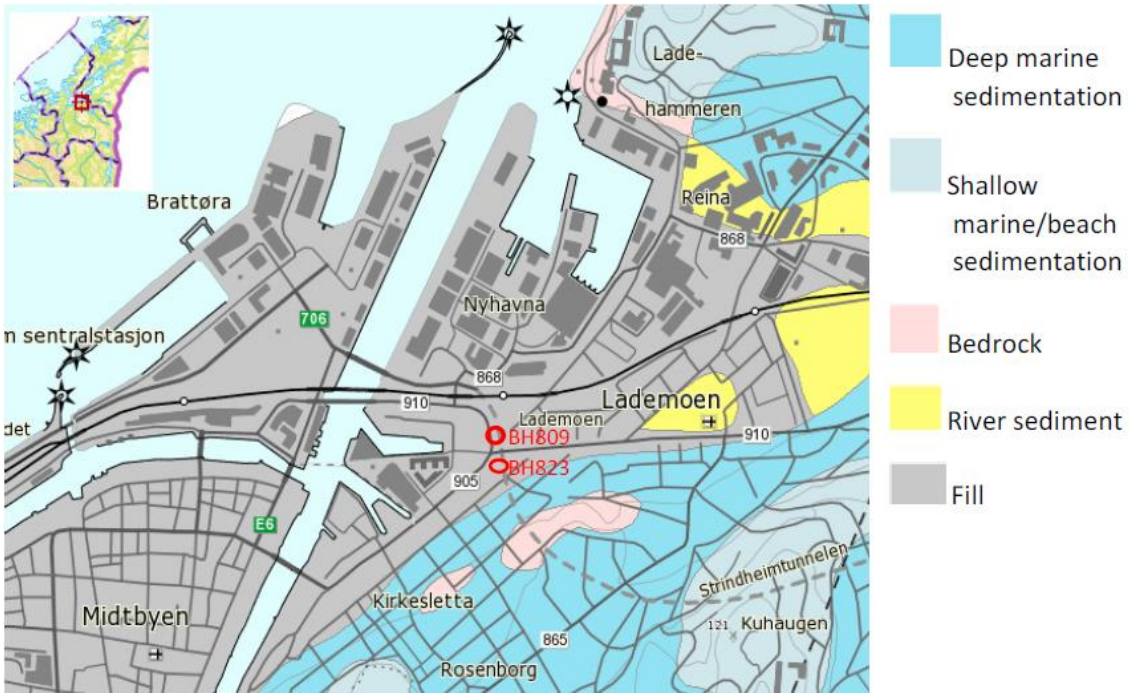

(a)

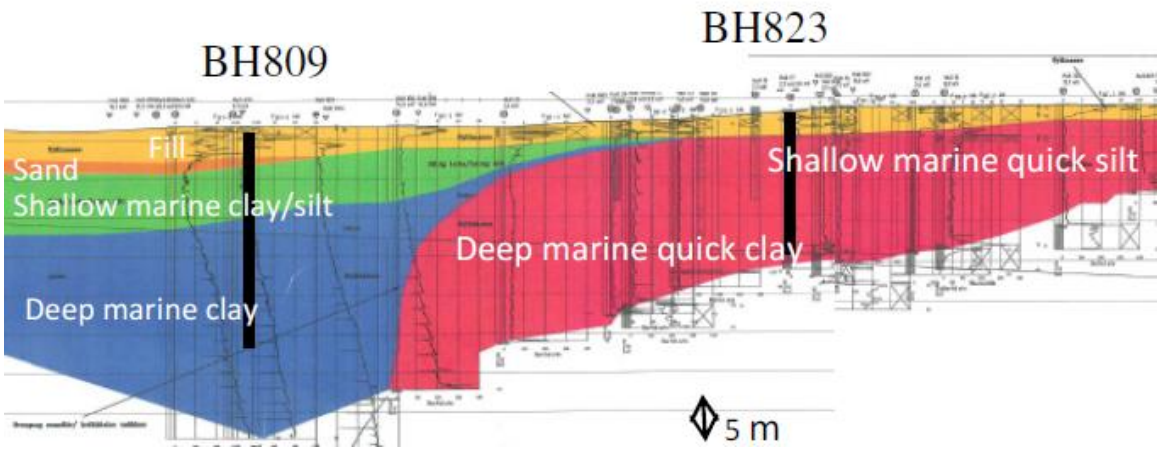

(b)

Figure 4.15 (a) Quaternary geology map of Trondheim with location of boreholes, adapted from NGU (2015), (b) Ground profile at the position of sampling in Site 12 adapted from VV (2007).

4.5 Basic geotechnical classification of soils studied

The basic geotechnical classification of the samples studied is presented in Table 4.3. Note, that for the varved clays the average properties are given and not properties specific to the individual varves. The wide range of soils tested is further confirmed when the soil classification from cone penetration (CPTU) tests are plotted (Robertson, 1990) in Figure 4.16 and the Skempton (1953) activity chart in Figure 4.17:

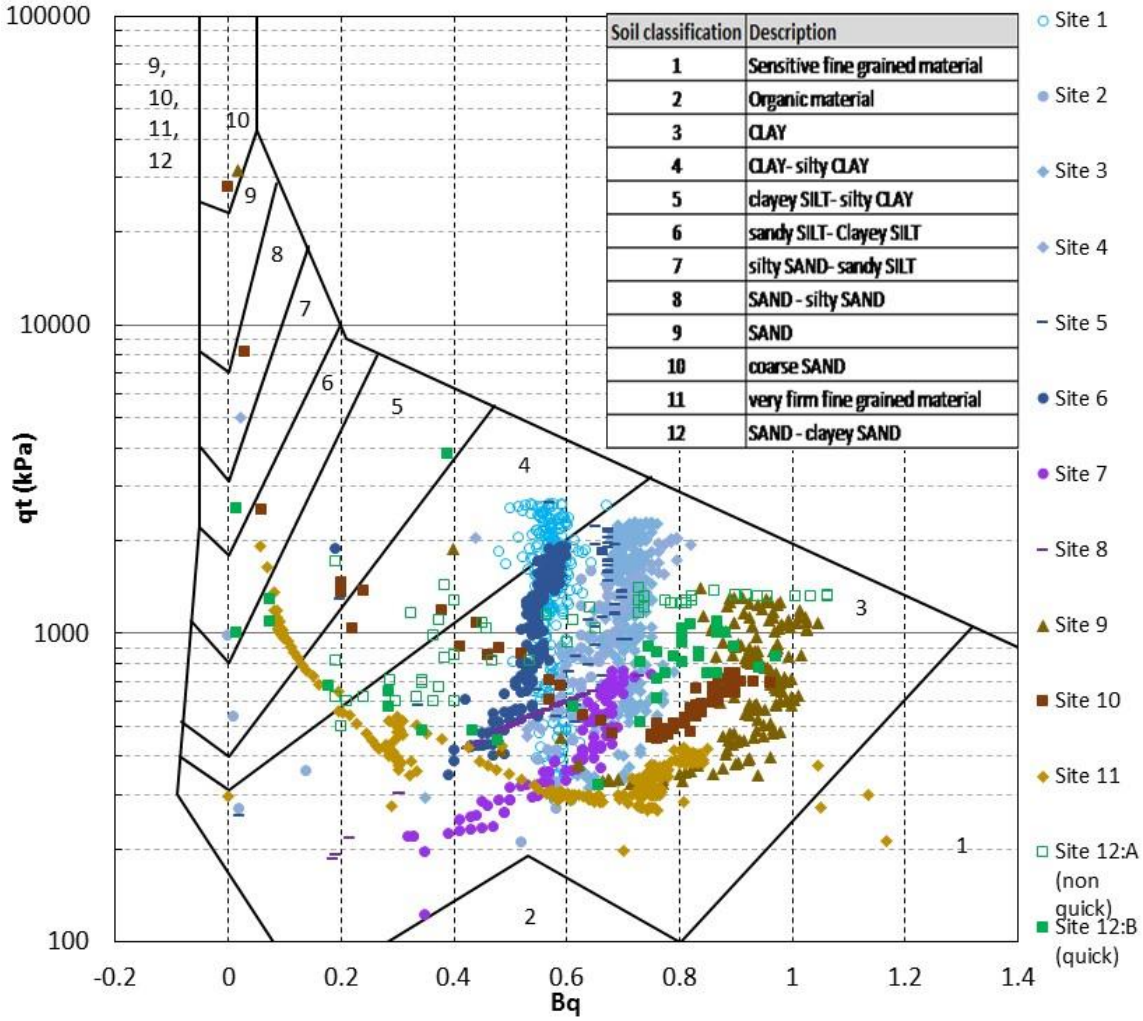

Figure 4.16 CPTU Robertson (1990) soil classification chart for the tested sites.

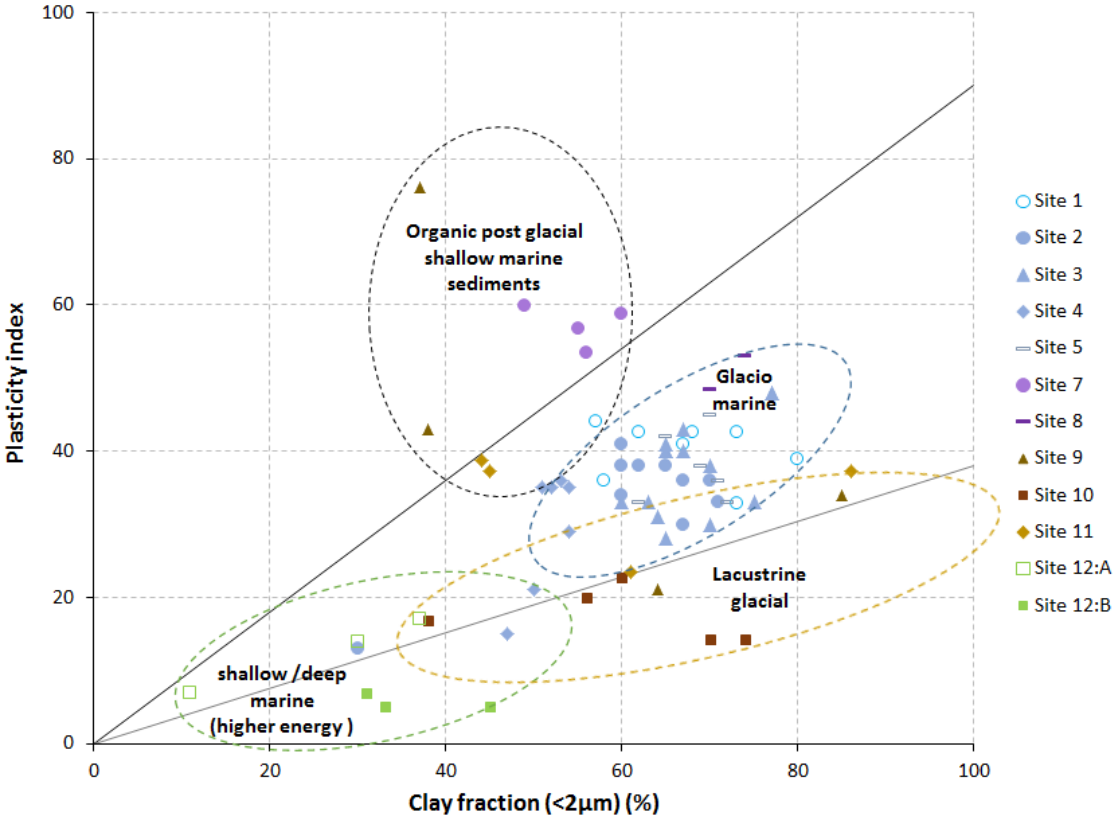

Figure 4.17 Skempton (1953) activity classification chart and sedimentation environment.

Table 4.3: Summary of soils and basic properties PG=post glacial, G= glacial, NC=normally consolidated, LC= lightly consolidated, OC= over consolidated.

Site No.	Soil Description (below fill/top crust 0.5-2 m)	Basic soil property range at sites							
		ρ t/m^3	W_N %	W_P %	W_L %	τ_v kPa	S_t $\frac{\tau_v}{\tau_{Rv}}$	% clay mass	*OCR* from CRS
1	LC PG organic silty marine clay to sulphide stained silty marine clay then G marine sulphide rich/stained silty clay to G marine sulphide varved silty clay (to ≈ 110 m)	1.55-1.68	71 - 59	31-26	100 -70	15-150	21 - 9	70 – 55	1.6 - 1.3
2	As above	1.54-1.64	84 - 61	41 - 31	72 - 49	19 - 55	30 - 4		1.44 1.33
3	As above	1.52 -1.66	94 - 59	43 - 27	84 - 59	21 - 112	33 12		1.4 1.2
4	As above- somewhat more silt present (clays to ≈ 44 m)	1.61-1.91	66-40	35-24	70-39	37 - 55	18-8	54 - 47	1.65 1.27
5	As above but clay from 8m-filled dock base (clays to 38m)	1.56-1.71	68-53	35-24	78-58	22 - 38			1.5 1.2
6	As above (clays to ≈ 110 m)	1.5-1.8	100 -50		95 - 40	5 - 90	30 -10		1.5 1.23
7	LC, PG silty clayey gyttja, LC-NCorganic PG silty marine clay (to 20 m)	1.47-1.56	100 - 74	36-29	99 - 71	11-25	15-8		1.4 1.1
8	OC quick G silty sulphide varved distal marine clay (clays to ≈ 12 m)	1.49	90			28-30	> 500	75-70	2
9	LC PG organic clayey marine silt, NC G clay and NC G lacustrine varved clay /evidence of landslide (vert. varves) (clays to ≈ 41 m)	1.39-1.89	106 - 32		122 - 41	14-44	22-5	90-36	1.3 1.0
10	OC to NC G lacustrine varved clay with silt and sand lamina (to ≈ 11 m)	1.73-1.88	55-32	20-18	50-36	17 - 21	28-7	70-55	3.0 - 1.0
11	LC PG organic silty marine clay over LC to NC PG lacustrine varved clay with silt and sand/ reworked in places (to ≈ 22 m)	1.58-1.81	77-45	46-20	82 - 46	12-34		86 - 44	1.7-1.0
12	OC-LC PG marine clayey silt and G silty clay /quick PG marine clayey silt and G silty clay (clays to ≈ 31 and 24 m)	1.89-2.05	35-24	23-16	38-27/ 21-25	59-34/ 15-9	22-4/ 15 2-97	45-10	2.5 – 1.2

where; ρ is the soil density, W_N is the natural water content, W_P is the Atterberg plastic limit, W_L is the Atterberg liquid limit, τ_v is the uncorrected undrained field vane strength, S_t is the sensitivity (typically determined from field vane), % clay < 2μ sized particles (by weight) based on particle sedimentation tests. The OCR in this table is given based on CRS tests, assessed using the Sällfors (1975) -this is not necessarily the same as the OCR in the field or from stepwise IL oedometer tests, discussed later.

4.6 Classification of sample quality of clay specimens studied

An assessment of sample quality is essential if the relevance and representativeness of laboratory tests to describe the *in situ* soil behaviour is to be appreciated. For the clay specimens studied within this work, an assessment of the degree of disturbance has been made with the help of the existing sample quality assessment methods. However, this is difficult to do convincingly due to the complexity of the natural clay samples, and the limitations of the assessment methods themselves. The different methods of assessment used are indicated in Table 4.4 which summarises the results of different quality assessment methods for a selection of 29 clay specimens out of 257 specimens assessed. The assessments presented in Table 4.4 reflect typical results for samples with different geological origins or different sample disturbance chains and test procedure. The existing assessment methods sometimes gave extremely varying assessments of quality. Thus when assessing sample disturbance in specimens one must continuously question the accuracy of the applied method, and its relevance to the specimen being assessed. When the same assessment of quality was defined for a given specimen using different assessment methods, this gave additional confidence however when large differences were noted greater weight was placed in the findings of the Lunne *et al.* (1997) pore volume criteria ($\Delta e/e_0$). Further discussion on the visual and volume change assessment methods is given below, while discussion on non-destructive quantative assessment methods based on suction and shear wave velocity can be found in Appendix A7.

Reflections on qualative methods: visual assessment ('touch' and 'sound')

When preparing samples a number of senses can be used to give an indication of disturbance. Visual observations comparing digital photos taken at extraction and at the time of testing were often very useful and could easily be integrated into standard laboratory procedures for both identification of mechanical damage, and the issues associated with chemical and biological changes during sample storage. In terms of mapping the changes during storage, this was particularly true for marine sediments as discolouration (related to chemical and biological changes during storage) of iron sulphide could easily be identified by photographic means and an assessment of the volume of the sample affected could be made. Some examples of the discolouration observed in different soils were given in Section 4.4. For lacustrine samples identification was more difficult, as the colour changes were more subtle. For these clays other "senses" were often more useful in identifying low disturbance samples, such as the "wetness" to the touch, or if the plastic foil placed on the sample at extraction was still completely adhered to the clay at the time of testing. In addition, during opening of sample tubes there was also a noise associated with less disturbed samples relating to air being drawn into the samples, when exposed to the atmosphere. This noise was not observed for desaturated or disturbed samples.

Table 4.4 Typical variations in quality assessments from different test specimens (darkness related to degree of assessed disturbance, white=low disturbance-very good to excellent quality, light grey= some disturbance-good to fair quality, dark grey=disturbed-poor quality, boxes with dots indicates that no data was available for that specific assessment method), refer to Table 3.13 for definition of parameters.

Specimen data and quality assessment								Larsson	Lunne	Landon	Tanaka	After Donohue and Long	
Site	Depth (tube) (m)	Sample Method	Test Procedure	Test Type	e_0	Age (days)	Visible change (colour change)	$\Delta V/V_0$	$\Delta e/e_0$	$\frac{V_{S\,unconf}}{V_{S\,field}}$	$\frac{u_r}{\sigma'_{V0}}$	L_{VT}	L_U*
1	10 (UT)	$STII_{slow}$	BES: Method B	CAUC	2.12	0	N	0.017	0.025	0.74	0.06	0.5	0.81
1	10 (MT)	$STII_{slow}$	Std: Method B	CAUE	2.12	2	N	0.018	0.026	0.70	0.07	0.43	0.76
1	10 (UT)	$STII_{slow}$	Standard rate	CRS	2.12	0	N	0.020	0.029	0.74	0.06	0.5	0.81
1	10 (MT)	$STII_{slow}$	24 hour steps	IL	2.12	4	N	0.028	0.041	0.70	0.07	0.43	0.76
1	10 (OT)	$STII_{slow}$	Std: Method B	DSS	2.12	11	Y (<10%)	0.013	0.018	0.65	0.03	0.58	0.91
3	11 (MT)	STII	BES:Method A	CAUC	1.87	84	Y (≈50%)	0.04	0.055	0.75			
3	4	$Block_{unconf}$	Standard rate	CRS	1.87	1	N	0.02	0.027	0.8	0.263	0.25	0.12
3	11 (MT)	$STII_{60\,L50}$	Std:Method A	CAUC	1.87	9	N	0.02	0.023	0.61			
3	11 (UT)	$STII_{60\,P50}$	Std:Method A	CAUC	1.87	11	Y (<10%)	0.03	0.041	0.51			
3	11 (UT)	$STII_{P38}$	BES:Method A	CAUC	1.87	84	Y (≈60%)	0.05	0.071	0.74			
1	18 (UT)	$STII_{slow}$	Std: Method B	CAUC	1.85	4	N	0.007	0.011	0.73	0.10	0.56	0.61
1	18 (MT)	$STII_{slow}$	BES: Method B	CAUE	1.85	0	N			0.87	0.17	0.41	0.44
1	18 (MT)	$STII_{slow}$	Standard rate	CRS	1.85	0	N	0.009	0.014	0.87	0.67	0.41	0.44
1	18 (UT)	$STII_{slow}$	24 hour steps	IL	1.85	4	N	0.024	0.037	0.73	0.14	0.56	0.61
1	18 (OT)	$STII_{slow}$	Std: Method B	DSS	1.85	5	N	0.009	0.014	0.65	0.07	0.53	0.72
1	35 (UT)	$STII_{slow}$	BES: Method B	CAUC	1.72	0	N	0.056	0.088	0.44	0.19	0.80	0.36
1	35 (MT)	$STII_{slow}$	Std: Method B	CAUE	1.72	27	Y(<10%)	0.050	0.078	0.36			
1	35 (UT)	$STII_{slow}$	Standard rate	CRS	1.72	0	N	0.045	0.071	0.44	0.19	0.80	0.79
1	35 (OT)	$STII_{slow}$	24 hour steps	IL	1.72	34	Y(20%)	0.179	0.283	0.32	0.02	0.97	0.93
1	35 (MT)	$STII_{slow}$	Std: Method B	DSS	1.72	6	Y	0.083	0.131	0.36	0.12	0.83	0.59
10	5 (MT)	STII	Std.Method A	CAUC	1.31	19	N	0.018	0.024	0.52	0.19		0.37
10	5 (MT)	STII	Standard rate	CRS	1.25	13	N	0.02	0.036	0.52			
10	5 (MT)	STII	Std.Method A	DSS	1.31	20	N	0.025	0.043	0.52			
10	6 (MT)	STII	Std.Method A	CAUC	1.23	17	N	0.025	0.045	0.38	0.941		-2.1
10	6 (MT)	STII	Standard rate	CRS	1.28	15	N	0.026	0.047	0.38			
10	6 (MT)	STII	24 hour steps	IL	1.31	15	N	0.036	0.063	0.38			
8	5	$Block_{conf}$	Standard rate	CRS	2.41	20	N	0.01	0.014	0.91			
8	5	$Block_{conf}$	24 hour steps	IL	2.41	34	N	0.002	0.003	0.87			
8	5	$Block_{conf}$	Std.Method A	DSS	2.41	10	N	0.013	0.019	0.91			
8	5	$Block_{conf}$	Std.Method A	CAUC	2.41	7	N	0.002	0.002	0.91	0.57	0.18	-0.89

Reflections on the use of pore volume change methods (Lunne/Larsson methods)

As can be seen in Table 4.4 there was generally very little variation between the Lunne and Larsson assessments as one would expect given that the Larsson method has developed from the work of Lunne *et al.* (1997). However, when differences were observed the Lunne criteria gave a more pessimistic assessment of quality. Both methods were developed from studies on oedometer samples. Assessments for other types of test (CRS, DSS, triaxial) are, however, consistent with oedometer values and are thought to be a reasonable indicator of sample quality even for the other types of laboratory testing. That is true, provided samples are not desaturated or biologically or chemically altered. In Figure 4.18 the triaxial samples tested specifically for this thesis are plotted in terms of the pore volume changes during reconsolidation to *in situ* stresses and storage time, in the first plot (a) the size of the marker reflects the initial void ratio of the sample, while in (b) the size of the marker reflects the depth from which samples were extracted. There is a greater variation of $\Delta e/e_0$ for piston samples. In particular the East Coast clays had a slight tendency for these values to increase with time. All of the

block samples fell within the highest Lunne quality criteria, while only 57 % of piston samples achieved this. No significant differences were noted for confined block samples transported in straw or bubble wrap filled containers. However, block samples transported unconfined in Clingfilm and later confined with wax and cling film in the laboratory gave the largest values of $\Delta e/e_0$ for block samples. Deep piston samples tended to have larger pore volume change as did samples with lower initial void ratio. However, if samples were tested within one week differences were minimised. Trimmed piston samples (38 mm from STII samples and 50 mm from $STII_{60}$) had similar values to the extruded STII samples of a similar age. For similar reflections on suction and seismic quality assessment methods refer to Appendix A7.

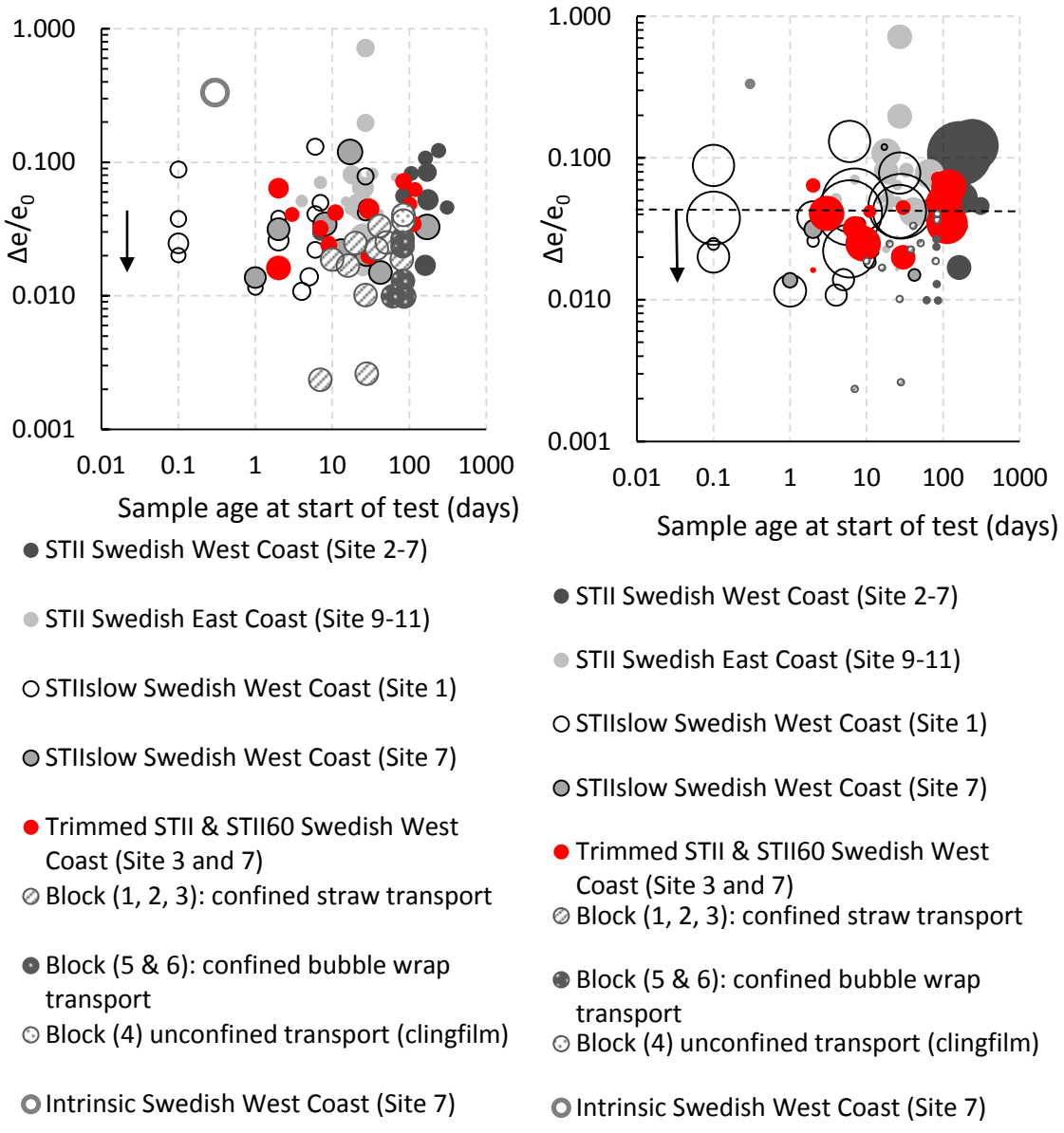

Figure 4.18 Triaxial sample pore volume change during reconsolidation (a) marker size relates to initial void ratio (e_0 = 2.6 to 0.9), (b) marker size relates to depth (3 to 55 m)

Conclusions and recommendations with regard to assessment of sample quality

A lot of effort was spent on the assessments of sample quality as it was identified early on in this research that only samples with low disturbance would be relevant for the study of soil behaviour in the laboratory, in particular within the small to medium strain

range. Unfortunately, none of the methods of assessment were completely reliable to this end. The Lunne pore volume method *(*$\Delta e/e_0$) would appear to be the best tool we have now, if samples are tested before any desaturation or chemical and biological changes occur (which generally means that testing should be conducted within 7 days from extraction). The Lunne method is, however, a "destructive" assessment method with sample quality assessment determined after testing, thus the assessments are retrospective. As the method stands today, it cannot identify the samples that are best suited for the study of small strain stiffness. It is also felt that some recalibration is undoubtedly required for samples extracted from large depths as these experience greater pore volume change, even when tested immediately following extraction, yet appear to be less disturbed than shallower samples with lower pore volume change. That addition calibration is required for deep samples is a sentiment that Lunne (2014) also conveyed, and is perhaps an area that warrants additional research.

It is an attractive idea that non-destructive quality assessment methods (suction/seismic/combined) could be used to identify only the best samples for advanced laboratory testing. Unfortunately, based on this research, these methods appear to give a useful quality indicator, but they are not reliable in their own right. Further research specific to this end is required to recalibrate the methods for Swedish clays, in addition to establishing alternative methods of quickly measuring "sample" suctions, as opposed to suction at the clay surface. The time taken to obtain results from filter paper tests make this method a useless decision-making tool in the light that Swedish soft clay samples should be tested within 7 days from extraction to avoid storage issues. There appears to be a longer "shelf life" of block samples provided the blocks are continuously confined from extraction until the day of testing. The "opening" of blocks triggered changes in pore volume changes, V_{S0} measurements and discoloration, even when immediately resealed.

None of the quantative methods were able to identify biologically and chemically altered (discoloured) and desaturated samples, thus it is imperative that a basic visual assessment is made.

The visual assessment of samples is a cheap method of identifying samples affected by alteration during storage. Protocols can easily be incorporated into standard laboratory procedures to record the degree of discoloration in samples and visual changes around any silt and sand partings (they become more and more visible due to water loss). Blocks which had been "opened", were more heavily affected by the chemical and biological changes. In these blocks discolouration was observed after around 30 days storage, while blocks that remained confined had very little discolouration even after 90 days storage. In piston samples the time taken for discoloration to occur varied between 2 to 30 days, with samples stored more than 90 days often found to be completely discoloured. The degree of discolouration (biological and chemical changes) occurring during storage is thought to relate to sample disturbance, or more specifically to the magnitude of excess pore water pressures exerted on the sample and their dissipation. The presence of more permeable interfaces (silt partings, pre-existing shear planes, shells, grass "holes", fissures) speed up this process, allowing changes to occur more quickly. Visual observations of colour changes were recorded digitally throughout this research as part of the quality assessment procedure and compared to digital images taken on extraction.

4.7 Mechanical properties of soils studied

The mechanical soil properties determined from laboratory and field testing for some of the sites are presented in this section, followed by some general observations. In addition to the testing conducted specifically for this research, some commercial test results are also included to provide additional data points in the profiles. Tests not conducted at CTH are indicated. Correlated soil properties from field tests (generally SDMT) are provided to indicate *in situ* variation, which when compared with laboratory test results helps give insight into the test specimen variation (including disturbance). Details of the mechanical properties for all sites and test data can be found in Appendix A8.

It should be noted that the assessment of the "simple" soil properties presented in this Section are by no means trivial, both in terms of assessment methods used and basic assumptions, such as the assumptions made for assessment of the *in situ* effective stresses. The seasonal pore water pressure variations, the presence of gas and human activity (notably dewatering at Site 9 to 11) all contribute to make the assessment of even the *in situ* effective stress (and reconsolidation stresses) difficult. Care has therefore been taken to utilize the average values of pore pressures based on long term *in situ* pore pressure measurements.

Some points on oedometer testing

Swedish CRS tests have displacement controlled loading. As such stiffer soils will be loaded more quickly. As a consequence, the rate of loading will vary both with sample quality and depth, even when the standard rate of displacement is used (0.0024 mm/min). At some sites CRS tests have been conducted at different rates of displacement, in which case this rate is indicated in the legend. These tests were done to better understand the rate-dependency. Comparison to IL tests (24 hour steps) and the triaxial tests (sheared at 0.01 mm/min) are also used to indicate the rate dependency of the different soils tested.

In determining the yield stress (σ'_c) Swedish CRS tests have been assessed based on the Sällfors (1975) method, even though this method should really be limited for use in the post glacial Gothenburg clays (for which the method was calibrated for). For design purposes it may be necessary to use alternative methods for samples with high residual effective stresses and for clays of other geological origins (East Coast Swedish clays and North West Coast Norwegian clays). At Site 12 it was not possible to use the Sällfors method, thus the NGI testing and assessment method (Sandbaekken, 1986) was used, which is comparable to the assessment method used for block samples by NGI at this site which are also presented in Appendix A8. Step-wise oedometer test interpretation of yield stress was done using the Casagrande (1936) method for all IL tests conducted.

Some remarks on undrained shear testing

All undrained triaxial tests were sheared at a rate of 0.01 mm/min, the assessment of yield stress (σ'_c) is in accordance with Larsson *et al.* (2007). All the triaxial test results presented were conducted at CTH at ≈7°C ambient conditions, except results for block samples from Site 12 which were tested at NGI in ambient temperatures of around 20°C.

In terms of undrained direct simple shear tests, the samples tested at CTH were sheared at 0.04 mm/min at 7 °C, while for tests conducted at other institutions the rate of shear varied between 0.015 to 0.05 mm/min, and the ambient temperatures would have been around 20°C during testing (no climate control). These procedural differences gave significant differences in the evaluated shear strengths, particularly at Site 11, refer to Appendix A8.

General observations in laboratory test results

A great deal of research has been conducted in Gothenburg and in particular around the Gothenburg Central Station area (Sites 1, 2, 3 and 5). This work dates back to the 1940's (Fellenius, 1955), and includes research by Alte *et al.* (1991), Persson (2004) and Olsson (2013). In addition, extensive commercial testing for a number of large infrastructure and building projects has also been conducted in this area. This has resulted in a large amount of test data (with testing conducted at CTH), which has been collated to give a basic understanding of the mechanical behaviour of Gothenburg clay, as well as the variation that can be observed in laboratory tests (differing degrees of disturbance). Figure 4.19(a) presents the compiled undrained strength test results for different modes of shear. A great degree of scatter in laboratory results can be observed, while the cone resistance profiles (q_t) from eight CPTU's in the area suggest very homogeneous conditions, refer to Figure 4.19(b). Much of the scatter in laboratory test results relates to differing sample disturbance, differing degrees of residual effective stress at the time of testing and the effects of partial desaturation and chemical/biological changes. Block samples and fresh piston samples with high residual effective stresses gave the upper bound undrained strengths (and stiffness), while the heavily discoloured "aged" samples tended to be at the lower bound.

Despite of the scatter in results, there is clear strength anisotropy between compression and extension modes of shearing. Direct simple shear tests (DSS) from the STII piston samples tended, however, to suggest undrained simple shear strengths were similar to the undrained triaxial extension shear strengths, despite being sheared four times faster and not lying between the undrained triaxial compression and extension shear strengths as one might expect. As such, the DSS tests on piston samples appear to give little insight into the simple shear strength properties of these clays. DSS tests conducted on the block sample from Site 3 did give undrained strengths that lay in between compression and extension values as one would expect. Both field vane (not corrected with respect to liquid limit) and the SDMT undrained strengths (Lunne *et al.* 1989 correlation) agreed fairly well to the DSS tests from $STII_{slow}$ piston samples, but as stated earlier the DSS tests generally do not indicate the shear strengths one would expect. This is thought to relate to the nature of the soils tested, the sample disturbance chain and the test procedure itself (the actual stresses acting on the sample during shearing are unknown in the CTH DSS apparatus as are the horizontal stresses during reconsolidation).

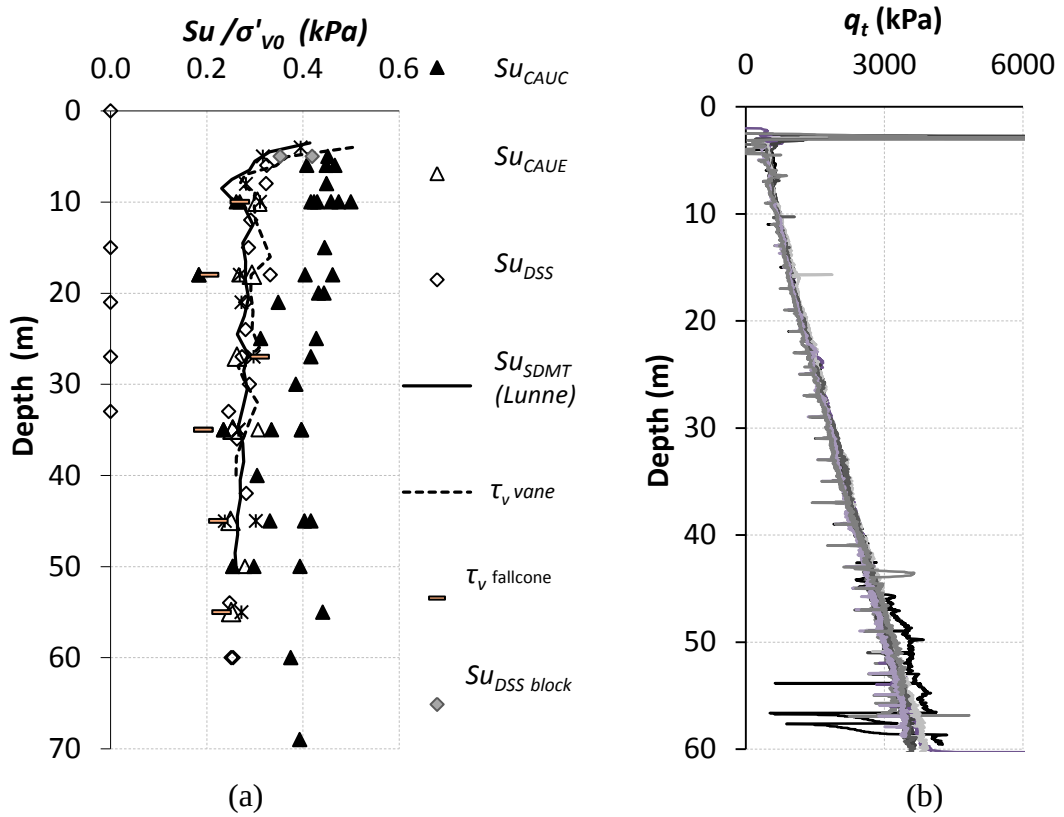

Figure 4.19 (a) Undrained strength for different modes of shear (normalised with σ'_{VC} (lab. based test) or σ'_{VO} (field based test), (b) Net cone resistance, q_t for 8 CPTU tests around Gothenburg central station area.

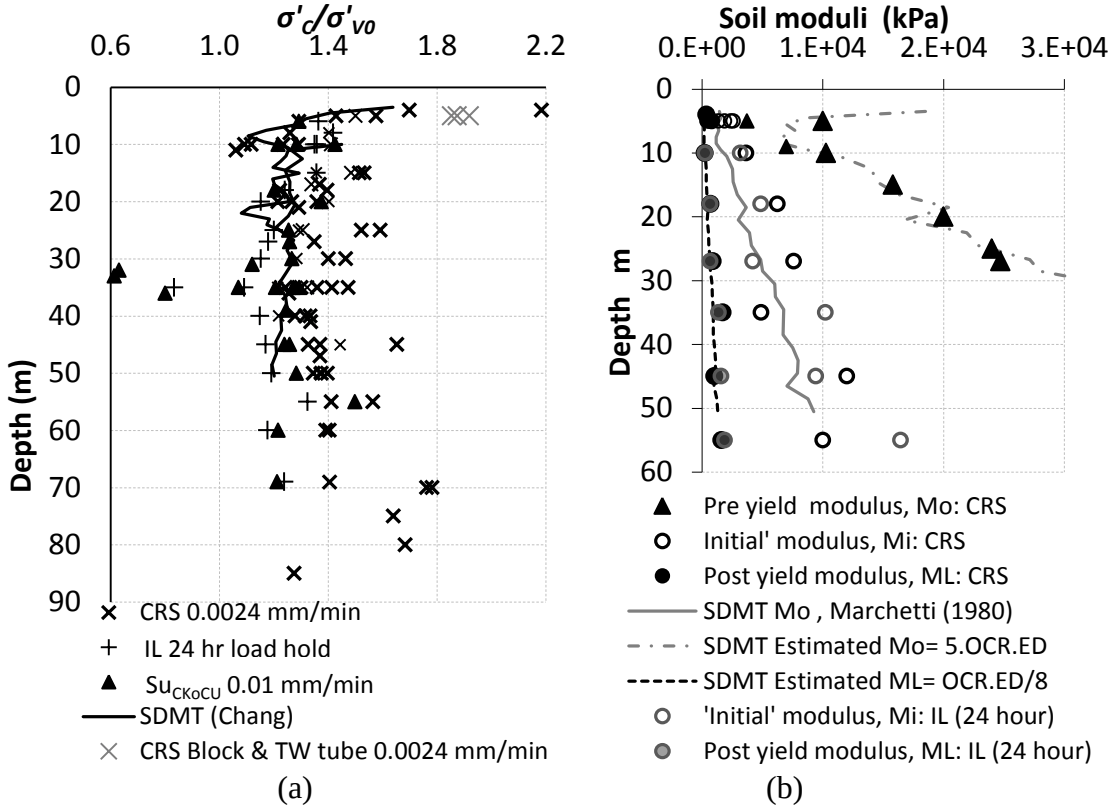

Figure 4.20 (a) Over-consolidation ratio assessed from different tests, (b) 1D moduli assessed from stepwise oedometer and CRS tests, refer to Section 3.3.4 for definition of M_0, M_i and M_L.

There is significant scatter in CRS oedometer results, as indicated in Figure 4.20(a). This is due to the differences in the rate of loading, as well as the underlying variations in the disturbance of samples, as discussed for the undrained shear tests. There is, however, an additional issue relating to the method of interpretation of yield stress, as the Sällfors method was calibrated primarily for the Zone 1 clays. In the Zone 1 clays the differences between assessments of yield stress from CRS, IL, SDMT and triaxial tests is small. However, below ≈12 m (Zone 2 and Zone 3 clays) the assessed yield stress varied by up to 40%, with the CRS tests providing the upper bound and IL tests providing the lower bound values (slowest loading rate). The SDMT (Chang, 1991) assessment related well to yield values determined from triaxial samples. In terms of 1D drained modulus the results from Site 1 are plotted for initial modulus, M_i and the 'elasto-plastic' modulus, M_L, while the reload moduli are from tests at Site 6. These results are, however, similar to IL tests from samples at Site 2 reported by Olsson (2013). The initial moduli (M_i) for the CRS tests was generally higher than IL tests, and roughly half that of the "elastic' modulus (M_0). This is most likely due to the CRS samples being mounted within 1 hour from sampling. Corresponding 'elasto-plastic' moduli for CRS tests were slightly lower, except for the disturbed sample at 35 m. The empirical relationships used to indicate in-situ M_L and M_0 appear a reasonable first estimate for these soils, while the M_{DMT} parameter proposed by Marchetti (1980) tends to agree with the 'initial' modulus of poor quality samples.

Thixotropy

A number of observations of thixotropic behaviour were made during this work, which will be shown to have an influence on the study of small strain stiffness in Chapter 5. However, some general findings are discussed in this Section. All piston samples, regardless of origin were observed to be in a "jelly like" state on extraction, however after a matter of minutes the samples were observably stiffer and more "clay like". The laboratory tests conducted on samples less than an hour after extraction were also noted to have slightly higher pore volume change during reconsolidation than samples that rested one day or more. The rapidly tested samples also exhibited more rapid degradation of stiffness in both CRS tests and triaxial tests.

The thixotropic behaviour of Swedish clays is prevalent, particularly the West Coast clays in field shear vane testing, as shown by Torstensson (1973) and Jendeby (1984), which is why it is imperative that shear vane tests are conducted in accordance with the Swedish standard (5 minutes rest then sheared over 3 minutes). Jendeby (1984) showed that a 24 hour rest period prior to shearing gave increases of shear strength of upto 60% in the glacial West Coast clays, while increases in the East Coast lacustrine varved clays were marginal (≈10%). It is also well known that thixotrophy affects the geotechnical bearing capacity of driven piles in Swedish soft clays, (often referred to as pile "set up"), as shown by Fellenius (1955) and Bengtsson (1977). Interestingly Torstensson (1973) observed no additional increase in shear strength if the 24 hour rest period was increased further.

Rate- dependency

Rate-dependency of Swedish soft clays has been studied using *in situ* field vanes by Torstensson (1973), Jendeby (1984) and Bengtsson (1977). Some of the differences in strength can be explained by partial drainage effects as discussed by Robinson & Brown (2013).That said the results suggest significant differences in rate-dependence of the soft clays originating from different geological layers. Differences were also observed

in the laboratory tests conducted within this research, both when comparing the assessed yield stress from stepwise IL tests (assessed using Casagrande , 1936), standard CRS tests (assessed using Sällfors, 1975) and triaxial compression tests (graphical method using stress paths in s', t stress space described by Larsson, 1977), and when comparing the CRS tests conducted at different displacement rates. The increased rate dependence of the older glacio-marine clays can be seen in Figure 4.20 (a) (difference between CRS and IL tests at depth) and from oedometer tests on intrinsic and natural samples in Figure 4.21. Similar results on intrinsic samples were obtained from 5 other tests. Additional comparisons of CRS tests performed on natural samples at different displacement rates, compared to IL tests, can be found in Appendix A8 both for tests on East Coast lacustrine and brackish clays, which like Jendeby (1984) confirmed reduced rate- dependency when compared to the West Coast glacio-marine clays.

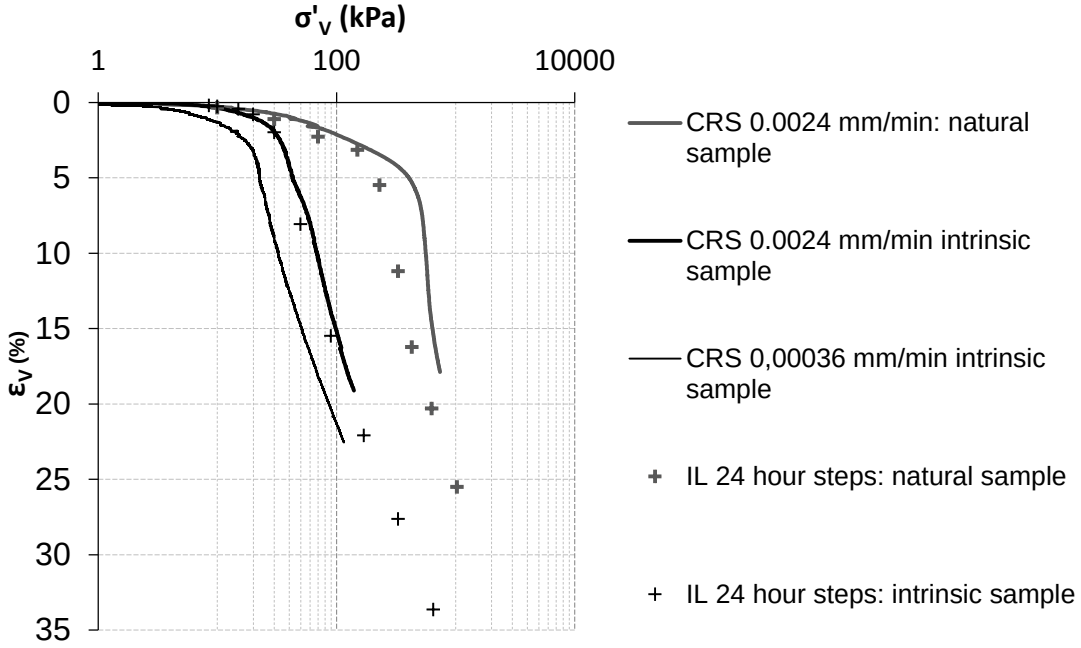

Figure 4.21 Typical results comparing of oedometer tests on natural and intrinsic samples, for different loading procedures, Site 1: 45m.

In terms of the stiffness, slower rates of loading gave lower stiffness prior to yield as one would expect, while post-yield they tended to be higher, thus is undoubtedly related to the fact the pore water pressures are significantly higher in samples loaded more rapidly giving lower effective stresses for comparable strains in slower CRS/IL tests during the progressive collapse of the clay structure.

Differences in the mechanical behaviour of block and piston samples

The study of the small strain stiffness and its degradation in the laboratory requires samples to be of the highest quality, if the results are to be of relevance to *in situ* conditions. In Section 4.6 it was shown that current assessment methods and criteria are perhaps not sufficient for this task. Much of the testing carried out in this research has been conducted on piston samples. These samples have often experienced more disturbance than if block samples (confined on extraction) had been used due to differences in the sample time line presented in Figure 3.1. To help visualise the differences experienced by the block and piston samples Figure 4.22 presents hypothetical effective stress paths experienced by samples during removal from the ground for these two cases. Typical changes in the shape of the state boundary surface

in situ compared to the laboratory specimens are also indicated in Figure 4.22 during removal of samples from the ground while differences experienced by samples in the overall sample time line up to the start of testing are presented in Figure 4.23.

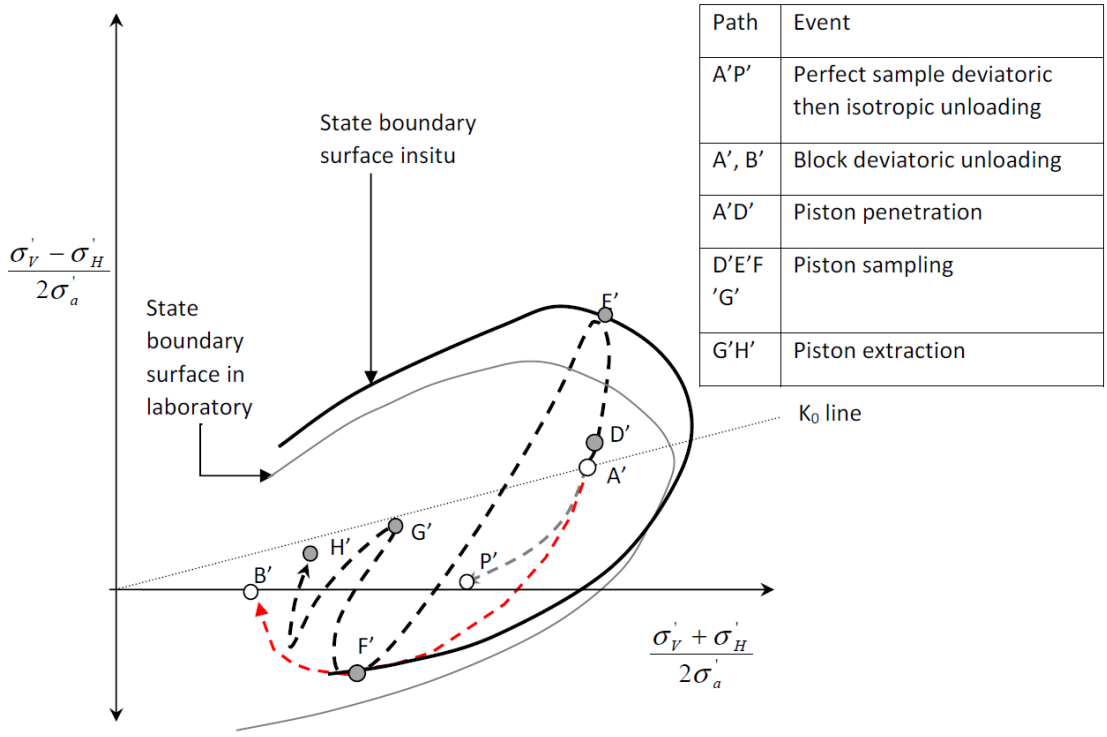

Path	Event
A'P'	Perfect sample deviatoric then isotropic unloading
A', B'	Block deviatoric unloading
A'D'	Piston penetration
D'E'F 'G'	Piston sampling
G'H'	Piston extraction

Figure 4.22 Hypothetical effective stress path response of light over-consolidated clay during sampling (dashed red line= block, dashed grey line= 'perfect' sampling and dashed black line= piston) presented in normalised triaxial space (normalised by axial consolidation stress σ'_a), adapted from Hight (2003), Ladd & De Groot (2003). Note, theoretical 'perfect' sampling (sample only experiences isotropic and deviotoric unloading as indicated by path A'P') is given for comparison.

In order to better understand how results from piston samples of Swedish soft clay might relate to the *in situ* conditions, the effective stress paths (ESP) during triaxial shearing are compared for piston and block samples tested at similar degrees of over-consolidation for the West Coast glacio-marine clays. The block samples are often indicative of "less disturbed" clay, as shown by Hight *et al.* (1992), and this appears consistent with observations of Swedish soft clays within this study, given the low pore volume change during reconsolidation ($\Delta e/e_0$ between 0.01 and 0.002) for test specimens taken from block samples that had remained confined since extraction. The stress paths of some of the block samples tested at varying initial states is shown in Figure 4.24. One of these tests was on a horizontally cut sample, which experienced very different evolution of anisotropy than the vertically cut samples. The near vertical stress path relates to shearing from OCR≈1.2, and is thought to represent behaviour typical of "undisturbed" Gothenburg post glacial clays (Zone 2C). The extension tests on vertically cut block samples indicated very little sensitivity to initial state. Unfortunately, some of the blocks tested had pre-existing shear bands, refer to Figure 4.12, which truncated the mode of failure thus results of these tests are omitted.

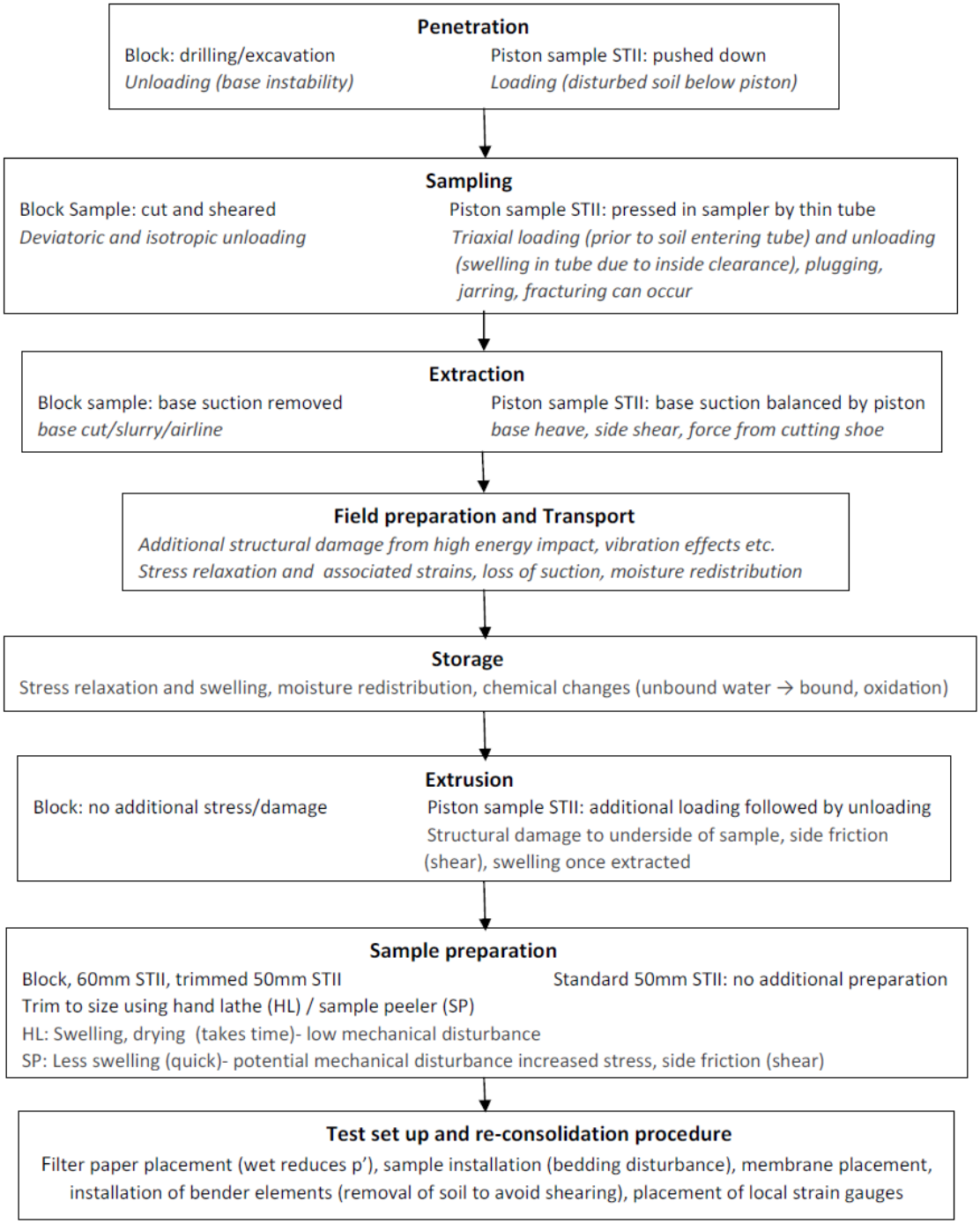

Figure 4.23 Stages affecting samples from in situ to triaxial testing for G_0 and G/G_0 using block and STII piston samples.

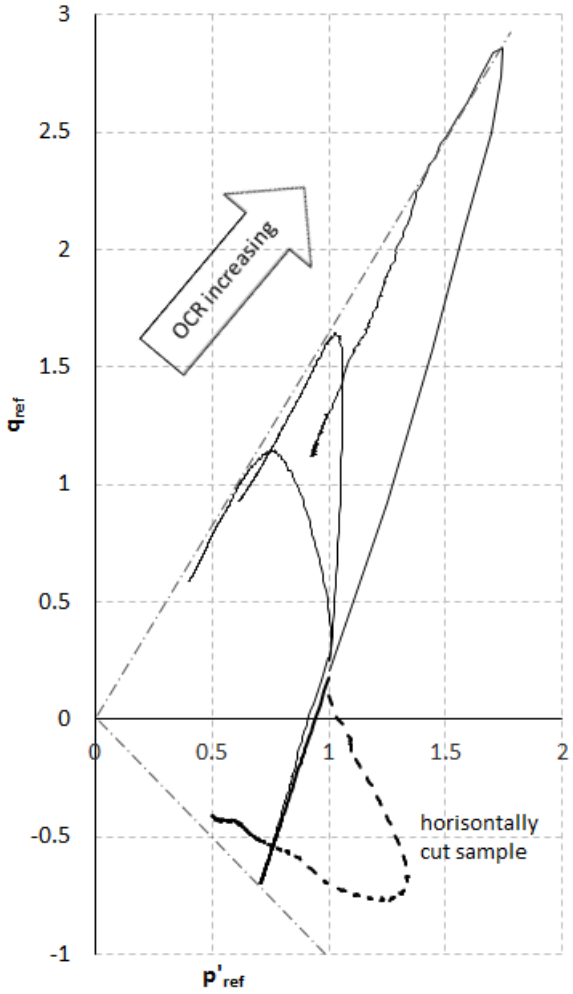

Figure 4.24 Variation in stress paths during shearing of block samples from Site 8 for different degrees of consolidation (OCR 6 to 1), where q_{ref} is the deviatoric stress normalised with the mean reconsolidation effective stress and p'ref is the mean effective stress normalised with the mean reconsolidation effective stress.

Block sample ESPs during triaxial shearing are used as a reference point in the following discussion on the impact of the sample timeline (primarily sampling method and alteration during storage) within this Section. These are presented together with the results from the different piston samples for the Swedish West Coast clays. In addition, the influence of sample disturbance is better understood with comparison to some tests on intrinsic samples. The intrinsic samples represent the lower bound of soil properties that can be expected, i.e. natural samples that are completely disturbed. As can be seen in Figure 4.25 (a), the undrained strengths of the intrinsic samples were up to 25% lower than observed for natural piston samples. This is opposite to Figure 4.21, where the intrinsic samples had higher values of post-yield stiffness, (M_L) than the natural piston samples. Thus, it would appear the effects of disturbance are different for different types of test.

In Figure 4.25(b) some examples of $STII_{slow}$ piston sample ESPs are shown for Site 7, where the Zone 1C and Zone 2 piston samples appear to lie within a similar framework to the to the block samples from Site 8 (Zone 2 clay). However, the Zone 1C piston sample falls to the left indicative of close proximity to the yield surface. The volume change during reconsolidation of this sample was $\Delta e/e_0$= 0.034, while the Zone 2 piston

sample had a volume change during reconsolidation of $\Delta e/e_0$= 0.014. This later sample clearly has much higher relative strength, which in combination with the reconsolidation pore volume change suggests lower disturbance. It seems therefore that the $STII_{slow}$ piston samples can in some cases give behaviour consistent with block samples, at least initially in compression, however when approaching the state boundary surface, differences are likely to occur leading to slightly lower relative strengths in the piston samples and differences in stiffness . This should mean however that the piston samples with low disturbance can be expected to give representative values of G_0 as the reconsolidation stress state is a significant distance from the state boundary surface, however stiffness degradation curves from small to large strains are likely to differ.

The ESP for the Zone 1A clay does not appear to lie within the same framework as the other ESPs in Figure 4.25(b), this may be associated with the proximity of the ground surface (5 m). Immediately above this level a significant increase in strength and stiffness was observed *in situ*, refer to Figure A8.2, Figure A8.3 and Figure 4.25(a) relating most likely to chemical and biological changes (weathering). Similar observations were made at Site 10 at this depth, refer to Figure 4.29(b).

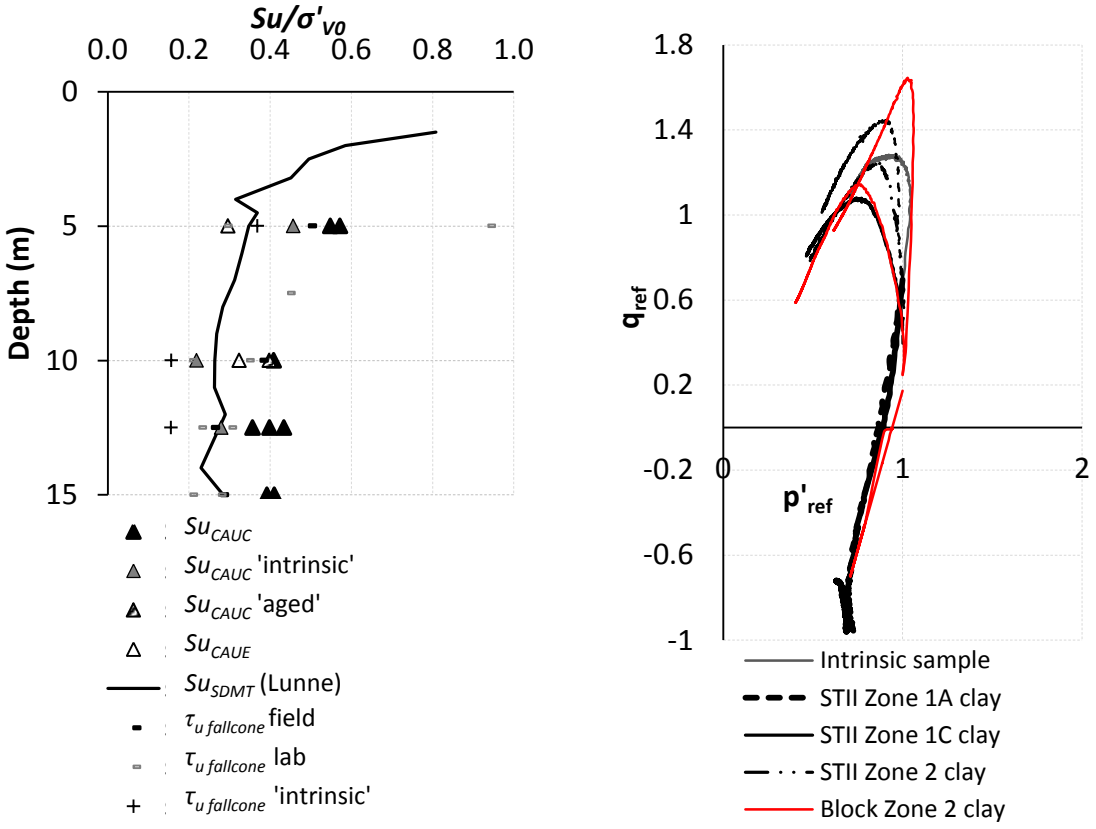

(a) (b)

Figure 4.25 Mechanical properties of natural and intrinsic samples of glacio marine clays (a) Undrained shear strengths from Site 7, (b) normalized ESP of ($STII_{slow}$) piston samples from Site 7 and block samples from Site 8 sheared from OCR 1(tending to the left) and 1.2 (slightly tending to the right) (normalized by p'_{VC}).

The intrinsic sample ESP in Figure 4.25(b) surprisingly suggests greater over-consolidation than the natural piston samples (tending to the right). The effective stress applied during resedimentation was around 16 kPa vertically (horizontal effective stress unknown), whereas during triaxial testing the intrinsic sample was reconsolidated to the

same stresses as the natural sample (σ'_v=25 kPa or p'=16 kPa). It is possible that the aging of the clay during the 4 month reconsolidation period was sufficient to allow the growth of the intrinsic yield surface through creep, although this is still far from the natural sample given the lower strengths that were achieved in fall cone tests. At large strains the intrinsic stress path tends towards a similar bounding surface as the natural samples, thus appear to fit within the critical state soil mechanics concept.

It is difficult to determine at what point within the sample timeline identified in Figure 3.1 the greatest changes occur, given both natural variation and differences experienced by samples during extraction. At Site 7 index testing was carried out in the field at 4 depths and repeated later in the laboratory over a period of 30 days. Of most note were the differences in fall cone shear strength measurements shown in Figure 4.25 (a), where measurements in the field can be compared to the laboratory results 36 hours later. Details of the changes occurring in the different index test parameters with time is presented in Figure 4.26 for one of these sampling levels (10m). Clearly the fall cone strengths, which initially experience a significant drop in strength, most likely due to dissipation of effective stresses, appear to recover with time, however, to what extent this is due to thixotropy or pore water redistribution /loss and chemical and biological change is unclear. The storage time however also appears to affect the liquid limit and the plastic limit and hence the plasticity index somewhat, which means that parameters determined using commonly used empirical correlations in Sweden will be affected by this. This gives an additional uncertainty to such correlations. The influence of the sample time-line on laboratory small strain stiffness is presented in Chapter 5 by tracking changes in shear wave velocity at each point in the sample timeline chain. Therefore, in this Section focus is on the differences in the typical mechanical behaviour observed in samples at medium to large strains during triaxial testing including specimens which have been biologically and/or chemically altered during storage (identified by extensive discolouration), hereto referred to as 'aged' samples.

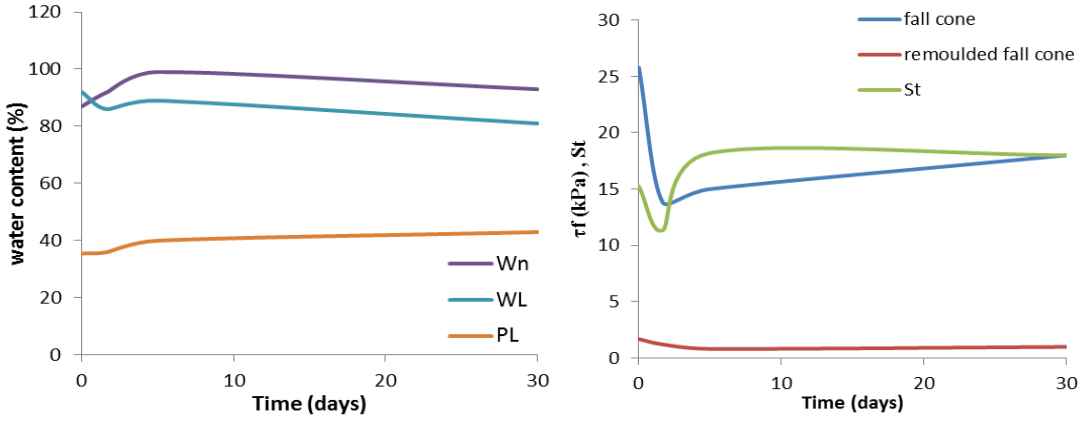

Figure 4.26 Changes in index properties from extraction (Site 7: 10m) and after transport and storage at 7°C and 100% humidity.

Difference in the mechanical behaviour of fresh and 'aged' samples was most significant in the Gothenburg clay. Undrained compressive strengths of 'aged' samples were up to 40% lower than those of the "fresh" samples, while in extension 'aged' samples were in some cases greater, refer to Figure 4.27(a) and Figure 4.28(a) and (b). The differences in undrained triaxial stiffness ($E_{u\ 50}$) of the fresh and aged samples was also significant, with aged triaxial compression specimens having similar $E_{u\ 50}$ stiffness, to fresh specimens under extension which were significantly lower that fresh specimens

tested in compression, refer to Figure 4.27 (b). Also note the higher stiffness of the block samples both in compression and extension, when compared to piston samples, which are sheared from similar *OCR* and mean effective stress. However, one piston sample at 18 m also indicated very high stiffness. This specimen ($STII_{slow}$ sample) was tested after 4 days, and experienced a relative pore volume change of $\Delta e/e_0$=0.011 (ie. similar to block samples). At extraction this sample was noted to have very little silt partings and measured suctions were high. It is thought therefore that this sample experienced less pore water pressure equalisation, which allowed the sample to maintain more of its inherent natural structure, in a similar manner to block samples.

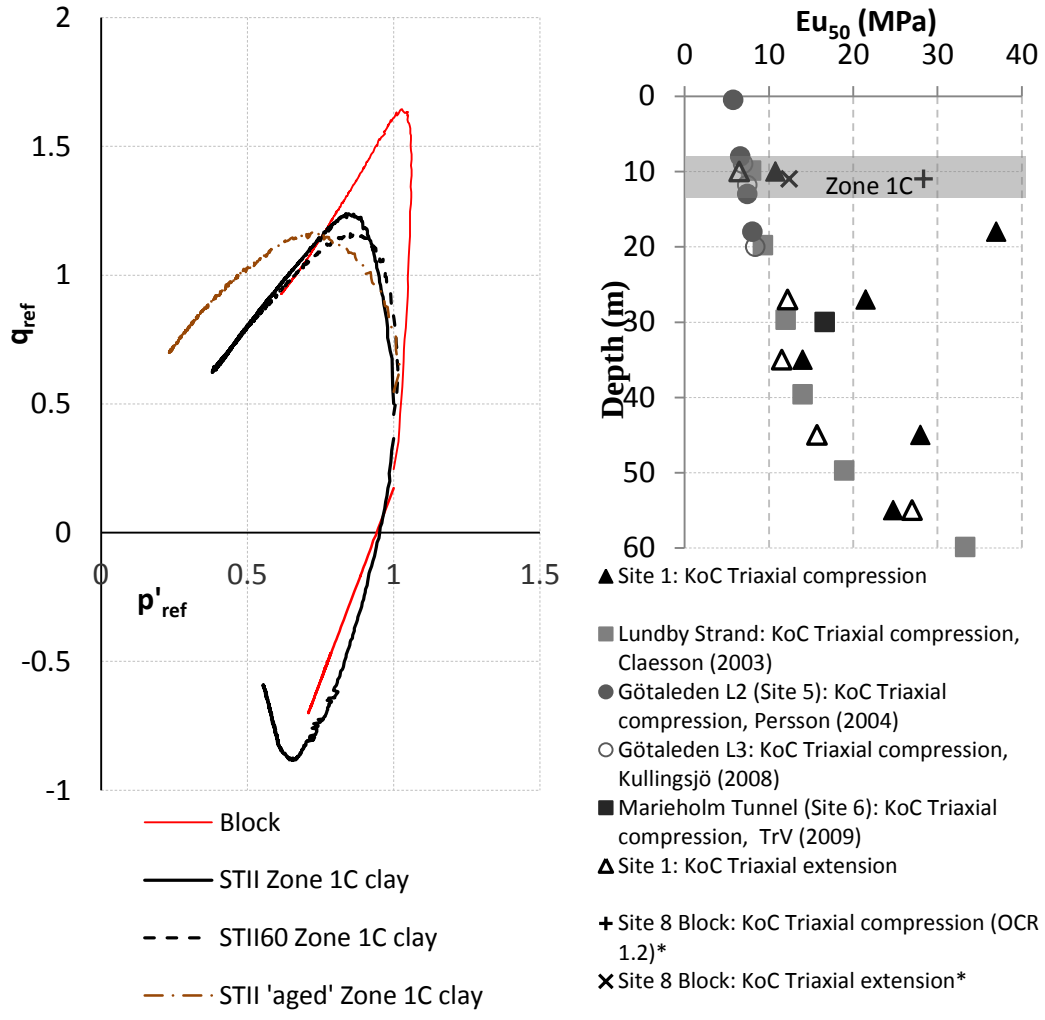

*Figure 4.27 (a) Normalized ESP of STII piston samples from Site 1 and 3 and block samples from Site 8 (normalized by mean reconsolidation effective stress, p'_{VC}), (b) Undrained secant Young's modulus at 50% of peak strength for Gothenburg clays, only tests at Site 1 are on "fresh" samples and block samples sheared for similar OCR, * equivalent depth based on p' used for these samples.*

Also shown in Figure 4.27(a) are test results on $STII_{60}$ piston samples trimmed to 50 mm for the post-glacial clays, while Figure 4.28(a) presents comparisons for the glacial Zone 3a clay. Both the $STII_{slow}$ and the $STII_{60}$ test results presented are from specimens less than 7 days old, and illustrate typical behaviour observed in 9 separate comparisons at two locations (Site 1/3 and Site 7). The $STII_{60}$ samples have undergone an additional process in the sample timeline, in order to trim to the diameter required for the triaxial

apparatus (50 mm). These samples often had slightly lower strengths and ESP that initially fell more to the left, indicative of increased disturbance. The differences were, however, small in terms of the stress paths followed, but differences in the undrained stiffness were, however, were larger. Based on these initial findings there would appear to be some additional damage to the $STII_{60}$ samples. It is not clear if the source of this additional damage relates to sampling or sample trimming and preparation. Comparative studies of the effect of different methods of trimming on both STII and $STII_{60}$ samples (hand lathe or sample peeler) were inconclusive, undoubtedly due to initial differences in the underlying samples.

Based on over 50 triaxial tests conducted on the Swedish West Coast clays within this work there are clear differences in the mechanical behaviour of the main geological deposits. The differences in the Zone 1B and Zone 1C clays at medium to large strains appears small for high quality samples, ie. they appear to fit within a similar critical state framework, while shallow Zone 1A clays are slightly different, most likely due to chemical weathering. The Zone 2 clays also appear to fit within a similar framework to the Zone 1 B and C clays, however, the relative stiffness of these clays is often higher for the high quality samples, suggesting there are still differences in structure. These clays are highly anisotropic both in terms of shear strength and undrained stiffness. The glacial Zone 3a and Zone 3b clays behave quite differently to the post-glacial clays, they appear to have a lower friction angle and exhibit increasing anisotropy with depth, seen by the compression and extension ESP's tending more to the right and left, respectively, until the state boundary surface is approached. As such numerical modelling of these soils needs to be tailored for each geological deposit.

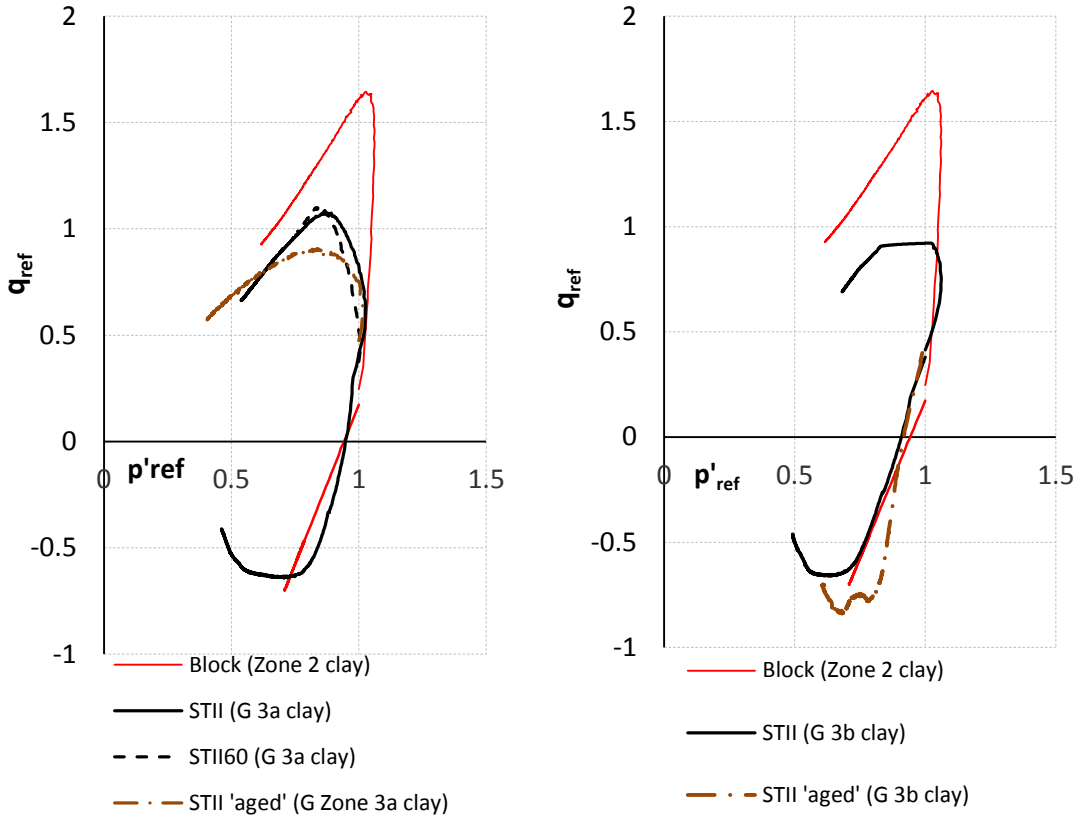

Figure 4.28 (a)Comparison of triaxial stress paths for STII and $STII_{60}$ glacial Zone 3a piston samples from Site 1 & 3 and Block samples from Site 8 sheared from OCR 1.2 (b) Comparison of triaxial stress paths for STII glacial Zone 3b piston samples from 55m ('aged' sample) (normalized by mean reconsolidation stress, p'_{VC}).

For the East Coast clays only standard STII piston samples were studied, however, by reviewing the shape of the stress paths with reference to the volume change during reconsolidation similar observations can made to the West Coast clays. Samples with higher pore volume change tended the give ESP that tended to the left, resulting in lower strengths and stiffness at medium to large strains as suggested by Figure 4.29. The sediments from the Litorina and Post Litorina sea, organic clays and clayey silts in (a), indicate high friction angles associated with the high silt content. The sample from 9m (Litoric Sea) was more disturbed than the sample from 3.5 m based on assessment using the Lunne criteria, which is consistent with the much flatter shape of the ESP that tends to the left. The lacustrine samples from Site 9 and 10 appear to have a consistent angle of friction at critical state even when the 25m sample has been rotated through ≈90 degrees during geological reworking, however the apparent cohesion appears to vary. This may relate to differences in digenesis (chemical weathering). The shape of the geologically reworked lacustrine sample ESP from Site 9 (25m) and Site 10 (10.5m) in Figure 4.29 (a) and (b) respectively suggest significant disturbance as one would expect. In addition similarities between the higher apparent cohesion of the fresh "dry crust" lacustrine sample from Site 10 and the 'aged' glacio marine clay samples may suggest that chemical and biological alteration occurring near surface in the field and in stored samples is similar.

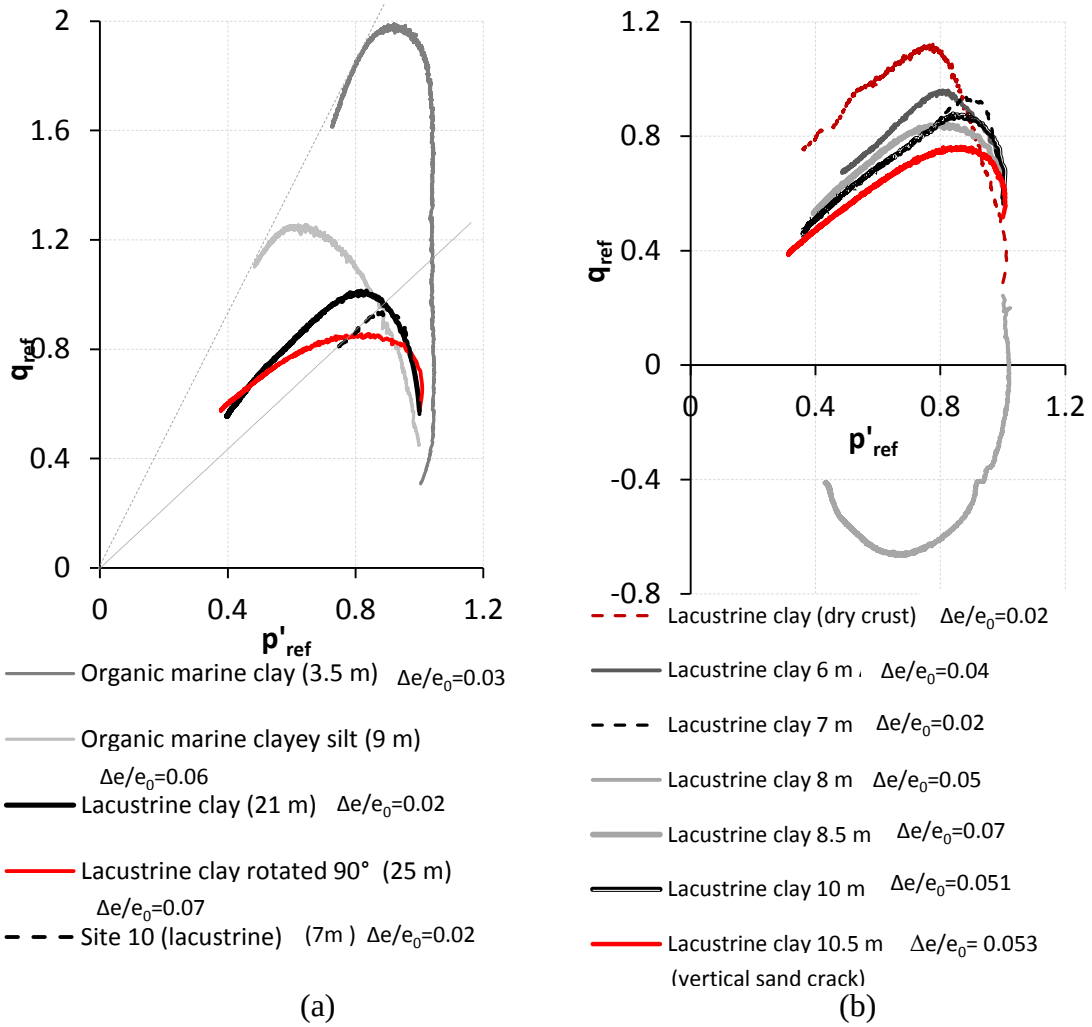

Figure 4.29 Comparison of triaxial effective stress paths for STII piston samples (a) Site 9 all tests with comparison to best quality sample from Site 10 (b) Site 10 all tests, (normalized by mean reconsolidation stress, p'$_{VC}$).

4.8 Summary of the materials studied

All the soft clays studied have some degree of anisotropy, rate-dependency, and furthermore are influenced by different sample histories (stress and strain history). A number of piston samples have been obtained that exhibit excellent quality, however these still appear to have undergone more disturbance than block samples when comparing results in the same geological deposit. For this reason the block samples are primarily used to try and understand small strain stiffness and its degradation, and the sample disturbance chain, whereas the tests on piston samples are given more for comparison purposes. Refer to Appendix A8 for full details of test results for specific sites in the medium to large strain range.

A number of different methods for sample disturbance assessment have been utilised, both destructive and non-destructive for identifying the samples that might best represent *in situ* conditions in the small strain range. None of the assessment methods were conclusive thus a multiple assessment approach is most likely the best way forward.

Clearly in terms of numerical modelling using finite element methods for deep excavation problems the validity of the results will be highly dependent on the quality of the samples used to define the constitutive model parameters and as well as the quality of field testing used to determine the ground profile and define the initial *in situ* state. Clearly the ability of the constitutive model to reproduce soft clay behaviour is also an important factor and is discussed in more detail in Chapter 6.

The homogeneity of the Swedish West Coast clays is helpful in this matter, providing one understands the ground profile and identifies the different geological deposits. As their homogeneity enables test results from wide reaching sites to be directly compared providing they are appropriately normalised. This is unfortunately not the case for the Swedish East Coast clays given their complex geological history. Certain trends seem however to exist within the different geological deposits at a given site. For the Norwegian West Coast clays determination of realistic soil parameters from laboratory testing is extremely difficult given their high silt content which makes them particularly sensitive to the sample disturbance chain. Even use of the Sherbrook block sampler within the Trondheim E6 project was only able to provide four of twelve soil samples that were able to meet the highest Lunne *et al.* (1997) quality criteria in samples used for triaxial testing. The best sample had a value of $\Delta e/e_0$=0.025 which is still considerably higher than the best block samples from Site 8 ($\Delta e/e_0$=0.002) and some piston samples from both the East and West Coast sites. It would appear therefore that different strategies will be required in different clays for clay characterisation and numerical model validation.

5 RESULTS OF SMALL STRAIN STIFFNESS MEASUREMENTS

5.1 Introduction

The focus of this Chapter is on the presentation of small strain stiffness data, as derived from shear wave velocity based techniques in the field and in the laboratory. After presenting the small strain data, the evolution of this property as function of time and strain history will be elaborated. Subsequently, a comparison is made with some existing empirical relations, before finalising with recommendations regarding small strain stiffness measurement in Swedish clays.

5.2 Test programme

A short summary on the executed shear wave velocity based small strain stiffness (G_0) tests is given for the 12 test sites in Table 5.1. Most samples are taken using the standard Swedish STII piston sampler however at 2 sites a widened version referred to as the $STII_{60}$ was also used, and at two sites block samples have been hand carved (refer to column 2). For the latter a qualitative indication of the general sample quality at each site using the Lunne criteria is given.

The direct measurements of the *in situ* (field) shear wave velocities are generally performed with the seismic dilatometer (SDMT) however at Site 12 test results of seismic cone penetration testing (SCPT) from the Tiller research site presented by Takke Eide (2015) are used (located approximately 8 km south in the same geological deposit. At some sites surface seismics (MASW) is also available, which for Site 12 again relates to testing presented by Takke Eide (2015) at the Tiller research site (see column 3). Subsequent testing of the samples in the laboratory using the GDS and/or CTH bender element system yielded the complementary laboratory value for a number of sampling levels (columns 4 & 5). The samples are tested for four different conditions:

1. Confined: the sample is still contained in the sample tube when tested. Some stress remaining (mainly lateral).
2. Unconfined: the sample is unconfined (in fresh samples some suction remaining) when tested in the mobile bender element testing rig.
3. Reconsolidated: the samples are reconsolidated to the anisotropic *in situ* stress level (estimated from unit weight and dilatometer pressures) before being sheared.
4. Intrinsic: the samples were reconstituted (resedimented) in the laboratory to the approximate initial void ratio of natural samples

The majority of the laboratory bender element tests have been performed in transmission in the direction that coincides with the geological deposition (vertical) giving V_{Svh}, however some tests were conducted on block samples of a similar height/width to investigate if any substantial differences could be observed between V_{Svh} and $V_{Shh.}$ It was found, however, that very different responses were noted for block samples tested horizontally when the bender element was placed in different seasonal layers (black or grey varves).

Table 5.1 Test overview for the reported shear wave velocity based G_0 tests.

Site No.	Sampler (quality)	SDMT or SCPT/ MASW	No. levels	Bender on confined/ unconfined/ reconsolidated/ intrinsic	Notes
1	ST_{II} (very good)	yes/no	6	conf/unconf/recons/intr	slow extraction
2	ST_{II} (good)	yes/no	4	unconf/recons	
3	ST_{II} & ST_{II60} (good) Block (excellent)	yes/no	3	conf/ unconf/recons	
4	ST_{II} (good)	yes/no	1	conf/unconf/recons	
5	ST_{II} (fair)	yes/no	4	recons	Lab. data from Persson (2004)
6	ST_{II} (good)	no/yes	4	conf/unconf/recons	diff stress histories
7	ST_{II},ST_{II60}(very)good	yes/yes	8	conf/unconf/recons/intr	(slow extraction) old
8	Block (excellent)	no/no	1: 6 block	conf/unconf/recons	diff stress histories
9	ST_{II} (good)	yes/no	4	conf/unconf/recons	
10	ST_{II} (good)	yes/no	7	conf/unconf/recons	diff stress histories
11	ST_{II} (fair)	yes/no	3	conf/unconf/recons	
12	STII (fair)	yes/yes (tests from Tiller research site)	2	conf/unconf/recons	diff stress histories field data & lab data on shallow samples from Takke Eide (2015)

5.3 Field measurements of G_0

It was shown in Chapter 4 that the clays within the city of Gothenburg were homogeneous, however, the different geological deposits were not always easy to identify with CPTU and field vane tests. A total of seven seismic V_S profiles were obtained within the city of Gothenburg using the SDMT equipment and are compiled in Figure 5.1. Also shown are the geological boundaries that correspond with Figure 4.7. The seismic measurements appear to be a useful profiling tool both in terms of geology

and identifying areas with different stress history. For example the higher values of V_S at Site 5 between elevation -4 m and -8 m relate to effects of the in filled dock, while, higher values of V_S at Site 4 and 5 around elevation -11 m, -14 m and -30 m relate to frictional layers within the clay. The MASW tests (Site 6) are able to pick up the same trend as the SDMT tests (Site 1, 2, 4 & 5) in the first 10 meters or so. Greater depths may be possible with a larger excitation source. Differences in MASW profiles (elevation 2 m to -3 m) relate to the presence of more organic matter at S15 and perhaps saturation (S16 is immediately adjacent to the Göta River). The similarity of SDMT and MASW results corroborate findings in literature (e.g. Donohue *et al.* 2012).

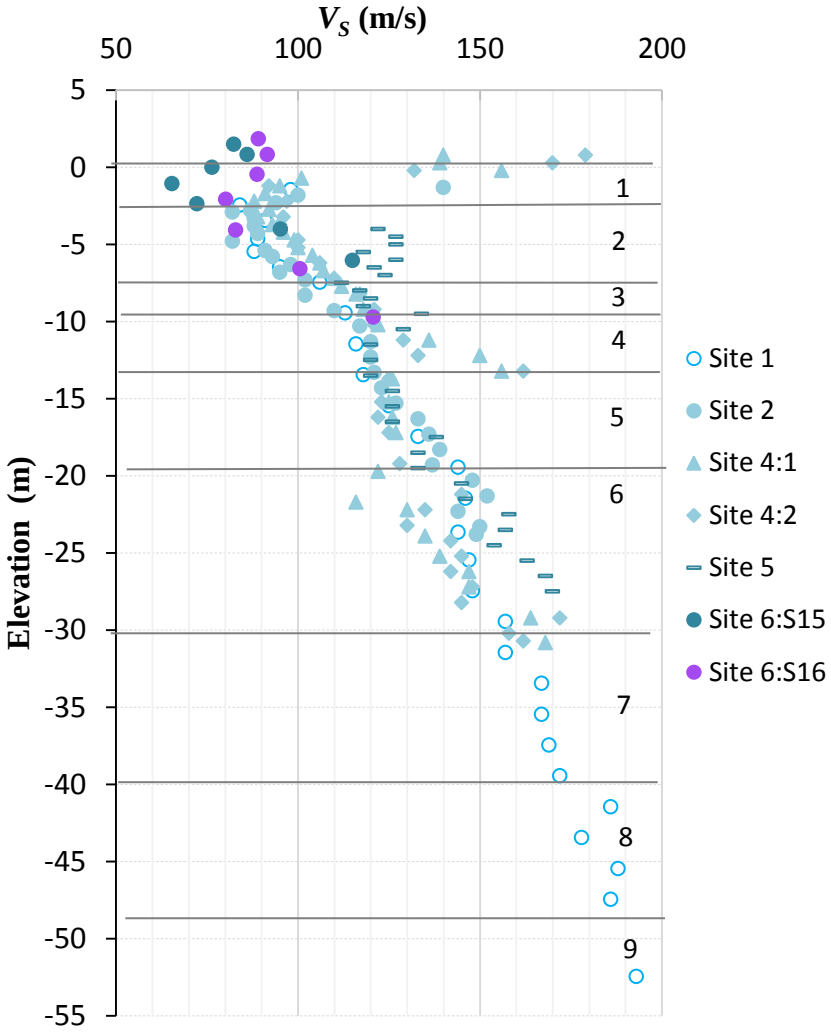

Figure 5.1 Comparison of field measurements of shear wave velocities using SDMT (Sites 1, 2, 4 and 5) and shallow surface seismics, MASW (Site 6), approximate position of geological boundaries also indicated.

In the following figures the measurements of V_S from field testing have been used to determine the small strain shear modulus G_0 *in situ* using Eq. 2-1. The stiffness data is de-trended using the *in situ* effective mean stress level *p'* and plotted against different soil parameters. For Site 12 the G_{0field} data is taken from the Tiller research site which is located approximately 8 km south of Site 12 but has very similar properties and shares the same geological history however where test data from the Tiller site was available these are presented in Figures 5.2 to 5.5 and not values determined specifically at Site 12. While this may be the source of some scatter in the Site 12 data this is not thought to be the case given the similarity of laboratory test results at Site 12 and the Tiller site

within the small strain stiffness strain range. In Figure 5.2 soil activity (i.e. the plasticity index divided by the percentage of clay particles < 2 μm) connection to G_0 is presented. This proved the most revealing relation between soil classification and G_0. Most of the clays tested can be considered inactive or normal, and only a tentative relation is found.

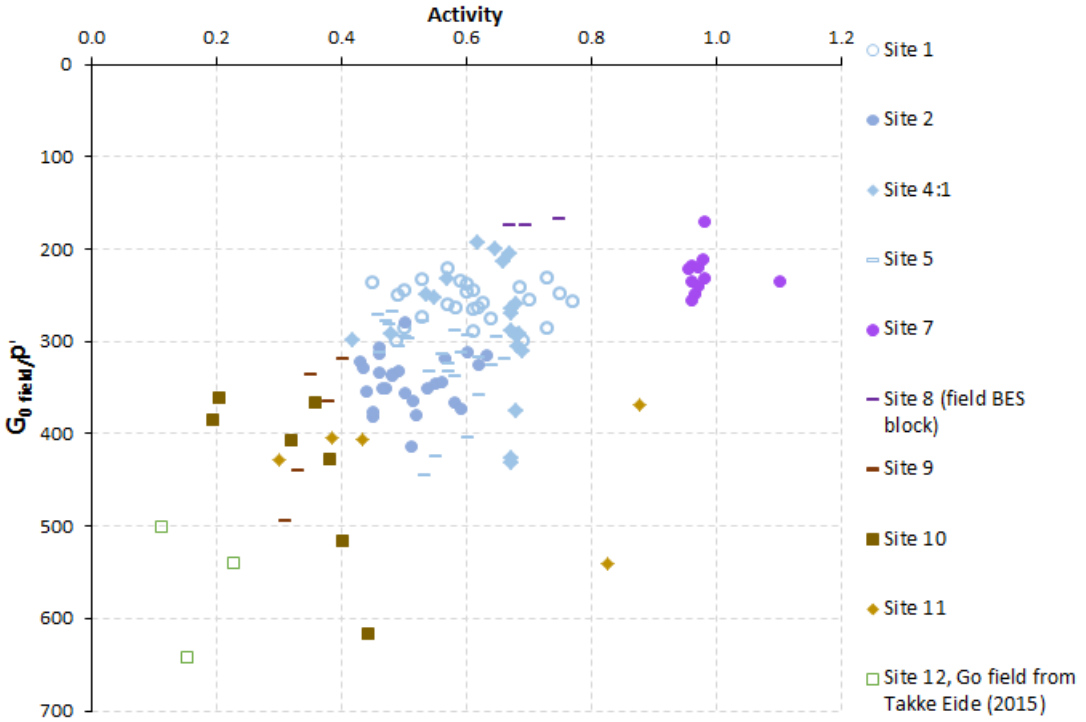

Figure 5.2 Field values for small strain shear modulus G_0 as function of soil activity.

No clear relation of G_0 with cone penetration data is found either, as shown in Figure 5.3 where the G_0 is normalised with the corrected cone resistance q_t and plotted against B_q which is a normalised pore water pressure measure. This is not completely unexpected, given the large strain failure modes around a CPT cone during penetration.

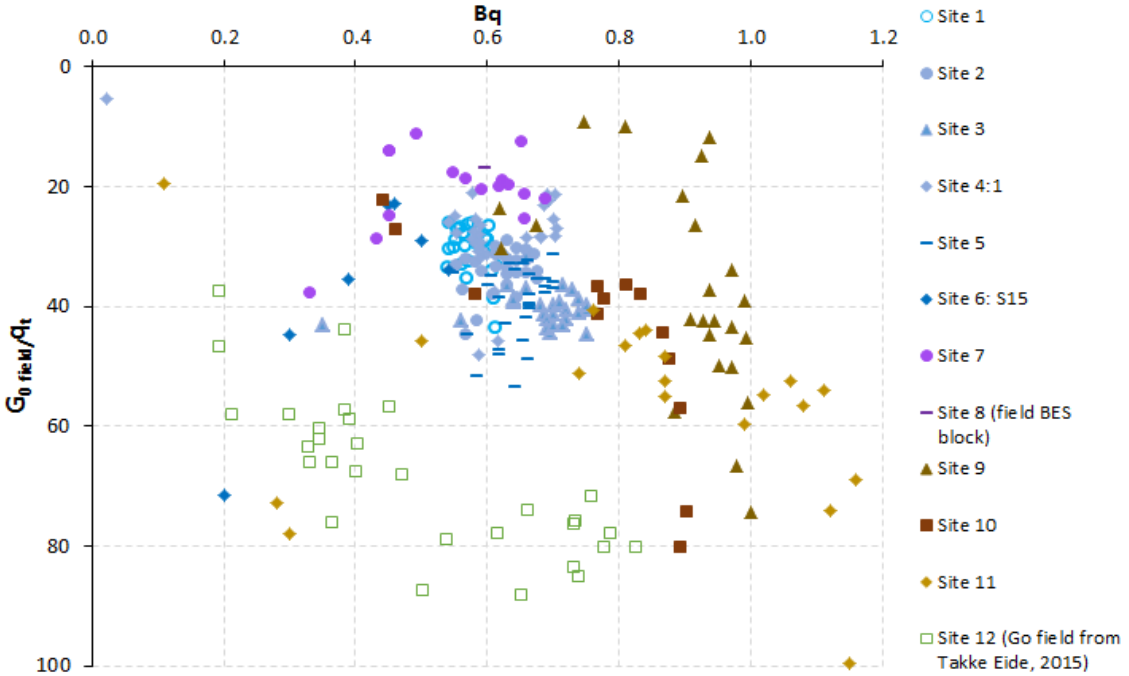

Figure 5.3 Field values for small strain shear modulus G_0 as compared to normalised CPT data.

Likewise, for field vane results the spread is large even when de-trended from the liquid limit. Note that shear vanes strengths are left uncorrected with respect to liquid limit (Fig 5.4).

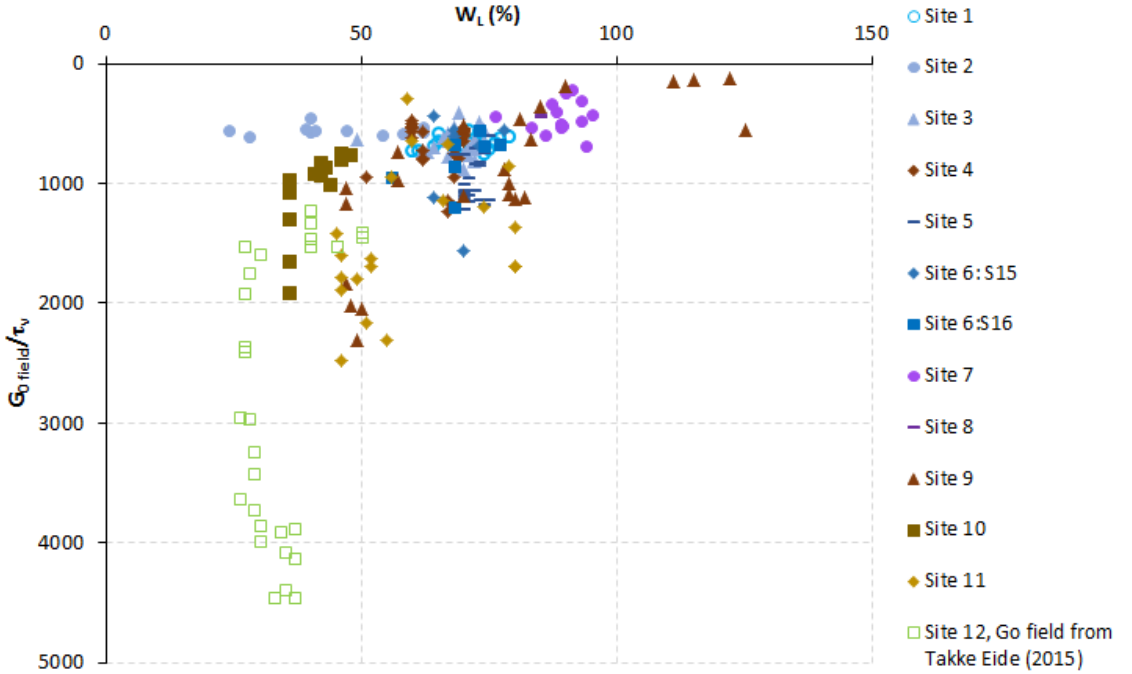

Figure 5.4 Field values for small strain shear modulus G_0 as compared to normalised field vane undrained strength and liquid limit.

A connection between the sensitivity S_t and G_0, was not found either, i.e. Figure 5.5. This is somewhat unexpected given the use of S_t to correlate to initial amount of bonding in some advanced constitutive models for soft soils.

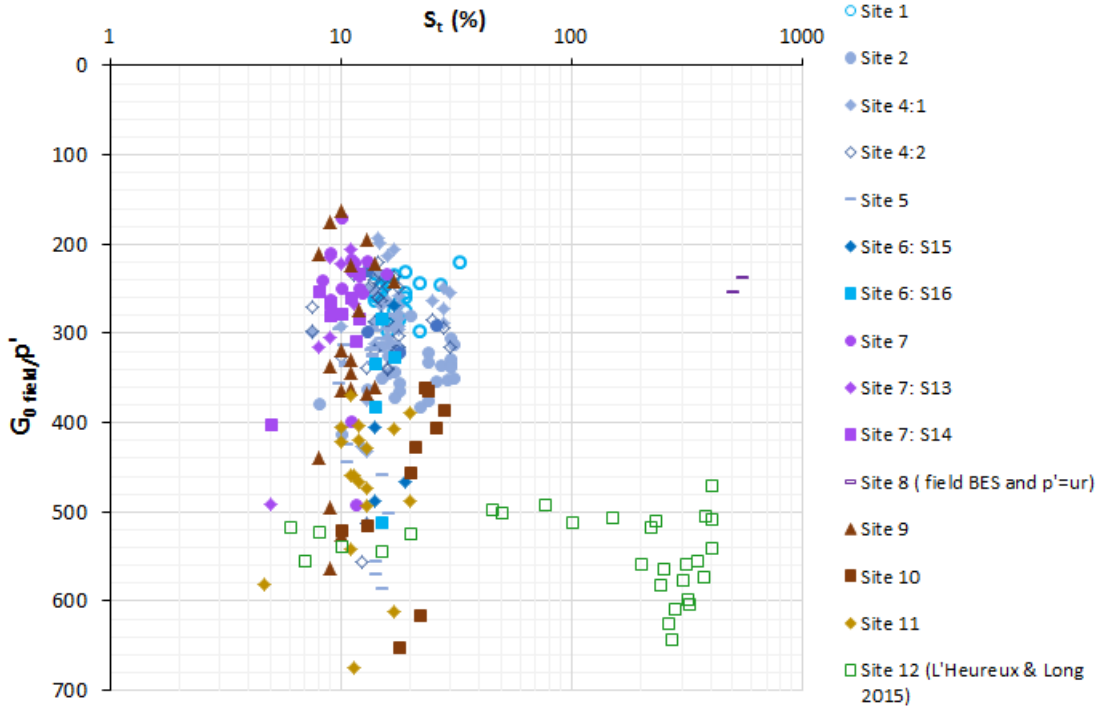

Figure 5.5 Field values for small strain shear modulus G_0 as compared to sensitivity.

5.4 Laboratory measurements of G_0

Subsequent measurements of the small strain shear modulus G_0 in the laboratory are directly compared to the values measured in field for Sites 1 - 12 in the cross-plot presented in Figure 5.6. Values falling above the line are conservative: the field value is larger than the one obtained in the complementary laboratory test.

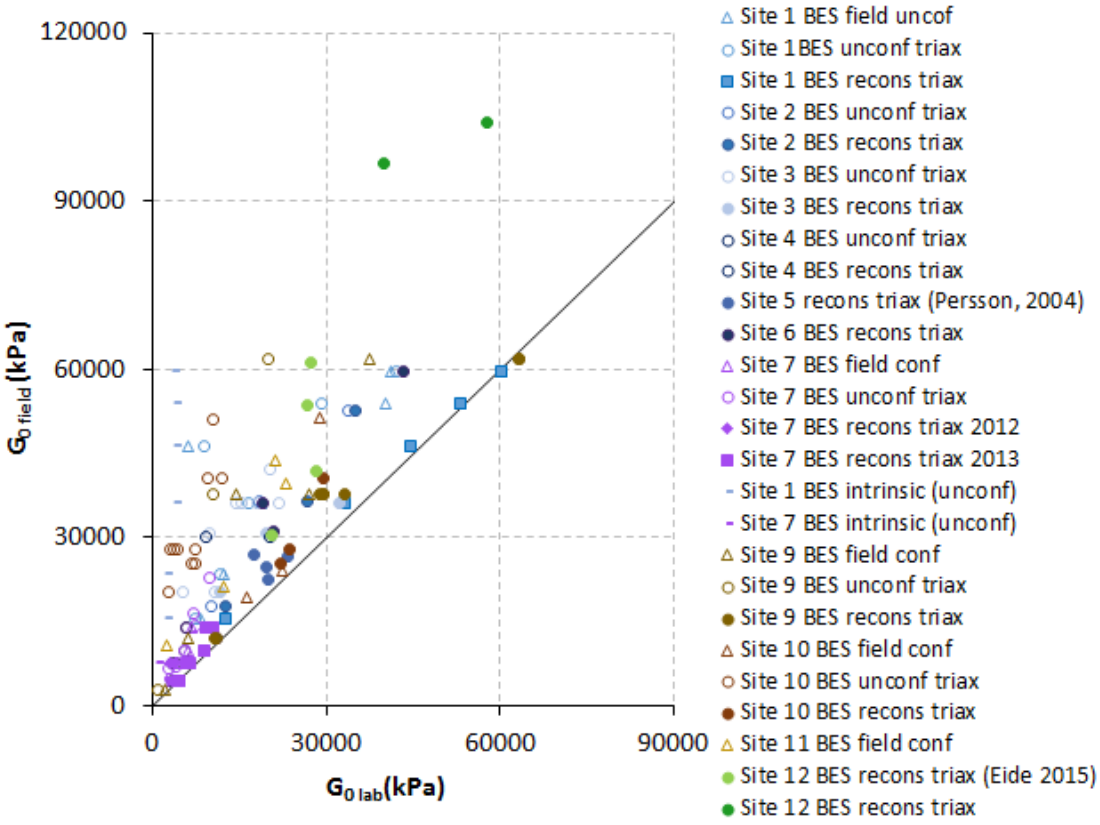

Figure 5.6 Comparison of field and laboratory values for G_0 for 12 test sites.

Closer study of the data presented in Figure 5.6 allows for the following observations:

1. The G_0 values found for confined samples that are reconsolidated in triaxial conditions to the anisotropic field stress level (denoted with 'recons triax' in the legend) are closet to the field values when the sample quality is sufficiently high.
2. Unconfined measurements are of limited value when performed in the laboratory after transport, storage and sample extrusion and/or manipulation. However, if the shear wave velocity is measured in the field directly after retrieving the sample the readings are reasonably close to the undisturbed measurements with SDMT. In this case suction is preserving some residual effective stress in the sample.
3. Intrinsic samples, that represent a worst case for disturbed natural samples, under-predict the stiffness by a large margin.
4. It is not trivial to obtain reliable G_0 measurements in the laboratory. The main influence is the sample degradation resulting from all sampling related activities, as well as difficulties in determining G_0 from BES measurements.

If only the laboratory based bender element results of piston samples reconsolidated to *in situ* stresses are plotted, tentative trends can be seen for samples from each region with suitability of G_{0lab} to describe G_{0field} decreasing with increasing values of G_{0field}

(increasing depth). Such discrepancies between field and laboratory values of G_0 have led to a number of corrections such as those found in Andréasson (1979) and Mitchell & Soga (1976). This new data indicates that corrections appear unnecessary for less disturbed samples, if they are tested quickly before any chemical or biological changes and while residual effective stresses remain within the sample. Based on the comparison of 'aged' and fresh samples around Site 1 and 7, changes associated with longer storage times may account for differences in G_{0lab} of up to 40%. However, underlying issues surrounding the interpretation of V_S from the bender element test data may also influence the scatter seen in these measurements. These issues are examined more thoroughly in the last part of this Chapter.

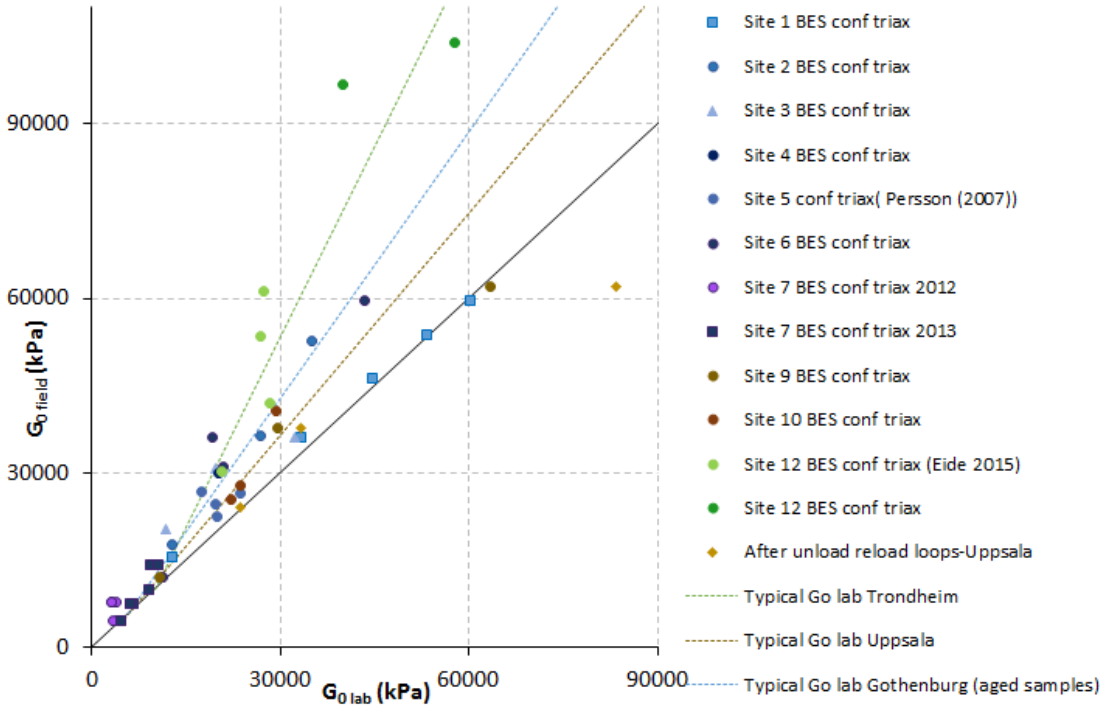

Figure 5.7 Comparison of field and BES laboratory values of G_0 for 12 test sites.

5.5 Factors influencing the G_0 timeline

The timelines of some samples are studied with particular focus on block samples (least disturbed samples) to help identify where the largest changes along the sample disturbance chain occur that undoubtedly contributes to poor agreement between $G_{0\,field}$ and $G_{0\,lab}$ that is often observed. All the results presented in this section are from bender element tests conducted with 10 kHz sine waves with interpretation of both phase velocity (time domain: Method A) and group velocity (frequency domain-cross correlation: Method B) unless otherwise indicated. If inconsistences between these two interpretation methods were present the 1st cross over (pick A) was used and a check made against the Lee & Santamaria (2005) method (when the reflected wave group was easy to identify).

Typical normalised sample time lines of shear wave velocity for different geological deposits and sample histories are presented in Figure 5.8. The smallest changes occur in the block samples (confined from site), i.e. the best quality samples, which is similar to findings by Donohue (2005). In general, the shear wave velocity of unconfined samples

was greatest at extraction, but then reduced after transport, storage and trimming. For two samples (Site 1: 27 m and Site 7:5 m $STII_{slow}$ samples), an increase in the shear velocity was observed during storage and is thought to relate to thixotropic effects. Of particular note is that the highly disturbed $STII_{slow}$ samples from Site 1:35 m (due to a frictional layer in the sample tube) gave shear wave velocity values when reconsolidated to *in situ* stresses that were very similar field values. It is not uncommon for disturbed samples to exhibit values of V_S equal to or higher than $V_{S\ field}$ and is one of the reasons why sample quality cannot be determined by comparison of only $V_{S\ lab}$ and $V_{S\ field.}$ Aged samples were less sensitive to sample trimming and mounting, but experienced smaller increase in shear wave velocity after reconsolidation, in many of the aged samples (heavily discoloured) only marginal increases of V_S were observed with increasing triaxial stress. Lacustrine samples experienced the largest changes in the shear wave velocity after transport, storage and trimming, however, these samples often recovered well. All samples experienced significant reduction in shear wave velocity after failure (ε >15%) consistent with loss of structure during strain softening.

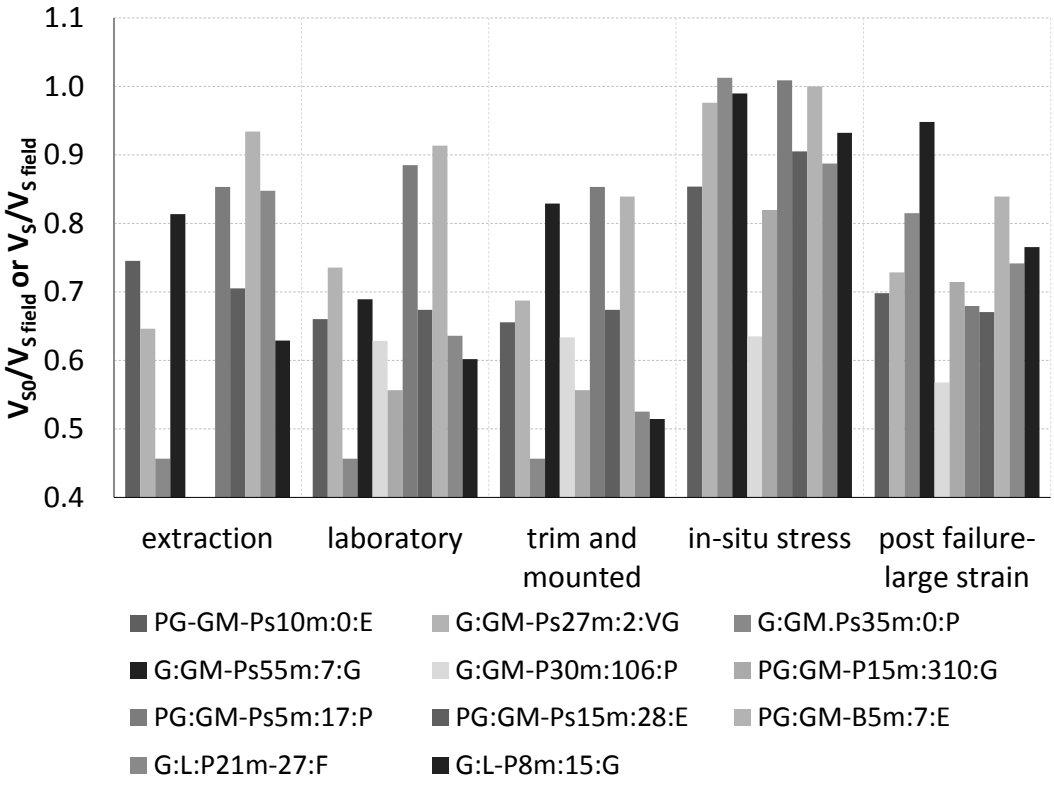

Figure 5.8 Sample timelines for; varying soils (PG=post glacial, G=glacial, GM= glacio marine, L=lacustrine), sample type (Ps=slow STII piston, P=STII piston, B=Block), depth, age at start of test and sample quality (Lunne criteria) E=excellent, VG= very good; G=good, F=fair, P=poor.

The disturbance observed in samples, affecting laboratory values of G_0, relates to the whole 'disturbance chain' from the extraction through to start of testing. Differences occurring in the disturbance chain between block and standard piston samples were presented in Figure 4.22 and Figure 4.23. Differences in the disturbance occurring in piston samples during extraction, makes it difficult to study the effects of secondary disturbance following sample extraction. However for the six block samples extracted

from Site 8 the amount of disturbance during extraction is similar thus these blocks can be used to study the influence of transport, storage, trimming and sample preparation, mounting in triaxial test apparatus, loading procedures etc. A detailed description of a block sample timeline in terms of both shear wave velocity and phase change across the transmitted shear wave (indicative of degree of dispersion / multi-model vibrations) is presented in Figure 5.9. For a fuller description of the stages in the sample timeline refer to Figure 4.23.

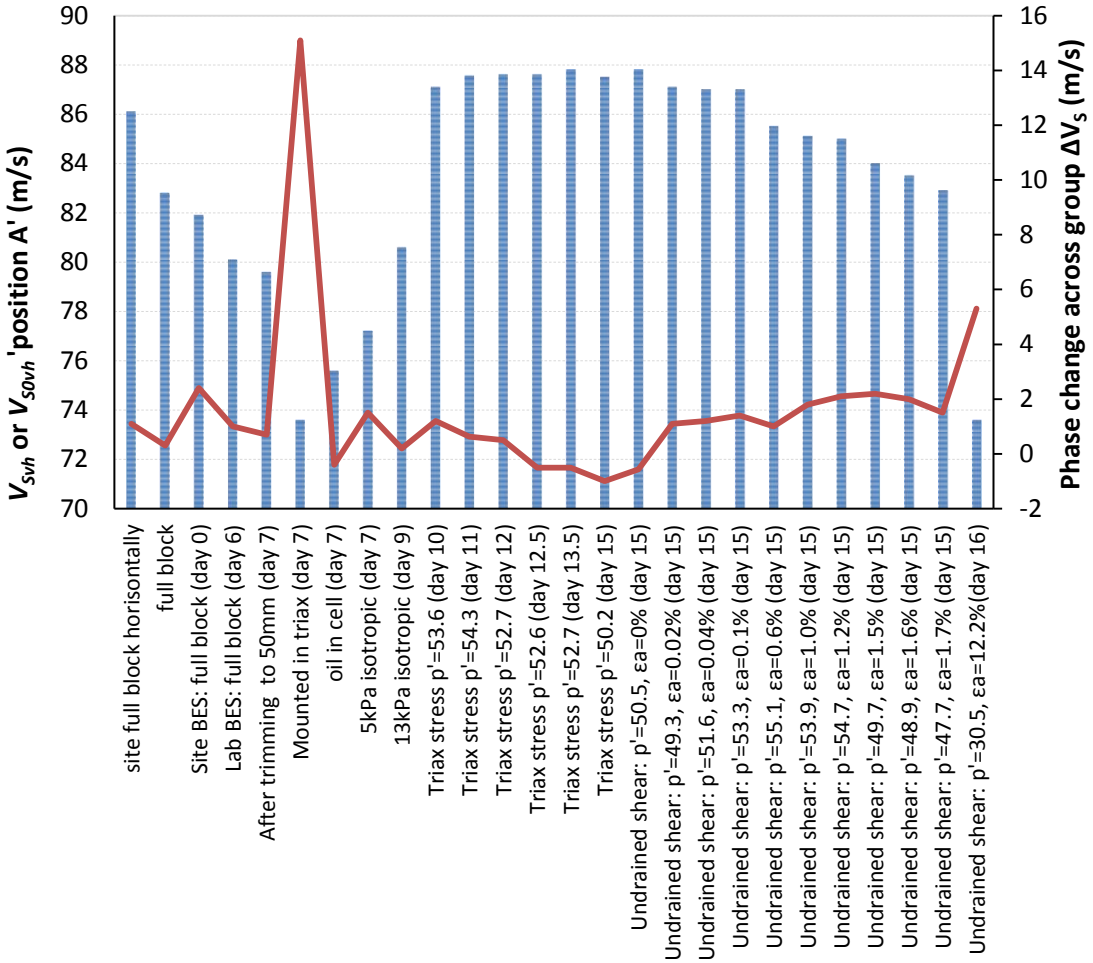

Figure 5.9 Changes in shear wave velocity measurements for a block sample along the sample time line.

5.5.1 **Influence of extraction method**

In Figure 5.10 the results of BES testing on (a) samples prior to testing and (b) at *in situ* stress are presented in terms of different sample extraction methods, and in some cases preparation methods (intrinsic, $STII_{38}$). The highest Lunne quality factor is also indicated in these plots. Clearly the low pore volume change relates well to values of $V_{S0}/V_{S\ field}$ and $V_S/V_{S\ field}$ that tend to 1 (*in situ* values) with block samples clearly indicating the least amount of disturbance, closely followed by $STII_{slow}$ samples and $STII_{60}$ (middle tube) samples that were tested within 7 days. Two high values of $V_{S0}/V_{S\ field}$ for $STII_{60}$ samples is thought to relate to densification of the sample associated with mechanical damage. Values of $V_{S0}/V_{S\ field}$ of the intrinsic samples act as a lower bound,

however, some STII samples (from East Coast) can be observed at similar values indicative of significant disturbance. The majority of the $V_{S0}/V_{S\ field}$ values exceed the Landon "best" criterion ($V_{S0}/V_{S;field} \geq 0.6$), however, not all these tests achieve the Lunne "class 1" criterion.

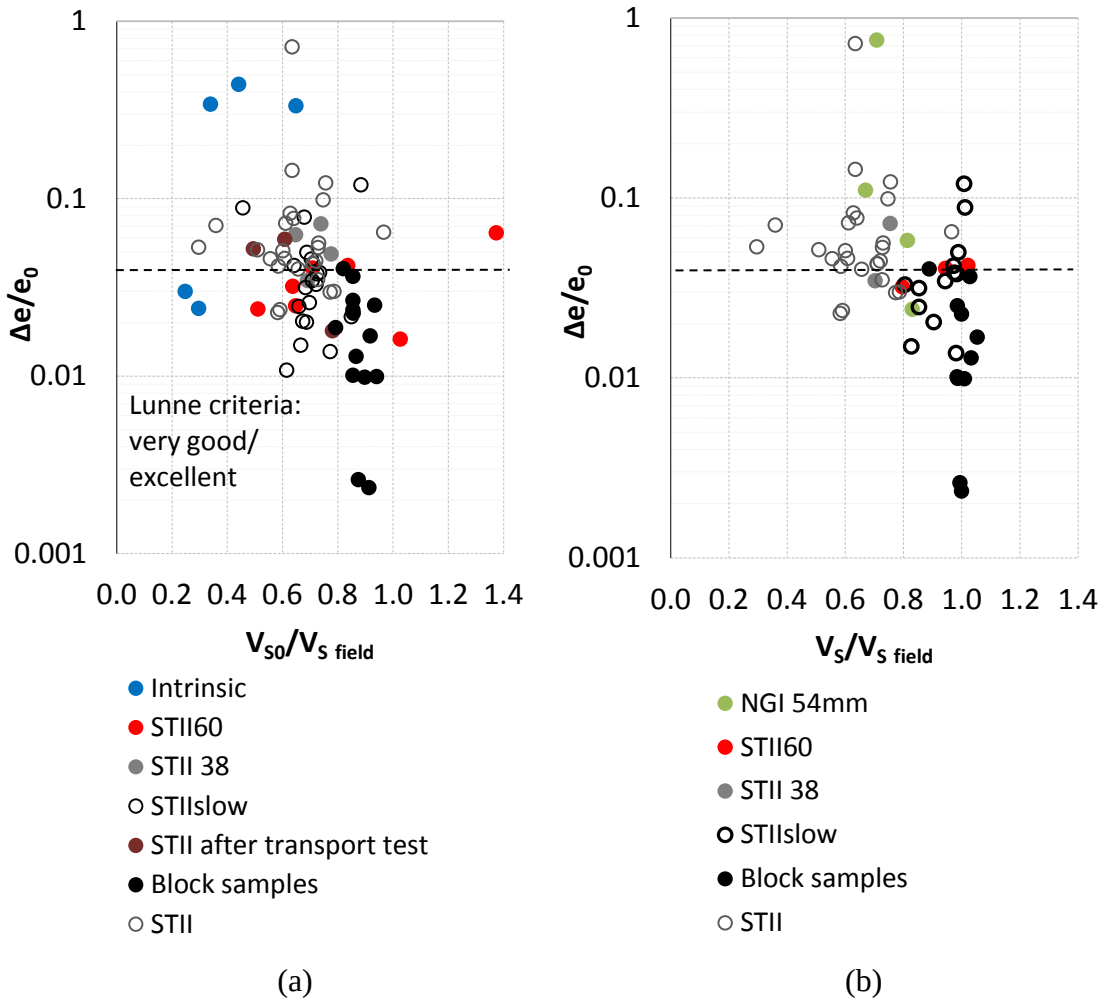

(a) (b)

Figure 5.10 Variations in shear wave velocity for different sample extractation and trimming methods (a) unconfined BES prior to testing, (b) confined BES at in situ stresses

5.5.2 Transportation and storage effects

In order to understand the impact of different transport procedures and storage, some of the BES results on 'less disturbed' block samples are used. Three methods of transport were used for these samples; Block 1, 2 and 3 were confined on site (wax and muslin 3 layers) and transported in a straw filled container, Block 4 was wrapped in cling film (3 layers) and transported on the back seat of a pick-up truck and Block 5 and 6 were wrapped in cling film (3 layers) and placed in a bubble wrap filled containers for transport. On arrival at the laboratory additional wax and muslin layers were added to Block 5 and 6, while these were not added to Block 4 until after CRS tests were done 2 days later. When the blocks were opened, the remaining parts of the sample (not needed for testing) were wrapped in 3 layers of wax and cling film, as it was found difficult to remove the wax and muslin layers without causing damage to the block.

In Figure 5.11 the received signals of BES tests on block samples are compared at extraction and after transport and storage at 7°C and 100% humidity. There are some striking differences. The stored samples had lower residual effective stress due to dissipation of excess pore water pressures but in all other ways the block used in the comparison is the same.

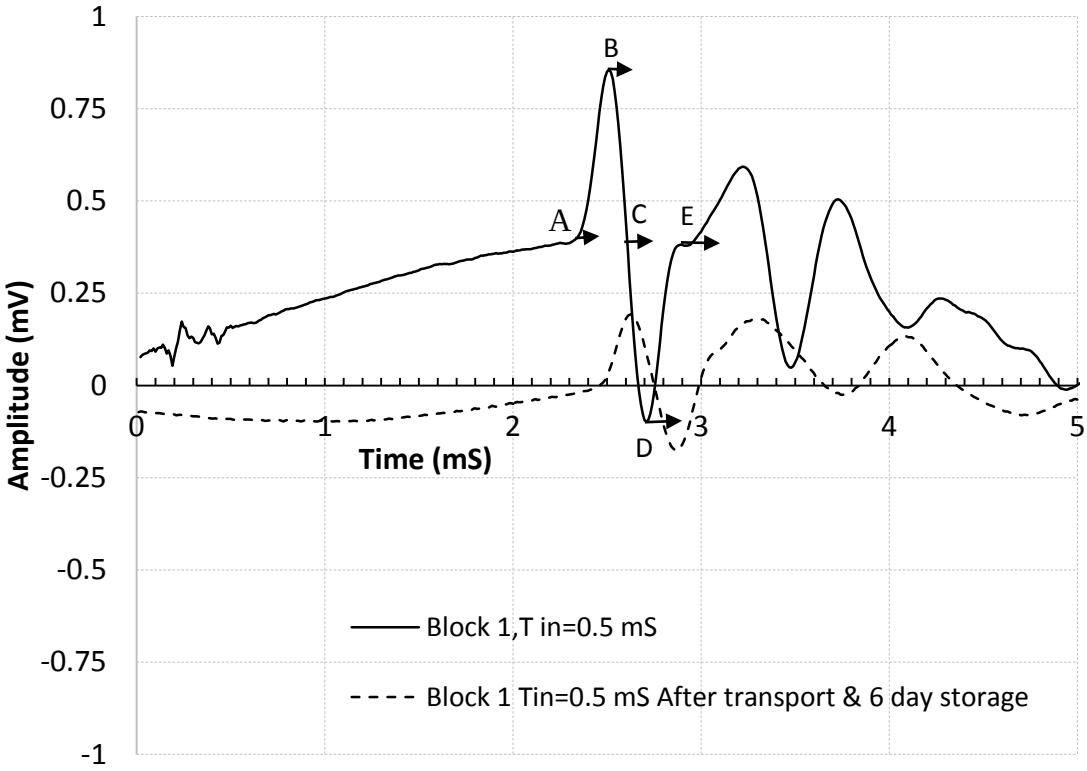

Figure 5.11 Observed changes in unconfined BES measurements (2kHz sine input wave) for a block sample.

There is almost twice the amount of signal attenuation in the sample that has been transported and stored and additional dispersion which leads to differences in the phase and group velocity for this test.

If the unconfined vertical shear wave velocity data for block samples (and three STII samples) is plotted in a bubble diagram, where the measurements on individual samples can be seen in addition to the magnitude of the shear wave velocity phase change across the received wave (differences between position A to E in the time domain is given by the size of the marker) it can be seen in Figure 5.12 that when V_{S0} is low this is often connected to larger velocity phase change, indicative of greater dispersion of the received wave. When blocks were first opened from site the highest values of V_{S0} were observed which often had very little dispersion. The arrows indicate changes when block samples have been divided. It appears that providing block samples remain confined from the day of extraction similar magnitudes of shear wave velocity from field values can be obtained even after storage of up to 62 days. However, if the blocks are opened, even if only for short periods of time, the shear wave velocity reduces. It would seem prudent therefore to leave block samples confined whenever possible. The measurements of V_{S0} of the STII samples were both higher and lower than block samples with an obvious increase in V_{S0} for the STII samples with the lowest values on extraction. While the latter is most likely related to thixotropic effects it is thought the

large discrepancy in V_{S0} may be related to issues with interpretation however reflected waves were not clear enough to allow alternative interpretation methods such as comparing the first arrival and reflected waves in line with Lee and Santamaria (2005). The phase change in the transmitted waves was significant for all the STII BE tests consistent with increased sample disturbance but also issues relating to geometrical effects caused by closer rigid horizontal boundary that would cause additional distortion and multimodal vibrations, refer to O'Donovan *et al.* (2015).

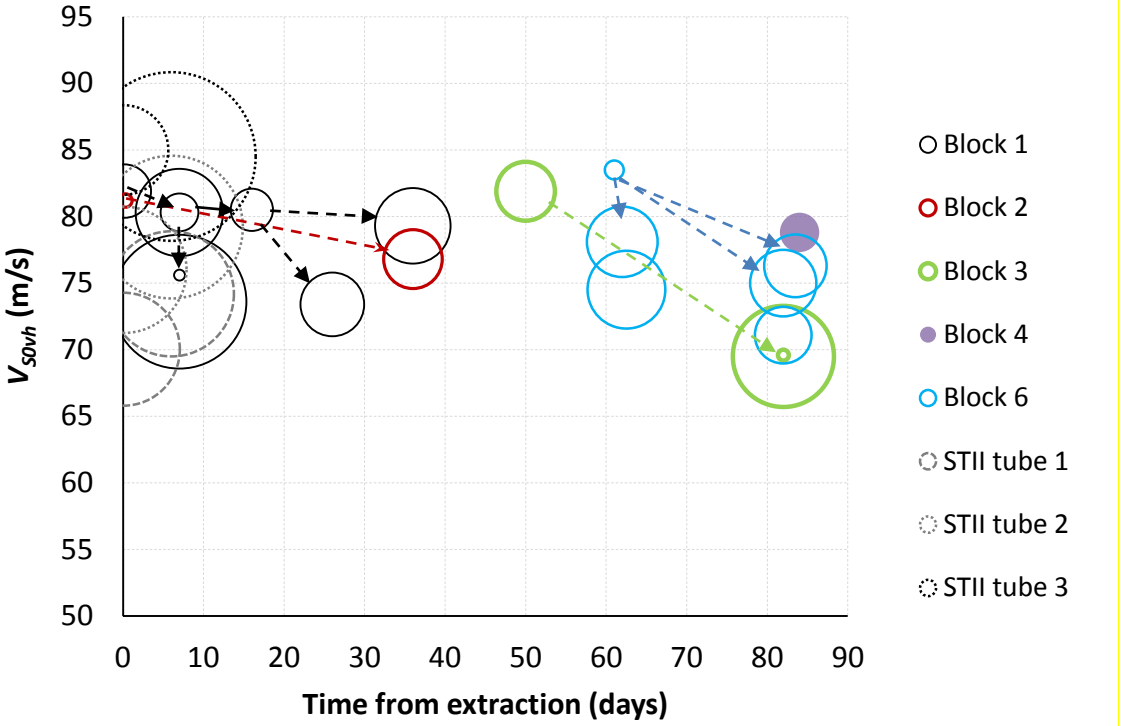

Figure 5.12 Summary of unconfined V_{Svh} tests from site to installation in triaxial apparatus with bubble size representing the extent of phase change across the first shear wave arrival for Block and STII samples from Site 8.

The test results from confined bender element tests on block samples are plotted in Figure 5.13 with respect to shear wave velocity in (a) and phase velocity change in (b) (difference in V_S between positions A and E using Method A) in two respective bubble diagrams but this time bubble size relates to sample age, it can be seen that younger samples had less dispersion, making interpretation using linear interpretation methods more reasonable. This no doubt relates to the quality of the BE:soil connection. Negative values of phase change, ΔV_S, relate to samples which had a pre-existing shear band which caused refraction of the travelling wave and causing superposition within the initial wave group arrival.

In terms of the effects of different transportation methods on small strain stiffness, there were no significant differences between the block samples that were confined on site and transported in straw and the samples that were transported in bubble wrap filled containers and wrapped in cling film during transport and then confined on arrival in the laboratory. However for Block 4 which was transported on the car seat and left unconfined for 2 days shear wave velocity was lower (by 7.5%). This sample also had

significant mechanical damage on the edges of the sample that had been in contact with the car seat, thus differences are thought to relate to damage during transport.

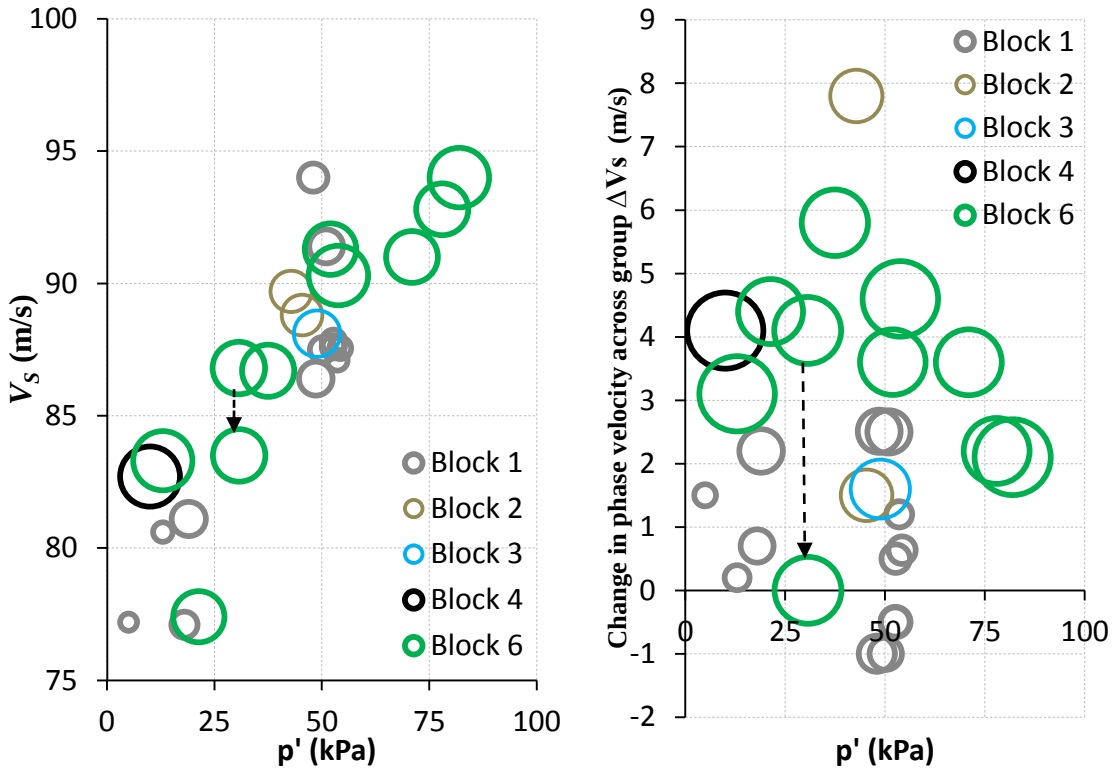

(a) (b)

Figure 5.13 Changes in V_S for confined triaxial samples at completion of each loading stage (stable pore pressures), Block 2 =V_{Shh} all others are V_{Svh} where size of bubble relates to sample age (6 to 85 day)

Some of the findings presented above are further corroborated by the unconfined measurements conducted on block samples and STII samples from Site 8 presented in Figure 5.14. In addition to the vertical shear wave velocity, also the horizontal shear wave velocity of unconfined block samples are shown (within the grey varves). The horizontal shear wave velocity were up to 9% higher than vertical shear wave velocity and experienced negligible degradation during storage, while vertical shear wave velocity reduced by up to 17% over a period of 86 days. The differences between the horizontal and vertical shear wave velocity of unconfined block samples appears to compare well to differences in field measurements presented by Andréasson (1979) and Larsson & Mulabdic (1991).

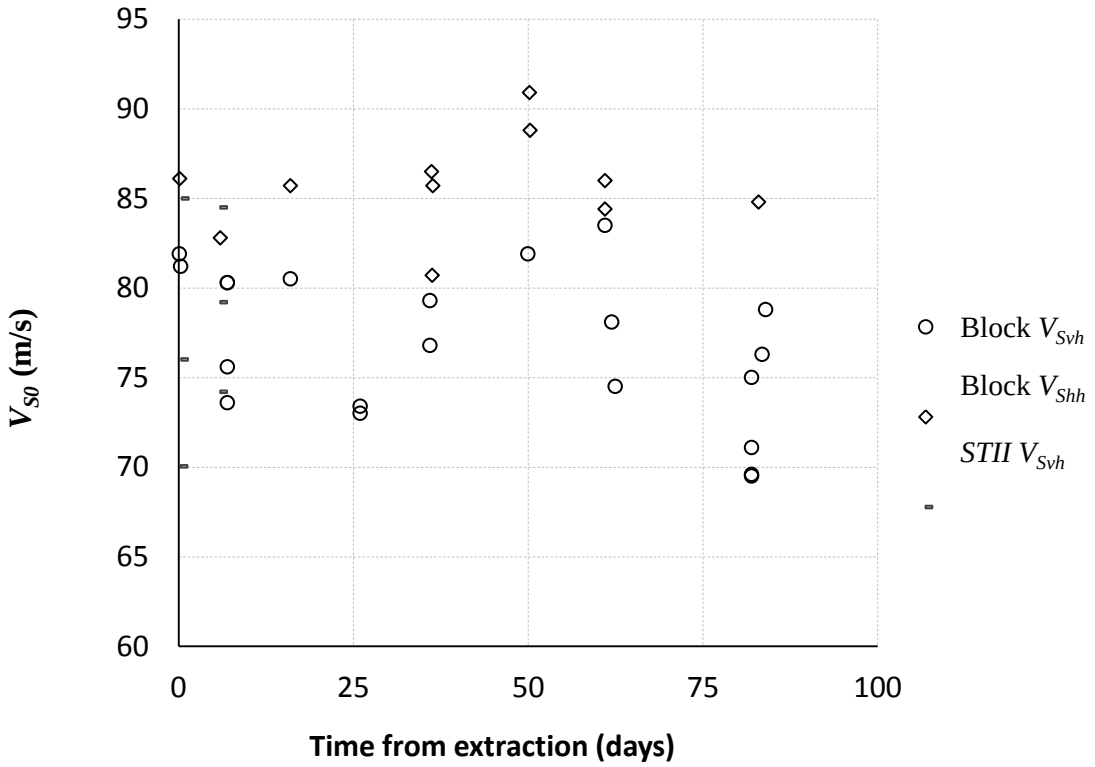

Figure 5.14 Variation in unconfined shear wave velocity in vertical and horizontal direction with time for block samples from Site 8 (Zone 2 glacio-marine clay).

When piston samples were transported from Site 7 in 2013 accelerometers were used to measure how much vibration samples experience during transport, vibrations that may well lead to increased disturbance and degradation of G_0. This site was around 20 kilometres closer to Gothenburg than Site 8 (but lay on the same transport route) thus similar vibrations are likely to have been experienced by samples transported from Site 8. In this study identical sample boxes were used (foam lined) but transported by car and pickup truck. A comparison of the vertical accelerations experienced by the sample boxes are presented in Figure 5.15. Transportation from the Site 7 involved both motorway and town driving as indicated. The pickup truck was towing a mobile laboratory (horse box) thus took 36 minutes to reach the university as opposed to 27 minutes for the car. The difference in the travel time was mainly within the town (different traffic light stops). Samples experienced greater accelerations within the town relating to breaking and accelerations at road junctions. The vertical acceleration peaks experienced by samples transported by car were more frequent with 40 peaks of magnitude ≥1.5 g, whereas the samples transported by pickup truck experienced around 20 peaks ≥1.5 g. It is not clear how much of this greater acceleration experienced by the car samples relates to the damping mattress placed under the sample box and how much relates to the car suspension system in this comparison.

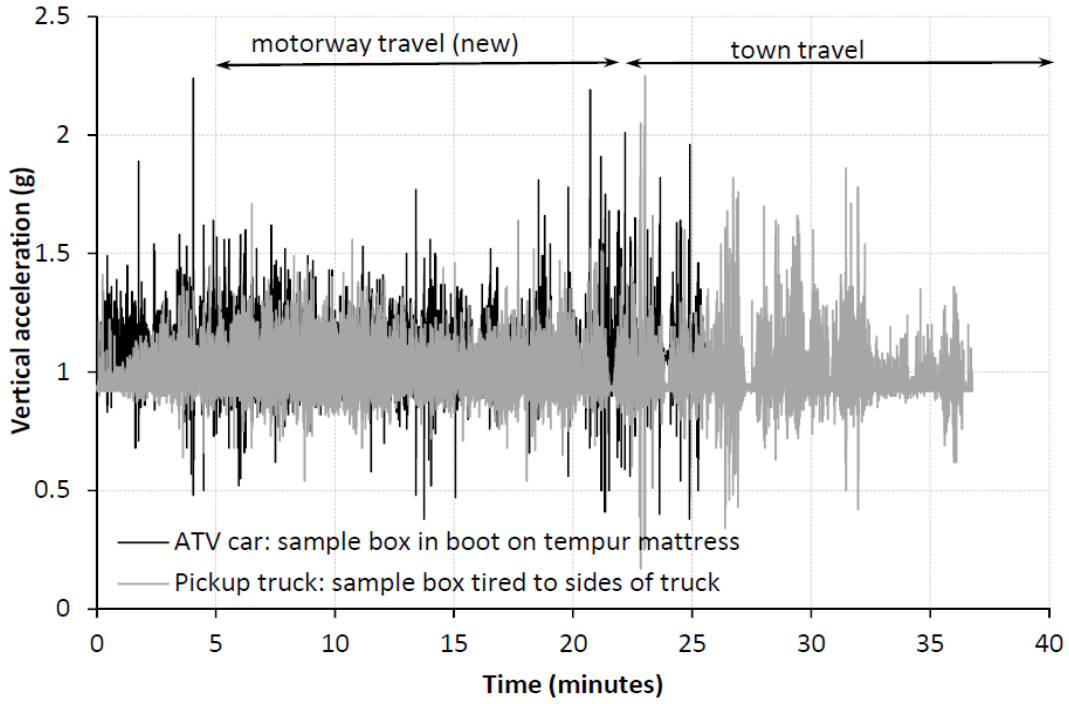

(a)

Figure 5.15 Accelerations experienced by different transport boxes during transportation from Site 7 (50 km from CTH).

In general samples transported in the car on a damping mattress experienced more acceleration peaks than samples transported in the pickup truck (typically used for commercial site investigations) provided the sample box was tied down. Both vehicles were driven with the utmost care to avoid disturbance, yet still a number of large peaks were experienced. In order to understand the impact of such peaks on small strain stiffness clay piston samples from Site 7 and 11 were placed in the foam lined box after measurements of V_{S0vh} prior to a second transport test and were measured again after 45 minutes of town driving, the results are shown in Figure 5.16. The increase in V_{S0} from field to laboratory for Site 11 samples can potentially be explained by thixotropy. However, V_{S0} increases further during the 100 day storage period which is thought to be an effect of chemical changes such as oxidation, changes in hydrogen bonding (free water becoming fixed) and desaturation. After the 45 minute transport study there was a large drop in shear wave velocity due to vibration induced disturbance for both samples. CRS tests conducted on these samples gave an estimated sample quality using the Lunne criteria of good ($\Delta e/e_0$=0.052) for the sample from Site 7 and excellent ($\Delta e/e_0$=0.018) for the sample from Site 11. Assessments on corresponding fresh samples were very good ($\Delta e/e_0$=0.039) for Site 7 and excellent ($\Delta e/e_0$=0.028) for Site 11. Unfortunately neither of the samples used for this second transport test were fresh, it is likely that fresh samples would have experienced even greater changes in shear wave velocity.

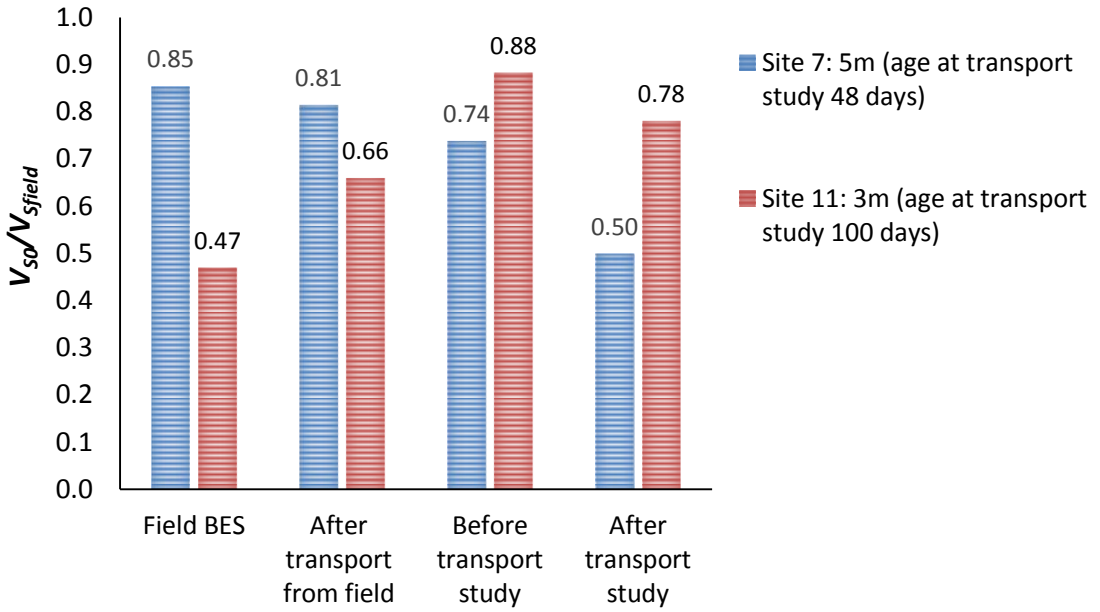

Figure 5.16 Impact of transport (and storage time) on STII piston samples

Specific studies on the effects of transport have been conducted on a limited number of samples. Based on these limited results, a number of tentative conclusions are drawn:

- Vibrations induced during transport induce changes in small strain stiffness.
- Aged samples are less sensitive to disturbance most likely due post sampling chemical changes.
- Transportation should be done using "careful" driving (slow breaking, acceleration, curves).
- The transportation distance should be minimised and route selected to avoid poor road surfaces, junctions; speed bumps, etc. where ever possible.
- Use of damping mats below sample boxes can increase disturbance. Focus instead on sample box linings that have good damping properties
- Mobile site laboratories may be a better alternative, provided the test environment (temperature, vibrations) can be adequately controlled and samples are rested at least 1 day to recover from sample extraction.

5.5.3 **Influence of re-consolidation time**

There are changes that occur both at the BE:soil interface and within the sample itself during hold periods at in-situ stresses. How this equates to changes in G_0 is shown in Figure 5.17.

While changes in the excellent quality high plasticity clay block sample from Site 8 and low plasticity clay piston sample from Site 9 is negligible, the changes in the aged high plasticity clay sample from Site 2 was significant even though the sample quality was good ($\Delta e/e_0$= 0.043). Figure 5.18 shows the change in G_0 for this sample which can be defined by a hyperbolic function that could be used to allow extrapolation to a longer hold period and is similar to the approach used to derive of corrections to $G_{0\,lab}$ found in literature. Clearly based on Figure 5.17 such corrections appear unwarranted for some clay samples thus should be used with caution.

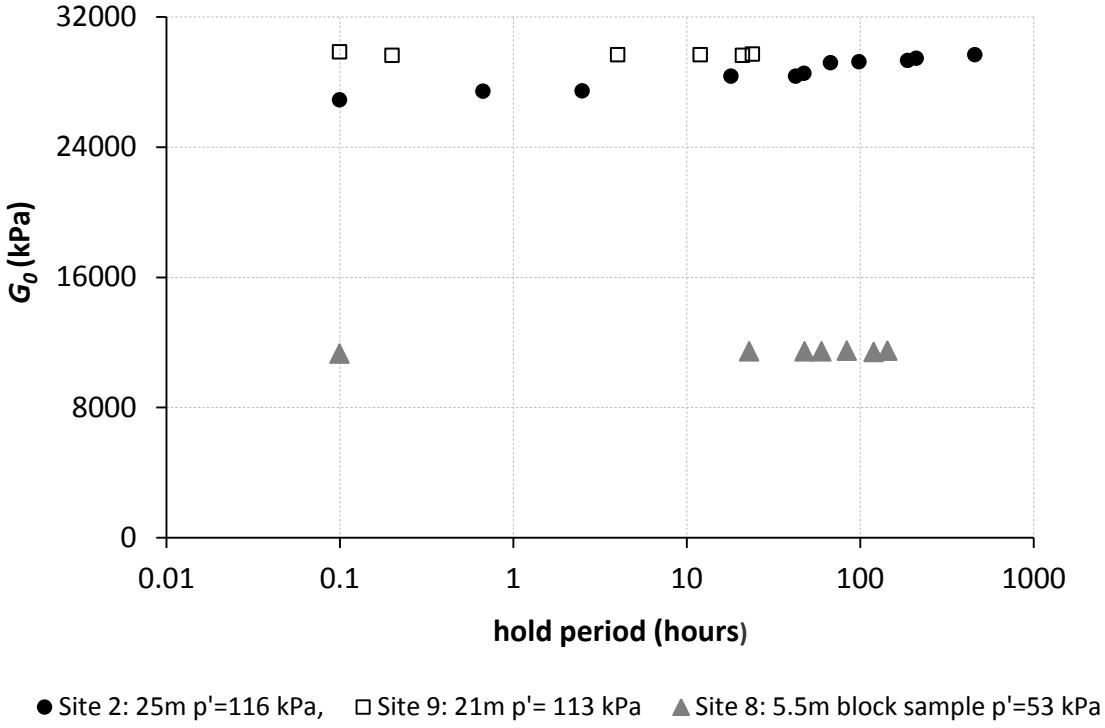

Figure 5.17 Variation in G_0 of different samples during hold period at in-situ stress

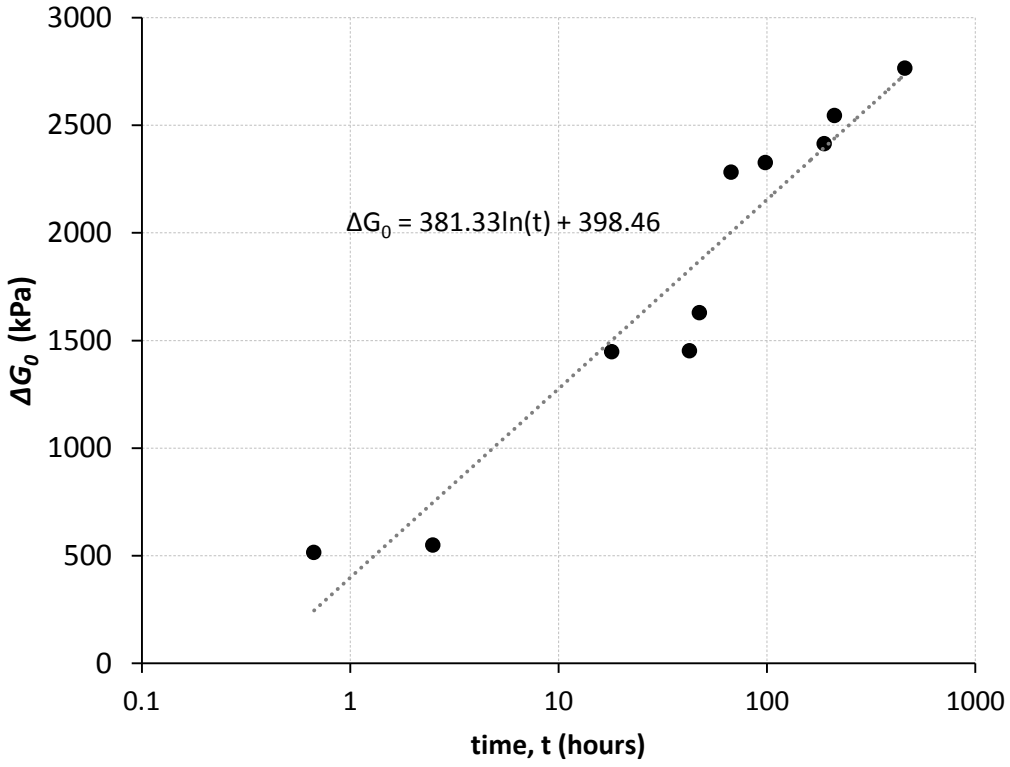

Figure 5.18 Effect of consolidation time at in-situ stress on the change in G_0 for an aged STII sample (Site 2:25m).

5.6 Effect of stress and strain history on G_0

5.6.1 Stress history

A number of samples were first loaded to *in situ* stresses (similar to Method 1 reconsolidation procedure) before being subjected to additional loads followed by unloading back to *in situ* stresses (Method 2 reconsolidation procedure), refer to Table 3.10. The differences observed in V_S on returning to in-situ stress are presented in Figure 5.19, together with the values obtained when first arriving at *in situ* stresses, in line with Method 1(after the necessary hold period required to allow stabilization of the BE:soil interface). Differences were small thus may just relate to resolution.

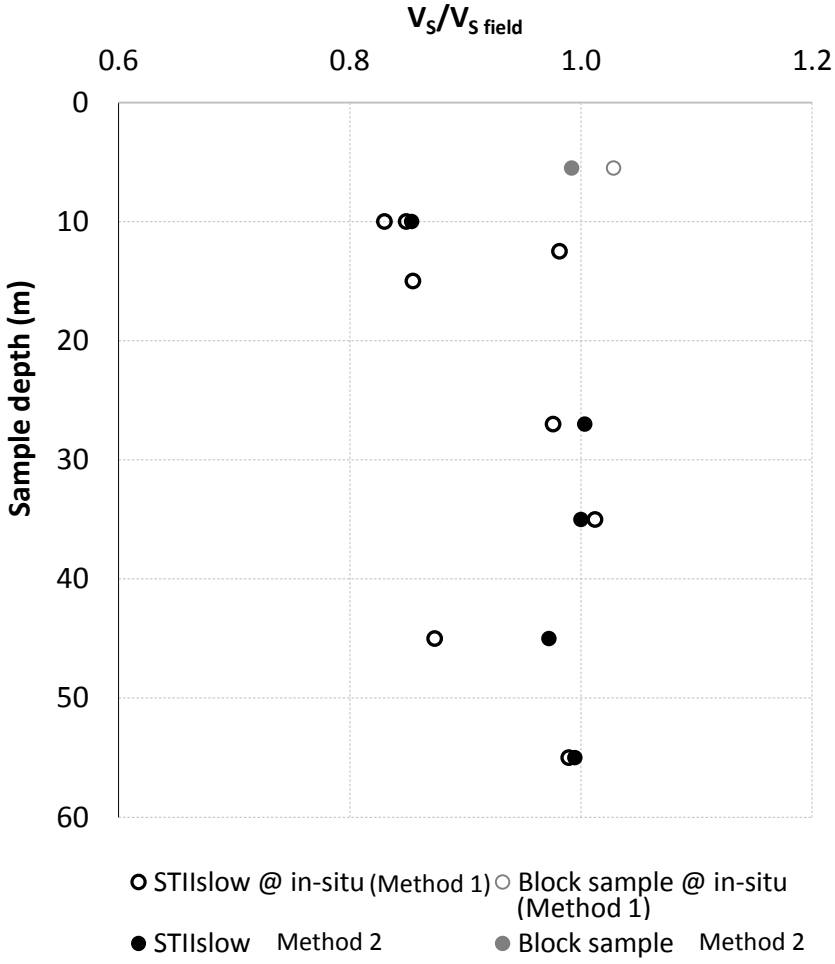

Figure 5.19 Influence of reconsolidation procedure on bender element measurements at in situ stress.

No significant changes of G_0 were noted after drained unloading and reloading loops in fresh glacio-marine samples (reconsolidation methods 3, 4 and 5 in Table 3.10). However, for lacustrine samples some variations were found for large unload-reload loops (to OCR 4), particularly in the most disturbed samples as seen in Figure 5.20, and is thought to relate to restructuring and strain hardening within the sample. Similar tests on high quality block samples or field testing would need to be conducted before any

conclusions can be drawn as to whether increases in G_0 can be expected in the field for unloading reloading loops beyond OCR 2.

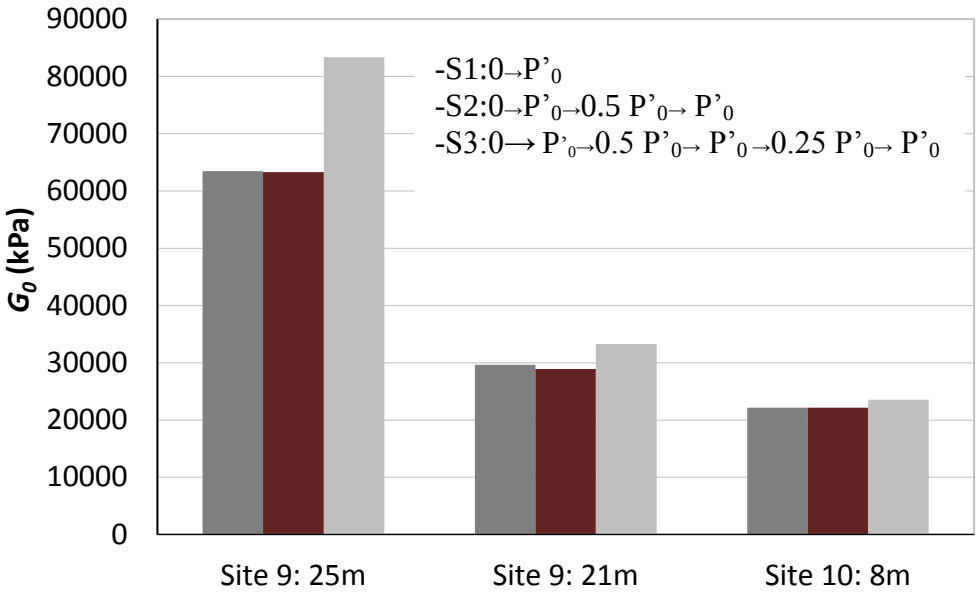

Figure 5.20 Influence of unload reload loops for BES tests on lacustrine clay of varying quality, Site 9:25m $\Delta e/e_0$= 0.077, Site 9:21m $\Delta e/e_0$= 0.071, Site 10:8m $\Delta e/e_0$= 0.051.

5.6.2 **Degradation in G_0 with increasing shear strain**

The small strain stiffness is affected by strain and relates often to the softening and destructuration of the soil. Measurement of the changes in shear wave velocity (at the difference phase positions) during shearing is presented in Figure 5.21 for a high quality block sample (with a pre-existing shear band). The shear wave velocities generally decrease with strain, however, when the pre-existing shear band is mobilised just before peak shear stress there is a sharp increase in shear wave velocity which then quickly reduces.

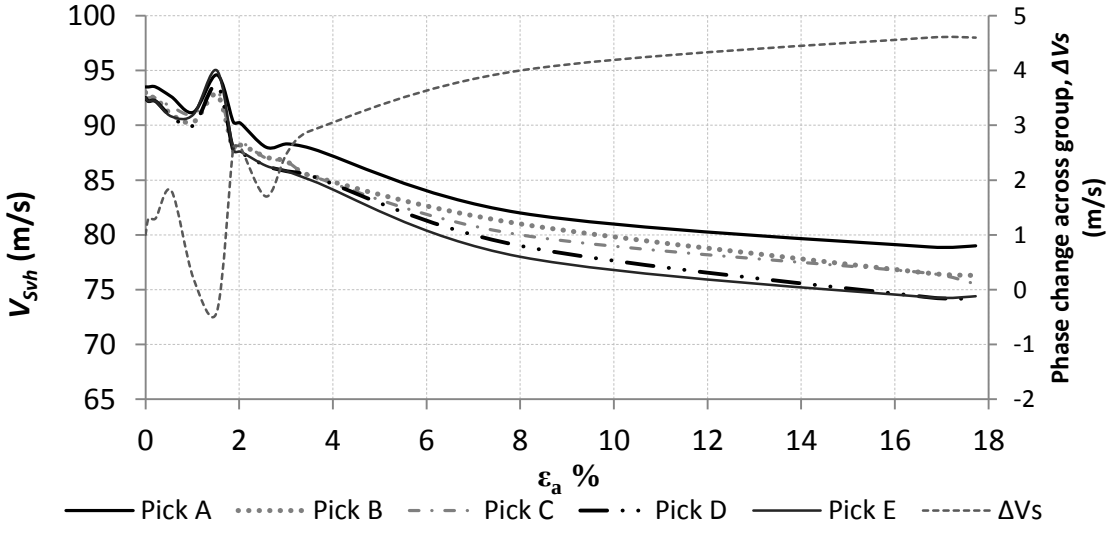

Figure 5.21 Variation in shear wave velocity and phase change across the initial wave group arrival during undrained shearing on Block 1 from Site 8.

In Figure 5.22 the variation in shear wave velocity during shearing of a number of block samples is shown, a number of which have undergone different stress history and modes of shear as outlined in Table 3.10. For tests sheared with increasing vertical stress (grey lines) degradation is similar when stress paths prior to shearing are similar. However, for the heavily over-consolidated sample there is very little change in V_S initially until failure, after which degradation of V_S is more rapid. For samples tested in extension a similar shape is observed with rapid degradation associated with the onset of failure, no doubt related to the evolution of anisotropy during shearing, refer to Karstunen (2013). The horizontal sample followed a very different stress path, which resulted in slower degradation in V_S initially but after failure of the sample (ε_a > 2%), the degradation was more rapid, in line with the extension tests on vertical samples. Clearly stress state, stress path direction and mode of shear all influence the degradation of small strain stiffness with increasing strains. It would be prudent, therefore, to allow for such changes when modelling small strain stiffness for real projects where the direction of the stress paths changes during construction and/or in service.

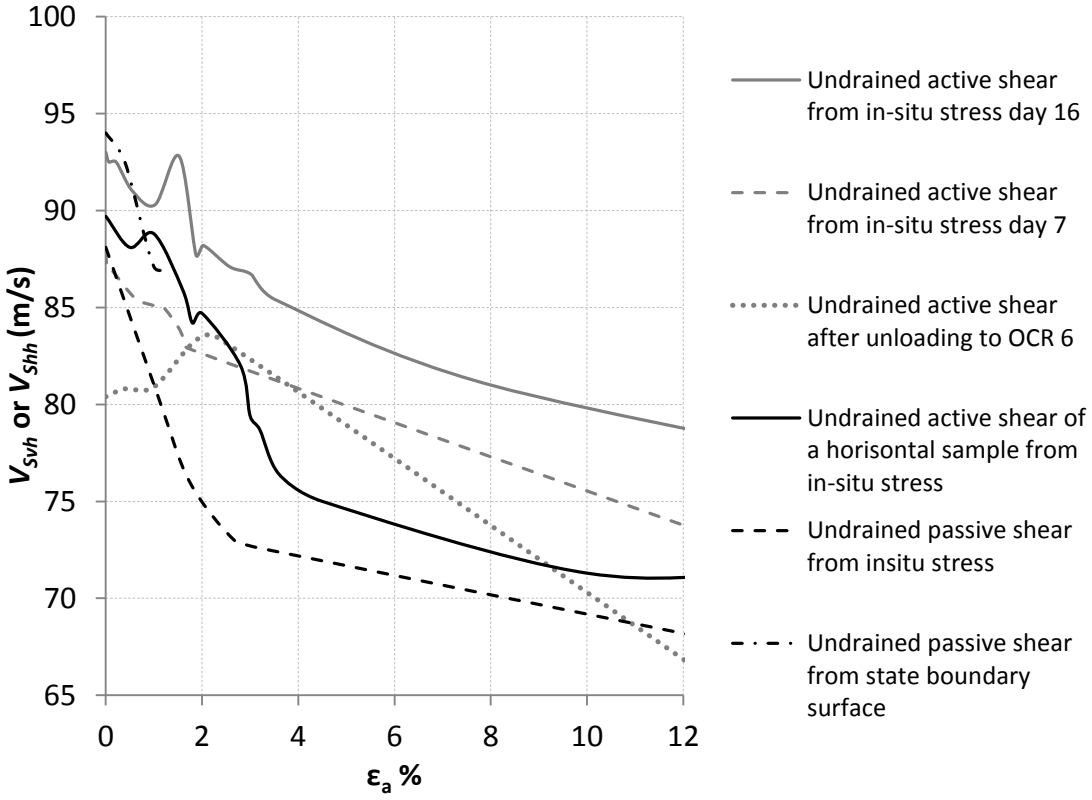

Figure 5.22 Variation in shear wave velocity for block samples with different loading procedures prior to shearing.

5.7 Degradation in G/G_0 with increasing shear strain

The work presented primarily relates to the degradation in shear modulus observed during different modes of undrained triaxial shearing for samples from 11 out of the 12 study sites. The small strain stiffness degradation is presented in terms of the variation of shear modulus (G/G_0) with respect to shear strain. The stiffness is normalised with the initial reading at small strain from the bender element tests conducted after reconsolidation to *in situ* stresses in order to easily compare the results from different stress levels (similar to approaches found in literature, e.g. Hardin & Drevnich 1972). Most work on the degradation of shear modulus has been conducted using resonant column techniques. As such the degradation is plotted with respect to increasing shear strain amplitude, and not increasing shear strain mobilised in the sample. The latter is far more relevant for deep excavations and other static problems, thus is the chosen method for presenting stiffness degradation data.

The degradation of Scandinavian soft clays has been studied in the laboratory within a series of 75 triaxial tests sheared either in compression and extension within this work. Within these tests 56 specimens were fitted with local instrumentation to allow accurate determination of secant shear modulus degradation. The shape of the degradation curves obtained varies tremendously for the soils tested as seen in Figure 5.23. All tests conducted show dramatic reduction of the normalised secant shear modulus with strain; however, the typical S-curves found in literature were not always captured. It should be remembered, however, that many G/G_0 degradation curves found in literature are plotted in terms of shear strain amplitude. It was found, similar to laboratory measurement of G_0 that the sample disturbance chain often influences the shape of the degradation curve, as well as the measurement accuracy of the testing equipment used (indicated by the error bars for each data point in Figure 5.23) and the frequency of data measurements and loading procedures.

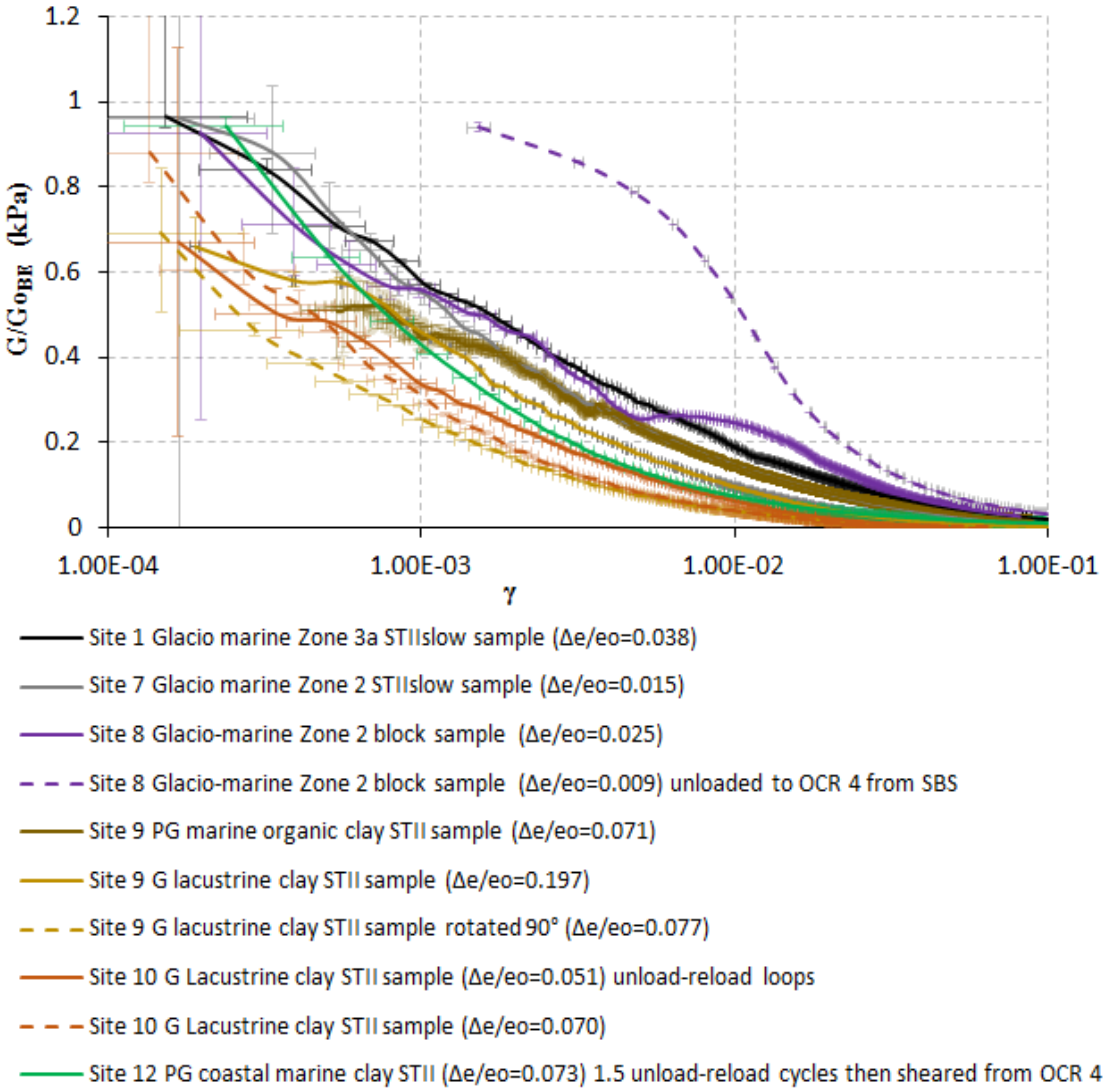

Figure 5.23 Selection of shear modulus degradation curves from laboratory measurements within the triaxial test apparatus.

5.7.1 Effects of disturbance chain on G/G_0

Similarly to G_0 the shape of the degradation curve is also affected by the disturbance chain, i.e. sample extraction, transport, storage, preparation, and re-consolidation. These effects are not as pronounced after normalization, as both G and G_0 are affected by the disturbance as indicated by Figure 5.24 (a). Clearly, Lunne's sample quality criterion is not conclusive, as differences between samples taken with the same sampler are small, whilst the superior block sample from Site 8 indicates significantly less rapid degradation initially when compared to comparable piston samples from Site 7 as indicated in Figure 5.24 (b).

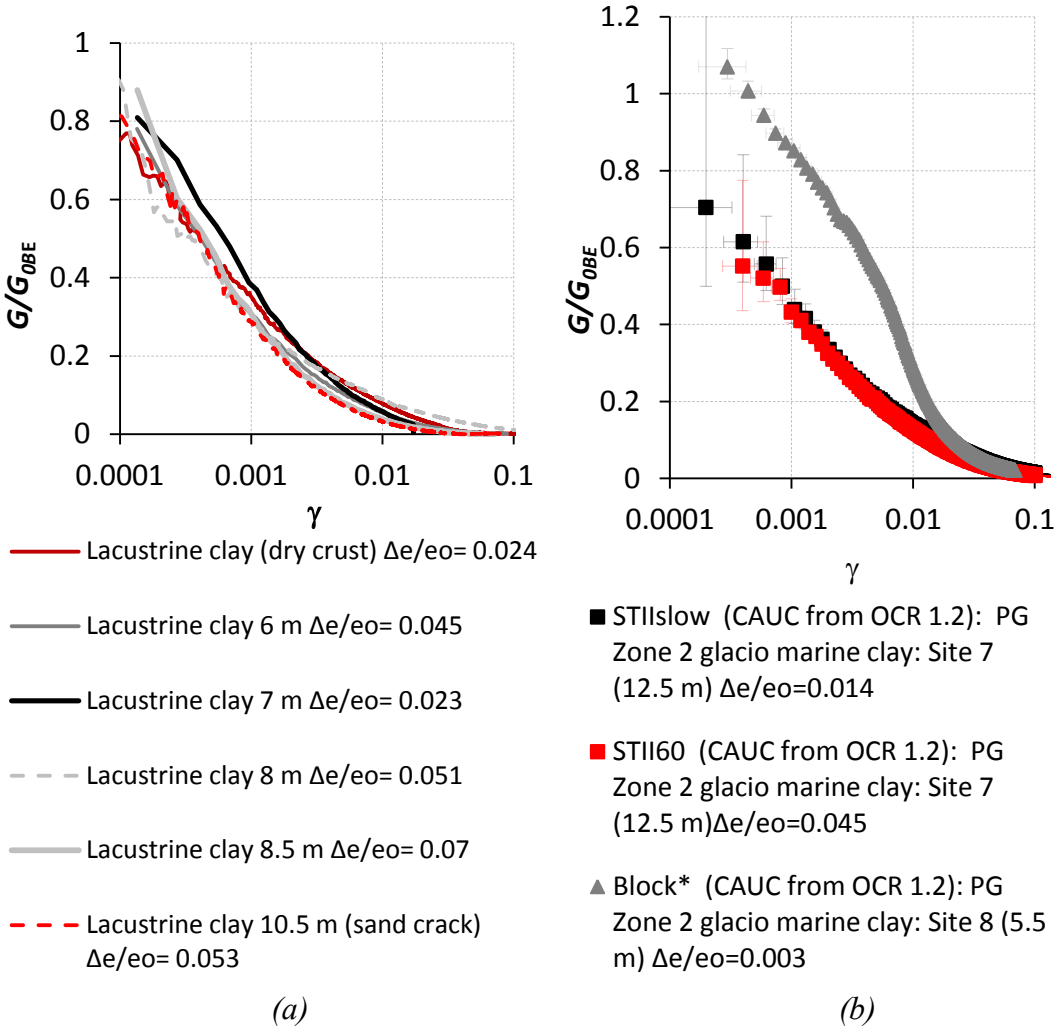

*Figure 5.24 Impact of sample quality in terms of $\Delta e/e_0$ on the shape of degradation curves for (a) Lacustrine samples from Site 10, (b) Post glacial glacio-marine samples from Site 7 and 8. *assessed G_{0BE} using Figure 5.13(a).*

No triaxial tests were conducted following specific transport studies, however it is expected that the degradation behaviour would also be affected. Storage time was found to have a profound effect on the resulting normalised degradation curve for all the Swedish West Coast sites. Figure 5.25 shows that with time the curves shift towards larger values for G/G_0 (here G_0 is measured at the start of the test after storage). This substantial difference in behaviour is also reflected in the decreasing Lunne metric from 0.038 at day 2 to 0.033 at day 170. The increase in the stiffness most probably is related to chemical changes in the sample.

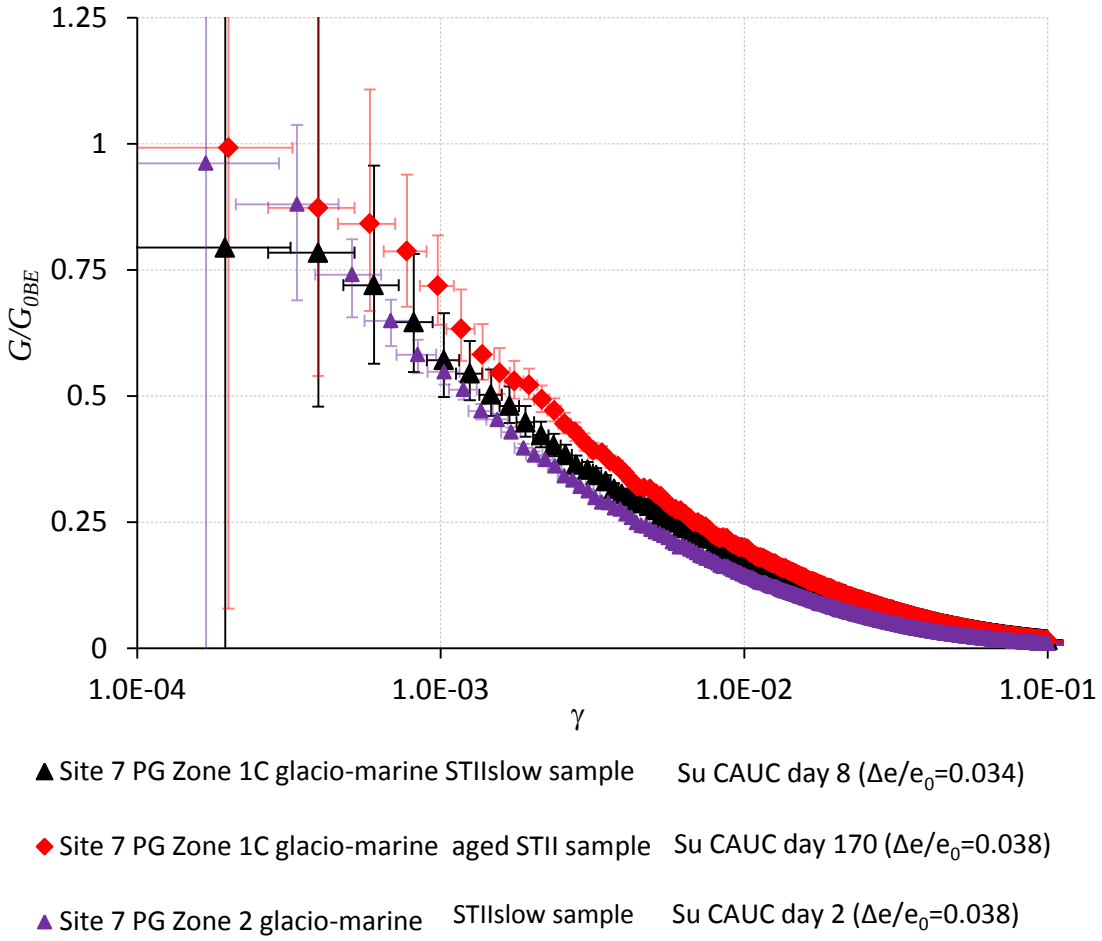

Figure 5.25 Degradation curves determined on piston samples from site 7 after various storage times.

Similarly to any laboratory test on natural samples of soft soil, the sample preparation technique, e.g. sample trimming, and choice of sample dimensions (boundary effects) can influence the results. The limited number of tests conducted on some of these aspects within this research (not presented) highlight that any difference that occurs mostly influences the stress-strain response up to 0.1% of strain. Therefore, any form of sample handling, cutting, trimming, etc. needs to be minimised in order to obtain consistent results for G/G_0.

5.7.2 Influence of anisotropy and direction of shear

The degradation of stiffness from small to large strain is an important feature of soil behaviour, which needs to be captured in serviceability limit state calculations. As expected, the standard element tests (presented in Chapter 4 and Appendix A8) on natural clay samples show strong anisotropy. In addition to the observed differences in the small strain stiffness G_0 (Figure 5.14) the normalised degradation curves, also show different responses during shearing along different stress paths, with most rapid degradation in the horizontally oriented samples (Figure 5.26a). Another indicator of anisotropy is the difference in the clay response when shearing in compression and extension. Figure 5.26(b) shows that across the small strain range, the shear modulus in

extension is larger than in compression which is similar to findings by Long *et al*. (2003).

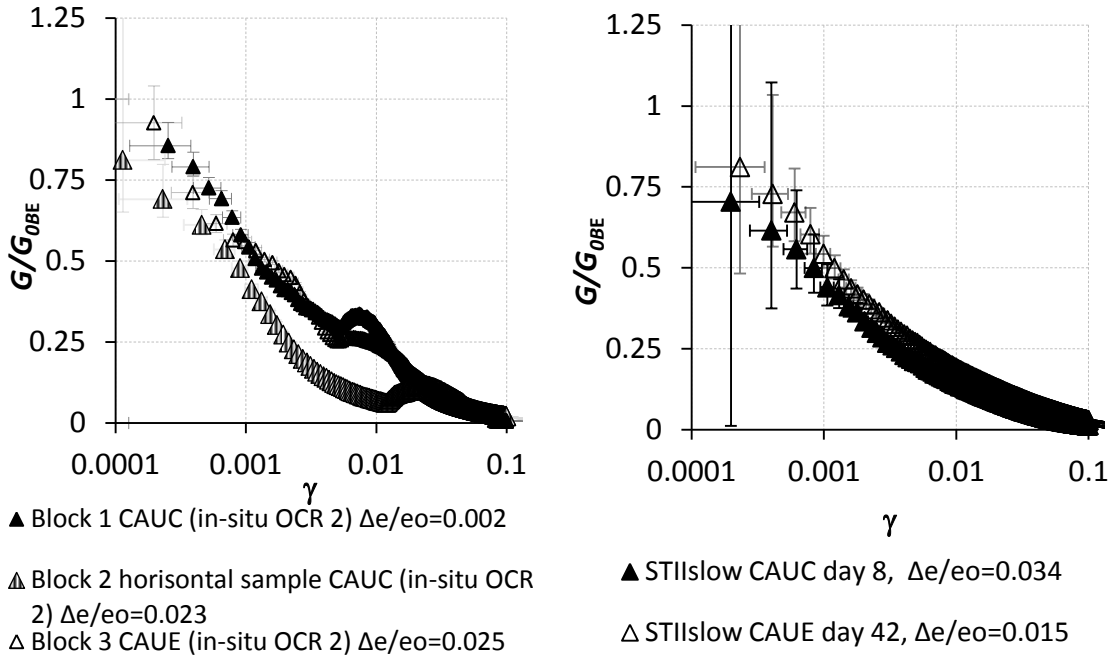

(a) (b)

Figure 5.26 Comparison of degradtion curves in undrained compression (CAUC) and extension (CAUE) for PG glacio-marine clays (a) STIIslow sampels Site 7:10 m, (b)Block samples Site 8: 5.5 m.

Most soils display stress history dependent soil response, or in this case differences in degradation curves of samples that have followed different stress paths prior to being sheared from the same stress level. The limited number of tests conducted with artificially increased OCR levels within the current research were affected by some experimental difficulties, resulting in some missing bender element data in the small strain range which is discussed in more detail in Section 5.9.4. The tentative results however corroborate the findings of Smith (1992) that increasing OCR by unloading, the curve shifts towards higher stiffness levels at small strains. This can be expected as it is well documented that most soft soils demonstrate larger re-loading stiffness after unloading.

5.8 Comparison with existing empirical relations

5.8.1 G_0

In Swedish engineering practice it is rather common, in absence of direct measurements, to relate the small strain shear modulus G_0 with the undrained shear strength. A number of existing empirical relations were tested for two different geological deposits, the glacio-marine clays at Site 1 and the lacustrine deposits at Site 10, to see how the empirically derived estimate of small strain modulus, $G_{0\ empirical}$, compared to field values, $G_{0\ field}$. Details of the empirical relationships used can be found in Appendix A1. In the following comparisons results from laboratory tests on high quality samples (shown as spheres) and/or field tests (shown as rings) are used so that results are comparable with the origin of the undrained shear strengths originally

used to define the empirical formulations that are applied. The results are presented in the cross-plots shown in Figure 5.27 and Figure 5.28 for Site 1 and Site 10, respectively. The size of the spheres indicates the degree of sample disturbance in the laboratory test results used, i.e. the larger the bubble the larger the sample disturbance (derived using Lunne criterion). The ring markers (field tests) are assumed to be of very good quality ($\Delta e/e_0$=0.04) and their size corresponds to this value, and thus can be used to assess the relative size of the spheres (laboratory tests).

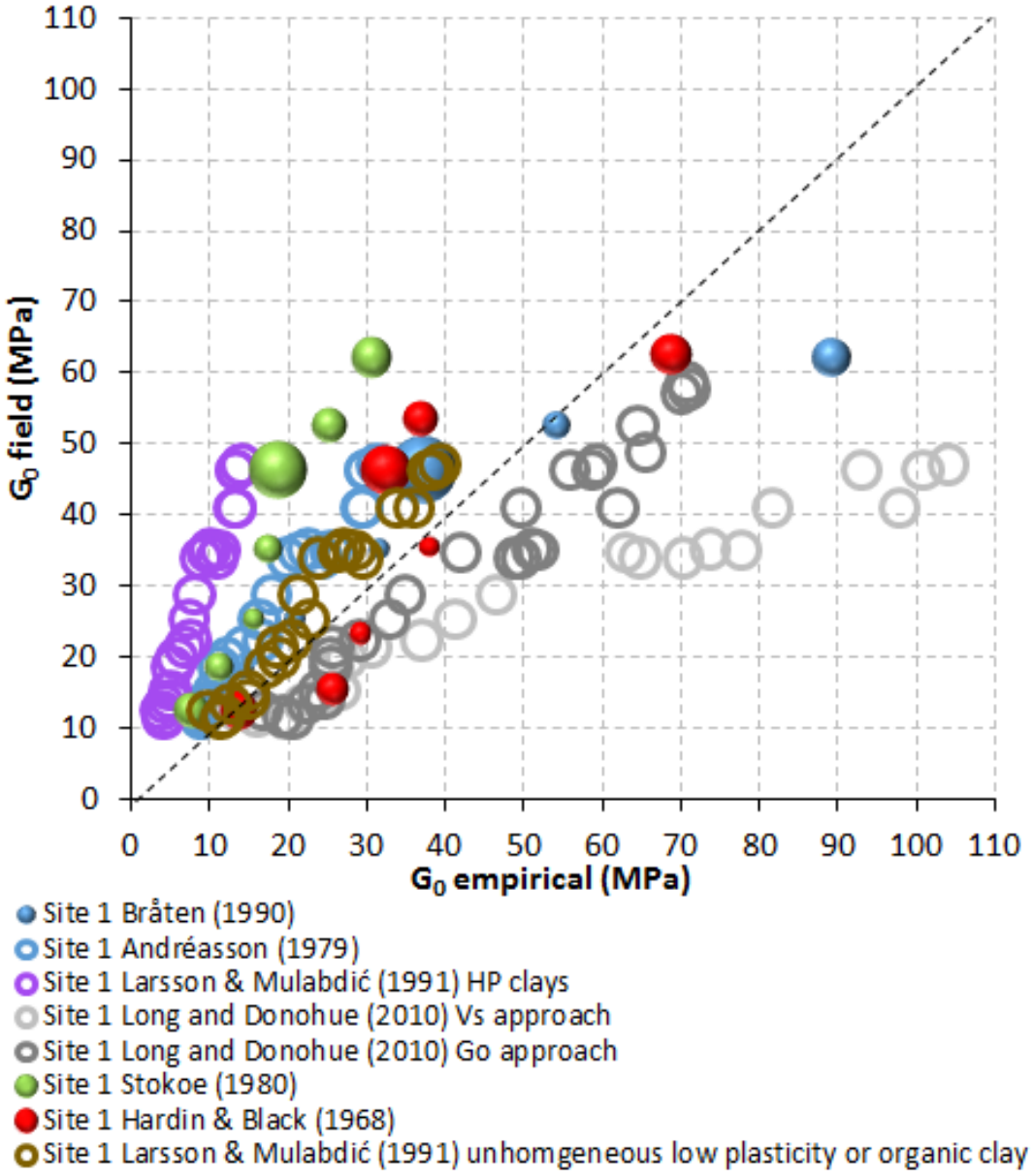

Figure 5.27 Comparison of empirical derived G_0 against field measurements for Site 1 (HP clay); larger spheres indicates larger sample disturbance. Circle size normalised on sample quality corresponding to very good.

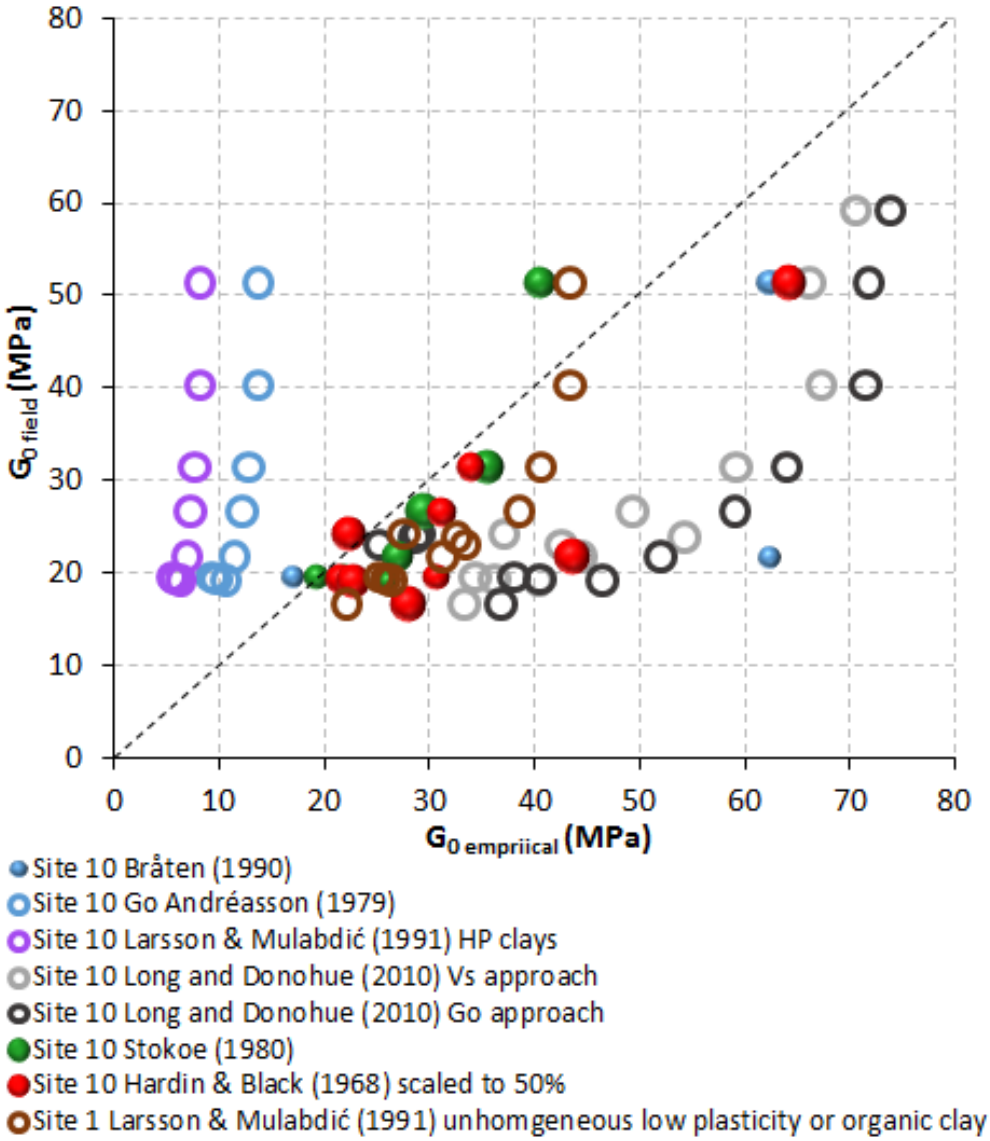

Figure 5.28 Comparison of empirical derived G_0 against field measurements for Site 10 (LP clay); larger markers indicates larger sample disturbance. Circle size normalised on sample quality corresponding to very good.

5.8.2 G/G_0

The shear modulus degradation curves are highly dependent on sample quality, over consolidation, soil type, loading procedures, mode of shear, etc. It is therefore not reasonable to expect empirical relationships to give an accurate estimation of G/G_0. To understand how empirical and laboratory curves may differ, degradation curves from Site 1 are presented in Figure 5.29, with some reference field values superimposed. For the latter SDMT data is used. The small strain measurement is from the SDMT shear wave velocity and the large strain value from the DMT pressure meter reading (where the strain level is estimated using a cavity expansion solution). Between these points the Hardin & Drnevich (1972) relationship is used to determine a curve for the glacial clays and post glacial clays. It should be remembered that this relationship is based on shear strain amplitude (resonant column tests) and not shear strain. There is a considerable

range in the laboratory degradation curves even though the samples have been reconsolidated in the same way (Method 2). The Hardin and Drnevich relationship has reasonable agreement for extension tests for the glacial clay, however, in compression this agreement is poor with significant over prediction of the magnitude of 'elastic zone' especially in the post-glacial clays (upper 20 m of the profile) with reference strains at 70% degradation differing by more than 100%. Similar issues are seen for all the soils tested.

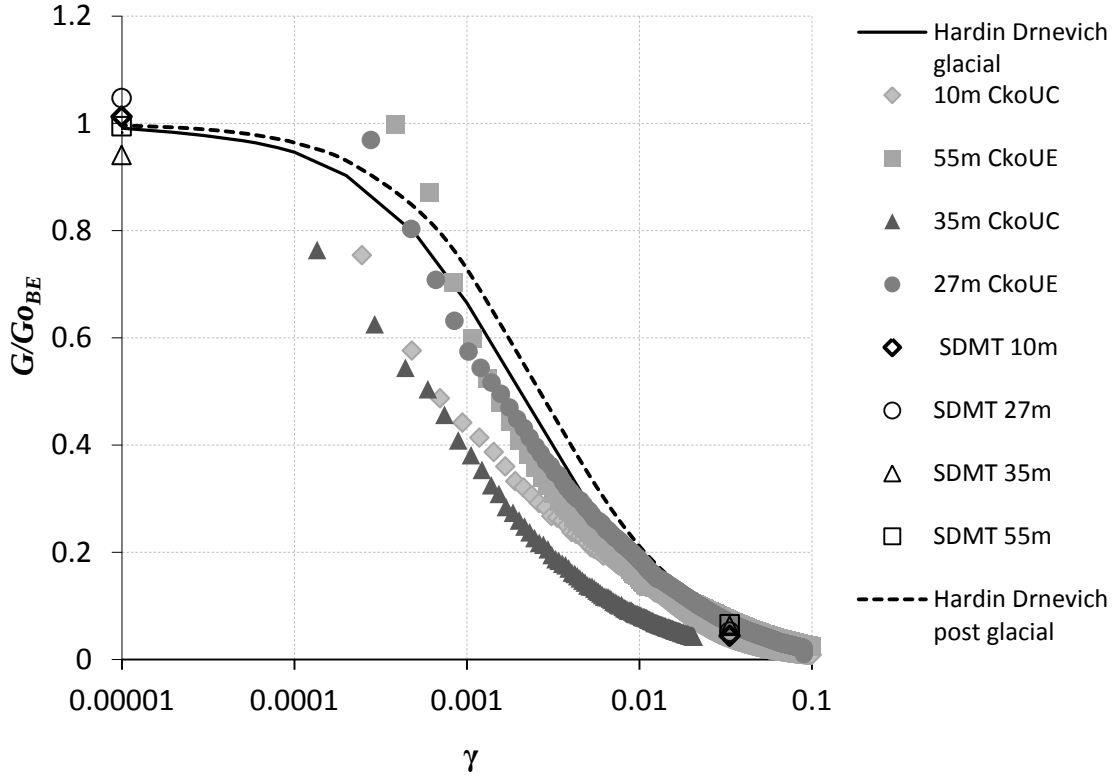

Figure 5.29 Shear modulus degradation curves from laboratory and in-situ measurements, also shown are empirically derived curves for post glacial and glacial clays.

5.9 Sensitivity of measurement results

5.9.1 Sensitivity of SDMT test results

Both the repeatability and the influence of excitation energy on SDMT seismic probe measurements were investigated at Site 4. For the repeatability test two SDMT profiles, 2 m apart were used. A comparison of the resulting V_S profiles is given in Figure 5.30, which indicates very good repeatability. A coarse sand layer just below 15 m, which was approximately 1 m thick, gave some differences in the profile immediately above this deposit which is thought to relate partly due to actual differences in this layer based on interpretation of the DMT measurements and partly the difference in the position of the layer relative to the geophones (the value of *Vs* is an average value over 0.5m). A similar discrepancy between the two V_S profiles is also identified at around 25m, which is again picked up by the DMT measurement.

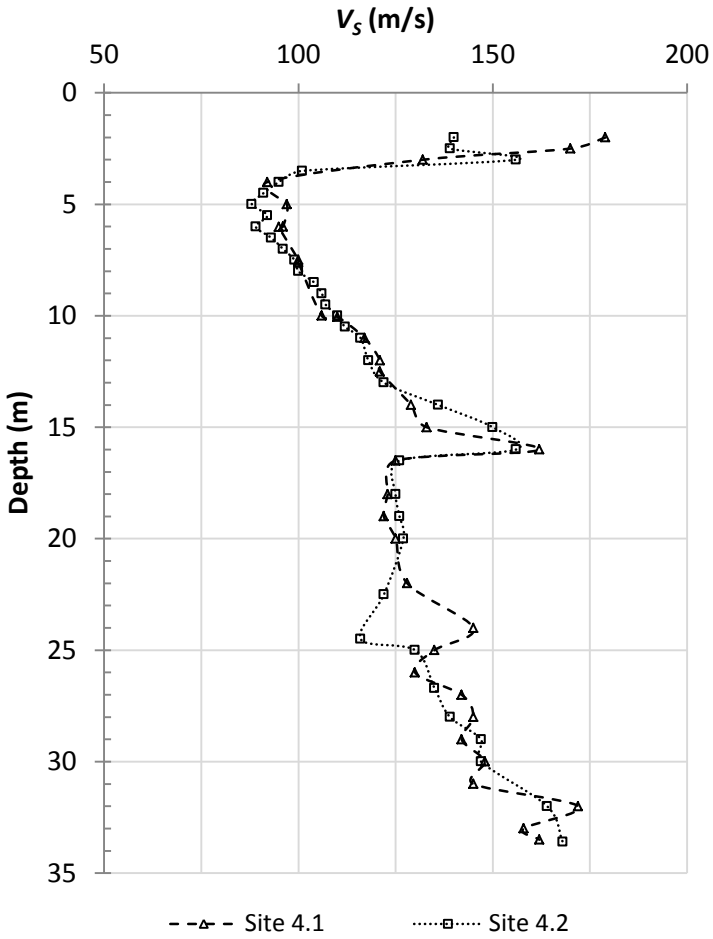

Figure 5.30 Repeatability test of V_S profile from SDMT seismic probe tests at Site 4.

In this study SDMT tests utilise a single excitation event and shear wave arrival is measured at two different depths, with V_S being assessed using cross-correlation of the two received signals (not a single point). Investigations into the influence of the excitation energy were conducted at two depths 6.5 m and 10.5 m at Site 4, and the value of V_S for five different tests assessed for two magnitudes of excitation energy. The results are shown in Table 5.2 and indicate very little influence. At 6.5 m some variation, related to the beam-soil contact, of *Vs* was observed. It was therefore concluded that adjustment of the field measurements with respect to shear strain was not required, provided that multiple tests were conducted at each level such that the variation coefficients of *Vs* results from repeated tests were kept low. In general only 3 tests were conducted and interpreted at each test depth for which the co-efficient of variation was generally <1%.

Table 5.2 Sensitivity of V_S to excitation energy applied to the shear beam.

Depth (m)	Applied energy (*kJ*)	*Vs* (m/s)
6.5	8.83	92, 97, 93, 101, 91
6.5	88.3	97, 97, 97, 97, 97
10.5	8.83	111, 110, 110, 110, 110
10.5	88.3	110, 113, 110, 110, 110

5.9.2 **Sensitivity of MASW results**

The MASW tests are a diffuse method of determining V_S and are influenced by the inversion process. All the MASW test results presented in Section 5.3 were interpreted using the Kansas University inversion software Surfseis. To try and understand the impact of the inversion process on V_S when using this software a sensitivity analysis was conducted on one of the MASW profiles from Site 7 (S14) in collaboration with APEX Geoservices and compared to interpretations done by University College Dublin (UCD) who interpreted all of the MASW tests conducted for this study using an 8 layer earth model as outlined in Section 3.3.2. A 10 layer earth model was used for the sensitivity analyses, which initially was allowed to automatically determine the input parameters for the earth model used in the inversion. The points selected for fitting the dispersion curve were selected to be as close as possible to the original "picks" chosen by UCD using an 8 layer model. The iteration accuracy stop criteria were set to a typical value of 5%. It was found that the densities automatically generated by the Surfseis software were too high so the inversion process was repeated with actual densities assessed for this site and with the accuracy condition reduced to 1%. The change in the V_S profile was up to 16% at a given depth which resulted in differences in G_0 of up to 35%. A third assessment of V_S was then conducted where the same earth model parameters were used (actual density) and iteration stop criteria (1%) but that that the picks for the inversion were selected to best fit the dispersion curve instead of trying to select the same picks of the original analysis conducted with the 8 layer model. This resulted in a reduction of V_S throughout the profile of around 21%, corresponding to differences in G_0 of around 30%.

The impact of the different inversion procedures on the interpreted V_S profile for the MASW Site 7, S14 test is indicated in Figure 5.31. Differences were greatest for the thickest earth model layers, thus one method to reduce sensitivity in the inversion may be have more layers in the earth model as it is the average value of V_S for each layer that is computed. Similar to the tests in Gothenburg at Site 6, MASW tests at Site 7 gave assessments of V_S to depths of around 11 m (mid point of the second to last layer in the earth model, the final layer is not used as this layer is of infinite depth in the inversion thus is not accurate).

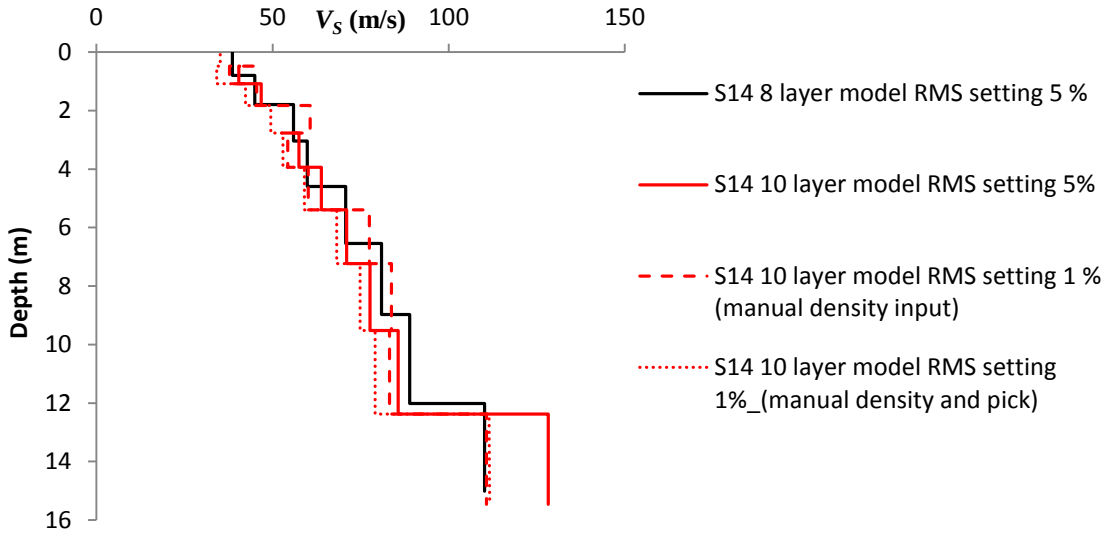

Figure 5.31 Sensitivity analysis of C assessed using MASW (profile S14).

A comparison of the field V_S profiles from MASW and SDMT tests, in addition to laboratory bender element tests at *in situ* stresses from Site 7 are shown in Figure 5.32. The SDMT test was conducted following a very cold period (frozen ground) and the effects of this cold appear to continue to a depth of around 4 m, giving larger shear wave velocities in this zone. In terms of site variation, comparison of the two MASW profiles suggests some differences are present, with higher values of *Vs* for the profile located perpendicular to the Göta River (S14). This may be an effect of drawdown of the groundwater table near the edge of the riverbank, rather than the unloading effects of ongoing river erosion, similar to Site 6. The SDMT V_S profile has a better agreement with the S13 MASW V_S profile, as do the laboratory results on fresh samples. In general agreement between the V_S profiles determined from the different methods of assessment was very good.

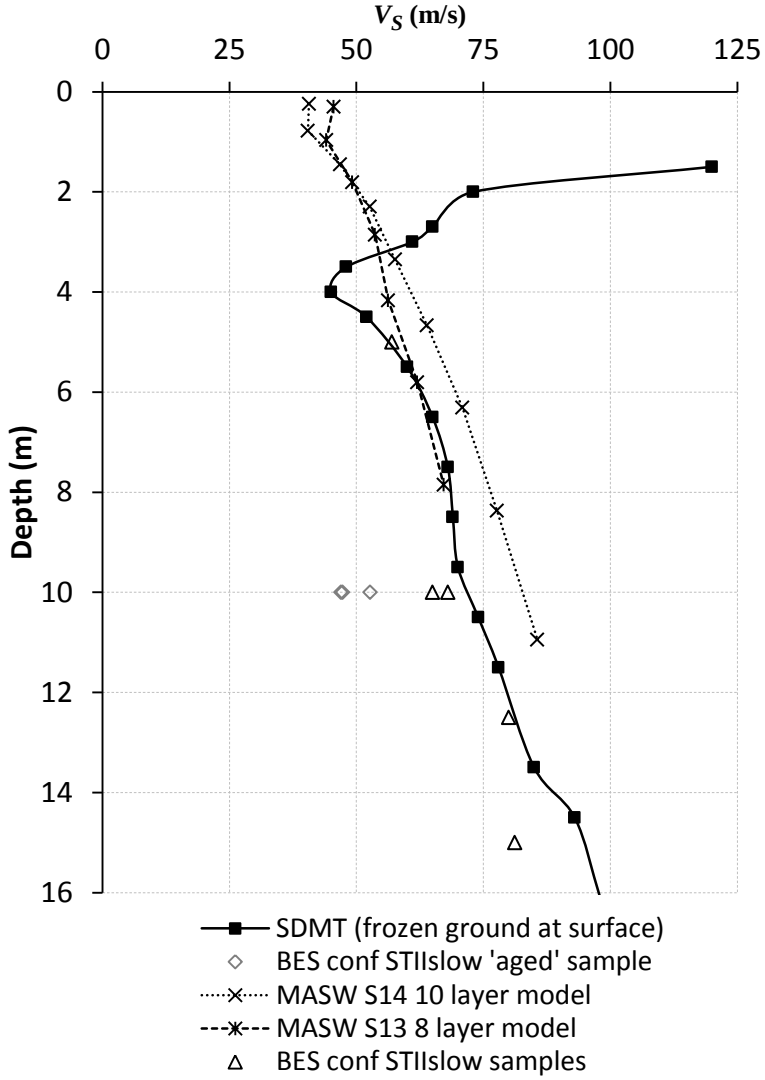

Figure 5.32 Comparison of shear wave velocity profiles obtained using different methods of measurement from Site 7.

5.9.3 **Sensitivity of V_S interpretation in BES laboratory tests**

One of the major challenges of BES interpretation is that the system is not linear due to attenuation, dispersion and multimodal vibration (multiple waves). Linearity is a basic assumption within the most commonly used interpretation methods (time domain,

frequency domain, cross correlation). In a truly linear system there should not be differences in the phase and group velocities of transported waves, and no frequency dependence on V_S, thus these features can be used to identify when significant non-linearity exists and help identify tests in which linear based methods may be unreliable. It was generally found that the greatest degree of non-linearity was found in samples that were most disturbed, while the highest quality samples often gave the appearance of linearity (no phase or group velocity differences and little frequency dependence).

The measurements proved to be sensitive to the contact between the bender element and the soil. Even in high plasticity clays striking differences are found. For example the time dependency of the BE:soil interface depends on both the nature of the soil tested the magnitude of stress change and the degree of disturbance (particularly chemical/biological). The time dependence if the BE:soil interface was most evident in aged glacial glacio-marine samples as seen in Figure 5.33 (a) by the large difference in signal amplitude before and after a 10 day hold period, consistent with thixotropic effects occurring after disturbance of the clay following insertion of the BE device. For very fresh $STII_{slow}$ samples of glacial glacio-marine clays no time dependency in the BE tests during a hold were noted (similar to block samples). In Figure 5.33 (b) BE tests on lacustrine samples also show very little change during hold periods, suggesting limited evolution of the BE:soil interface and changes in the sample due to potential thixotropic effects.

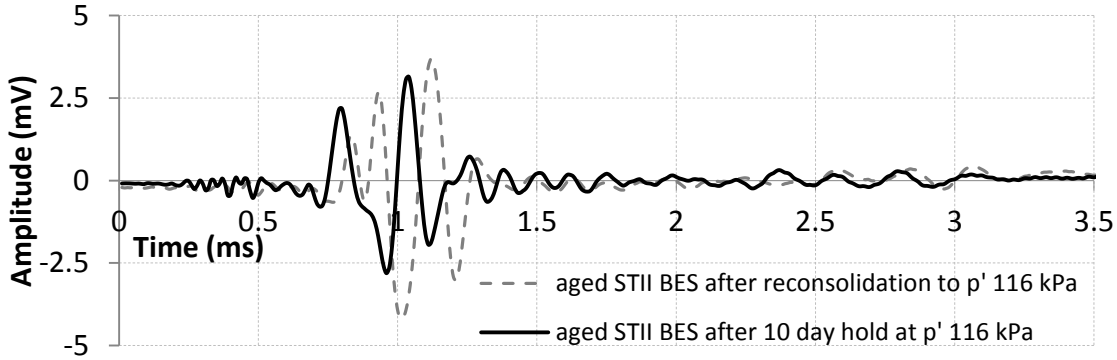

(a)

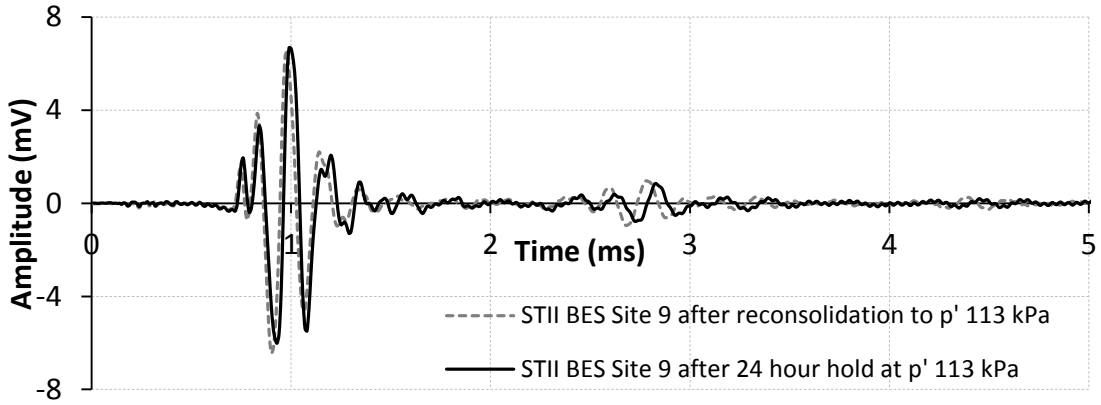

(b)

Figure 5.33 Variation in received BES signals for piston samples, 10kHz sine wave 200 sample stack (a) aged glacio marine clay sample (Site 2:25.5m) (b) lacustrine varved clay sample (Site 9:21 m)

It appears that the greatest issue with linear V_S interpretation occurs when samples are somewhat disturbed (both mechanically and/or chemically). A typical example where non-linearity was present is given in Figure 5.34 where both input (sine and square wave) and output signals from bender element tests on an aged sample (Site 2) are compared. Both tests experience the same degree of attenuation (loss of amplitude) with 2 distinct sets of peaks and troughs, however the square waves (that contains more high frequency signal components) experiences more distortion (change of shape). Both signals are affected by multi modal vibration with waves superimposing upon each other in the initial part of the 1st wave group arrival (giving a crooked 1st peak). In the 2nd wave group additional filtering caused by the clay has changed the shape of the transmitted waves, particularly in its initial part. Other BE tests where the presence of superimposed waves was observed was where BE tests were conducted during undrained triaxial shearing just after failure. In this instance an additional peak and trough was observed in the initial part of the first wave group (caused by waves reflected at the shear band). Received signals affected by multiple waves often had higher amplitude (due to superposition) interpretation of which often gave the impression of higher shear wave velocities due to the shape of the superimposed peak and troughs when using Method A and B. The impact of multimodal vibration, attenuation and dispersion on interpretation of V_S using Method A (time domain) at different phase positions is indicated in Table 5.3 for various excitation signals and signal stacking quantities. The largest variations were observed in the rectangular signals which equate to differences in G_0 of up to 40%, whereas differences in sine wave signals were up to 10% this lower value relates to the fact these signals have undergone less distortion. It was found that the variation in phase velocities (time domain) and group velocity (frequency domain) was a useful indicator of multimodal vibration and could be used to identify when a more advanced interpretation was required. Signal stacking was found to be a useful method of removing background noise from the signal data thus large stacks (100-200 shots) were generally used however this was not always necessary as seen in Table 5.3.

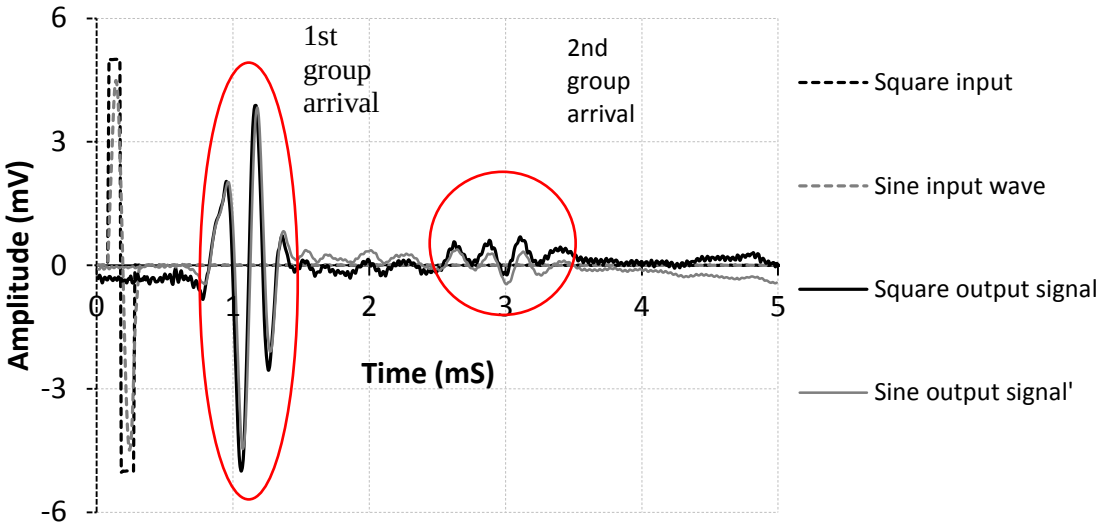

Figure 5.34 Comparison of stacked BES tests with Sine and square wave input signal on aged STII sample from Site 2 (30 m).

Table 5.3 Impact of no. of stacked tests (1,10,100), signal shape (S=sine, R=square) for 25.5 m piston sample from Site 2.

Phase Position	*Vs* (m/s) 1 test (S: +10V)	*Vs* (m/s) 10 tests (S:+10V)	*Vs* (m/s) 10 tests (S:-10V)	*Vs* (m/s) 100 tests (S:+10V)	*Vs* (m/s) 1 tests (R:+10V)	*Vs* (m/s) 10 tests (R:+10V)
A	154.5	154.4	154.4	154	160	162.7
B (mid-point)	152	152	152	152	153	153
C	152	152	152	152	148	153
D (mid-point)	148	147.5	147	147	134	136
E	152	152.5	152	152	138	141

When different BES systems (PC based and traditional oscilloscope based) were compared using the same fresh clay sample in a bench marking exercise (refer to Appendix A5) it was found there was significant variation in the shear wave velocity at low frequencies however at higher frequencies (≥ 10 *kHz)* the results were very similar for PC based and oscilloscope based BES, in agreement with Schmalz *et al.* (2007).

Based on discussion in this section it is clear that the assessed small strain stiffness, G_0 of a sample can vary, depending on soil type, the disturbance chain and procedural (and assessment) differences (stress level, loading strategies etc.). Generally differences were very small (< 5%) using the 10kHz sine wave input signal for linear based interpretation methods (at least for 1st cross over or 1st peak in time domain). There can be some sensitivity of the "pick" positions when using the time domain, if care was not taken thus cross-correlation techniques were useful in removing potential bias. However, given the multimodal nature of the received signal, additional adjustment was normally required as standard cross-correlation formulations identify the largest peak, which in many cases within this work was not the first peak from the initial shear wave, but a later superimposed multimodal wave form, which gave a significant underestimation of V_S and V_{S0}.

5.9.4 **Sensitivity in G/G_0 measurement**

When conducting triaxial tests it is necessary to select the frequency of data acquisition (time between each measurement). This choice is a balance between having sufficient points to capture the soil behaviour and having data files that are of a manageable size. The standard frequency of data acquisition used at CTH for triaxial tests is every 120 seconds and this was used for some of the tests. Unfortunately, this meant that the initial part of the degradation curve was not completely captured for all tests. In general degradation was captured from G/G_0=0.9, however for one of the lacustrine samples (10 m Site 10) that was very stiff only degradation from G/G_0=0.68 was captured (stiffer samples are loaded more quickly as shearing is displacement controlled). A number of tests were conducted with data acquisition set to every 10 seconds, and in Figure 5.34 a comparison is shown between curves obtained with 10 and 120 second data acquisition for two comparable samples from Site 10. The less frequent data acquisition smooth's the data, as much of the scatter in the measurement is not captured. The curves are however of a similar shape.

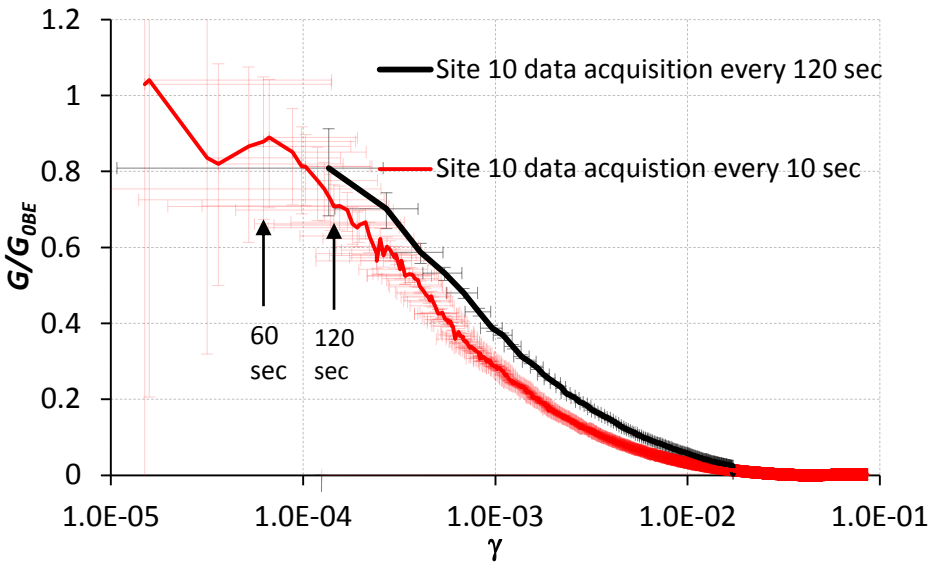

Figure 5.35 Influence of sampling frequency of data measurement

The speed at which degradation occurs can be observed in the curve for 10 second data acquisition with the help of the error bars which lie at 10 second intervals; arrows are used to illustrate degradation that had occurred after 60 seconds and 120 seconds. Clearly to capture the full degradation curve, it is necessary to have 10 second data acquisition. In total 10 of the 75 tests were done with 10 second data acquisition, however, as seen by the size of the vertical error bars in Figure 5.34 the potential error in G/G_0 and shear strains of these initial measurements rendered them unreliable. For this reason data below shear strains of 10^{-4} has been cut from the degradation curves that are presented in this thesis.

There is often much focus on the accuracy of strain measurements when discussing stiffness degradation. The DVRT transducers used here had a strain resolution down to $4x10^{-5}$ whereas the radial Hall-effect device had strain resolution to $4.8x10^{-4}$. The magnitude of radial strain during shearing was often small compared to the axial strain, so it is primarily the axial strain measurement that influences the magnitude of the shear strains. A number of comparisons of local and external measurements of vertical strain have been made between externally and locally measured axial strains in the range 0 to 2 % similar to comparisons presented by Jardine *et al.* (1984). However, when these comparisons were made within this work using the GDS local strain gauge (Hall effect) and Penny and Giles linear potentiometer for external measurements two observations were made that led to the decision not to use local vertical instrumentation. The first was that the data obtained was erratic despite being averaged over the two vertical gauges as shown in Figure 5.36. The second was that placement of such a device on soft clay samples appeared to effect the failure mechanism of the sample which infers it may also affect the degradation curves. The scatter of the data points in the Hall effect measurements is most likely due to a number of reasons: transducer resolution, resolution of the analogue to digital converter, performance of attachment method, slip and variations in elastic properties of the membrane, as discussed by Goto *et al.* (1991). However, there were more fundamental problems in the testing soft soil samples in this work with the device available which relates to the stroke length of the Hall effect transducer, the magnitude of reconsolidation strains and the size of the device relative to the sample.

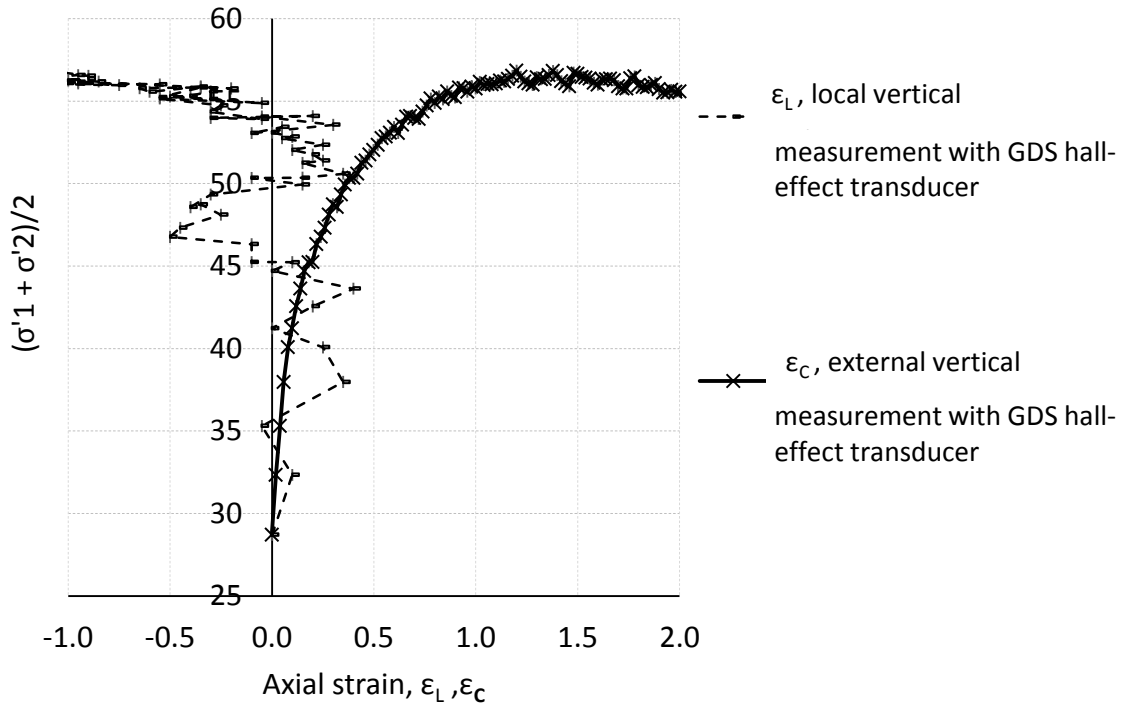

Figure 5.36 Comparison of external and local measurement of axial strain.

The sample represented in Figure 5.36 experienced vertical displacements during reconsolidation of 3.74 mm, while the range of the GDS local vertical strain device was ± 3 mm. This means that the device was beyond its linear range at the start of shear. In addition the length of the device was 70 mm, thus it could not capture changes in the middle third of the (initially) 100 mm sample as is often intended with local vertical strain measurement, but rather the middle two thirds. The device is quite clearly designed for stiffer soils (smaller reconsolidation strains) and sample heights of 200 mm, as is typical in the UK where the device was developed.

The shape of the external measurement curve in Figure 5.36 is very similar to the local measurement curve presented by Jardine *et al.* (1984). It was felt therefore that many of the issues that often cause differences between local and external measurements (system compliance, bedding errors, tilt of top cap etc.) in the 'relatively' small to medium strain range are not a significant issue for the soils tested, given the way in which samples are prepared and mounted and given their low stiffness relative to the system stiffness. It was therefore decided to proceed with triaxial testing without local vertical strain measurement and accept the loss of data within the smallest strain range. As a check the shape of the degradation curves obtained for the high quality glacio-marine samples within this work was compared with similar tests reported by Long *et al.* (2003) on Onsøy clay (which has very similar geological history and index properties to the Swedish west coast clays) and were found to be in good agreement, refer to Figure 5.37. Thus it is felt that degradation curves produced during this work give a reasonable indication of stiffness degradation from shear strains of around 10^{-4} despite the lack of vertical local strain measurement data, except perhaps for the few cases where the potential error in G/G_0 was high (very soft samples) which is discussed below.

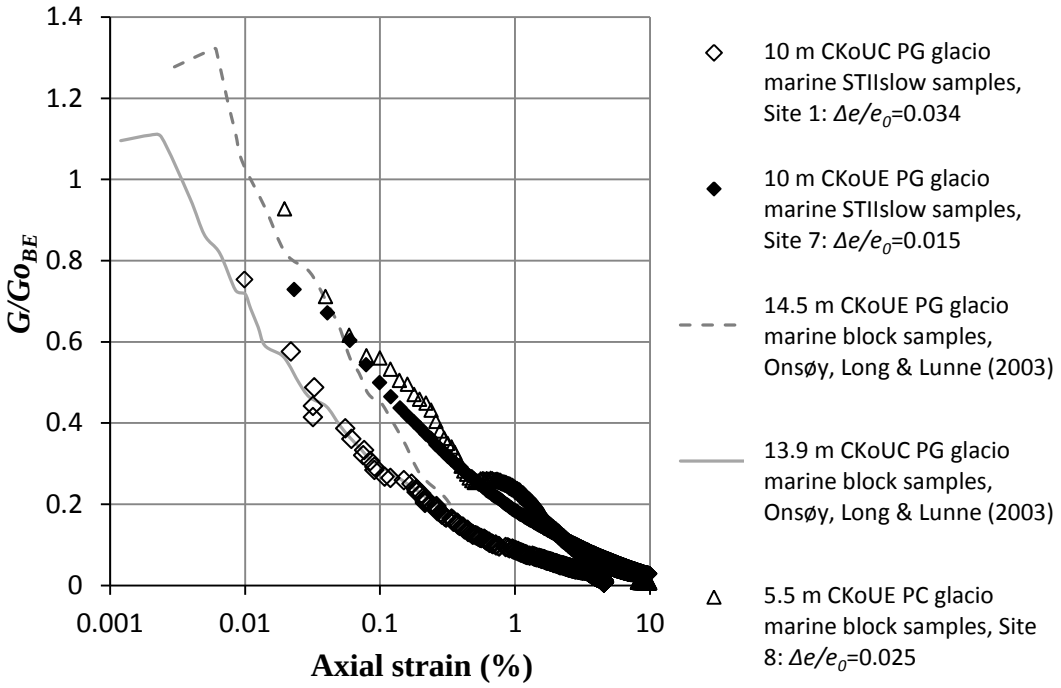

Figure 5.37 Comparison of degradation curves for post glacial marine clays from Swedish West Coast and Onsøy.

The potential errors in G/G_0 relate to: the accuracy in shear strain measurement and stress measurement, which combine to give the accuracy of the shear modulus and the accuracy in determination of G_0. In order to formulate the positive error bars for G/G_0 errors leading to a maximum value of G and a minimum value of G_0 were calculated. For the negative error bars errors associated with minimum values of G and maximum values of G_0 were calculated. A standard error of ±10% of G_{0BE} was assumed for all tests. The accuracy of secant shear modulus (G) is highly dependent on the shear stress interval from the start of shearing. As stated earlier, triaxial tests used displacement control during shearing, with a standard displacement rate of 0.01 mm/min. This means that for the softest clays the magnitude of the shear stress interval between data acquisition points used to determine shear modulus was in some cases smaller than the potential error in the stress measurement alone. For these cases (very soft samples) potential errors in G/G_0 were unreasonable until strains of around $5x10^{-4}$. For the stiffest soils the error in G/G_0 is low.

5.10 Summary of the findings

The similarity of the measurements of small strain stiffness from field testing both when comparing repeated tests in similar soils and different test methods (direct measurement with the SDMT seismic probe) and diffuse measurement with multiple analysis surface wave (MASW) measurements suggest that the tests give a good insight into small strain stiffness behaviour in the field. The results are, however, based on state-of-the-art testing and interpretation methods, for which sensitivity analyses have been conducted (repeated shots for each test and sensitivity checks for the interpretation procedures).

In the laboratory the similarity of $G_{0\ lab}$ to $G_{0\ field}$ was highly dependent on the effects of the sample disturbance chain and the BES interpretation method. Similarly G/G_0 also

appears to be strongly affected by disturbances occurring prior to testing as well as reconsolidation stress path. Given the potential loss of small strain stiffness behaviour of laboratory samples due to the sample disturbance chain, it may be better to focus on field testing, particularly for low plasticity clays. Even when it is possible to take high quality samples, without field testing uncertainty will remain in the reliability of the results due to the issues associated with the interpretation of shear wave velocity, affecting both bender element tests but also resonant column tests (Long *et al.* 2003).

Interpretation of bender element tests was most consistent for the methods selected (first wave arrival: time domain (phase velocity) and frequency domain (group velocity)) when the dispersion was low, which occurred in fresh very high quality natural samples, or intrinsic samples. This appears to relate to the quality of the BE:soil interface. For these samples there was no frequency dependency in V_S as is often reported in literature in the range 2-10 *kHz*.

There is some uncertainty in the initial part of some of the G/G_0 degradation curves in this work. This uncertainty relates to the resolution of the measurement system used and/or the frequency of measurements when determining the shear modulus and led to some of this data being cut at strains of 10^{-4}. The DVRT device used to measure local radial strains worked well while the Hall-effect device did not, for this reason the latter device was only used on two samples, for further comparisons of the performance of these two devices refer to Appendix A6. Some tests with local vertical strain measurement using two hall-effect devices were conducted but the size of these devices and their stroke length ± 3 mm made this device incompatible with the clays studied given the deformation occurring during reconsolidation and shearing. Thus in general axial vertical strains are based on external measurement.

A method of determining local strains with high accuracy and precision without attachment of devices to the sample (such as optical techniques) needs to be developed for these soils so that reliable measurement of small strains can be obtained even after large deformation during testing. In addition, a more accurate measurement system for the determination shear stress (pore pressure, cell pressure, and load cell) would improve reliability of the results as would better resolution of the data acquisition system.

6 THE EFFECT OF G_0 IN DEEP EXCAVATIONS

6.1 Introduction

The results presented in Chapter 5 confirm that small strain stiffness and its degradation are an integral part of Swedish soft clay behaviour, similar to anisotropy, structure and creep. It was shown that if state-of-the-art techniques are used, laboratory and field assessments of G_0 can have good agreement, provided fresh high quality samples are used. In terms of small strain stiffness degradation, behaviour observed in the laboratory varied significantly due to differences in the clays tested, sample timeline effects and stress/strain history. Of considerable note was the degradation of G_0 with strain during undrained shearing, the difference in magnitude of strains for which small strain stiffness was observed, and the anisotropy both in G_0 and G/G_0, all of which could have implications when modelling both static and dynamic boundary value problems in the serviceability limit state. The analysis of soil-structure interaction problems forms a major challenge in geotechnical engineering. Not only the stiffness of the structure, but also the stiffness of the soil affects the subsequent system response. As discussed in Section 1.1 the magnitude of the soil stiffness, i.e. the small strain shear modulus is stress-dependent and strain magnitude –dependent (Figure 1.2). This soil behaviour should be incorporated in the analysis of deep excavations in soft clays.

In Sweden measurement of small strain stiffness and its degradation in soft clays has generally only been conducted at research level for a limited number of Swedish clay sites. In practice reliance has been placed on empirical relationships. Unfortunately none of the relationships typically used in Sweden were found to give reliable estimations of G_0 or G/G_0 for the sites studied in this thesis. In particular, the empirical relationships that tend to be used for G/G_0 are based on shear strain amplitude (dynamic testing) and not shear strains (obtained by triaxial testing), the latter being most relevant for static boundary value problems presented in Figure 1.2. Clearly these two are not directly comparable, and it is unclear how the two relate; this difference appears sometimes to be overlooked in practice, such as when using the small strain finite element model developed by Benz (2007), which is gaining popularity in Sweden. Empirical relationships should be used with caution and not for detailed design. When used for preliminary design, it is important to use the same basis of assessment of input parameters as originally defined, for example if the relationship is based on uncorrected field vane results (such as the relationship by Andréasson, 1979) then this is what should be used, not the corrected field vane values. Otherwise the user is applying the relationship to data that it was never intended for.

What is clear from this work is that the sample timeline has a significant effect on the behaviour observed in the laboratory. Prior to this work, the laboratory measurements of G_0 in Sweden (and in fact triaxial tests in general) had generally been conducted on old samples (> 6 months). These were found to give laboratory values of G_0 that were significantly lower than observed in the field (also identified by Andréasson, 1979, Persson, 2004, Burland, 1989). Andréasson (1979) suggests corrections based on extrapolation of the increase in G_0 with time during the 'hold' period at *in situ* stresses in the laboratory tests. Work in this thesis suggests, however, that this increase relates to sample timeline effects and that very fresh high quality samples experience very little

change. In such cases further correction of the laboratory data would lead to over estimation of G_0 in the field. The best way forward is clearly to measure G_0 *in situ,* and if it is necessary to measure in the laboratory, one should minimise the effects of the sample timeline.

Attempts have been made in this work to examine where the changes in G_0 occur within the sample timeline. A significant potential source of change lies in the method of sampling, the magnitude of which depends both on sampling method and to clay type. Carefully extracted piston samples in higher plasticity clays (Swedish West Coast) generally exhibited less disturbance during sampling than low plasticity samples (Swedish East Coast; Norwegian West Coast) thus laboratory samples were able to give a better indication of $G_{0\ \text{field}}$ provided they were tested quickly ('fresh' samples), as did block samples. If however the same piston samples were stored significant periods of time ('aged' samples), the agreement was poor. For block samples the period with which samples remained 'fresh' was much longer, provided the blocks remained confined from extraction. Clearly the changes occurring during storage depend on storage conditions, clay type and the initial disturbance during sample extraction. In most of the clays tested changes in samples during storage could be seen visually by a change in colour or the presence of precipitates (typically salt) or mould on the surface of samples.

In general, block samples experienced less disturbance than the piston samples, however they are generally significantly more expensive to extract and test (due to additional preparation time) unless hand cut blocks can be taken within the scope of planned excavation works. The use of block samplers (Sherbrook/mini block) can normally only be conducted for practical reasons to depths of around 25 m. Thus it would be foolish to suggest that block samples should always be used to determine the soil parameters for design from a practical standpoint. However, for some soils, that are difficult to extract without significant disturbance when using piston samplers, and/or where there is a boundary value problems that requires realistic small strain parameters, a few carefully selected block samples together with more focus on direct *in situ* testing (calibrating with the help of the block samples) would appear a more reliable way forward. Such an approach worked very successfully for the E6 cut and cover tunnel project at Site 12.

Significant effort was placed on testing existing methods of sample disturbance. The Lunne *et al.* (1997) sample quality criteria appeared to work well in identifying triaxial samples (block and piston) that were less disturbed ($\Delta e/e_0$<0.04) and which tended to give laboratory values of G_0 similar to field values, providing samples were 'fresh'. No field testing of small strain stiffness degradation was conducted within this work, thus it is unclear how well the laboratory values of G/G_0 relate to the field. Large differences were observed, however, both in terms of stress paths followed during undrained shearing, and the rate of stiffness degradation for comparable piston and block samples, even though both were of the highest quality ($\Delta e/e_0$<0.04). Large differences in G/G_0 were also observed in block samples when identical samples were subjected to different stress paths prior to undrained shearing from the same stress state. It would appear, therefore, that the degradation behaviour is very sensitive to the sample stress/strain history (sample timeline and test procedures).

In Sweden the importance of allowance for non-linear behaviour in the serviceability limit state design of deep excavations was highlighted in the 1970's by Hansbo & Sellgren (1979). Although finite element analysis (FEA) was in its early stages of development, Hansbo & Sellgren (1979) presented the results of FE calculations using an undrained hyperbolic stress-strain model with anisotropic strength and stiffness properties. When comparing FE predictions to field monitoring results for a 6 m deep 13 m wide excavation in Gothenburg (stresses and deformation) the predictions were poor due to:

- The inability to model the actual soil behaviour,
- The inability to model time aspects (consolidation),
- The geometrical simplifications and
- The effects of construction activities (piling, etc.).

However, Hansbo & Sellgren (1979) concluded that in the future improved soil models should be available for use in FEA, and that such developments may provide the only method capable of providing realistic predictions of soft clay behaviour during deep excavation. Similar conclusions were drawn by Potts, (2003), Jardine *et al.* (1991), Kullingsjö (2007), Wood (2008) and Wood (2010). Other forms of analyses are possible for the design of deep excavation problems, such as the Winkler beam methods, the strain path methods, the finite difference methods, the strength mobilisation methods, etc. However, none of these are well proven in Sweden nor incorporate the small strain stiffness, and thus will not be discussed.

During interaction with industry during this research project a great deal of scepticism has been voiced over the need to allow for small strain stiffness of deep excavations in Swedish soft clays. For this reason, the results of field and laboratory measurements from Site 1 are used to conduct FEA for a theoretical case of a 10 m deep excavation with and without allowance for small strain stiffness. Two different families of constitutive models are used, discussed further in Section 6.2. There is currently no constitutive model available for design of deep excavations that is able to capture all facets of Swedish soft clay behaviour, namely; anisotropy (large and small strain), creep, small strain stiffness, structure. It will be shown however that development of such a model is clearly warranted, giving the projects that lie ahead.

In practice most deep foundation works in Sweden involve piles (almost exclusively driven piles) which means soil, soil:pile and soil:retaining wall behaviour needs to be captured. An overview of the design stages recommended when using FEA for design of deep excavations is presented in Table 6.1. For simplicity only the soil and soil:retaining wall interaction is considered in this thesis. Stages relating to piles, and validation at boundary level are omitted in this work, as are sensitivity analyses (Stage 8 in Table 6.1). The purpose of the analyses presented in this section, therefore, is to understand and highlight the impact of using FEA with and without allowance for small strain stiffness with models that are currently available. Extensive validation and sensitivity analyses for deep foundations can be found in Wood (2014) and shows there are significant differences in the results of FE simulations relating to the design assumptions made such as: recent stress history effects (*in situ* state), ground profile,

design parameters (quality of samples used), constitutive models and the assumed construction activities (piles installed before or after excavation).

Table 6.1 Overview of recommended modelling stages for deep foundations using FEA in soft clays.

Stage Number	Design Task	Verification of design assumptions
1	Specify ground & hydrological profile and understand variability	Review multiple site and profiling methods in the area
2	Understand real soil behaviour	Review relevant field and laboratory test data from multiple sites
3	Model characteristic soil behaviour and determine limitations	Comparison with high quality test data at element level
4	Understand individual pile behaviour	Review relevant case studies and identify trends
5	Model characteristic individual pile behaviour and determine limitations	Comparison of FE results with relevant full scale pile tests
6	Understand deep excavation and pile group behaviour	Review relevant case studies and identify trends
7	Model characteristic excavation and piled raft behaviour and determine limitations chosen models	Comparison of FE results with relevant long term case studies
8	Sensitivity analysis of behaviour to uncharacteristic loads, ground and hydrological profile, material properties and construction methods	Compare results with well winnowed experience and traditional ULS calculation results

6.2 Analysis of deep excavations

6.2.1 Background

In Sweden, the commercial finite element code PLAXIS and its double hardening non-linear elasto-plastic Hardening Soil (HS) model is routinely used to analyse deep excavation works in clay (Kennedy *et al.*, 2006, Persson, 2013, Hansson, 2014). More recently, the small strain overlay model by Benz (2007), the Hardening Soil Small (HSs) model is also gaining popularity. It is less clear, however, if the selected model parameters used for these models have been correctly validated, and if the associated limitations and reliability of the results are communicated to the end user, refer to Wood (2015). In particular the lack of allowance for initial anisotropy and its evolution, de-structurisation post-peak and creep may lead to erroneous estimates of factors of safety, deformations and structural loads in and around the retaining structures and the support systems. Work by Dawd & Trygg (2013) and Persson (2013) using developments of Cam Clay based models validated specifically for soft structured clays without incorporation of small strain stiffness (SCLAY1S, Karstunen *et al.* 2005 and Creep-SCLAY1S, Sivasithamparam *et al.*, 2015) suggest that differences may be great. Other soft soil models that have been developed for Scandinavian clays (but that do not consider small strain stiffness), and have been used for deep excavation problems in Sweden are: NGI-AN12 (Andresen, 2005) and e-ADP (Grimstad, 2009), a version of

which is available in the standard material model suite within the PLAXIS software. Both these models have been developed to account for anisotropy in undrained loading/unloading (total stress analysis), and are therefore by default not really suitable for studying deep excavation solutions, where partial drainage may occur (given the long period of time deep excavations remain open).

There are a number of numerical models incorporating small stiffness behaviour as indicated in Table 6.2. Unfortunately none of these models are either validated for soft Swedish clays, and/or incorporate the essential features required to model these soils realistically in the small to large strain range.

An additional feature of real excavations which is often ignored is the impact of time. The degree of excess pore water pressure dissipation that occurs during construction time for deep excavation projects may be of great importance to the safe design of deep excavation solutions, particularly for the various deep cut-and-cover tunnel projects that lie ahead in the city of Gothenburg. Traditionally, it has been common to only consider undrained conditions both in traditional limit equilibrium/stress field type analyses and finite element analyses. However, work by Vermeer (1998) suggests that undrained analysis should only be used when the dimensionless time factor, T_v conforms to $T_v < 0.1$ where T_v is defined as:

$$T_v = \frac{c_v}{D_r^2}.t \qquad \text{Eq. 6-1}$$

where c_v is the coefficient of consolidation (*in situ*), t is time and D_r is the drainage path length (which can often be set to the embedment depth of the retaining wall).

Using typical values of c_v assessed from very good quality samples of Gothenburg clay (using oedometer tests), this criteria would equate to a construction period of around 3-12 weeks, depending on the embedment depth of the retaining wall. Deep retaining wall projects often have considerably longer construction periods (typically 6 to 18 months), and therefore the effect of time should also be considered in the design. To illustrate the potential impact of time, one of the simulations presented in this Chapter also shows the effects of partial consolidation on the bending moments in a retaining wall when a consolidation phase of 365 days is considered.

Table 6.2 Numerical models incorporating small strain stiffness behaviour

Model Name	Description
Bi-linear model Hardin and Drnevich (1972)	Models non-linear elastic stress-strain response where stiffness decays as a function of strain for both sands and clays
Burland model Burland et al. (1979)	Kinematic yield surface based on strain space developed for analysis of deep excavations in over-consolidated marine clay
Jardine model, Jardine *et al.* (1986)	Uses a logarithmic function to model the non-linear elastic behaviour as a trigonometric function of strain. Constants of the function are found by curve fitting with triaxial tests.
Bubble model, Al Tabba & Wood (1989), Stallebrass (1990).	Multiple kinematic surfaces to allow for recent history on stress/strain behaviour using different hardening laws for the various surfaces
Brick Model, Simpson (1992)	Models stiffness decays in steps on load reversal based on strains on reversal of direction (like a man dragging bricks)
Hypoplastic models using intergranular strain, Mašín (2005)	Hypoplasticity principles applied within a Critical State soil mechanics framework. Model specifically developed for soft clay by Mašín (2005) incorporates a modified Cam Clay model with Matsuoka-Nakai failure surface. Non-linear behaviour specified with generalised hypo-plasticity, with small strain behaviour added using the concept of intergranular strain (strain history)
MIT-S1 model Pestana and Whittle (1999)	Advanced constitutive model to model the rate-independent non-linear behaviour of sands and clay. Features include kinematic hardening, evolution of anisotropy and non-associated flow rule. Definition of 15 input parameters many of which require specific advanced testing, used by Kullingsjö (2007)
Hardening Soil small model (HSs) Benz (2007)	Non-linear elastic double hardening overlay model using empirical description of stiffness decay with strain. The underlying constitutive model is the double-hardening HS model developed by Schanz (1998) from work presented by Vermeer (1978) for sands.
Kinematic bubble model (B-SCLAY), Sivasithamparam *et al.* (2010)	An extension of the anisotropic S-CLAY1 model (Wheeler *et al.* 1999, Wheeler *et al.* 2003) with introduction of a kinematic yield surface (bubble) which was used to simulate effects of cyclic loading and evolution of anisotropy of clays observed in laboratory tests.

6.2.2 **Details of constitutive models and FEA analyses**

In the following example, the effect of incorporating the proper small strain shear modulus in a FE constitutive model is discussed. For sake of simplicity the commercial finite element code PLAXIS and the incorporated constitutive model that includes shear and volumetric hardening and the Mohr-Coulomb failure envelope (Hardening Soil (HS), Schanz *et al.* 1999) and the extended model for small strain modelling (Hardening Soil small strain (HSs), Benz 2007) are compared. Due to the major limitations of these models when used in soft clay simulations, simulations were also conducted with an extension of the anisotropic elasto-visco-plastic model described by Sivasithamparam *et al.* (2015) which also allows for structure, namely the Creep- SCLAY1S model.

Both the HS and HSs models were primarily developed and validated for use in sands thus there are some issues when these models are applied to soft structured clays such as those found in Gothenburg. The results of simulations using the HS and HSs constitutive models are compared to give an indication of the impact that allowance for the small strain stiffness has in a deep excavation boundary value problem. Some major drawbacks of these models with respect to their use in the FEA of soft clays, (which makes them potentially unreliable for design of deep excavations, both in terms of serviceability limit state -deformation and structural loads and assessment of safety) are outlined below:

- Lack of initial anisotropy
- Lack of evolution of anisotropy during shearing
- Lack of allowance for creep
- Lack of allowance for destructuration (important for assessment of safety in sensitive clays)
- Model artefacts of the HS and the HSsmall constitutive models within the PLAXIS software implementation, which require that $E_{50}^{ref} > 2E_{ur}^{ref}$ and that E_{oed}^{ref} is sufficiently large relative to E_{50}^{ref}, even though these parameters are not mathematically linked within the underlying constitutive model. Limitations exist such that the actual assessed value of E_{oed}^{ref} has be multiplied by a factor ≈10 in order to gain acceptance for the stiffness parameter set ($E_{50}^{ref}, E_{oed}^{ref}, E_{ur}^{ref}$). Input of a representative stiffness parameter set for Swedish soft clays is not possible with the current implementation restraints[1].

[1] For deep excavation problems one has to prioritise representative values of E_{50}^{ref} and E_{ur}^{ref}, which results in the need to specify unrealistically large values of E_{oed}^{ref} in the input data. This is due to a condition of the model implementation, and not directly inferred from experimental data. These model artefacts should not be interpreted as real soil properties.

Simulations using the Creep-SCLAY1S model will be done with the model used in its original form with stress dependent pre-yield stiffness (logarithmic scale) represented by κ^* (the modified swelling index), as well as a separate analysis where the small strain stiffness values of pre yield stiffness, referred to herewith as κ^*_{SS}, are defined outside the main excavation area instead of κ^*, as indicated in Figure 6.1.

This is clearly a very rudimentary way of incorporating some small strain stiffness effects, and is only done to help illustrate the effect that incorporation of small stiffness into a model developed specifically for soft sensitive soils would have.

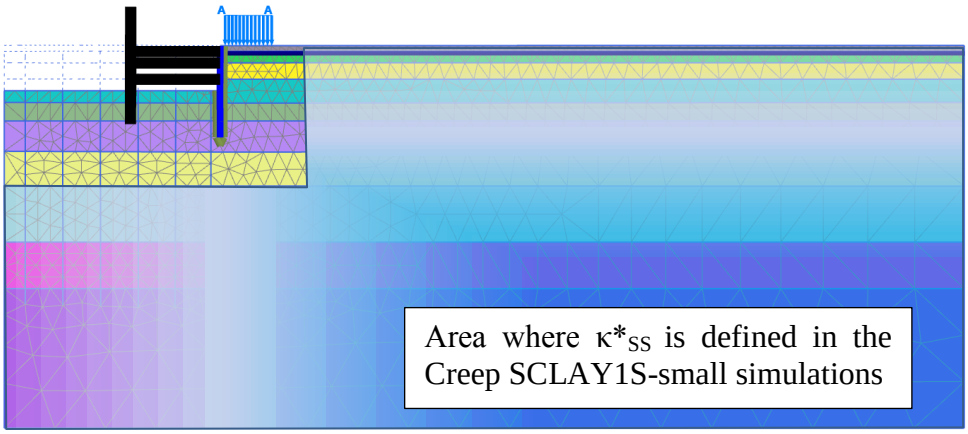

Figure 6.1 FEA Model and mesh at excavated depth (10 m), surcharge applied 13 kPa.

Unfortunately IL tests on fresh piston samples at Site 1 did not contain unload-reload loops, thus existing test data from Site 2 (Vägverket, 2014) were used to define κ*. The samples from Site 2 were between 6 to 8 months old, and in some cases indicated very high unloading stiffness (during unloading yield point to around OCR 2) which is thought may relate to changes occurring in the sample during storage, rather than real clay behaviour. For this reason the reloading stiffness was used to determine κ* rather the average unload-reload stiffness, which is normally the case, values differed by a factor ≈2. Clearly for a real boundary value problem IL unload reload tests on fresh samples would be required to determine more realistic values of κ*.

The value of κ^*_{SS} was based on the G_0 values determined using the seismic dilatometer at Site 1. The values of κ^*_{SS} were determined using the assumptions of isotropic porous elasticity by converting G_0 to E_0 using Eq. 2.3, and then converting E_0 to M_0 using Eq. 6-2. The value of κ^*_{SS} was then defined using a slightly adapted version of the formulation by Olsson (2010), given in Eq. 6-3. In its original form this formulation gives reasonable estimations of κ^* for clays with K_0^{NC} of around 0.5 which is the case at Site 1.

$$M_0 = E_0 \frac{(1-\nu_0)}{(1+\nu_0)(1-2\nu_0)} \qquad \text{Eq. 6-2}$$

where ν_0 is Poisson's ratio at small strain = 0.15 based on K_0 triaxial unloading tests by Persson (2004) on STII piston samples extracted close to Site 1, 2 and 3.

$$\kappa^*_{SS} = \frac{2\sigma'_V}{M_0} \qquad \text{Eq. 6-3}$$

where σ'_v is taken as the *in situ* vertical effective stress at the depth of measurement of G_0.

The parameters used to define the initial state were the same for all analyses as indicated in Table 6.3 whilst the parameters used for the different constitutive models are presented in Table 6.4 and Table 6.5.

Table 6.3 Definition of initial state in FEA analyses (definition of yield stress utilised highlighted in grey), extent of clay layers indicated in Figure 4.7.

	γ' (kN/m^3)	OCR	*POP* (kPa)	k_x, k_z m/day	K_0
Fill 1	18	1		7.65	0.42
Fill 2	17	1		7.65	0.5
Clay 1	16.5	2		1.00	0.7
Clay 2	15.5	1.65		4.00E-05	0.7
Clay 3	15.7	1.3	32	2.00E-04	0.63
Clay 4	16.4	1.29	32	4.00E-05	0.61
Clay 5	16.2	1.22	32	4.00E-05	0.61
Clay 6	16.2	1.16	32	3.00E-05	0.58
Clay 7	16.4	1.14		5.00E-05	0.57
Clay 8	16.5	1.14		7.00E-05	0.56
Clay 9	16.9	1.35	120	2.00E-05	0.57

Table 6.4 Definition of standard HS and HSs model parameters based on extent layers indicated in Figure 4.7, note Poisson's ratio, υ, was set to 0.15.

		HS and HSs model								HSs model	
	c' (kPa)	HS φ' (°)	HSs φ' (°)	ψ' (°)	E_{50}^{ref} (kPa)	E_{oed}^{ref} (kPa)	E_{ur}^{ref} (kPa)	m	K_{0nc}	$G_{0\ ref}$ (kPa)	$\gamma_{0,7}$
Fill 1	0	35	35	20	10000	7000	30000	0.5	Jaky	90000	0.0004
Clay 1	3/1	32	36	0	7000	3002	27000	1	0.53	77483	0.0004
Clay 2	3/1	32	36	0	7000	3400	33700	1	0.53	39699	0.0004
Clay 3	3/1	32	36	0	7000	3070	24250	1	0.53	40213	0.0004
Clay 4	3/1	32	36	0	15400	8300	30800	1	0.53	38128	0.0004
Clay 5	3/1	32	36	0	33000	17700	66 300	1	0.53	40325	0.0004
Clay 6	0	30.5	30.5	0	13100	5095	26200	1	0.49	40960	0.0006
Clay 7	0	30.5	30.5	0	13100	5744	26200	1	0.49	36056	0.0008
Clay 8	0	30.5	30.5	0	10500	4604	21000	1	0.49	37460	0.0009
Clay 9	0	30.5	30.5	0	7000	2773	17440	1	0.49	33686	0.0003

Table 6.5 Definition of parameters used in the Creep-SCLAY1S analyses based on extent layers indicated in Figure 4.7.

Creep-SCLAY1S	Clay 1	Clay 2	Clay 3	Clay 4	Clay 5	Clay 6	Clay 7	Clay 8	Clay 9
κ^*	0.032	0.025	0.018	0.025	0.018	0.025	0.0175	0.017	0.018
κ^*_{ss}	0.0029	0.0048	0.0041	0.0045	0.0044	0.0048	0.0049	0.0049	0.0051
υ	0.15	0.15	0.15	0.15	0.15	0.15	0.15	0.15	0.15
λ_i^*	0.09	0.09	0.09	0.09	0.09	0.085	0.085	0.085	0.085
M_c	1.4	1.55	1.6	1.6	1.6	1.35	1.3	1.23	1
M_e	1.2	1.15	1.15	1.15	1.15	1.1	1.1	0.9	0.95
ω	120	100	100	100	100	110	110	100	100
ω_d	0.3	0.1	0.1	0.1	0.1	0.2	0.2	0.2	0.2
ξ	9	12	12	12	12	12	12	12	12
ξ_d	0.2	0.4	0.4	0.4	0.5	0.2	0.2	0.2	0.2
e_0	1.4	2.1	2.1	1.71	1.8	1.57	1,74	1.65	1.55
α_0	0.5	0.7	0.7	0.7	0.7	0.35	0.35	0.4	0.4
χ_0	10	8	9	8	6	9	8	8	8
τ	1	1	1	1	1	1	1	1	1
μ^*	0.003	0.003	0.004	0.0033	0.0028	0.0022	0.0022	0.0018	0.0034

6.3 Comparison of element level simulations

The fitting of model parameters presented in Section 6.2.2 were generally based on high quality fresh samples ($\Delta e/e_0$ <0.4) taken from Site 1. However for the determination of the Creep-SCLAY1S model parameters relating to anisotropy, some clay layer properties were defined with the help of high quality samples fresh samples from Site 3 (Clay 3) and Site 7 (Clay 1 and 4), given that in Chapter 4 it was found that samples at different sites in the same geological deposits gave very similar behaviour. For the HS and HSs model parameters, the strength parameters were initially defined based on an overall assessment of all the undrained triaxial compression tests from Site 1 for post-glacial and glacial clays, respectively, in the p'-q –space, and then again checked at element level, in addition to shear stress with axial strain, τ-ε_a . For the deviatoric stiffness parameter E_{50}^{ref} values were determined using E_{u50} determined from undrained triaxial tests, which was then converted to E'_{50} using the empirical relationship in CUR 195. Checks were made to with the few drained triaxial results conducted in the area, and were found to give reasonable agreement, for further details refer to Wood (2014). The values of E_{ur}^{ref} were determined from oedometer unload reload tests (M_{reload}) and converted to E_{ur} assuming elastic theory for isotropic porous elastic material using the relationship given in Eq- 6.2. In the original derivation of the HS and HSs models isotopic drained triaxial unload-reload tests were used, however isotropic tests are not able to capture the true behaviour of soft clays, thus such tests were not conducted. The HS and HSs models are isotropic, and thus are unable to reproduce the initial anisotropy observed in the triaxial compression and extension tests in soft Swedish clays, refer to Figure 6.2 and no attempts were made to fit an alternative parameter set for unloading, as the evolution of anisotropy during shearing would still not be captured. As discussed

earlier, the laboratory determined values of E_{oed}^{ref} could not be input to the model so the lowest acceptable value was used. Clearly this means that the HS and HSs data sets cannot be used where loads are close to or beyond yield.

For the Creep-SCLAY1S model parameters, both undrained compression and extension tests were used to define strength (M_c and M_e) and anisotropy parameters (α_0, ω and ω_d). For determination of M_c *and* M_e it was checked that a stable stress ratio was achieved in the test and that variation in pore pressures in this range were small, and therefore could be considered indicative of the critical state. The structure parameters (ξ, ξ_d, χ_0) were determined primarily using IL oedometer tests although some checks against CRS oedometer tests were made. The values of λ_i* used to define the modified intrinsic compression line was determined using the tests performed on intrinsic samples prepared within this research.

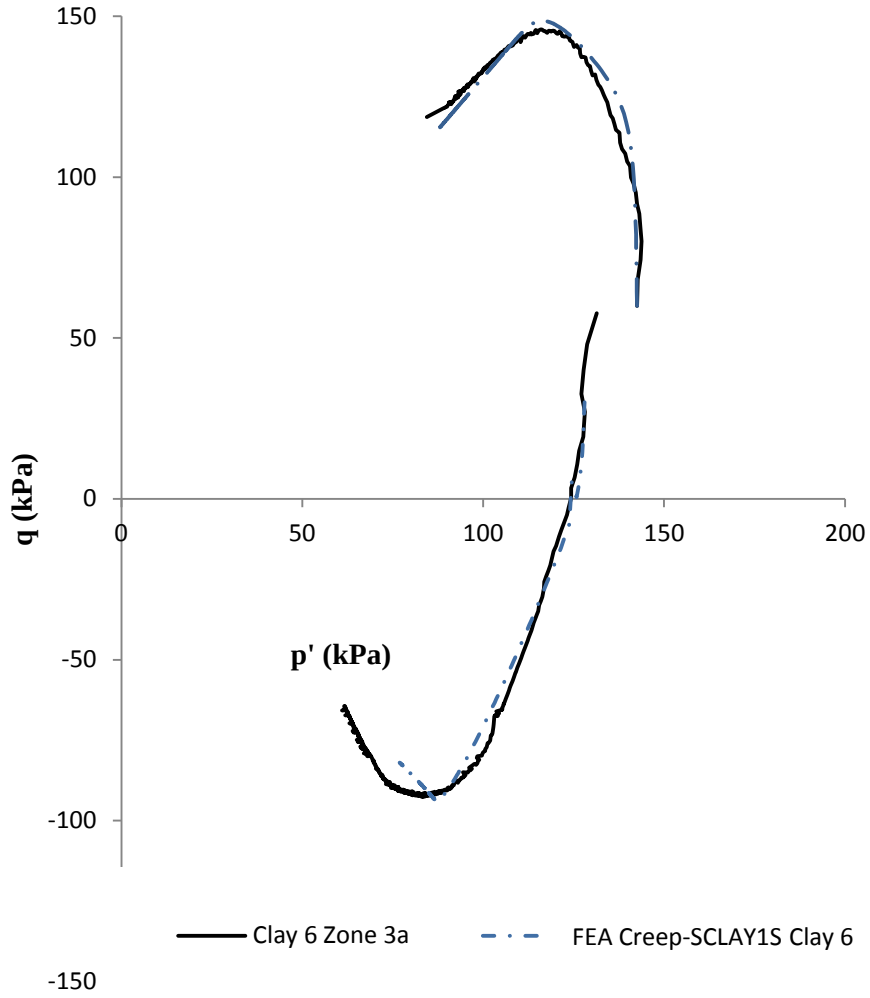

Figure 6.2 Effective stress paths during undrained triaxial shearing of high quality piston samples of Zone 3a Gothenburg glacial clays from Site 1, 27 m and simulated behaviour using Creep SCLAY1S model.

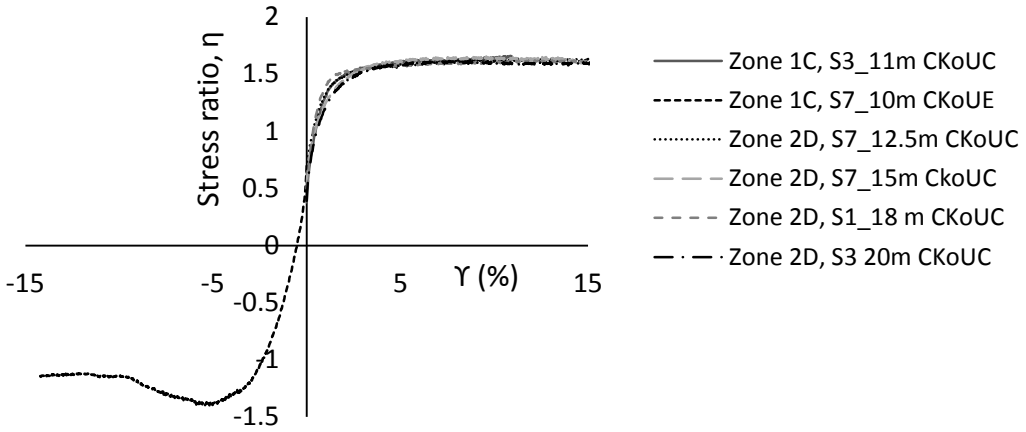

Figure 6.3 Variation in stress ratio during undrained triaxial compression and extension tests for Zone 1C and 2D Gothenburg post glacial clays from various sites on the Swedish West Coast ($STII_{slow}$ piston samples).

The results of some of the element level simulations for IL oedometer tests on the post glacial Gothenburg clays are presented in Figure 6.4. The effect of the extremely high values of E_{oed}^{ref} in the HS and HSs models beyond the yield surface is clearly evident in Figure 6.4.(a), however the initial stiffness (pre-yield) behaviour of the Creep-SCLAY1S, HS and HSs models is similar as is the reloading behaviour of the Site 2 IL test. Differences in the initial stiffness of the Creep-SCLAY1S simulations relate to different assumptions of initial stress at the start of the test. For the Site 1 tests, the initial stress specified was based on measured suction at the time of test. In Figure 6.4(b) the agreement with the Site 1 IL test and Creep-SCLAY1S simulation is good, whilst in the Site 2 IL test with unload- reload agreement is only fair. The initial unloading loop pre-yield in Creep-SCLAY1S is not visible, as only pre-yield stiffness is defined and the creep induced strain are negligible. However, in the post-yield unload-reload loop, the unloading behaviour can more clearly be seen. The dataset was not fitted exactly to the Site 2 IL curve given the age of the sample.

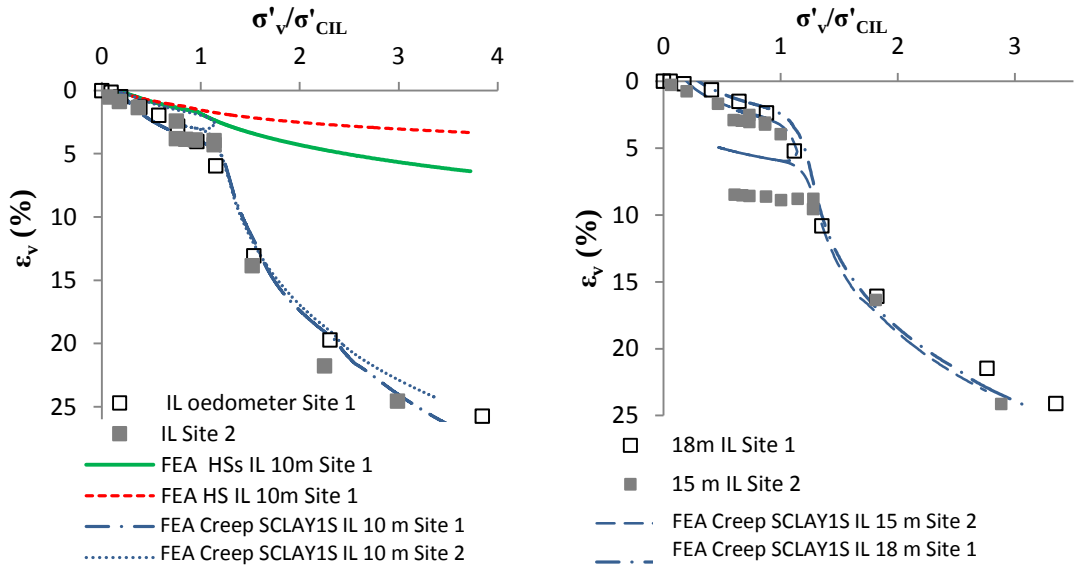

(a) (b)

Figure 6.4 Model calibration for (a) Clay 3 and (b) Clay 5, note: Site 1 tests are fresh samples (4 days) while Site 2 tests were around 6 months old, Site 2 data reproduced from Trafikverket (2014).

In the simulations of pre-yield unloading and reloading loops quite different behaviour is captured in the HS, HSs and Creep-SCLAY1S models as seen in Figure 6.5, differences in the unload-reload stiffness relate to the age of the samples that were simulated.

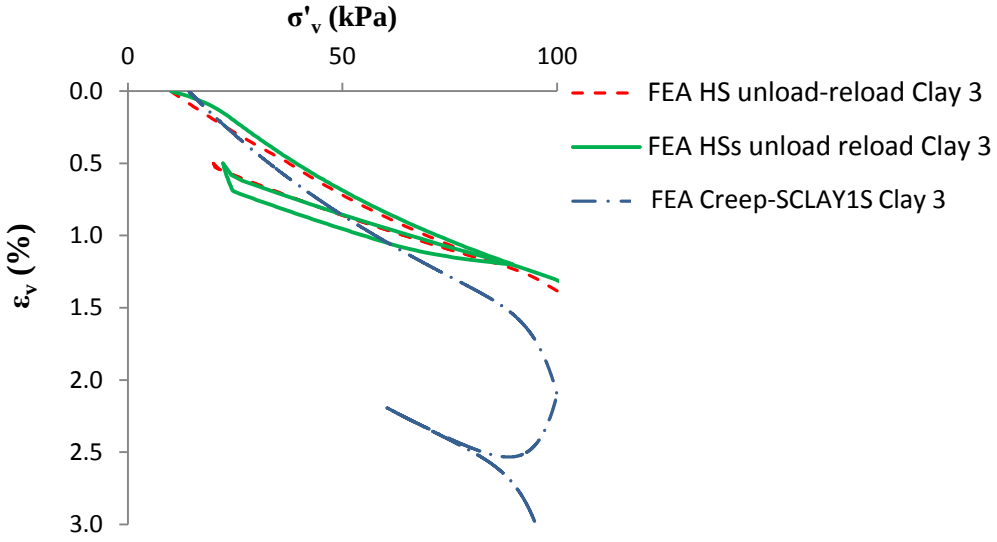

Figure 6.5 Unloading reloading loops in IL tests from in Zone 1C clay from Site 2 (6 month old sample), Trafikverket (2014), using Creep-SCLAY1S, and Site 6 (1 year old sample) using HS and HSs, Trafikverket (2013).

The simulations and IL test results for the Gothenburg glacial clays from Site 1 are presented in together with results for Site 2 unload-reload. Similar to the post glacial clays, the agreement with the laboratory data and Creep-SCLAY1S simulations is reasonable. Results of HS and HSs simulations are not presented given the poor agreement that is achieved due to the falsely high values of E_{oed}^{ref} one is forced to use.

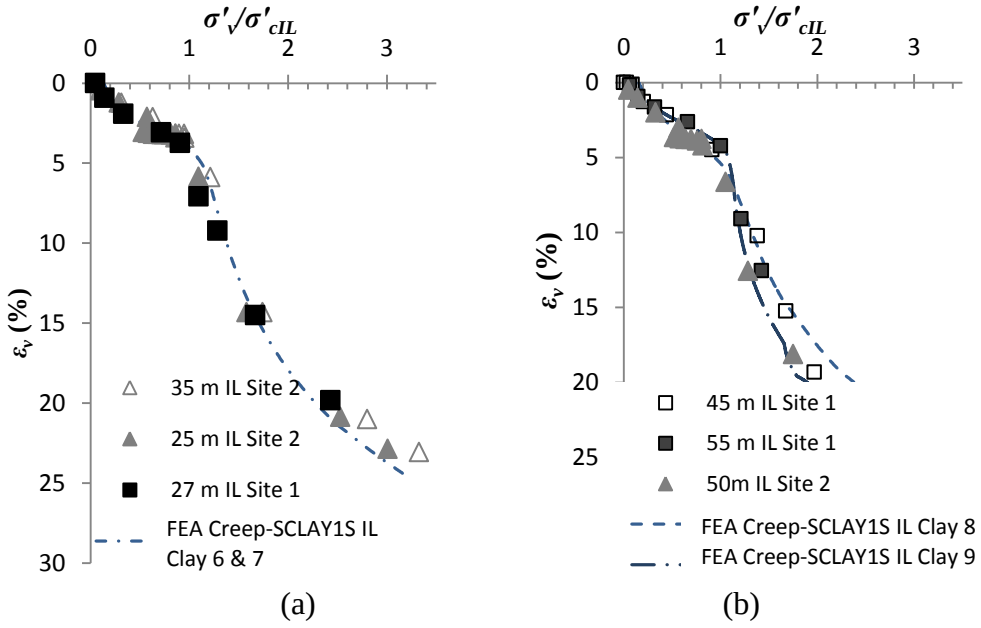

Figure 6.6 Model calibration on IL oedometer tests for Clay 6 and 7 (a) and Clay 8 and 9(b). Note: Site 1 tests are fresh samples around 30 days) while Site 2 tests were around 6-8 months old, Site 2 data is reproduced from Trafikverket (2014).

A comparison of some of the laboratory data and simulations for undrained triaxial tests on Site 1 samples are presented in Figure 6.7 and Figure 6.8.All the models were able to reproduce the behaviour observed up to peak failure strength in triaxial compression reasonably well, however post yield softening could clearly not be captured by the HS and HSs models. This can have repercussions at boundary level when determining factors of safety against failure, which is commonly required in deep foundation design. In addition the laboratory value of $\gamma_{0.7}$ determined for Clay 5 had to be reduced in order to obtain a reasonable fit. This sample was of extremely high quality with very high values of E_{u50}, thus the lack of fit with the laboratory values will relate to differences in the actual stiffness degradation with the empirical relationship used in the model. What is worrying is the huge over-prediction of stiffness in extension with these models and their failure to reproduce realistic stress paths in unloading. This can have significant consequences at boundary level both in terms deformations predicted close to and in the retaining wall (under estimated), but also in structural loads determined in the retaining wall. Clearly it is very important to consider such uncertainties when determining structural design loads by way of the load factor that is applied. In terms of failure strength in extension, the HS and HSs gave lower undrained strengths in extension than in compression given the shape of the Mohr Coulomb failure criteria specified within the model, but these values slightly over- predicted actual values.

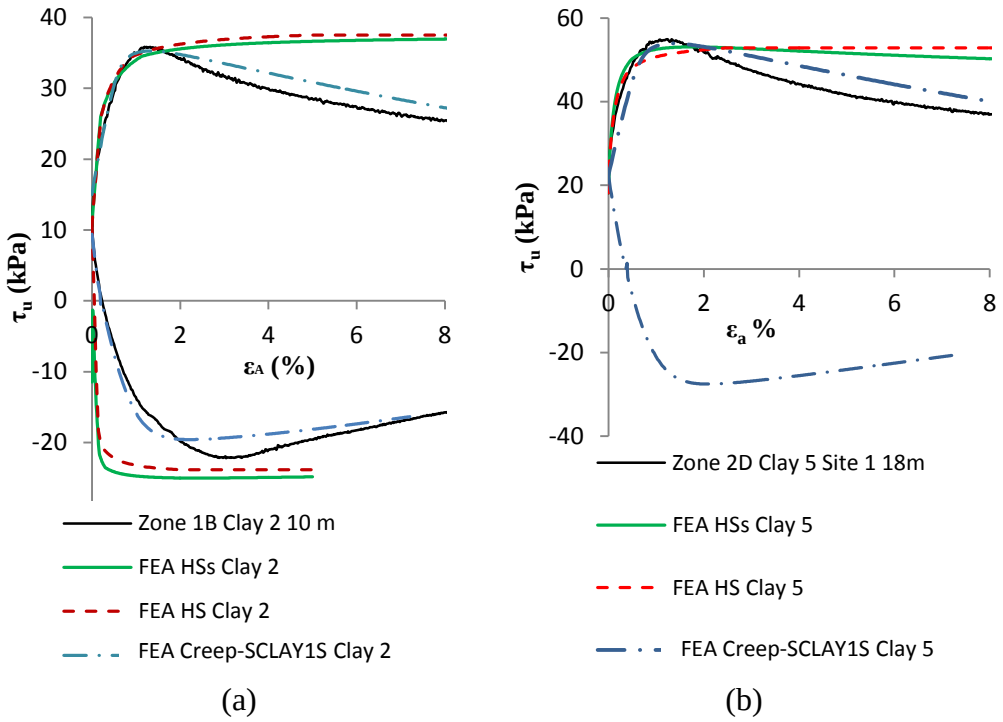

Figure 6.7 Model calibrations on undrained triaxial tests in compression and extension for Site 1 post glacial clays, Clay 2 (a) and Clay 5(b).

In the simulations of the undrained triaxial tests using the Creep-SCLAY1S model both the behaviour in compression and extension is captured reasonably well. However, to truly validate the model for a real problem more advanced triaxial tests are required to confirm the validity of the dataset used. These tests would reproduce the stress paths predicted from the boundary value problem simulations at key points of interest, and then a second round of element level simulations would be conducted and compared to the more advanced tests, with any necessary amendments to the dataset.

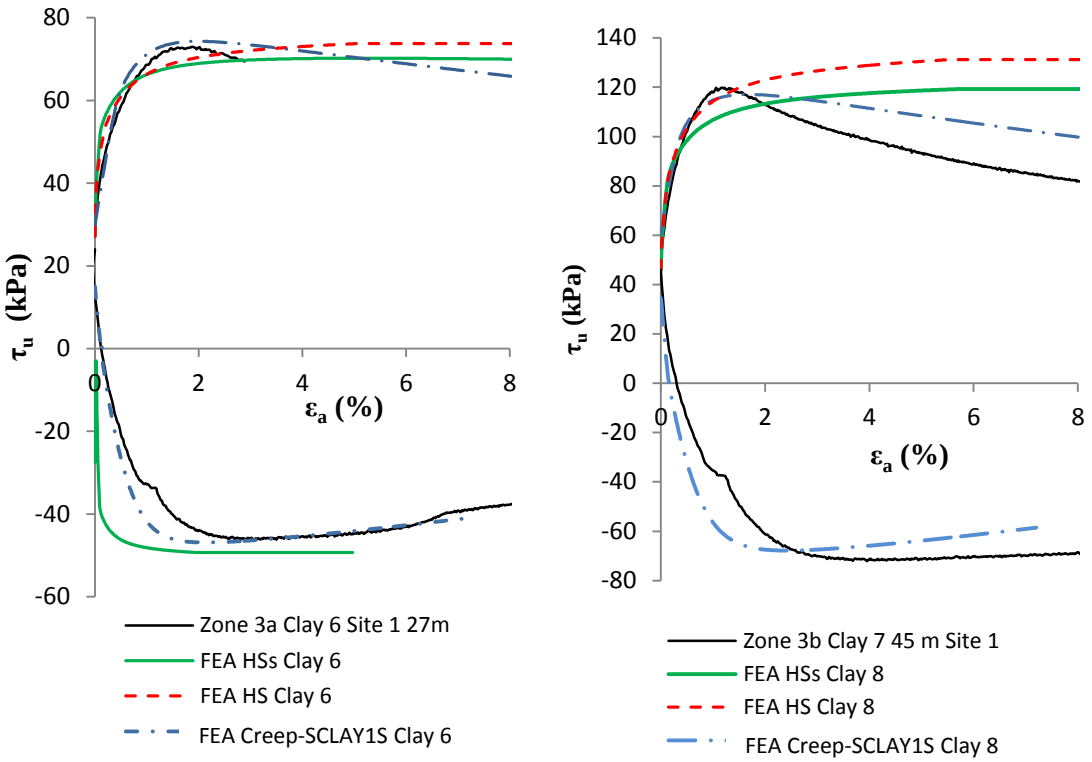

(a) (b)

Figure 6.8 Model calibrations on undrained triaxial tests in compression and extension for Site 1 glacial clays, Clay 6(a) and Clay 8(b).

6.4 Comparison of FEA simulations of deep excavations

In order to illustrate the effect of small strain stiffness in a realistic excavation scenario a theoretical case for a 10 m deep excavation is modelled for the Gothenburg soil profile where the soft clay extends to around 100 m. This is indicative of ground profiles found at Site 1, 2, 3 and 6. The mesh discretisation and layering was shown in Figure 6.1, in accordance with Figure 4.7, and the modelling stages for the HS and HSs simulations are detailed in Table 5.4. For the Creep-SCLAY1S simulations, the initial loading caused by land reclamation was omitted as to model this would require using input parameters that were relevant in the 1800's and not the values determined from laboratory testing. In the HS and HSs simulation the excess pore pressures relating to this reconsolidation stage were small (5 *kPa*) which is similar to pore pressures measured in the field. Failure to ignore this reconsolidation stage in the HS and HSs models gave unrealistically large heave at depth and was not consistent with measured behaviour of deep excavations in the area. It is not possible to perform factor of safety analyses with the Creep-SCLAY1S model, thus these too are omitted from the calculation stages performed. The stages in the Creep-SCLAY1S model simulations are presented in Table 6.7.

Table 6.6 Analysis stages used in the Finite Element simulations with the HS and HSs models.

Identification	Phase no.	Start from	Calculation	Loading input	Pore pressure	Time
Initial phase	0	N/A	K0 procedure	Unassigned	Phreatic	0.00 day
Consolidation lan...	24	0	Consolidation (UM)	Staged construction	Phreatic	47200.00 ...
install SSP	1	24	Plastic	Staged construction	Phreatic	0.00 day
Excavate to prop 1	2	1	Plastic	Staged construction	Phreatic	0.00 day
install prop 1	3	2	Plastic	Staged construction	Phreatic	0.00 day
Excavate to 5m ...	4	3	Plastic	Staged construction	Phreatic	0.00 day
Safety 1 prop Ex...	6	4	Safety	Incremental multipli...	From previous ...	0.00 day
install prop 2	13	4	Plastic	Staged construction	Phreatic	0.00 day
Excavate to 7m ...	8	13	Plastic	Staged construction	Phreatic	0.00 day
safety 7m 2 prop	21	8	Safety	Incremental multipli...	From previous ...	0.00 day
Excavate t0 10m	7	8	Plastic	Staged construction	Phreatic	0.00 day
consolidation exc...	22	7	Consolidation	Staged construction	Phreatic	365.00 day
safety consolidat...	23	22	Safety	Incremental multipli...	From previous ...	0.00 day
safety at full exc...	9	7	Safety	Incremental multipli...	From previous ...	0.00 day

Table 6.7 Analysis stages used in the Finite Element simulations with the creep SCLAY1S and the creep SCLAY1S small strain adaption.

Identification	Phase no.	Start from	Calculation	Loading input	Pore pressure	Time
Initial phase	0	N/A	K0 procedure	Unassigned	Phreatic	0.00 day
Install SSP	1	0	Plastic	Staged construction	Phreatic	0.00 day
Excavation prop 1	2	1	Plastic	Staged construction	Phreatic	0.00 day
Prop 1	3	2	Plastic	Staged construction	Phreatic	0.00 day
Excavation to pr...	4	3	Plastic	Staged construction	Phreatic	0.00 day
Prop 2	5	4	Plastic	Staged construction	Phreatic	0.00 day
Excavation to pr...	6	5	Plastic	Staged construction	Phreatic	0.00 day
Prop 3	7	6	Plastic	Staged construction	Phreatic	0.00 day
Excavation 10 m	8	7	Plastic	Staged construction	Phreatic	0.00 day

Four data sets are investigated, and the deformations and the structural loads in the retaining wall system are compared. As discussed earlier, the strength reduction analyses using the PLAXIS safety calculation (*c-ϕ*' reduction) are not possible with the Creep-SCLAY1S model. However, safety analyses using the HS and HSs models show that similar failure mechanism, as seen in Figure 6.9and factors of safety determined at the various safety calculation stages were almost identical, except for the final excavation stage where values were F=1.98 for the HSs model and F=1.92 for the HS model. Clearly, the small strain stiffness has marginal effect on the safety against failure in the ground, but could have consequences with regard to failure in structural elements as will be shown later.

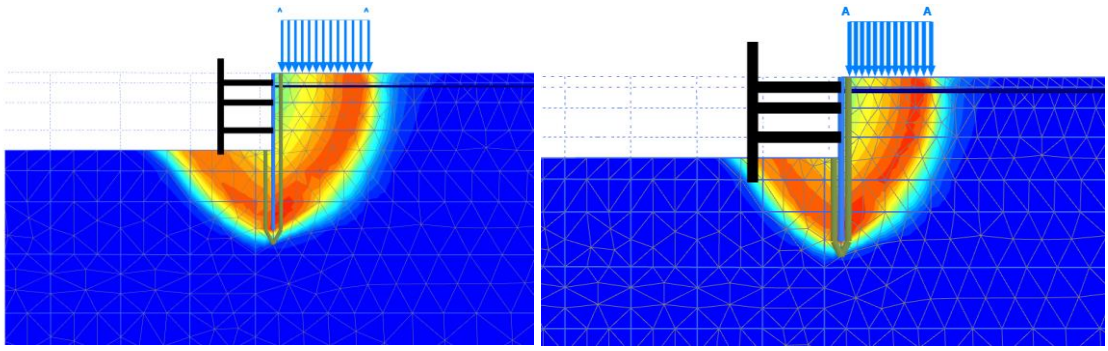

(a) (b)

Figure 6.9 Failure mechanism at full depth (undrained) (incremental displacement) (a) HSs data set, (b) HS data set.

Differences in displacements fields

The average simulated displacement to a distance of 160 m from the retaining wall for the four data sets is presented in Figure 6.10.These simulations are plotted on the same scale (red=200 mm, dark blue=0 mm). The difference in the 4 simulations is large. The HSs simulations indicate less impact on the immediate surroundings beyond the influence of the assumed surcharge load of 13 *kPa* than the HS simulations. Similar differences are noted between the Creep-SCLAY1S small strain and Creep-SCLAY1S simulations. The largest movements are generated in the Creep-SCLAY1S simulations and is caused partly due to the allowance for anisotropy, but also due to the influence of movements well outside the area of influence of the retaining wall, and are therefore judged to unrealistic, as are the displacements predicted with the HS model. The rudimentary allowance for some small strain stiffness in the Creep-SCLAY1S small strain analysis has a significant effect, and yields displacements that are only slightly larger than the HSs model generally. Away from the retaining wall this is not surprising given that no degradation of stiffness is included, and adjacent to the wall the larger displacements relate to anisotropy which is captured well with this model as shown in Section 6.3. Thus is this instance is thought that the Creep-SCLAY1S small strain analysis captures best the behaviour close to the retaining wall.

The differences in the predictions close to the retaining wall are further confirmed in Figure 6.11, which indicates the horizontal movements of the SSP retaining wall. Somewhat surprising is the large difference between the Creep-SCLAY1S and Creep-SCLAY1S small strain simulations given that κ^*_{SS} is only specified at a horizontal distance of 15 m from the retaining wall and 20 m below the final excavated depth. Differences between the HSs simulation and the Creep-SCLAY1S small strain simulation are consistent with element level comparisons, and relate to the Creep-SCLAY1S small strain simulations being able to more realistically capture the anisotropic behaviour of Gothenburg clays during shearing.

In Figure 6.12 the predicted displacement in the ground surface behind the retaining wall is presented. In the simulations without allowance for small strain stiffness, the displacements away from the retaining wall are unrealistic. In the simulations with allowance for small strains it is difficult to say which is the more realistic as generally there is very little data available for movements within the ground surface. In practice the displacement at specific points of the retaining wall is normally measured, or the horizontal displacement in the ground with the help of inclinometers, however these tend to lie a few meters from the wall. The vertical displacements are very similar suggesting that the differences in the horizontal displacements most likely relate to the effects of anisotropy.

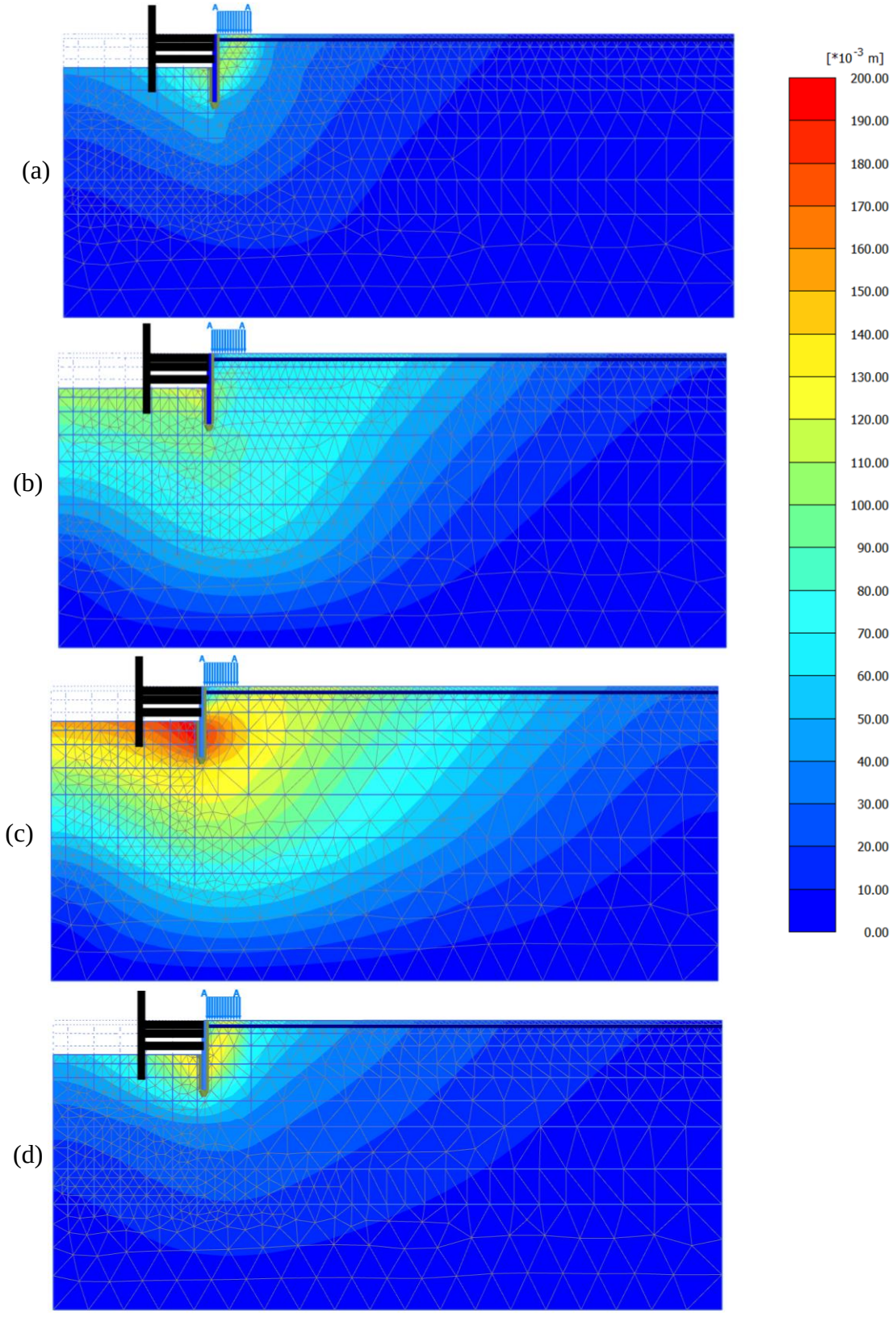

Figure 6.10 Displacements at full depth (undrained): (a) FEA HSs (0.114 m max) (b) FEA HS (0.124 m max) (c) FEA creep-SCLAY1S (0.197 m max) (d) FEA creep-SCLAY1S small strain (κ^*_{SS} in the area outside the main excavation works as indicated in Figure 6.1) (0.137 m max).

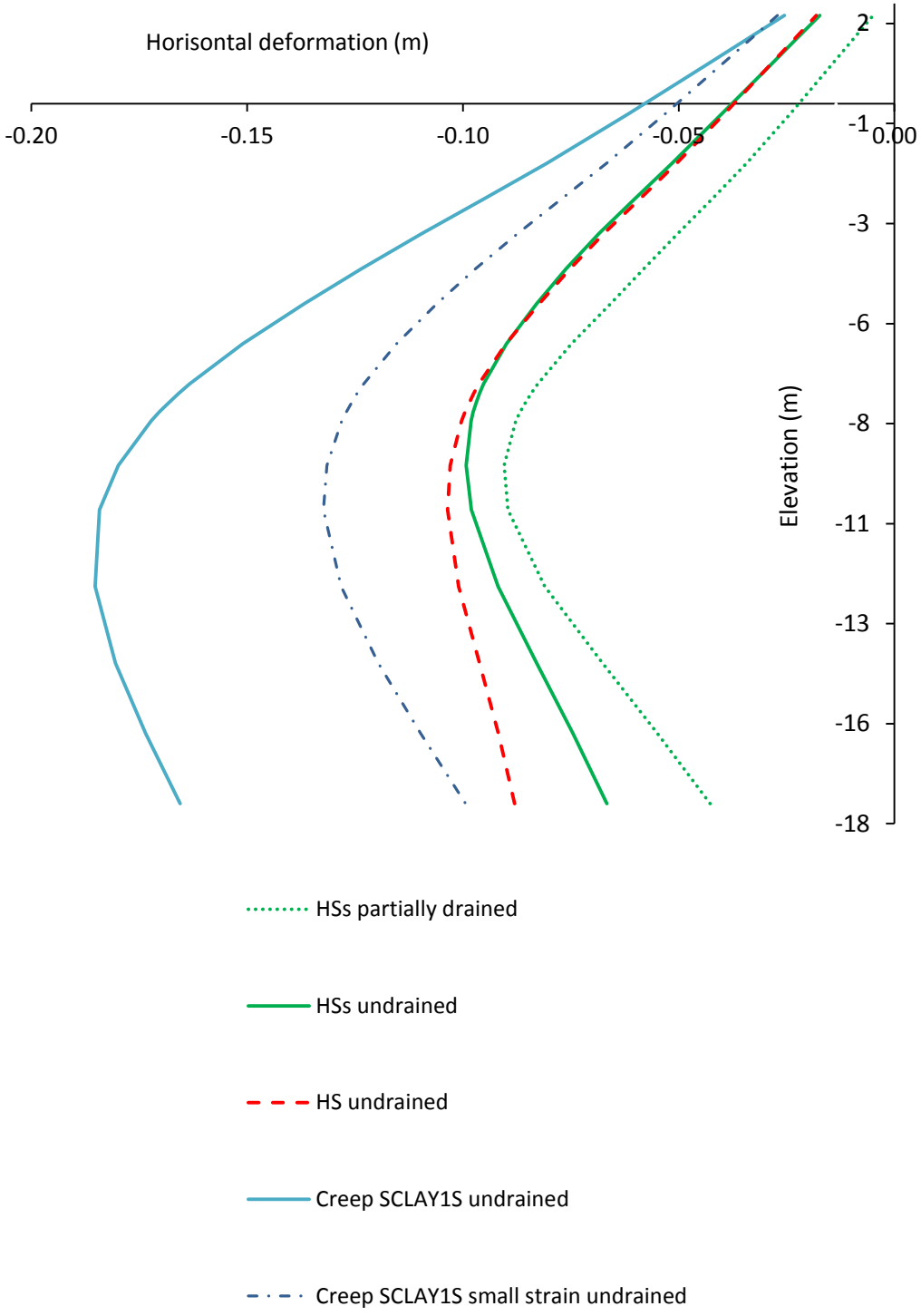

Figure 6.11 Predicted horizontal displacement of the SSP wall at 10m excavation (-ve towards excavation).

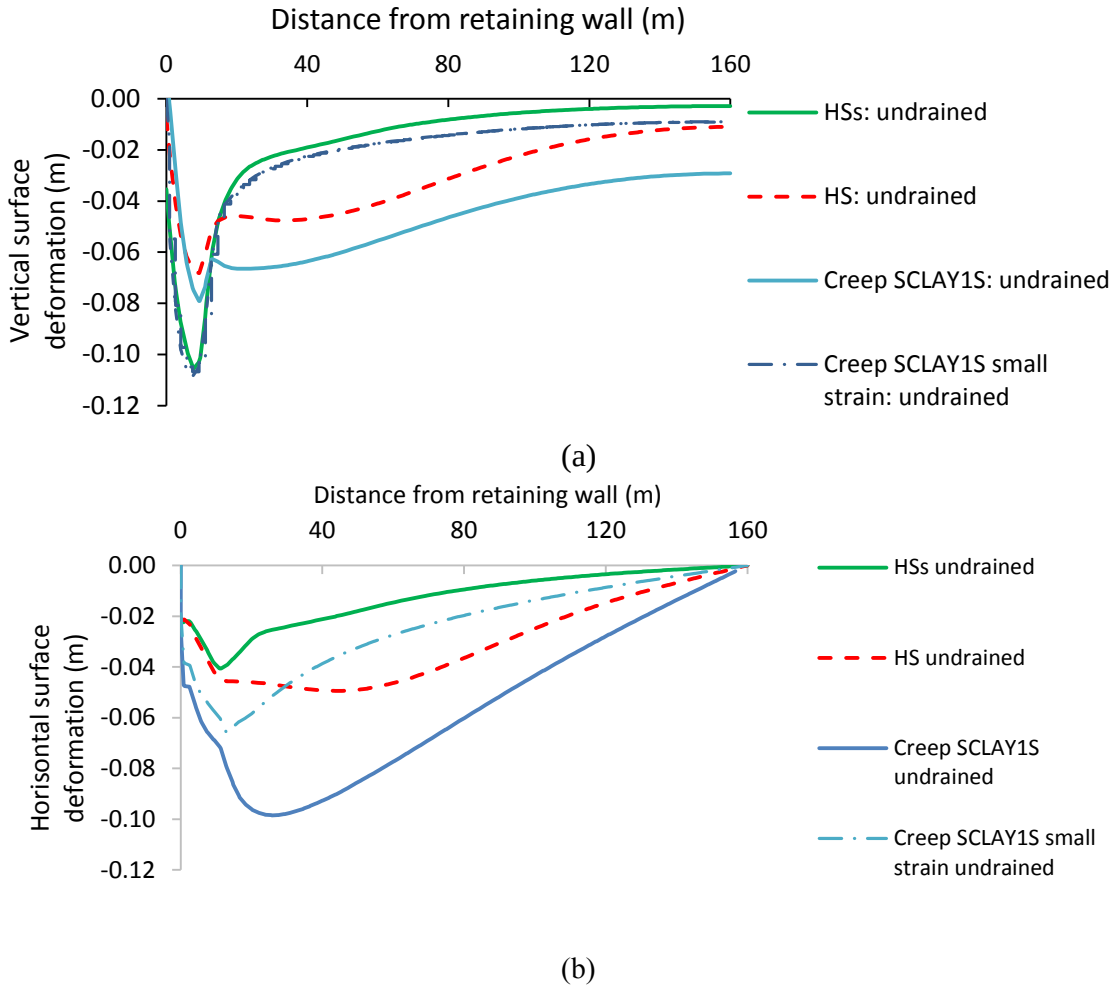

Figure 6.12 Predicted movement of ground surface behind SSP retaining wall (a) Vertical displacement, (b) Horizontal displacement.

Influence on structural loads of temporary works structures

It is well understood that stiffer retaining wall systems (soil:retaining wall:support) experience higher structural loads. Thus, it is interesting to examine what influence allowance for small strain stiffness has on structural loads. For simplicity bending moment in the retaining wall and maximum prop loads only are compared. However, what is of more concern based on the differences observed between the HSs undrained and partially drained simulations is that the undrained analysis will not capture a conservative upper bound in terms of structural loads for project durations of 1 year, typical for large infrastructure considered (Figure 6.13 and Table 6.8). Such issues lie outside the focus of this thesis, thus further discussion is limited to undrained conditions or close to (T_v<0.1) and differences between analysis with and without small strain stiffness.

In Table 6.8 the maximum loads occurring in the three props are indicated. The magnitude of load in the upper two props is fairly similar although the Creep-SCLAY1S small strain simulations are smaller consistent with the greater deformation of the retaining wall. The largest loads obtained with the Creep-SCLAY1S simulations was somewhat surprising initially, however on closer scrutiny this simulation had fewer plastic points along the retaining wall than the Creep-SCLAY1S small strain simulations as the mobilised strengths were lower, thus the retaining wall is taking a

greater share of the loads. It is perhaps important to point out that the mobilised strengths in the Creep-SCLAY1S small strain simulations alter very abruptly at the boundary of the assumed small strain stiffness zone. Comparisons of the HS and HSs models indicate increased structural loads with allowance for small strain stiffness when at full excavation depth.

Table 6.8 Summary of prop load (800 mm diameter 40m long steel props) undrained conditions.

	Serviceability state prop load (kN/m)			
Construction phase	HSs undrained /partially drained	HS undrained	Creep-SCLAY1S undrained	Creep-SCLAY1S small strain undrained
Excavation 4m + 1 prop	130/130	107	152	122
Excavation 7m + 2 prop	306/306	336	363	285
Excavation 10m + 3 prop	291/445	279	254	197

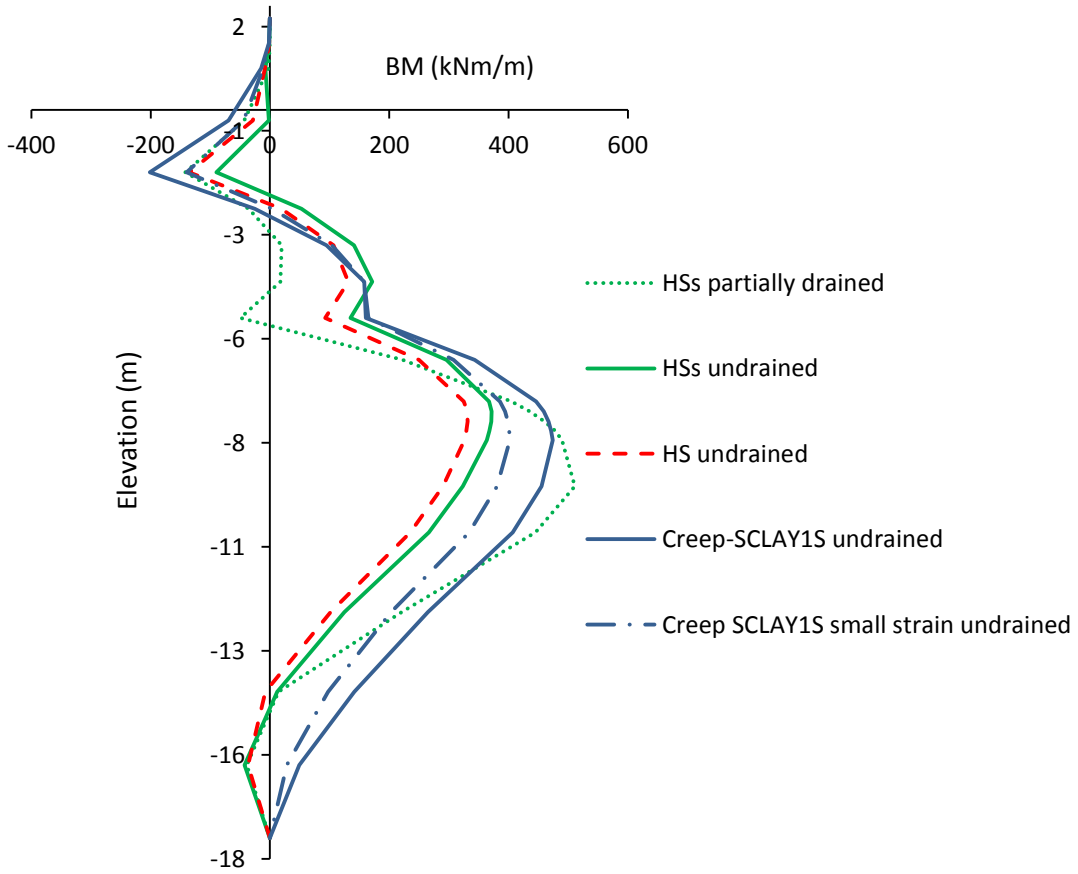

Figure 6.13 Comparison of simulated bending moments using the HS and HSs model data sets for 10 m excavation.

Conclusions with regard to FE simulations

For Finite Element (FE) simulations of deep excavations in soft Scandinavian clay, it is recommended that a more advanced model is utilised, which can capture anisotropy, small strain stiffness, structure and creep. Without this much trust has to put in the hands of the executor of the numerical analyses to implicitly allow for model limitations and their choice of model parameters and FEA implementation. However, lower stiffness and strength parameters do not lead to a safer (more conservative) design.

It would seem prudent to insist that for critical deep excavation projects where FEA is performed, the consistency of the model parameters is demonstrated with element test simulations. In this way the behaviour of the chosen parameter set can easily be understood. The laboratory element tests used for calibrating the constitutive model should only consider fresh high quality samples with relevant undrained and drained triaxial stress paths as an initial stage in the calibration process. Boundary level simulations can be performed so that the expected stress paths can be determined to enable more relevant advanced testing. These advanced tests should attempt to simulate different stress paths occurring around the retaining wall structure. Such tests may include K_0 consolidated tests which are unloaded undrained and then be allowed to consolidate under drained conditions, drained extension/compression tests with reload-unload loops pre-failure to determine the deviatoric unload –reload moduli and drained triaxial tests at various stress states (minimum of 3) in order to determine drained strength characteristics more easily for each geological deposit. When determining design parameters for Finite Element simulations of real excavations, one must consider the influence of sample quality of the samples used for calibration, the construction methods to be applied (duration of excavation stages, drainage conditions), as well as model assumptions with respect to ground profile, stress history and pore pressure generation method during consolidation stages within a sensitivity analysis. Failure to do this may lead to unsafe design.

The simulations with allowance for small strains appear to reflect the deformations that one would expect during undrained conditions. It is difficult to say which of the small stain simulations gives more realistic structural loads, probably neither. For better reliability a Creep-SCLAY1S type model with small strain stiffness incorporated within the model would be required. Ideally such a model would not only incorporate more realistic stiffness degradation behaviour than the HSs model, but also incorporate the small strain anisotropy and changes in small strain stiffness occurring with strains. Until such a model is available numerical users need to be very careful when using FE simulations to determine structural loads. The uncertainty surrounding them should be reflected in the partial factors applied when determining design loads. Use of a robust sensitivity analyses will however add confidence. That said, the FE methods will be more reliable than the traditional methods used in Sweden for deep excavations (> 7 m) when correct validation is applied. The traditional methods are either empirically based (on shallower excavations), such as when considering base heave, or involve no consideration of soil: structure interaction, such as when determining earth pressures using Rankine approach. Lack of allowance for soil:structure interaction (and associated higher stiffness) in deep excavations has been shown to give unsafe structural loads in the ultimate limit state, whereas estimations of loads in the serviceability limit state using FEA reflected actual loads well, refer to Wood (2010).

7 CONCLUSIONS AND RECOMMENDATIONS

7.1 Conclusions

The extensive testing programme comprised of a wide range of Swedish clays and used a multitude of shear wave velocity based methods identified from literature, in the field and in the laboratory. The subsequent interpretation of small strain shear modulus from this data using time and frequency based methods leads to the following conclusions:

1. The consistency in the results indicates that shear wave velocity based measurement methods are suitable for measuring the small strain shear modulus of Swedish clays as those clays have minimal signal dispersion and reasonably small attenuation.
2. The following techniques work best:
    a. In the field
        i. Multiple receiver direct methods (e.g. SDMT or SCPT).
        ii. Surface seismic methods (e.g. MASW), if state of the art inversion methods are used.
        iii. Direct shear wave velocity measurements using bender elements on freshly retrieved samples that still retain a large degree of suction.
    b. In the laboratory
        i. Bender element methods when used on high quality samples that are tested quickly after extraction and are re-consolidated in a test cell to in-situ anisotropic stress level.
        ii. In the latter, a high bandwidth data acquisition system should be used in conjunction with contemporary signal processing (stacking of samples, digital filtering of signal)
3. No reliable relation between small strain shear modulus G_0 and index properties (soil classification) has been identified for the clays tested. Currently, the G_0 value normalised by mean effective stress related to soil activity (i.e. the plasticity index that is normalised by the clay fraction <2 μm), appears the best approach for a generalised relationship, however, significant spread remains.
4. Similarly, Cone Penetration Test (CPT) based soil classification relations with G_0 were not reliable either. Most of the uncertainty in these methods stems from the uncertainty in the assumed in-situ pore pressure profile used for the evaluation.
5. Local (site specific trends) appear to exist, but more extensive testing would be required to enable reliable determination of site specific relationships.
6. Empirical relations to G_0, based on undrained shear strength, commonly used in Sweden, are unreliable and appear highly site specific. The TKGEO (2013) is overly conservative in high to medium plasticity clays, whereas the CPT based relation proposed by Long and co-workers (Long & Donohue 2010) are overly optimistic for the cases presented.
7. The influence of the sample time-line (disturbance chain) is evident in all samples tested in the laboratory to varying degrees, and therefore in many cases will affect the geotechnical parameters determined. Apart from the initial disturbance during sample extraction, long storage times even under optimum conditions (7°C and 100% humidity) can have considerable impact on observed behaviour. The effect on small strain stiffness and its degradation with strain were particularly affected. When testing small strain stiffness behaviour in the laboratory the best way forward is to minimise sources of disturbance wherever possible. This means careful selection of sample extraction methods and sample extraction positions, (as some

soft clays cannot be extracted with STII piston samples without causing significant disturbance), minimising transport distances and vibrations during transport, testing samples quickly (preferably within 2 days), limiting the time samples remain unconfined during sample preparation and following reconsolidation paths that do not involve loading too far beyond the estimated *in situ* stresses, i.e. no use of SHANSEP type reconsolidation procedures. When this is not possible, use field tests such as the seismic dilatometer (SDMT) or seismic pressuremeter testing (SbPMT) is a better way forward.

8. Based on studies of high quality block samples, the magnitude of small strain stiffness, G_0, varies with shear strain. This means that for deep foundations involving unloading and then reloading it is not the initial small strain stiffness values that should be used when analysing the reloading behaviour, but rather the reduced values. The size of the latter will depend on the magnitude of the strains occurring during unloading. This may also have significant consequences for dynamic analyses and cyclic loading.
9. Stiffness degradation is significant for the soils tested. Existing relations such as those internationally proposed (and implemented in the Hardening Soil Small Strain model) are unreliable and non-conservative. They are, however, preferred over the formulation presented in TKGEO (2013) 5.2.2.3.5 (unloading modulus).
10. The majority of the laboratory tests presented were performed on piston samples with an excellent to very good rating. Still the signal interpretation of the bender element tests required extra care. The limited tests on the block samples show superior signal quality, and therefore ease of interpretation with less uncertainty. As a result, the reported values for the shear modulus are expected to be a reliable lower bound for the small strain shear modulus.
11. The numerical analyses using standard commercial constitutive models clearly indicate the profound effect of small strain shear stiffness of the soil on the structural response. Whilst the predicted deformations are generally of smaller magnitude, the corresponding bending moments in the wall are significantly larger. These differences are even more pronounced when realistic partial drainage conditions are considered.
12. Numerical analysis with an advanced constitutive model tailored specifically to soft structured clays for medium to large strains gave significantly larger deformations at the retaining wall (with or without a rudimentary allowance for small strain stiffness in the far field) given the models ability to more realistically model soft clay behaviour during deviatoric unloading. This is clearly of importance when using observational techniques in real situations. Differences in the predictions of deformation with and without allowance for small strain in the far field were large, as were differences in structural loads in the retaining wall system. Clearly the effects of small strain stiffness are significant in deep excavations in soft clays and a constitutive model is required that can capture this, and the other important features of these clays (anisotropy, structure, creep).

7.2 Recommendations

1. The small strain shear modulus requires more systematic experimental probing of stiffness degradation following different stress paths and intermediate strain magnitudes. This includes unloading/re-loading paths simulating geotechnically relevant building sequences, cyclic loading and large amplitude shear waves such as with high speed rail. In addition to using bender elements in conventional test cells a resonant column or cyclic torsional shear apparatus should also be considered.

2. Development of high resolution local strain measurement techniques without the need to attach any devices to soft clay sample is needed, possibly using optical techniques if sufficient accuracy can be achieved.

3. Investigations into the viability of field methods such as the seismic SbPMT tests to define small strain stiffness and degradation *in situ*.

4. Expansion of the G_0 database in terms of field and laboratory measurements with more tests conducted on block samples.

5. It would seem prudent for clients to insist that for critical deep excavation projects where Finite Element Analyses are performed, consistency of the model parameters is demonstrated with element test simulations where the behaviour of the chosen parameter set can easily be understood.

6. The laboratory element tests used for calibrating the constitutive model should only consider high quality samples with relevant undrained and drained triaxial stress paths. These advanced tests should attempt to simulate different stress paths occurring around the retaining wall structure. Such tests may include K_0 consolidated tests, which are unloaded undrained, and then be allowed to consolidate under drained conditions, drained/undrained extension/compression tests with reload-unload loops pre-failure to determine the deviatoric unload – reload moduli, and drained triaxial tests at various stress states (minimum of 3) in order to determine drained strength characteristics more easily for each geological deposit.

REFERENCES

Alén, A., Sällförs, G., Bengtsson, P.E. and Baker, S. (2006) "Test embankments National road 45/Nordlänken: Embankments on lime cement stabilized soil-calculation method for settlement." Report 15: Swedish Deep Stabilization Research Centre, Linköping. (In Swedish).

Alén, C. Jendeby, L. (1996) "Hävning vid schaktning – Ullevi, ett praktikfall". Proceedings. of Nordic Geotechnical Meeting, pp. 353-358. (In Swedish).

Alte, B., Olsson, T., Sällförs, G. and Bergsten, H. (1989). "Djupdykning I Göteborgsleran", Chalmers Technical University. (In Swedish).

Alvarado, G. and Coop, M. R. (2012). "On the performance of bender elements in triaxial tests." Géotechnique 62(1), pp. 1-17.

Alvarado, G. and Coop, M. R. (2007). Influence of stress level in bender element performance for triaxial tests. Proc. 4th Int. conf. on earthquake and geotechnical engineering, Thessaloniki, Paper 1419, pp. 1–11.

Al Tabba, A. and Muir Wood, D. (1989) "An experimentally based 'bubble' model for clay." In Pietruszczak, S. and Pande, G.N., (Ed.), Numerical models in geomechanics: NUMOG III, London, Elsevier Applied Science, pp. 91-99.

Andresen, L. and Jostad, H.P. (2005) "A constitutive model for anisotropic and strain-softening clay." International Journal for Numerical and Analytical methods in Geomechanics." 36(4), pp. 483-497.

Andresen, A. and Kolstad, P. (1979). "The NGI 54 mm samplers for undisturbed sampling of clays and representative sampling of coarser materials". Proc. of international symposium on soil sampling, Singapore, pp. 13-21.

Andréasson, B. (1979). Deformation characteristics of soft, high-plastic clays under dynamic loading conditions. PhD thesis, Chalmers University of Technology, Gothenburg, Sweden.

Arman, A. and McManis, K. L. (1976). "Effects of storage and extrusion on sample properties." Soil specimen preparation for laboratory testing, ASTM, STP 599, pp. 66-87.

Arroyo, M. Muir Wood, D. Greening, P.D. Medina, L. and Rio, J. (2006) "Effects of sample size on bender-based Axial G_0 measurements." Géotechnique, 56(1), pp. 39-52.

Arulnathan, R., Boulanger, R. W., and Riemer. M. F. (1998). "Analysis of bender element tests." Geotechnical Testing Journal, ASTM, 21(2), pp. 120-131.

Atkinson, J.H, Allman, M. A., and Beose, R. J. (1992). "Influence of laboratory sample preparation procedures on the strength and stiffness of intact Bothkennar soil recovered using the Laval sampler". Géotechnique, 42(2), pp. 349-354.

Atkinson, J.H. and Sällfors G. (1991). "Experimental determination of soil properties." Proc. of the 10th ECSMFE, Vol. 3, Florence, Italy, pp. 915-956.

Atkinson, J., Richardson, D. and Stallebrass, S. (1990). "Effect of recent stress history on the stiffness of over consolidated soil." Géotechnique, 40(4), pp. 531-540.

Atkinson. J, (1975). "Anisotropic elastic deformations in laboratory tests on undisturbed London clay." Géotechnique, 25(2), pp. 357-374.

Baligh, M. M., Azzouz, A. S., Chin, C. T. (1987). "Disturbances due to ¨ideal¨ tube sampling". Journal of Geotechnical Engineering, 113(7), pp. 739-757.

Baligh, M. M. (1985) "Strain path method." Journal of Geotechnical Engineering, 111(9), pp. 1108-1136.

Bengtsson, P. E. (1977) ”Dragpåle i lös lera (Belastningsförsök i Trägårdsföreningens park i Göteborg)”. Intern rapport, Chalmers Tekniska Högskola, Gothenburg, Sweden. (In Swedish).

Benz, T. (2007). “Small-strain stiffness of soils and its numerical consequences.” PhD thesis, University of Stuttgart, Institution für Geotechnik.

Berre, T. Schjetne, K. and Sollie, S.(1969). “Sample disturbance of soft marine clays.” Proceedings of the 7th ICSMFE, Special Session, Mexico, Vol. 1, pp. 21-24.

Bergsten, H. (1991). “Late Weichselian-Holocene stratigraphy and environment conditions in the Göteborg area, south-western Sweden. “ PhD Thesis, Chalmers University of Technology, Göteborg, Sweden.

Bhandari, A.R., Powrie, W. and Harkness, R.M. (2012). “A digital image based deformation measurement system for triaxial tests.” Geotechnical Testing Journal, 35(2), pp. 209-226.

Bjerrum, L. (1973). “Problems of soil mechanics and construction on soft clays.” State of art report to session IV, 8th International Conference on Soil Mechanics and Foundation Engineering, Moscow. Vol. 3, pp. 111-159.

Bjerrum, L. (1967). “Engineering geology of Norwegian normally consolidated marine clays as related to settlement of buildings." Géotechnique, 17(2), pp. 81-118.

Blewett, J., Blewett, I.J. and Woodward, P.K. (1999). “Measurement of shear-wave velocity using phase sensitive detection technique.” Canadian Geotechnical Journal, 36(5), pp. 934-939.

Bodare, A. and Massarsch, K.R. (1984). “Determination of shear wave velocity by different cross hole methods.” Proceedings of the 8th world conference on Earthquake Engineering, pp. 39-45.

Bonal, J., Donohue, S. and McNally, C. (2012). “Wavelet analysis of bender element signals.” Géotechnique, 62(3), pp. 243-252.

Bozouk, M. (1976). “Effects of sampling and storage on test results for marine clays.” Sampling of Soil and Rock. ASTM STP 483, pp. 121 - 131.

Brignoli, E., M. Gotti and K. H. Stokoe (1996). "Measurement of shear waves in laboratory specimens by means of piezoelectric transducers." ASTM geotechnical testing journal 19(4): 384-397.

Brinkgreve, R., Swolfs, W., Engin, E., Waterman, D., Chesaru, A., Bonnier, P. and Galavi, V. (2010). "PLAXIS 2D 2010." User manual, Plaxis bv.

Britto, A.M., and Kusakabe, O. (1982). “Stability of unsupported axisymmetric excavations in soft clays.” *Géotechnique*, 32(3), pp. 261-270.

Brocanelli, D. and Rinaldi, V. (1998). "Measurement of low-strain material damping and wave velocity with bender elements in the frequency domain." Canadian Geotechnical Journal 35(6), pp. 1032-1040.

Bråten, C. Døssland, Å. L. Gjestvang, M., Kaynia, A.M. Loe, M. M., Løset, Ø. (2010). ”Dimensionering for jordskjelv”. Rådgivande Ingenjørers Forening. (In Norwegian)

Budhu & Wu, (1992). “Numerical analysis of sampling disturbances in clay soils.” International Journal Numerical Analytical Methods in Geomechanics, Vol. 16, pp. 467–492.

Bulut, R., Lytton, R.L., and Wray, W.K. (2001). “Soil suction measurements by filter paper.” In Expansive clay soils and vegetative influence on shallow foundations, ASCE, pp. 243-261.

Burland, J. B (2012). “Chapter 4: The geotechnical triangle.” In ICE manual of geotechnical engineering, Burland, J., Chapham, T., Skinner, H. and Brown, M. (Ed.), Thomas Telford, pp. 17-26.

Burland, J.B. (2001). " Ground Profiles." Course notes from MSc in Advanced Soil Mechanics, Imperial College, University London.

Burland, J. B.(1990). "On the compressibility and shear strength of natural clays." Géotechnique, 42(2), pp. 349-354.

Burland, J. (1989). "Ninth Laurits Bjerrum Memorial Lecture:" Small is beautiful"-the stiffness of soils at small strains." Canadian Geotechnical Journal, 26(4), pp. 499-516.

Burland, J.B (1987). "The teaching of soil mechanics: a personal view." Proceedings of 9th European conference on soil mechanics and foundation engineering, Dublin, Vol. 3, pp. 1427-1447.

Burland, J.B., Moore, J.F., Smith, P.D. (1972). "A simple precise borehole extensometer." Géotechnique, 22(1), pp.174-177.

Burland, J.B. and Symes, M.(1982). "Simple axial displacement gauge for use in the triaxial apparatus.", Géotechnique, 32(1), pp. 62-65.

Burland, J.B., Simpson, B., St. John, H.D. (1979). "Movements around excavations in London Clay." Proc. of the 7th European Soil Mechanics and Foundation Engineering Conference, Vol. 1, pp. 13-30, Brighton, UK.

Butcher, A. and Powell, J. (1996). "Practical considerations for field geophysical techniques used to assess ground stiffness". Proc. of the International Conference Advances in Site Investigation Practice, London, 30-31 March 1995, pp. 701-711.

Butcher, A.P. Campanella, R.G. Kaynia, A.M. Massarsch, K.R. (2005) "Seismic cone down hole procedure to measure shear wave velocity- a guideline prepared by ISSMGE TC10: Geophysical Testing in Geotechnical Engineering", TC 10 Report.

Callisto, L. and Rampello, S. (2002)."Shear strength and small-strain stiffness of a natural clay under general stress conditions." *Géotechnique*, 52(8), pp. 547-560.

Camaco – Tauta, J., Cascante, G. Santos, J.A. and Fonseca, A.V.D. (2011). "Measurement of shear wave velocity by resonant-column test, bender element test and miniature accelerometers." Proc. of Pan-Am CGS geotechnical conference, Canada, Vol. 949, pp.1-9.

Campanella, R., Robertson, P. and Gillespie, D. (1986). "Seismic cone penetration test". In Use of In Situ Tests in Geotechnical Engineering, ASCE, pp. 116-130.

Casegrande, A. (1936). "The determination of the pre-consolidation load and its practical significance." Proceedings of the 1st International Conference of Soil Mechanics and Foundation Engineering, Harvard, pp. 60-64.

Chandler, R.J. and Gutierrez, C.I. (1986), "The filter-paper method of suction measurement." Géotechnique, 36(2), pp. 265-268.

Chang, M. F. (1991). "Interpretation of over consolidation ratio from in situ tests in recent clay deposits in Singapore and Malaysia." Canadian Geotechnical Journal, 28(2), pp. 210-225.

Chang, M.F. (1988). "Some Experience with the Dilatometer Test in Singapore", Proceedings 1st International Symposium on Penetration Testing, Vol. 1, pp. 489-496.

Claesson, P. (2003). " Long term settlements in soft clays." Department of Geotechnical Engineering, PhD Thesis, Chalmers University of Technology, Gothenburg.

Clayton, C. (2011). "Stiffness at small strain: research and practice." Géotechnique, 61(1), pp.5-37.

Clayton, C., Theron, M. and Best, A. (2004). "The measurement of vertical shear-wave velocity using side-mounted bender elements in the triaxial apparatus." Géotechnique, 54(7), pp. 495-498.

Clayton, C., Siddique, A. and Hopper, R.J. (1998). “Effects of sampler design on tube sampling disturbance- Numerical and analytical investigations.” Géotechnique, 48(6,), pp. 847-867.

Clayton, C., Mathews, M.C. and Simons. N.E. (1995). “Site Investigation.” 2nd Edition, Department of Civil Engineering, University of Surrey.

Clayton, C..R., Hight, D.W., and Hopper, R.J (1992). “Progressive destructuring of Bothkennar clay: Implications for sampling and reconsolidation procedures Géotechnique, 42(2), pp. 219-239.

Clayton, C. R., Khatrush, S., Bica, A. and Siddique, A. (1989). "The use of Hall effect semiconductors in geotechnical instrumentation." ASTM Geotechnical Testing Journal 12(1): 69-76.

Connolly, T. and Kuwano, J. (1999). “Shear stiffness anisotropy measured by multi-directional bender element transducers.” Pre-failure Deformation Characteristics of Geomaterials: Proc, of 2nd International Symposium on Pre-Failure Deformation Characteristics of Geomaterials: Torino 99: Torino, Italy 28-30 September, 1999, Vol. 1: 205 CRC Press.

Collins, I.F. and Hounsby, G.T. (1997). “Application of thermo mechanical principles to the modelling of geotechnical materials.” Proceedings of the Royal Society London, A: Mathematical, Physical and Engineering Sciences, Vol. 453, pp. 1975-2001. The Royal Society.

Cornwell, J.W. and Morse J.C. (1987). “Analysis and distribution of iron sulphide minerals in recent anoxic marine sediments.” Marine Chemistry, 22(1), pp.55-69.

Comina, C., Foti, S. Musso, G. and Romero, E. (2008). “EIT Oedometer: An advanced cell to monitor spatial and time variability in soil with electrical and seismic measurements.” Geotechnical Testing Journal, 31(5): pp. 1-9.

Crice, D. (2002). “Borehole shear-wave surveys for engineering site investigations.” Sartoga,CA:Geostuff. www.geomatrix.co.uk/tools/applicationnotes/Shearwaves.pdf.

Cruse, T.A. and Rizzo, F.J. (1968). “A direct formulation and numerical solution of the general transient elastodynamic problem.” Journal of Mathematical Analysis and Applications, 22, pp. 244-259.

Darendeli, M. B. (2001).”Development of a new family of normalised modulus reduction and material damping curves”. PhD Thesis, University of Texas, Austin, USA.

Dawd, S. & Trygg, R. (2013). “FE analyses of horizontal deformations due to excavation processes in deep layers of soft Gothenburg clay.” Master Thesis 2013:80. Chalmers University of Technology,Gothenburg, Sweden.

DeGroot, D.J., Lunne, T., Sheahan, T.C. and Ryan, R.M. (2003). “Experience with down hole block sampling in soft clays.” Proc. 12th Pan-American Conference on Soil Mechanics and Geotechnical Engineering, Boston, USA, pp. 521-526.

Dobry, R. (1991). “Soil properties and earthquake ground response.” Proc. of Offshore Technology Conference, Soil Mechanics and Foundation Engineering’s Association, Florencia, Italy.

Dobry, R and Vucetic, M. (1987). “Dynamic properties and seismic response of soft clay deposits.” Proc. of International symposium on geotechnical engineering of soft soils, Ciuad de Mexico, Agosto, Vol. 2, pp. 49-85.

Donohue, S., Long, M., L’Heureux, J. S., Solberg, I. L., Sauvin, G. Römoen, M. Kalscheuer, T., Bastani, M., Persson, L., Lecomte, I. and O’Connor, P. (2014). “Use of geophysics for sensitive clay investigations.” Advances in Natural and Technological Hazards Research; 36, Landslides in Sensitive clays. From Geosciences to Risk Management, Springer, pp. 159-178.

Donohue, S., Long, M., O'Connor, P. Eide Helle, T., Pfaffhuber, A., Rømoen, M. (2012). "Multi-method geophysical mapping of quick clay." Near Surface Geophysics, 10(3), pp. 207-219.

Donohue, S and Long, M. (2010). "Assessment of sample quality in soft clay using shear wave velocity and suction measurements." Géotechnique, 60(11), pp. 883-889.

Donohue, S. and Long, M. (2008). "Assessment of an MASW approach incorporating discrete particle modelling." Journal of Environmental & Engineering Geophysics 13(2): pp. 57-68.

Donohue, S. (2005). "Assessment of sample disturbance in soft clay using shear wave velocity and suction measurements." PhD Thesis, University College Dublin.

Donohue, S., M. Long, P. O'Connor and K. Gavin (2004). "Use of multichannel analysis of surface waves in determining Gmax for soft clay." Proceedings of the 2nd International. Conference on Geotechnical Site Characterisation, ISC, Vol. 2, pp. 459-466.

Doran, I.G., Sivakumar, V. Graham, J. and Johnson, A. (2000). "Estimation of in situ stresses using anisotropic elasticity and suction measurements." Géotechnique, 50(2), pp. 189-196.

Dorman, J. and Ewing, M. (1962). "Numerical inversion of seismic surface wave dispersion data and crust-mantle structure in the New York-Pennsylvania area." Journal of Geophysical Research 67(13), pp. 5227-5241.

Drnevich, V.P. and Massarsch, K. R. (1979). "Sample disturbance and stress-strain behaviour." Journal of Geotechnical and Geoenvironmental Engineering, ASCE, Vol. 105. No. GT9, pp. 1001-1016.

Drnevich, V., Hardin, B. and Shippy, D. (1978). "Modulus and damping of soils by the resonant column method." Dynamic Geotechnical Testing, ASTM STP 654, pp. 91-125.

Dyvik, R. and Madshus, C. (1985). "Lab measurements of Gmax using bender elements." Annual Convention on advances in the art of testing soils under cyclic conditions, ASCE, Detroit, Michigan, pp. 186-196.

Eide, H. T. (2015). "On shear wave velocity testing in clay." MSc Thesis, Norwegian University of Science and Technology, Department of Civil and Transport Engineering, NTNU, Trondheim.

Emdal, A. Gylland, A., Amundsen, H.A. Kåsin, K. and Long, M. (2016)." Mini-block sampler." Canadian Geotechnical Journal, 53(8), pp. 1235-1245.

Fellenius, B. (1955). Resultat från pålprovningar vid Göteborg C. Geotechnical Department, Swedish State Railways, Bulletin No. 5, Sweden. (In Swedish)

Fonseca, A.V., Ferreira, C., Fahey, M. (2009). "A framework interpreting bender element tests, combining time-domain and frequency-domain methods." Geotechnical Testing Journal, 32(2),

Freden, C. (1986). "Quaternary marine deposits in the region of Uddevalla and Lake Vänern." Sveriges Geologiska Undersökning, rapporter och meddelanden 46.

GDS Advanced Digital Controller Handbook (2000)

Gens, A. (1982). "Stress-strain and strength characteristics of a low plasticity clay, PhD Thesis, University of London, London, UK.

Ghose, R. (2012). "A microelectromechanical system digital 3C array seismic cone penetrometer". Geophysics, 77(3), pp. 99-107.

Ghose, R. and Goudswaard, J. (2004)."Integrating S-wave seismic-reflection data and cone penetration test data using a multiangle multiscale approach." Geophysics, 69(2), pp. 440-459.

Goto, S., Tatsuoka, F. Shibuya, S. Kim, Y.S., Sato, T. (1991). "A simple gauge for local small strain measurements in the laboratory" Soils and Foundations, 31(1), pp. 169-180.

Graham, J. and Lau, S. L. –K. (1998). "Influence of stress-release disturbance, storage, and reconsolidation procedures on the shear behaviour of reconstituted underwater clay." Géotechnique, 38(2), pp. 279-300.

Greening, P. D. & Nash, D. F. T. (2004). "Frequency domain determination of G_0 using bender elements." Geotechnical Testing Journal, 27(3), pp. 288–294.

Greening, P.D., Nash, D.F.T., Benahmed, N. Viana da Fonseca, A. and Ferreira, C. (2003) "Comparison of shear wave velocity measurements in different materials using time and frequency domain techniques, " Proc. of Deformation Characteristics of Geomaterials, Lyon, France, 22-24 September, Balkema, Rotterdam, pp. 381-386.

Grimstad, G. (2009) "Development of effective stress based anisotropic models for soft clays." PhD Thesis, Norwegian University of Science and Technology, Trondheim.

Hamblin, A.P. (1981). "Filter-paper method for routine measurement of field water potential." Journal of Hydrology, 53, pp. 355-360.

Hansbo, S. and Sellgren, E. (1980). "Deep excavation in soft, highly plastic clay: Performance and possibility of prediction." Väg och vattenbyggaren, No. 7-8, Mälartryckeriet, AB, Stockholm.

Hardin, B. O. and Black, W. l. (1968). "Vibration modulus of normally consolidated clay." Journal of Soil Mechanics and Foundations, ASCE, 94(2), pp. 353-369.

Hardin, B. O. and Drnevich, V. P. (1972). "Shear modulus and damping in soils." Journal of the Soil Mechanics and Foundations, 98(7): part 1 pp. 603-624, part 2 pp. 667-692.

Heisey, J., K. Stokoe II, W. Hudson and A. Meyer (1982). "Determination of in situ shear-wave velocity from spectral analysis of surface waves: Research Report No. 256-2." Centre for Transportation Research, University of Texas at Austin, December.

Henriksson, M. and Carlsten, P. (1994) "The effect of storage time of samples taken with the standard piston sampler." Varia 430, Swedish Geotechnical Institute (In Swedish).

Heymann, G. and Clayton, C.R.I. (1999). "Block sampling of soil: some practical considerations". In: Wardle, Blight and Fourie (Editors), Geotechnics for Developing Africa. Balkema, Rotterdam, pp. 331 - 339.

Hight, D.W. (2003), "Sampling effects in soft clay: An update on Ladd and Lambe (1963)." American Society of Civil Engineers, ASCE, Geotechnical Special Publication 119, pp. 86-121.

Hight D.W and Leroueil, S. (2003). "Characterization of soils for engineering purposes." Proc. of International workshop on characterization and engineering. properties of natural soils, Singapore, (1), pp. 255-360.

Hight, D.W. (2000). "Sampling effects in soft clay: an update". Proc. of 4th. International Geotechnical Conference, Cairo, Egypt.

Hight, D. W. (1998). "Soil characterisation: the importance of structure, anisotropy and natural variability". 38th Rankine Lecture.

Hight D.W and Higgins, K.G. (1994). "An approach to the prediction of ground movements in engineering practice: background and application." Proc. International symposium on pre-failure deformation characteristics of geomaterials –Measurement and application, Sapporo, Japan, (2), pp. 909-945.

Hight, D.W., Boese, R., Butcher, A.P., Clayton, C.R.I., and Smith, P.R (1992). "Disturbance of the Bothkennar clay prior to laboratory testing." Géotechnique, 42(2), pp.199-217.

Holm, G. and Holtz, R.D. (1977). "A study of large diameter piston samplers." Proc. of 9th International Conference on Soil Mechanics and Foundation Engineering, pp. 73-78.

Houlsby, G.T. (2000). "Critical state models and small strain stiffness." Proceedings of the Booker memorial symposium: Developments in theoretical geomechanics, pp. 295-312.

Hvorslev, M.J (1949). "Subsurface exploration and sampling of soils for civil engineering purposes". Report on a research project of the Committee on Sampling and Testing. Soil Mechanics and Foundation Division, American Society of Civil Engineers. Vicksburg, MS: waterways Experiment Station.

Idriss, I.M. (1990). "Response of soft soil sites during earthquakes." Proc. Of Bolton Seed Memorial Symposium, 2(4), University of California, Berkley.

Idriss, I.M., Dobry, R. and Singh, R.D. (1978). "Nonlinear behaviour of soft clays during cyclic loading." ASCE, Geotechnical Engineering Division Journal, GT12, Vol. 104, pp. 1427-1447.

Ismail, A., Stumpf, A., Anderson, N. and Dey, W. (2012). "Comparing shear wave velocity measurements from MASW and down hole seismic methods." 25th Symposium on the Application of Geophysics to Engineering & Environmental Problems. Tucson, Arizona, USA 25-29 March:196

Ishibashi, I. and Zhang, X. (1993). "Unified dynamic shear moduli and damping ratios of sand and clay." Soils and Foundations, 33(1), pp. 182-191.

Jakobson, B. (1954). "Influence of sampler type and testing method on shear strength of clay samples." SGI Proceedings 8, Swedish Geotechnical Institute, Stockholm.

Jamiolkowski, M. Lancellotta, R, Lo Presti, D.C.F. (1994)."Remarks on the stiffness of small strains of six Italian clays." In: Shibuya, S., Mitachi, T., Miura, S. (Eds.), Pre-failure Deformation of Geomaterials, Vol. 2, A.A. Balkema, pp. 817-836.

Jardine, R. (1995). "One perspective of the pre-failure deformation characteristics of some geomaterials." Proc. of the International Symposium on pre-failure deformation of geomaterials, 12-14 September 1994, Sapporo, Japan, Vol. 2, pp. 855-885.

Jardine, R. (1992). "Some observations on the kinematic nature of soil stiffness." Soils and Foundations, 32(2), pp.111-124.

Jardine,, R.J., St-John, H.D., Hight, D.W. & Potts, D.M. (1991). "Some practical applications of a non-linear ground model." Proc. of 10th European Conference on Soil Mechanics and Foundation Engineering., Florence, Italy, Vol. 1, pp. 223-228.

Jardine, R.J., Potts, D.M., Fourie, A.B. and Burland, J.B. (1986). "Studies of the influence of non-linear stress-strain characteristics in soil structure interaction." Géotechnique, 36(3), pp. 377-396.

Jardine, R., M. Symes and J. Burland (1984). "The measurement of soil stiffness in the triaxial apparatus." Géotechnique, 34(3), pp.323-340.

Jendeby, L. (1986) "Friction piled foundations in soft clay: A study of load transfer and settlements". PhD Thesis, Chalmers University of Technology, Gothenburg, Sweden.

Jensen, J.B., Bennike, O., Witkowski, A., Lemke, W. & Kuijpers, A. (1999). "Early Holocene history of the South Western Baltic Sea: the Ancylus Lake stage." Boreas 29, pp. 437–453.

Johanson, B. and Jendeby, L. (1998). “Portrycksökningar till följd av pålslagning och dess betydelser för stabilitet.” Rapport B 1998:4, Chalmers Technical University, Gothenburg, Sweden. (In Swedish)

Jones, R. (1958). "In-situ measurement of the dynamic properties of soil by vibration methods." Géotechnique, 8(1), pp.1-21.

Jovićič, V., Coop, M. R. and Simić, M. (1996). “Objective criteria for determining Gmax from bender element test.” Géotechnique, 46(2), pp. 357–362.

Kallstenius, T. (1972). “Secondary mechanical disturbance: Effects in cohesive soil samples.” In: Quality in Soil Sampling, Supplement to the “Proceedings” and Meddelanden” of the Institute, No. 45, Swedish Geotechnical Institute, Svenska Reproduktions AB, Stockholm, pp. 30-39.

Kallstenius, T. (1963). “Studies on clay samples taken with standard piston sampler.” Statens Geotekniska Institut, SGI. Proceedings 21, Stockholm. Ivar Hæggströms boktyckeri AB.

Kallstenius, T. (1958). “Mechanical disturbances in clay samples taken with piston samplers.” Statens Geotekniska Institut, SGI. Proceedings 16, Stockholm. Ivar Hæggströms boktyckeri AB.

Karlsrud and Hermandex – Martinez, F. G., (2013). “Strength and deformation properties of Norwegian clays from laboratory tests on high-quality block samples.” Canadian Geotechnical Journal, 50, pp. 1273 – 1293.

Karlsrud, K. (2003), “Deformation properties for use in geotechnical calculations.” Technical Note 2G-201, Oslo (In Norwegian).

Karlsson, M., Bergström, A. and Dijkstra, J. (2016). “Comparison of the performance of mini-block and piston sampling in high plasticity clay.” Technical report: Chalmers University of Technology, Gothenburg, Sweden.

Karstunen, M. (2013). Modelling rate-dependent behaviour of structured clays. Proc. of Installation effects in geotechnical engineering, Taylor & Francis Group, London, pp. 43-50.

Karstunen, M., Kreen, H., Wheeler, S.J., Koskinen, M. and Zentar, R. (2005). “Effect of anisotropy and destructuration on the behaviour of Murro test embankment.” International Journal of Geomechanics, pp. 87-97.

Kawaguchi, T. Mitachi, T. Shibuya, S. and Sato, S. (2003) “Evaluation of deformation modulus of clay at small strains based on isotropic elasticity.” Proceedings of the 3rd International Symposium on Deformation Characteristics of Geomaterials, Di Benedetto, H., Doanh, T., Geoffroy, H. and Sauzeat, C. (Eds), Lyon, France, Lisse, pp. 211-219.

Kawaguchi, T., T. Mitachi and S. Shibuya (2001). “Evaluation of shear wave travel time in laboratory bender element test.” Proceedings of the International conference on soil mechanics and geotechnical engineering, Vol. 1, pp. 155-158, AA Balkema Publishers.

Kennedy, H.K. and Jendeby, L. (2004). “Deformation due to deep excavation in soft clay- comparison of calculated and measured movement.” Proc. of the Nordic geotechnical meeting, NGM XIV, Ystad, Sweden, pp. 101-111. (In Swedish)

KGS (2015). Kansas Geotechnical Society website,
(http://www.kgs.ku.edu/software/surfseis/downl.html)

Kilpatrick, W.M., and Khan, A.J. (1984). “The reaction of clays to sampling stress relief.” Géotechnique, 36(4), pp.511-525.

Kimura, T. and Saitch, K. (1982). “The influence of disturbance due to sample preparation on the undrained strength of saturated cohesive soil.” Soils and

Foundations, 22(4), Japanese Society of Soil Mechanics and Foundation Engineering, pp. 109-120.

Klingberg, F., Påsse, T. and Levander, J. (2006). "Bottenförhållanden och geologisk utveckling i Göta älv." Geological Survey of Sweden report K43, Uppsala. (In Swedish)

Kullingsjö, A. (2007). "Effects of deep excavations in soft clay on the immediate surroundings-Analysis of the possibility to predict deformations and reactions against the retaining system", PhD Thesis, Chalmers University of Technology, Gothenburg, Sweden.

Kuwano, R., Connolly, T.M. and Kuwano, J. (1999). "Shear stiffness anisotropy measured in multi-directional bender element transducers." Pre-Failure Deformation Characteristics of Geomaterials, Jamiolkowski, Lancelotta and Lo Presti (Eds), Balkema, Rotterdam, Vol. 1, pp. 205-212.

Lacasse, S. Nadim, F. and Høeg, K. (2003). "Risk assessment in soil and rock engineering." Proceedings of Soil and Rock America, Pan-American Conference on Soil Mechanics and Geotechnical Engineering, Cambridge, Mass, USA, Vol. 2, pp. 2743-2750.

Ladd, C. C and DeGroot, D.J (2003). Arthur Casagrande Lecture: Recommended Practice for Soft Ground Site Characterization, in Proc. of the 12th Pan American Conference on Soil Mechanics and Geotechnical Engineering, Massachusetts.

Ladd, C.C and Foot, R. (1974), "New design procedure for stability of soft clays. " Journal of Geotechnical Engineering, Div., ASCE, 100(GT7), pp. 763-786.

Ladd, C.C and & Lambe, T.W. (1963). "The strength of undisturbed clay determined from undrained tests. "Symp. Laboratory Shear Testing of Soils, ASTM STP 361, pp. 342-371.

Lai, C.G. and Rix, G.J. (1998). " Simultaneous inversion of Rayleigh phase velocity and attenuation for near-surface site characterization, Georgia Institute of Technology, USA.

Landon, M. M. (2007). "Development of a non-destructive sample quality assessment method for soft clays." PhD Thesis, University of Massachusetts Amherst, Amherst, USA, ProQuest.

Landon, M. DeGroot, D., and Sheahan, T. (2007). "Non-destructive sample quality assessment of shear wave velocity", Journal of geotechnical and geo-environmental engineering, 133(4), pp. 424-432.

Landon, M. M DeGroot, D.J., and Jakubowski, J. (2004) "Comparison of shear wave velocity measured in situ and on block samples of marine clay." Proc. of the 57th Canadian Geotechnical Conference, Canadian Geotechnical Society, Quebec, Canada.

Lanzky, R. & Palmquist, D. (2014). "Sample quality and disturbance in soft marine clay- A comparative study of the effects from using two different sized piston samplers." MSc Thesis, Department of Civil and Environmental Engineering, Chalmers University of Technology, Gothenburg, Sweden.

La Rochelle, P., Leroueil, S., and Tavenas, F. (1986). "Technique for long term storage of samples. " Canadian Geotechnical Journal, 23(4), pp. 602-605.

La Rochelle, P., Sarrailh, J., Tavenas, F., Roy, M., and Leroueil, S. (1981). "Causes of sampling disturbance and design of a new sampler for sensitive soils." Canadian Geotechnical Journal, 18(1), pp. 52-66.

La Rochelle, P., Sarraih, Roy, M. (1976). "Effect of storage and reconsolidation on the properties of champlain clays." In Soil Specimen Preparation for Laboratory Testing, ASTM STP 599, pp. 126-146.

La Rochelle, R. and Lefebvre, G. (1971). " Sampling disturbance in Champlain clays." Sampling of Soil and Rock, ASTM STP 483, pp. 143-163.

Larsson, O., Stevens, R.L. and Klingberg, F. (2007). " The transition from glaciomarine to marine conditions during the last deglaciation in Eastern Skagerrak." Marine Geology 241, Elsevier, pp. 45-61.

Larsson, R. (2011). "Manual for SGI 200mm diameter "Block sampler"-Undisturbed sampling in fine-grained soil." GÄU-delrapport No. 33, Swedish Geotechnical Institute, Linköping, Sweden.

Larsson, R. (2007). "The CPT test. Equipment, testing, evaluation. An in situ method for determination of stratigraphy and properties in soil profiles." SGI Information No. 15, Swedish Geotechnical Institution, Linköping, Sweden.

Larsson, R., Sällförs, G. Bengtsson, P.-E., Alén, C. Bergdahl, U. & Eriksson, L. (2007). "Skjuvhållfasthet-utvärdering I kohesionsjord." Swedish Geotechnical Institute (SGI), Information 3, Reviderad, Linköping. (In Swedish)

Larsson, R. and Mulabdic, M. (1991). "Shear moduli in Scandinavian clays; measurements of initial shear modulus with seismic cones; empirical correlations for the initial shear modulus in clay." Report No. 40, Swedish Geotechnical Institute, Linköping.

Larsson, R. (1989)."Dilatometerförsök- En in-situ metod för bestämning av lagerföljd och egenskaper i jord", SGI Information 10, Linköping, Sweden. (In Swedish)

Larsson, R. (1981)"Far vi några ostörda prover med standardkolvborren? En jamforelse mellan prover tagna med standardkolvborr och Laval-provtagaren." Svenska Geoteknisk Institut, Varia No. 60, Linköping, Sweden. (In Swedish)

Larsson, R. (1977). "Basic behaviour of Scandinavian soft clay." Swedish Geotechnical Institute Report No.4. Linköping, Sweden.

Lee, J.S. and Santamarina, J. C. (2005). "Bender elements: performance and signal interpretation." Journal of Geotechnical and Geoenvironmental Engineering, 131(9), pp.1063-1070.

Lefebvre, G and Poulin, C. (1979). " A new method of sampling in sensitive clay." Canadian Geotechnical Journal, 16(1), pp. 226-233.

Leong, E. C., J. Cahyadi and H. Rahardjo (2009). "Measuring shear and compression wave velocities of soil using bender-extender elements." Canadian Geotechnical Journal, 46(7), pp. 792-812.

Lessard, G. and Mitchell, J.K. (1985). "The causes and effects of aging in quick clays. Canadian Geotechnical Journal, 22(3), pp. 335-346.

Leroueil, S. (1996) Compressibility of clays: fundamental and practical aspects." Journal of Geotechnical Engineering, 122(7), pp. 534-543.

L'Heureux, S. and Long, M. (2015). "SP8- GEODIP: Correlations between shear wave velocity and geotechnical parameters in Norwegian clays." NGI Report 20150020-04-R, Oslo, Norway.

L'Heureux, S. and Kim, Y. (2013). "NIFA-N.6.4.3 Effekt av lagringstid på prøvkvalitet." State of art report, NGI Document number: 20130672. (In Norwegian)

Lind, B. "Skadekostnader i byggprocessen- en litteraturgenomgång". Statens Geotekniska Institut, Varia 642, Linköping, 2012. (In Swedish)

Lings, M., Pennington, D. and Nash, D. (2000). "Anisotropic stiffness parameters and their measurement in a stiff natural clay." Géotechnique 50(2): 109-125.

Lohani, T., Imai, G. and Shibuya, S. (1999). "Determination of shear wave velocity in bender element tests." Earthquake Geotechnical Engineering, pp. 101-106.

Long, M., Quigley, P. and O'Connor, P. (2013). "Undrained strength and stiffness of Irish glacial till from shear wave velocity." Ground Engineering, 46 (11), pp.26-27

Long, M., and Donohue, S. (2010). “Characterization of Norwegian marine clays with combined shear wave velocity and piezocone cone penetration test (CPTU) data.” Canadian Geotechnical Journal, 47(7), 709-718.

Long, M. and Donohue, S. (2007). "In situ shear wave velocity from multichannel analysis of surface waves (MASW) tests at eight Norwegian research sites." Canadian Geotechnical Journal 44(5), pp. 533-544.

Long, M., El Hadj, N and Hagberg, K. (2009). “Quality of conventional fixed piston samples of Norwegian soft clay.” Journal of Geotechnical and Geoenvironmental Engineering, 135(2), pp. 185-198.

Long, M., Lunne, T. and Forsberg, C.F. (2003). “Characterisation and engineering properties of Onsøy clay.” Characterisation and engineering properties of natural soils, 1, Swets and Zeitlinger, Lisse, pp. 395-428.

Long, M., Quigley, P. and O'Connor, P. (2013). “Undrained strength and stiffness of Irish glacial till from shear wave velocity.” Ground Engineering, 46 (11), pp.26-27

Low, H.E., Lunne, T., Andersen, T., Sjursen, K.H., Li, M.A. and Randolph, M.F. (2010). “Estimation of intact and remoulded undrained shear strengths from penetration tests in soft clays.” Géotechnique, 60(11), pp. 843-859.

Lunne, T. (2015). “Discussion in seminar: Sample aging and quality of soft clays.” Norwegian Geotechnical Institute, 17th November, 2014, Oslo, Norway.

Lunne, T., Berre, T., Andersen, K.H. Strandvik, S. and Sjursen, M. (2006). “Effects of sample disturbance and consolidation procedures on measured shear strength of soft marine Norwegian clays”, Canadian Geotechnical Journal, 46, pp. 726-750.

Lunne, T., Berre, T. and Stranvik, S. (1998) “Sample disturbance effects in deep water soil investigations.” Proceedings of Society of Underwater Technology International conference on Offshore site investigations and foundation behaviour: New Frontiers, London, pp. 199-220.

Lunne, T., T. Berre and S. Strandvik (1997). “Sample disturbance effects in soft low plastic Norwegian clay.” Symposium on Recent Developments in Soil and Pavement Mechanics., M. Almeida (ed.), Balkema Rotterdam, pp. 81-102.

Lunne, T., S. Lacasse and N. Rad (1989). State of the art report on in situ testing of soils. Proceedings of XII ICSMFE, Rio de Janeiro, Vol. 4, pp. 2339-2403.

Luo, Y., Xia, J., Liu, J., Liu, Q., & Xu, S. (2007). ”Joint inversion of high-frequency surface waves with fundamental and higher modes. “Journal of Applied Geophysics, 62(4), pp.375-384.

Löfroth, H. (2012). “Sampling in normal and high sensitive clay – a comparison of results from specimens taken with the SGI large-diameter sampler and the standard piston sampler St II.” Varia 637. Swedish Geotechnical Institute. Linköping.

Magnusson, O., Sällfors, G., Larsson, R. (1989). “Ödometerförsök enligt CRS-metoden”. Rapport R44:1989. Statens råd för byggnadsforskning. Stockholm: Svenskt Tryck. (In Swedish.)

Mair, R.J. (1993). “Developments in geotechnical engineering research: Application to tunnels and deep excavations.” Unwin Memorial Lecture 1992, Proc. of the Institution of Civil Engineers-Civil Engineering, 97(1), Thomas Telford, pp. 27-41.

Malehmir, A., Umar Saleem, M. and Bastani, M. (2013). “High resolution reflection seismic investigations of quick clay and associated formations at a landslide scar in southwest Sweden.” Journal of Applied Geophysics, 92, Elsevier, pp. 84-102.

Mancuso, C., Simonelli, A.L. and Vinale, F. (1989). “Numerical analysis on in situ S-wave measurement.” Proc. of 12th International Conference on Soil Mechanics and Foundation Engineering, Rio de Janerio, Brazil, Vol. 1, pp. 277-280.

Marchetti, S. (2012) "The Seismic Dilatometer For In Situ Soil Investigations." Proc. of Indian Geotechnical Conference, December 3-15, 2012, Delhi (Paper No. C312).

Marchetti, S., Monaco, P. Totani, G. and Marchetti, D. (2008). "In situ tests by seismic dilatometer (SDMT)." From Research to Practice in Geotechnical Engineering, ASCE Geotechnical Specialist Publication 18: pp. 292-311.

Marchetti, S., Monaco P., Totani, G. and Calabrese M. (2001). "The Flat Dilatometer Test (DMT) in Soil Investigations." A Report by the ISSMGE Committee TC16. Proc. of IN SITU 2001, International Conference on In situ Measurement of Soil Properties, Bali, Indonesia, May 2001, 41 pp.

Marchetti, S. (1980). "In situ tests by flat dilatometer." Journal of the Geotechnical Engineering Division 106.3, 299-321.

Marek, M. (2010). "Seismik-fånga bergnivån och mycket mer" Session in Temadag: Geofysik för geotekniska tillämpningar i Göteborg, 18 March, 2010, Swedish Geotechnical Society. (In Swedish).

Mataic, I. (2012) Personal Written Communication on "Preparation of reconstituted samples", 27 September 2012, Aalto University, Finland.

Mayne, P.W., Coop, M.R., Springman, S.M., Huang, A.B. and Zornberg, J.G. (2009). "Geomaterial behaviour and testing." Proc. of 17th International Conference on Soil Mechanics and Geotechnical Engineering, M. Hamza et al. (Ed.), IOS Press, pp. 2777-2872.

Mayne, P.W. and Rix, G.J. (1995). "Correlations between shear wave velocity and cone tip resistance in natural clays." Soils and Foundations, 35(2), pp. 107-110.

Mayne, P. W., Schneider, J. A. and Martin, G. K. (1999). "Small-and large-strain soil properties from seismic flat dilatometer tests." Proc. of the 2nd International Symposium on Pre-Failure Deformation Characteristics of Geomaterials, Torino. Vol. 1.

Mayne, P.W. and Kullaway, F. (1982) "Ko-OCR (At rest pressure-Over consolidation Ratio) relationships in soil", ASCE, Geotechnical Engineering Division, Journal 108 (GT6), pp. 851-872.

Mašín, (2005). "A hypoplastic constitutive model for clays." International Journal for Numerical and Analytical Methods in Geomechanics, 29(4), Wiley & Sons, Ltd. pp. 311-366.

Meyerhof, G.G. (1976). "Bearing capacity and settlement of pile foundations." Journal of Geotechnical Engineering, 102, pp.197-228.

Miller, R.D., Xia, J., Park, C.B. and Ivanov, J.M. (1999). "Multichannel analysis of surface waves to map bedrock." The Leading Edge, December 1999, pp. 1392-1396.

Mitchell, J. K. and K. Soga (1976). Fundamentals of Soil Behaviour, Wiley, New York.

Mohsin, A. and D. Airey (2003). "Automating Gmax measurement in triaxial tests." Proc. of Prefailure deformation characteristics of geomaterials, Lyon, France, pp. 73-80.

Nazarian, S. and K. H. Stokoe (1985). "In situ determination of elastic moduli of pavement systems by spectral analysis of surface wave method: practical aspects." Research report 368-1F, Centre for Transportation Research, University of Texas, Austin, USA.

NCC (2012a). "Rapport Geoteknik- Västra Orgeln, Uppsala." Projekterings underlag 2012-07-03, Ref. No. 7178314. (In Swedish)

NCC (2012b). "PM Geoteknik-beskrivning av planerad grundläggning och markarbeten: Kvarntorget, Uppsala." Ref. No. 7178282. (In Swedish)

NGI (2007). "E6 Trondheim- Stjørdal, parsell Trondheim: Blokkprøvetagning og laboratorieundersøkelser. Datarapport. Rapport No. 20071380-1. (In Norwegian)

NGU (2015). “Quaternary geology map.” Norwegian Geological Institute (NGU), digital map. (In Norwegian)

Norconsult (2012) “Rapport Geoteknik, RGeo-Allianshallen, Gränby, Uppsala.” Report No. 102 42 49. (In Swedish)

O’Donovan, J., O’Sullivan, C., Marketos, G. and Wood, D.M. (2015). “Analysis of bender element test interpretation using the discrete element method.” Granular Matter, 17(2), pp.197-216.

Olsson, M. (2013). “On Rate-Dependency of Gothenburg Clay”, PhD thesis, Chalmers University of Technology, Gothenburg, Sweden.

Olsson, M. (2010). “Calculating long-term settlement in soft clays- with special focus on the Gothenburg region.” Licentiate Thesis, Chalmers University of Technology, Gothenburg, Sweden.

Olsson, M., Edstam, T. and Alén, C. (2009). “Some experiences from full scale test embankments on floating lime-cement columns.” Proc. of 2nd International Workshop on Geotechnics of Soft Soils, Glasgow, Scotland. CRC Press/Balkema, pp. 77-86.

Olsson, J. (1925). “Kolvborr, ny typ för upptagning av lerprov.” Teknisk Tidskrift, Väg och vattenbyggnadskonst 55, pp. 13-16. (In Swedish).

Oppenheim, A. V., Schafer, R. W., & Buck, J. R. (1989). Discrete-time Signal Processing (Vol. 2). Englewood Cliffs, NJ: Prentice hall.

Pan, H., Yang, Q. and Pei-Yong, L. (2010). “Direct and indirect measurement of soil suction in the laboratory.” Electronic Journal of Geotechnical Engineering, 15(3), pp. 1-14.

Park, C. B. and R. D. Miller (2008). "Roadside passive multichannel analysis of surface waves (MASW)." Journal of Environmental and Engineering Geophysics, 13(1), pp. 1-11.

Park, C.B., Miller, R.D., Ryden, N., Xia, J. and Ivanov, J. (2005). “Combined use of active and passive surface waves.” Journal of Environmental and Engineering Geophysics, 10(3), pp. 323-334.

Park, C.B., Miller, R.D. and Xia, J. (1999). “Multichannel analysis of surface waves.” Geophysics, 64(3), pp. 800-808.

Park, C.B., Miller, R.D., and Xia, J. (1998). “Imaging dispersion curves of surface waves on multi-channel record.” In SEG Expanded Abstracts, 17(1), pp. 1377-1380.

Pennington, D., Nash, D. and Lings, M. (1997). "Anisotropy of G_0 shear stiffness in Gault Clay." Géotechnique 47(3), pp.391-398.

Persson, J. (2013). “Modelling of an excavation in sensitive soil with strain rate dependency.” MSc Thesis 2013:42, Chalmers Technical University, Gothenburg, Sweden.

Persson, J. (2007). “Hydrogeological methods in geotechnical engineering: applied to settlements caused by underground construction.” PhD Thesis, Chalmers University of Technology, Gothenburg, Sweden.

Persson, J. (2004). "The Unloading Modulus of Soft Soil: A Field and Laboratory Study." Licentiate Thesis. Chalmers University of Technology, Gothenburg, Sweden.

Persson, M. (2014). “Predicting spatial and stratigraphic quick-clay distribution in SW Sweden.” PhD Thesis, Gothenburg University, Gothenburg, Sweden.

Pestana, J.M. and Whittle, A.J. (1999). “Formulation of a unified constitutive model for clays and sands.” International Journal for Numerical and Analytical Methods in Geomechanics, 23, pp. 1215-1243.

Poirer, S.E., DeGroot, D.J. and Sheahan, T.J. (2005). "Measurement of suction in a marine clay as an indicator of sample disturbance." Proc. of the GeoFrontiers Conference, ASCE, Austin, USA.

Potts, D.M. (2003). "Numerical analysis: a virtual dream or practical reality." *Géotechnique*, 53(6), pp. 535-573.

Pusch, R. (1970). "Clay Microstructure", Byggforskningrådet, Dokument D8:1970, Stockholm.

Pusch, R. (1966). "Investigation of clay microstructure by using ultra-thin sections." Supplement to the "Proceedings" and "Meddelanden" of the Institute, No. 15, Swedish Geotechnical Institute, Stockholm.

Quigley, P., M. Long and S. Donohue (2011). "Undrained shear strength and stiffness of Irish glacial tills from shear wave velocity measurements." Geophysical Association of Ireland Seminar on Engineering Geophysics, University of Bath.

Richart, F.E., Hall, J.R. and Woods, R.D. (1970). "Vibrations of Soils and Foundations." Prentice-Hall.

Ridley, A.M., Dineen, K., Burland, J.B. and Vaughan, P.R. (2003). "Soil matrix suction: some examples of its measurement and application in geotechnical engineering." *Géotechnique*, 53(2), pp. 241-253.

Ridley, A.M. and Burland, J.B. (1993). "A new instrument for the measurement of soil moisture suction." *Géotechnique*, 43(2), pp. 321-325.

Rio, J. (2006). "Advances in laboratory geophysics using bender elements." PhD Thesis, University College London, University of London.

Robinson, S. & Brown, M. J. (2013). "Towards a framework for the prediction of installation rate effects", Proc. of the International Conference on Installation Effects in Geotechnical Engineering, ICIEGE 2013. London : CRC Press. pp. 128-134.

Robertson, P. (1990). "Soil classification using the cone penetration test." Canadian Geotechnical Journal, 27(1), pp.151-158.

Rowe, P.W. (1972). "Theoretical meaning and observed values of deformation parameters for soil." In Stress-strain Behaviour of Soils (Ed. Parry, R.H.G.), London:Foulis, pp. 143-194.

Russell, D.A. (2015). "Longitudinal and Transverse Wave Motion." In Acoustics and Vibration Animations, Graduate Program in Acoustics, The Pennsylvania State University, http:/www.acs.psu.edu/Drussell/demos.html.

Rønning, S., Hovem, S.G., Tørum, A., Schram Simonsen, A. and Athanasiu, C. (2009). " Deep excavation in soft, sensitive clay. A case study from Norway." Proc. of the 17th International Conference on Soil Mechanics and Geotechnical Engineering, Alexandria, Egypt.

Sanchez-Salinero, I., Roesset, J. M. and Stokoe, K. H. (1986). "Analytical studies of body wave propagation and attenuation." University of Texas at Austin, Civil Engineering Department, Geotechnical Engineering Report No. GR86-15.

Santagata, M.C. and Germaine, J.T. (2002). "Sampling disturbance effects in normally consolidated clays." Journal of Geotechnical and Geoenvironmental Engineering, 128(12), pp. 997-1006.

Santamarina, J. C. & Fam, M. A. (1997). Discussion: Interpretation of bender element tests. Géotechnique, 47(4), pp. 873–877.

Santos, J.A. and Gomes Correia, A. (2001). "Reference threshold shear strain of soils. Its application to obtain an unique strain-dependent shear modulus curve for soils." Proc. of the 15th International Conference on Soil Mechanics and Geotechnical Engineering, Istanbul, Turkey, AA Balkema, pp. 267-270.

Schanz, T., Vermeer, P. and Bonnier, P. (1999). "The hardening soil model: formulation and verification." Proc. of Plaxis Symposium "Beyond 2000 in Computational Geotechnics", Amsterdam, Balkema, pp. 281–296.

Schmalz, D., La Rochelle, E. and Sheahan, T. (2007). "Development and proof testing of a PC-based bender element system for shear wave measurements in soft soil." Proceedings of the 4th International Symposium on Deformation Characteristics of Geomaterials, Atlanta, USA, pp. 725-732.

Schmidt, B. (1966) "Earth pressures at rest related to stress history." Canadian Geotechnical Journal, 3(4), pp. 239-242.

SGF (2009)."Metodbeskrivning för provtagninng med standardprovtagare, Rapport 1:2009, Linköping:SGF, 2009. (In Swedish)

SGF (1996) "Fälthandbok" Rapport 1, Swedish Geotechnical Society, Linköping:SGF. (In Swedish)

SGI (1996). "Geotekniska skadekostnader och behov av ökad geoteknisk kunskap, Linköping, Statens Geotekniska Institut. (In Swedish).

SGU (2015) "Quaternary Geological Map-Lödöse" Swedish Geological Investigations (SGU), online digital maps (www.sgu.se)

SGU (1966) "Quaternary Geological Map-Uppsala" Swedish Geological Investigations (SGU), online digital maps (www.sgu.se).

Sherwood, D.E. (2011). " Systematic causes for failure of geotechnical works around the world." Proceedings of Grundläggningsdagen 2011: Avmaskerad geoteknik, Stockholm, pp. 47-74.

Shibuya, S. (2000). "Assessing structure of aged natural sedimentary clays." Soils and Foundations, 40(3), pp.1-16.

Shirley, D.J. and Hampton, L.D. (1978). "Shear-wave measurements in laboratory sediments." Journal of the Acoustical Society of America 63(2), pp. 607-613.

Simpson, B. (1992). "Retaining structures: displacement and design." Géotechnique, 42(4), pp. 541-576.

Sivasithamparam, N., Karstunen, M., Bonnier, P. (2015) "Modelling creep behaviour of anisotropic soft soils." Computers and Geotechnics, 69, Elsevier Ltd. pp. 46-57.

Sivasithamparam, N., Kamrat-Pietraszewska, D. and Karstunen, M. (2010). "An anisotropic bubble model for soft clays." Proc. of 7th European Conference on Numerical Methods in Geotechnical Engineering (NUMGEO), Trondheim, Norway, Benz, T., Nordal, S. (Eds.), CRC Press/Balkema:Rotterdam, pp. 21-26.

Skempton, A.W. and Sowa, V.A. (1963). "The behaviour of saturated clays during sampling and testing." Géotechnique, 13, pp. 269-290.

Smith, P.R. (1992). "Properties of high compressibility clays with reference to construction on soft ground." PhD Thesis, University of London, London, UK.

Smith, M. (1989). "Dilatometer tests in soft Swedish clays", MSc Thesis. Chalmers University of Technology, Gothenburg, Sweden.

Stallebrass, S.A. (1990). "Modelling the effect of recent stress history on the deformation of over consolidated soils." PhD Thesis, City University, London, UK.

Stevens, R. (1990). "Proximal and distal glaciomarine deposits in South Western Sweden: contrasts in Sedimentation", Geological Society, London, Special Publications, Vol. 53, pp. 307-316.

Stevens, R., April, R.H. and Wedel, P.O. (1987). "Sediment colour and weathered preglacial sources of Quaternary clays in south-western Sweden." GFF, 109(3), pp. 241-253.

Stokoe, K.H. Joh, S.H. and Woods, R.D. (2004). "Some contributions of insitu geophysical measurements to solving geotechnical engineering problems." Proc. of

the International Conference on Site Characterisation, ISC, Porto, Portugal, Vol. 1, pp.19-22.

Stokoe, K., Hwang, S. Lee, J.-K. and Andrus, R. D. (1995). "Effects of various parameters on the stiffness and damping of soils at small to medium strains." Proc. of the International Symposium on "Pre-failure deformation of geomaterials," 12-14 September 1994, Sapporo, Japan, Vol. 2, pp. 785-816.

Stokoe, K. H., Isenhower, W.M. and Hsu, J. (1980). "Dynamic properties of offshore silty samples." Proc. of the 12th Offshore Technology Conference, Houston, Vol. 2, pp. 289.

Stoke, K.H. and Nazarian, S. (1983). "Effectiveness of ground improvement from spectral analysis of surface waves." Proc. of the 8th European Conference on Soil Mechanics and Foundation Engineering, Helsinki, Finland, AA Balkema Publishers, Netherlands, pp. 91-95.

Sun, J.I., Ramin, G. and Nolton Seed, H. (1988). "Dynamic moduli and damping ratios for cohesive soils." Earthquake Engineering Research Centre, University of California, USA.

Suzuki, A. and Matsushima, T. (2015). "Meso-scale structural characteristics of clay deposit studied by 2D Discrete Element Method." Keynote lecture in Proc. of the International Symposium on Geomechanics from Micro to Macro, Vol. 1, Cambridge, UK, pp. 621-651

Svensson, M. (2001). "Application of the SASW-technique in geotechnical in-situ testing," PhD Thesis, Lund University, Lund, Sweden.

Swedish Committee on Piston Sampling, (1961) "Standard piston sampling" Proceedings no. 19, Swedish Geotechnical Institute, Stockholm, Ivar Hæggströms Boktyckeri AB.

Sällfors, G. (1975). "Preconsolidation pressure of soft, high-plastic clays", PhD Thesis, Chalmers University of Technology, Sweden. Stockholm: Libertryck.

Söderblom, (1969)."Salt in Swedish clays and its importance for quick clay formation: Results from some field and laboratory studies." Swedish Geotechnical Institute Proceedings No.22, Stockholm, Sweden.

Söderblom, (1974). "New lines in quick clay research." Supplement to the "Proceedings" and Meddelanden" of the Institute, No. 55, Swedish Geotechnical Institute, Svenska Reproduktions AB, Stockholm.

Takke Eide, H. (2015). "On shear wave velocity testing in clay." MSc Thesis, Norwegian University of Science and Technology, Department of Civil and Transport Engineering, NTNU, Trondheim.

Tanaka, H. and Tanaka, M. (2006). "Main factors governing residual effective stress for cohesive soils sampled by tube sampling." Soils and Foundations, 46(2), pp. 209-219.

Tanaka, H. (2000). "Sample quality of cohesive soils: lessons from three sites, Ariake, Bothkennar, and Dramme." Soils and foundations, 40(4), pp. 57-74.

Tanaka, H. and Tanaka, M. (1999). "Key factors governing sample quality." Proceedings of the International Symposium on the Characterisation of Soft Marine Clays- Bothkennar, Drammen, Quebec and Ariake Clays," Taylor and Larkin, pp. 57-81.

Tanaka, H., Sharma, P., Tsuchida, T. & Tanaka, M. (1996) "Comparative study on sample quality using several types of samplers", Soils and Foundations, Vol. 36 (2), pp. 57-68,

Terzaghi, K., Peck, R.B. and Mesri, G. (1996). "Soil Mechanics in Engineering Practice." John Wiley & Sons.

Tidfors, M. (1987). “Temperaturens påverkan på leras deformationsegenskaper- en laboratoriestudie.” Licentiatuppstats, Chalmers Technical University, Gothenburg, Sweden. (In Swedish)

TKGEO (2013). Trafikverkets tekniska krav för geokonstruktioner (In Swedish)

Tokimatsu, K., S. Kuwayama and S. Tamura (1991). Liquefaction potential evaluation based on Rayleigh wave investigation and its comparison with field behavior. Second International Conference on Recent Advances in Geotechnical Earthquake Engineering and Soil Dynamics (1991: March 11-15; St. Louis, Missouri), Missouri S&T (formerly the University of Missouri--Rolla).

Torrance, J.K. “Pore water extraction and the effect of sample storage on the pore water chemistry of Leda clay.” Soil Specimen Preparation for Laboratory Testing, ASTM International.

Torstensson, B. A.(1973) ”Kohesionspålar i lös lera: En fältstudie”. Statens Institute för byggforskning, Rapport R38:1973. (In Swedish)

Trafikverket (2013) ”7.1 Markteknisk Undersökningsrapport MUR, Geoteknik.” Project 85423612- Mariaholm Tunnel. (In Swedish)

Trafikverket (2014) ”Tillhör systemhandling 2014-12-01, PM Geotekniska material parametrar, Km 456+900 – 457+800, Station Centralen”, Västlänken document referens: PM F 05-010, 2014. (In Swedish)

Tørum, E. Kirkebø, S. and Athanasiu, C. (2009). “ A numerical study of a deep excavation in soft clay in Norway – Comparison of 2D and 3D FEM analyses.” Proc. of the 17th International Conference on Soil Mechanics and Geotechnical Engineering, Alexandria, Egypt.

Vermeer, P. and Neher, H. (1999). A soft soil model that accounts for creep. Proceedings of the International Symposium “Beyond 2000 in Computational Geotechnics.

Vermeer, P. (1978). “A double hardening model for sand.” Géotechnique, 28(4), pp. 413-433.

Viggiani, G. and Atkinson, J.H. (1995). “Stiffness of fine –grained soil at very small strains.” Géotechnique, 45(2), pp. 249-265.

Vucetic, M. and Dobry, R. (1991). "Effect of soil plasticity on cyclic response." Journal of Geotechnical Engineering, 117(1), pp. 89-107.

Vucetic, M. and Dobry, R. (1988). “Degradation of marine clays under cyclic loading.” Journal of Geotechnical Engineering, 114(2), pp.133-149.

VV (2007). “ Datarapport:Grunnundersøkelser.” E6 Trondheim-Stjørdal, parsell Trondheim, Rapport No. 412380-1. (In Norwegian)

Vägverket (2009). “Väg E45 Göteborg-Trollhattan delen Tingberg-Hönebäck, Objekt Nr. 545303. Rapport Geotekniskt undersökning, Rgeo För nybyggnad av Bro 15-1726-1 och -2 för väg E45 över Gårdaån.” Kontraktshandling 13.4, Dokument 3G130400.doc. (In Swedish).

Wang, Y. H., Lo, K. F., Yan, W. M., & Dong, X. B. (2007). “Measurement biases in the bender element test.” Journal of Geotechnical and Geoenvironmental Engineering,133(5), pp. 564-574.

Wheeler, S.J., Näätänen A., Karstunen, M., Lojander, M. (2003). “An anisotropic elastoplastic model for soft clays.” Canadian Geotechnical Journal, 40(2), pp. 403-418.

Wheeler, S.J., Karstunen, M. and Näätänen, A. (1999). “ Anisotropic hardening model for normally consolidated soft clay.” In the Proc. of 7th International Symposium on Numerical Models in Geomechanics (NUMOG VII), G.N. Pande, S. Pietruszczak and H.F. Schweiger (Ed.)Graz, Balkema, pp. 33-40.

Wohlfarth, B., Björck, S. Possnert, G. Lemdahl, G. Brunnberg, L. Ising, J., Olsson, S. and Svensson, N-O. (1993). "AMS dating Swedish varved clays of the last glacial/interglacial transition and the potential/difficulties of calibrating Late Weichselian "absolute" chronologies." BOREAS 22, pp. 113-128.

Wood, T. (2015). "Re-appraisal of the dilatometer for in-situ assessment of geotechnical properties of Swedish glacio-marine clays."In the Proc. of 3rd International Conference on the Flat Dilatometer, Rome, Italy.

Wood, T. (2014) "Phase 3 – Site Characterization and Sensitivity Analysis: Region City." Research Report 5023021, Chalmers University of Technology, Gothenburg, Sweden.

Wood, T and Kullingsjö, A. (2010). "A review of the design and performance of retaining walls in the Citytunnel project E101, Malmö." Proc. of the 11th International Conference on Piling and Deep Foundations, London.

Wood, T. (2008). "Investigation into installation effects of diaphragm walls." Proc. of Nordic Geotechnical Meeting, NGM, Sandefjord, Norway, pp. 546-554.

Wroth, C.P. (1973). "General theories of earth pressure and deformation." Proceedings of the 5th European Conference on Soil Mechanics and Foundation Engineering, Vol.2, Madrid, Spain, pp. 33-52.

Xia, J., R. D. Miller, C. B. Park and G. Tian (2003). "Inversion of high frequency surface waves with fundamental and higher modes." Journal of Applied Geophysics, 52(1), pp.45-57.

Xia, J., R. D. Miller, C. B. Park, J. A. Hunter, J. B. Harris and J. Ivanov (2002). "Comparing shear-wave velocity profiles inverted from multichannel surface wave with borehole measurements." Soil Dynamics and Earthquake Engineering, 22(3), pp.181-190.

Xia, J., R. D. Miller and C. B. Park (1999). "Estimation of near-surface shear-wave velocity by inversion of Rayleigh waves." Geophysics, 64(3), pp.691-700.

Yamashita, S., T. Kawaguchi, Y. Nakata, T. Mikami, T. Fujiwara and S. Shibuya (2009). "Interpretation of international parallel test on the measurement of Gmax using bender elements." Soils and Foundations 49(4), pp. 631-650.

Yimsiri, S. and Soga, K. (2011). "Cross-anisotropic elastic parameters of two natural stiff clays." Technical Note: Géotechnique,61(9), pp. 809-814.

Zapata-Medina, D.G., Finno, R.J. and Vega-Posada, C.A. (2014). "Stress history and sampling disturbance effects on monotonic and cyclic responses of over consolidated Bootlegger Cove clays." Canadian Geotechnical Journal, 51(6), pp. 599-609.

Åhnberg , H. Larsson, R. (2012) "Strength degradation of clay due to cyclic loadings and enforced deformation." Report 75, Swedish Geotechnical Institute, Linköping, Sweden.

Appendices

Appendix A1

Appendix A1: Empirical assessment of G_0 and degradation (G/G_0)

Numerous empirical assessments can be found in literature using both direct measurements and derived parameters from field and/or laboratory tests. Determination of small strain stiffness from field tests that involve large strains and failure of the soil during penetration such as CPT and DMT tests may be somewhat suspect if single shot:single measurement level has been utilised. Many direct correlations of field test relations with undrained shear strength have been established. Table A1.1 presents some commonly used correlations between small strain shear stiffness and undrained shear strength. These relations should be used as a last resort and only for the ground conditions studied by their authors. Furthermore, it is advised when using these equations that the assessment of undrained shears strength should be made in a similar fashion as the original work to account for the stress path dependency of the undrained shear strength (very case specific).

Table A1.1 Comparison of different correlations based on undrained shear strength for determination of G_0.

Source	Soils	Correlation
Andréasson (1979) (uncorrected shear vane)	High plasticity post glacial soft clays (Gothenburg Area)	$G_0 = 441\tau_V$
Stokoe (1980) (average Su from *CAUC*, *CAUE* & DSS)	Clays	$G_0 = \left(\frac{208}{W_P} + 250\right) Su_{av}$
Larsson & Mulabdic (1991) (corrected shear vane and at some sites Su_{DSS})	High- low plasticity soft clays (Western and central Sweden and Norway)	$G_0 = \left(\frac{208}{I_P} + 250\right) \tau_U$
Larsson & Mulabdic (1991) (corrected shear vane and at some sites Su_{DSS})	Low plastic and varved or otherwise inhomogeneous soils & organic clays	$G_0 = \left(\frac{504}{W_L}\right) \tau_U$ *
Bråten *et al.* (1991) (Su_{DSS})	Medium and low plasticity soft clays (Norway)	$G_0 = \left(\frac{55}{I_P^2} + 325\right) Su_{DSS}$
Long *et al.* (2013) (Su from CAUC tests)	Medium plasticity firm clays (Ireland)	*Eq2.1* with V_s from $Su_{cauc}=0.001V_s^2+0.016V_s+60.8$

Appendix A1

A large number of correlations based on cone penetration tests exist such as those presented by Mayne & Rix (1995). Correlations specific to Scandinavian (Norwegian) clays are presented by Long & Donohue (2010) and L'Heureux & Long (2015) who found better correlation of field and empirical assessments when shear wave velocity correlations were used directly to determine G_0. Two of these correlations are given in *Eq. A1-1* and *Eq. A1-2* while Eq. 2-8 presents the relationship by Hardin & Black (1968).

$$V_S = 1.961 q_t^{0.579} \left(1 + B_q\right)^{1.202}$$

Eq. A1-1

where q_t is the net cone resistance and B_q is the normalised pore water pressure

$$G_0 = 21.5 q_t^{0.79} \left(1 + B_q\right)^{4.59}$$

Eq- A1-2

where q_t is the net cone resistance and B_q is the normalised pore water pressure

$$\frac{G_0}{p_a} = 625 \left(\frac{OCR^{ki}}{0.3 + 0.7 e_0^2} \right) \left(p_a p'\right)^{0.5}$$

Eq. A1-3

where p_a is atmospheric pressure, p' is the mean effective stress, e_0 is the initial void ratio, OCR is the over consolidation ratio and k_i is determined from a hyperbolic curve with respect to plasticity index.

In Sweden the empirical method by Andréasson (1979) is commonly used in high plasticity clays but the relationship by Larsson and Mulabdic (1991) for low plastic and varved or otherwise inhomogeneous clays is incorporated in the current Road Transport Authorities Design Guidelines (advice document), TKGEO (2013) for use in normally and lightly over consolidated clays. Previous TKGEO documents have referred to Andréasson (1979) for high to medium plasticity clays and the relationship derived by Hardin & Black (1968) for low plasticity clays.

There are fewer empirical relationships relating to degradation of shear modulus from small strains, particularly for clays similar to soft Scandinavian structured clays. The work by Hardin & Drnevich (1972) if often used in practice, degradation is dependent on the reference strain γ_r determined using the large strain undrained peak shear strengths, refer to Eq. A1-4 and Eq.A1-5. Within this formulation there is no specific allowance for confining pressure or soil type which is known to affect the shape of the degradation curve significantly. A modified form of this relationship by Santos & Gomes Correia (2001) is incorporated in the

commercial constitutive model Hardening Soil Small (Benz, 2007). It should be noted that the Hardin & Drnevich relationship and variations of it are related to shear strain amplitude and not shear strain per sig.

$$G = \frac{G_0}{1 + \left|\frac{\gamma}{\gamma_r}\right|} \qquad \textit{Eq. A1-4}$$

where γ is the shear strain amplitude and γ_r is the threshold shear strain amplitude defined by:

$$\gamma_r = \frac{\tau_{\max}}{G_0} \qquad \textit{Eq. A1-5}$$

where τ_{max} is the shear stress at failure.

The influence of soil consistency on the stiffness degradation is indicated in Figure A1.1 which is why a number of empirical relationships with respect to plasticity index have been developed, such as Sun *et al.* (1988), Idriss (1990) and Vucetic & Dobry (1991). These formulations fail to take account of the confining stress and it was not until the work by Ishibashi & Zhang (1993) was published that allowance for both soil type and confining pressure could be accounted for empirical determination of the shape of the degradation curve. Since then many different empirical curves have been developed. The work by Darendeli (2001) is of note and consists of a family of normalised degradation curves based on extensive laboratory testing from 20 different sites and from depths of up to several hundred meters. This work took care to identify the factors influencing the shape of the stiffness degradation curves for different soils and from this developed a non-linear four parameter model which considered; reference strain, curvature coefficient, small strain damping ratio and a scaling co-efficient. The model parameters are determined from a family of curves based on statistical analysis of the extensive database. At a specific site use of these curves were shown to capture more realistic behaviour than earlier empirical correlations over a wide range of soil, stress/strain history and confining stresses.

Appendix A1

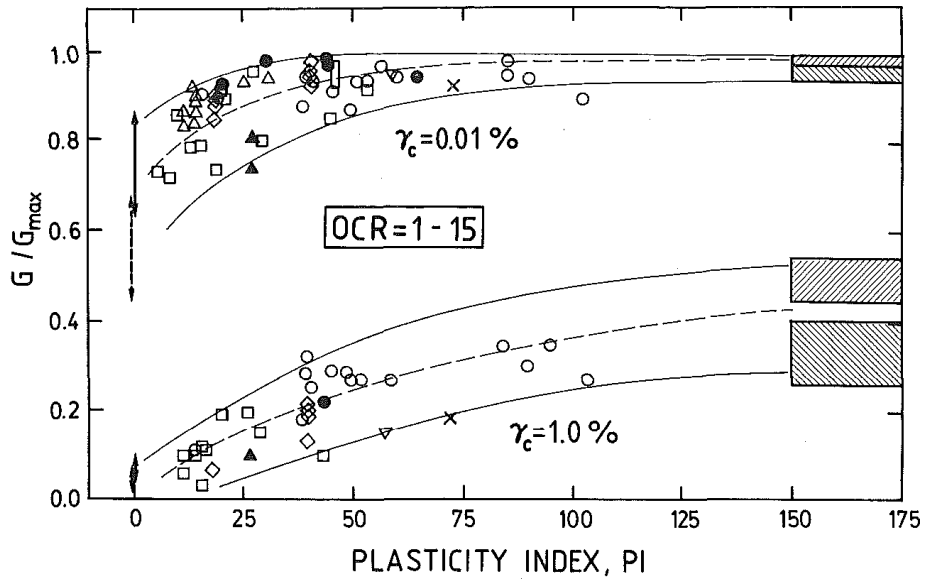

Figure A1.1 Influence of plasticity on degradation G/G_0 of small and medium cyclic strain, Vucetic and Dobry (1991).

Appendix A2

Appendix A2: Drawing of the Swedish standard STII fixed piston tube sampler

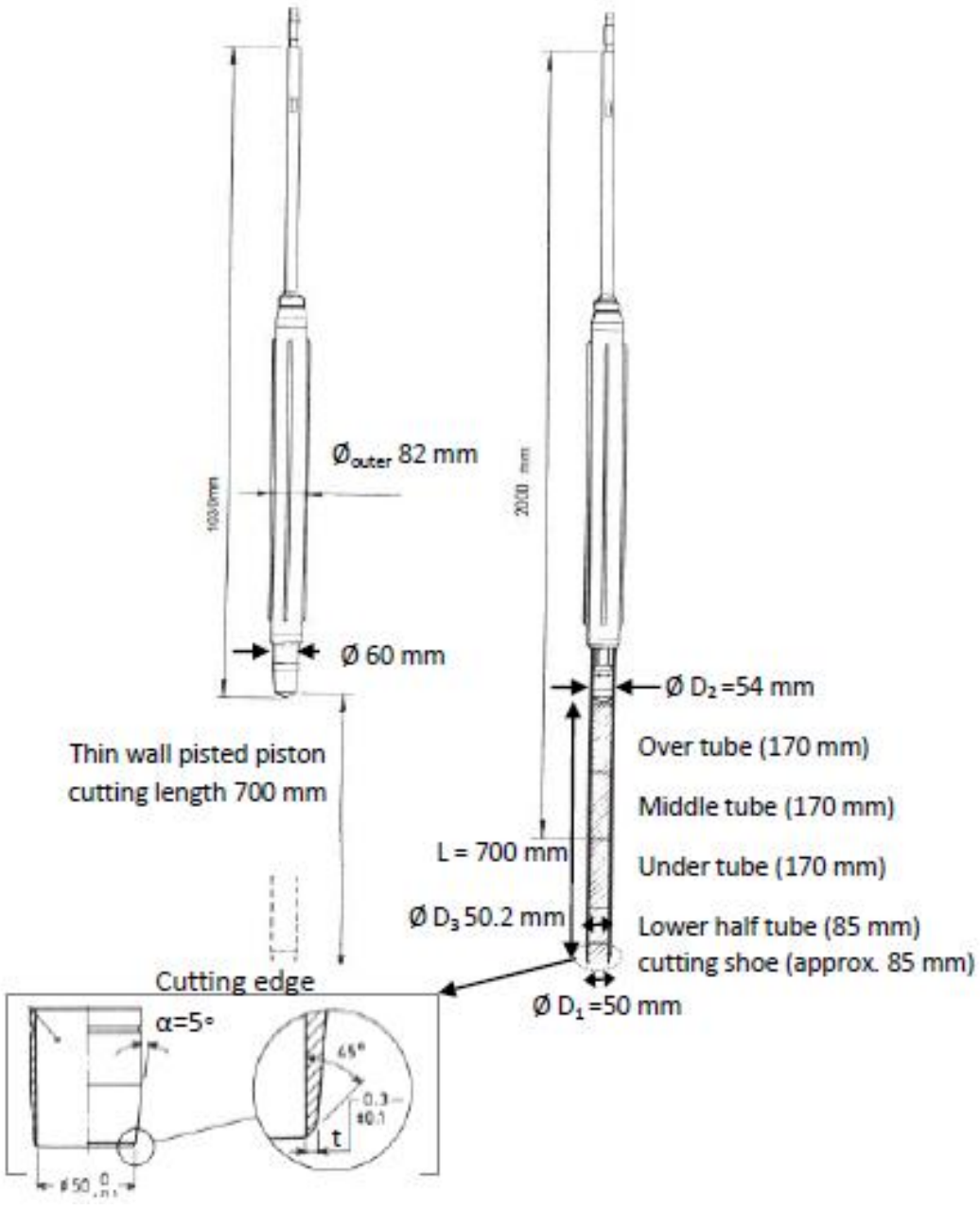

Figure A2.1 Details of the Standard Swedish STII sampler, SGF (2009).

Appendix A3

Appendix A3: Graphical steps in Surfseis (Version 3.0) analysis of MASW tests for 1D and 2D V_S profile

1: Compilation of shot gather (shot at midpoint or array shown here).

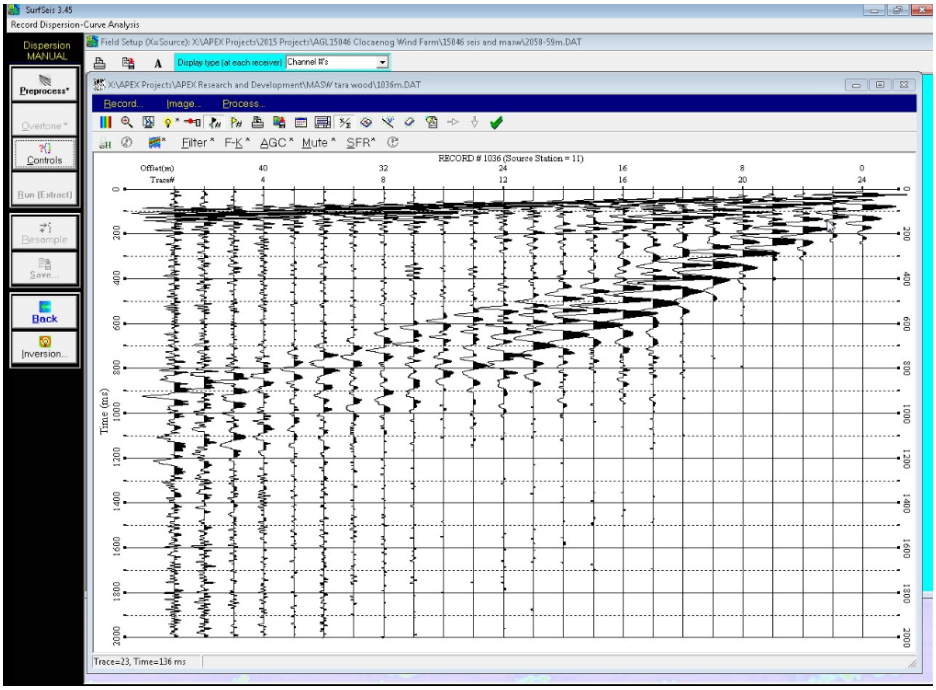

2: Automatic generation of dispersion curve using shot wave fields (soil response in red circle).

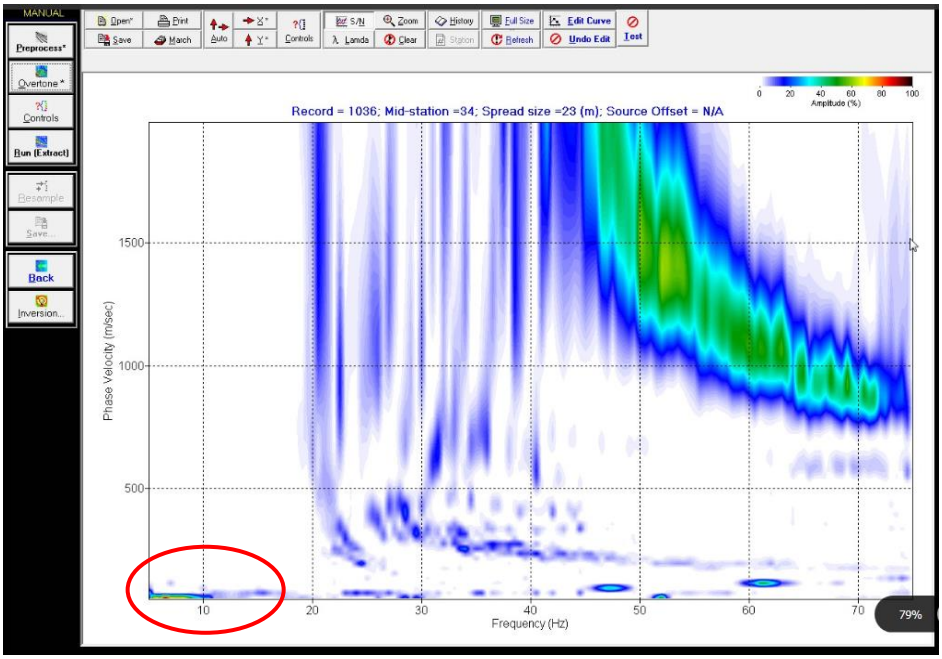

Appendix A3

3: Frequency cut off applied to data, revised dispersion curve.

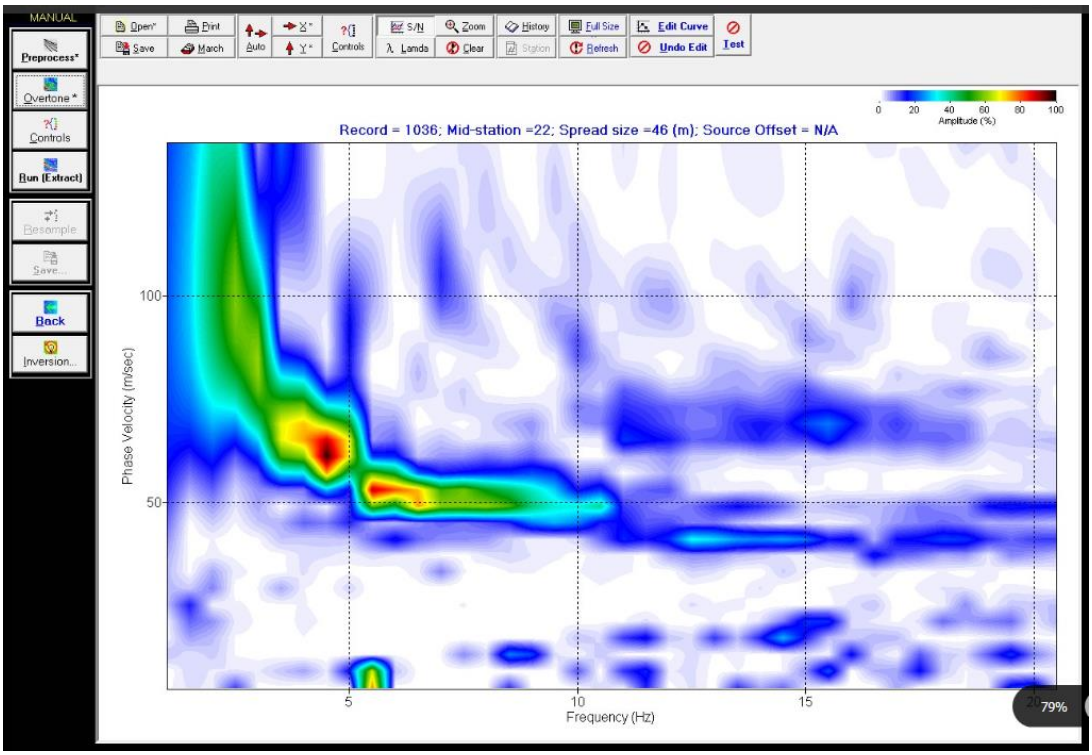

4: Inversion process: Picks applied to determine initial theoretical dispersion curve.

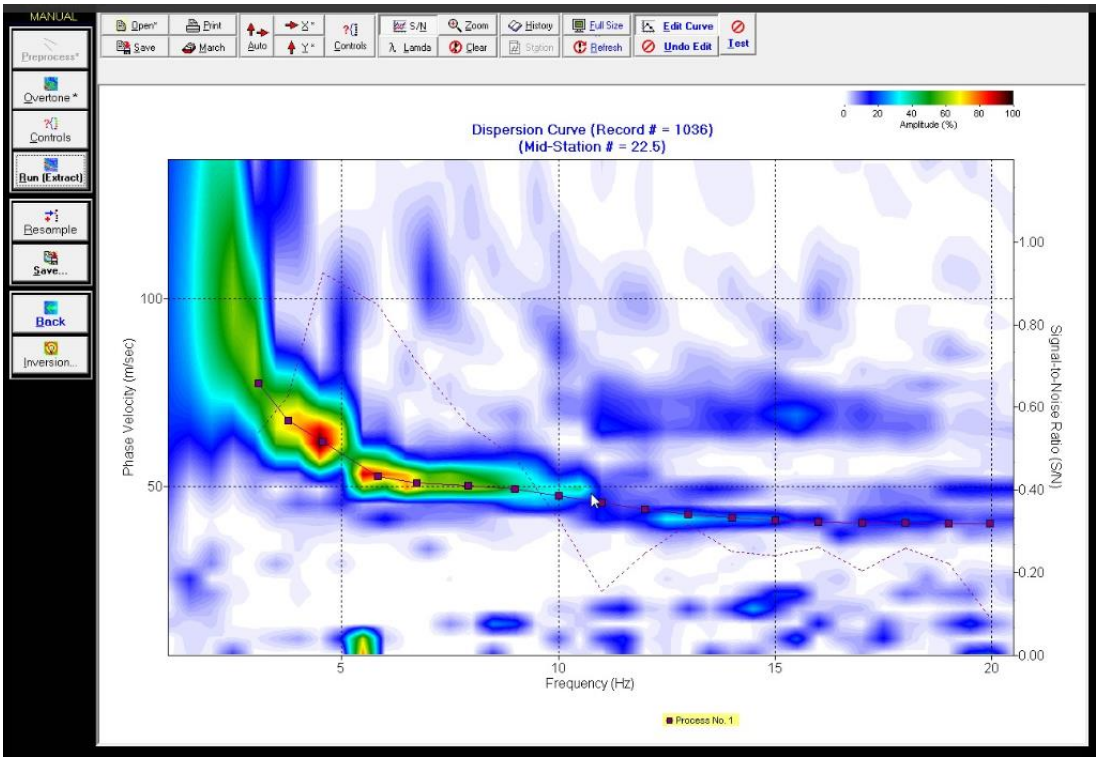

Appendix A3

5: Inversion process: definition of earth model geometry (10 layer model).

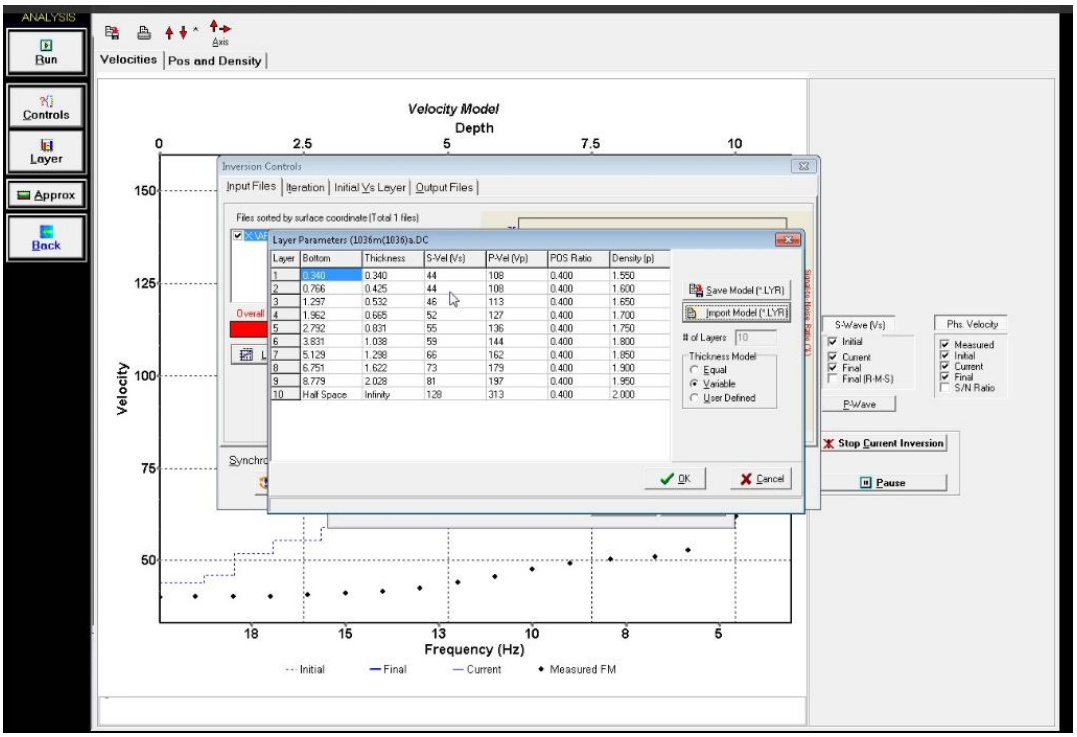

6: Inversion process: Iteration until RMS error reaches specified limit (initial profile shown by dotted line, final match by solid line). After 2 iterations RMS error is 0.94%, 1% was the specified limit.

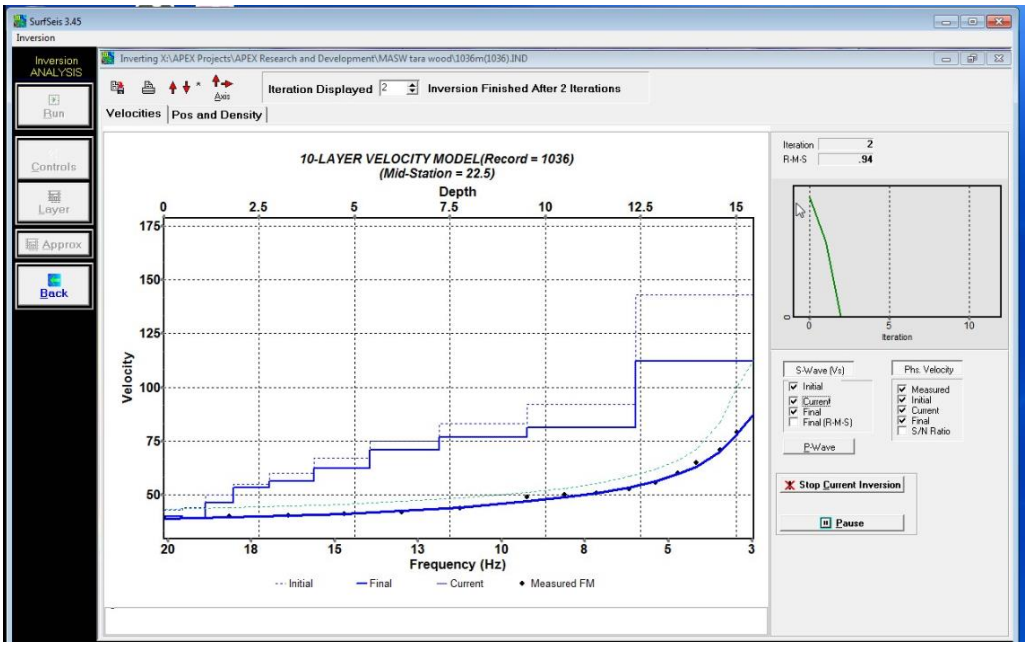

Appendix A3

7: Determination of 2D *Vs* profile within Surfseis, KGS (2015)

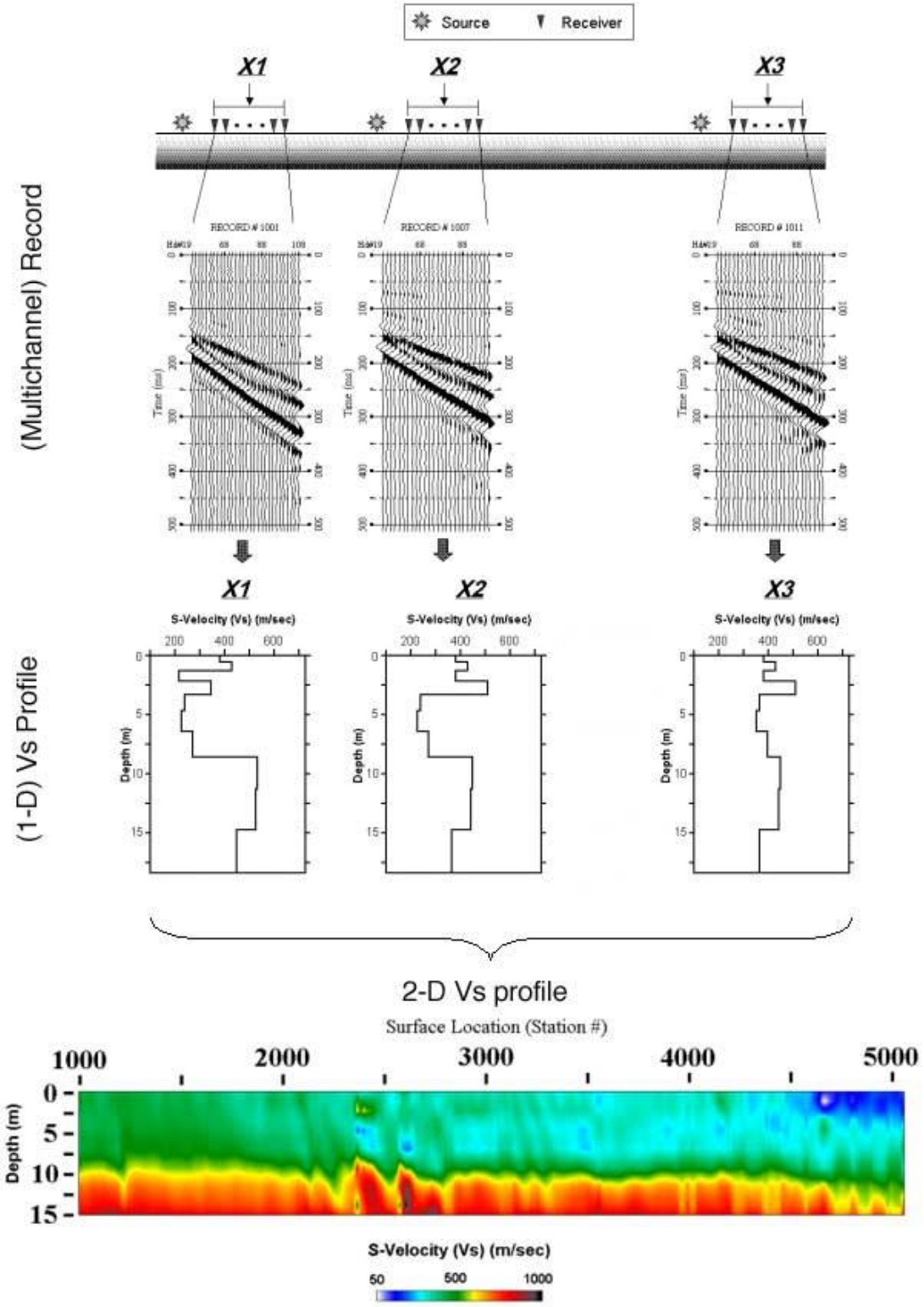

Appendix A4

Appendix A4: Graphical steps in SDMT test and analysis for 1D *Vs* profile

1: Source excitation: SDMT Source excitation with 9 kg swing hammer on beam subjected to downforce from the bore rig .

2: Field acqisition and analysis equipment.

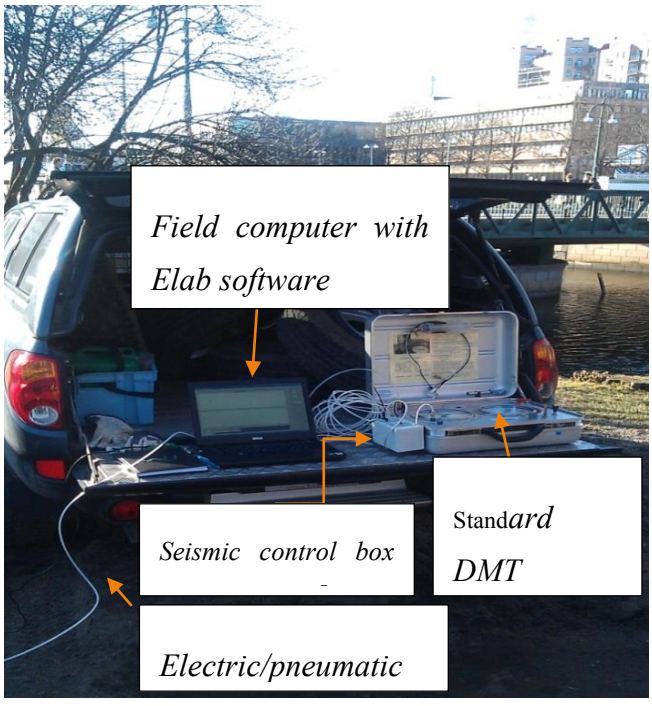

Appendix A4

3: SDMT Elab interface in which acquisition parameters are specified.

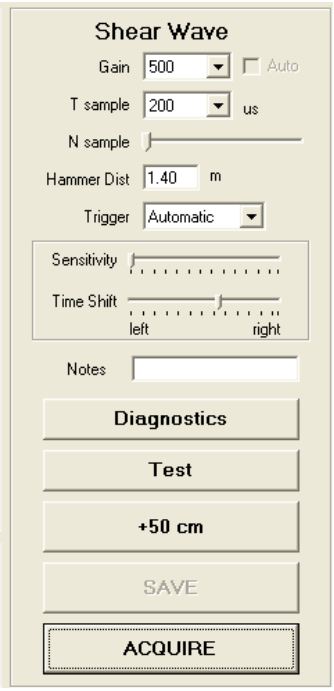

4: A number of different filters can be selected prior to analysis and frequency cut off to clean the signals. The same cut off and filter is applied to both signals.

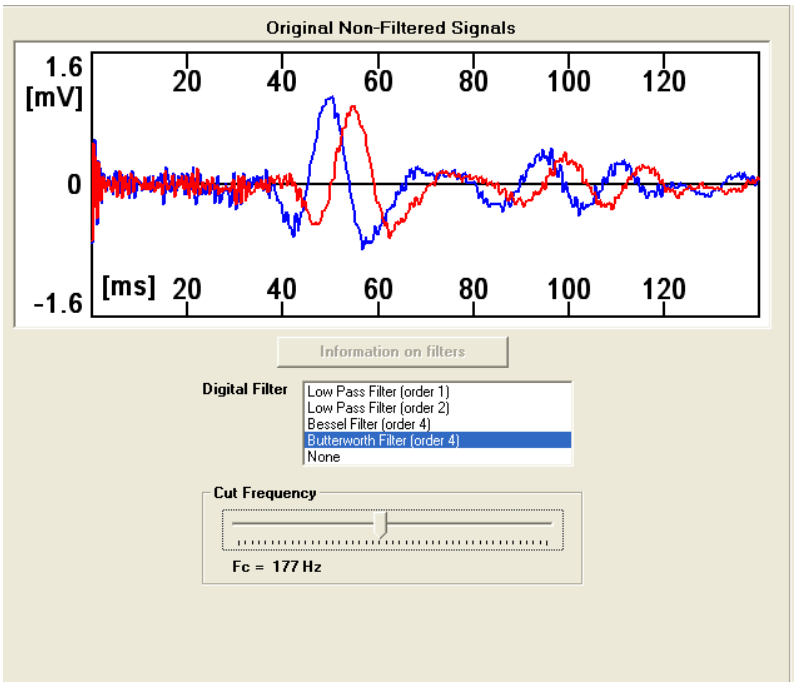

Appendix A4

5: Definition of window for cross correlation (selection shown by dotted lines); this can be defined manually or automatically by the program.

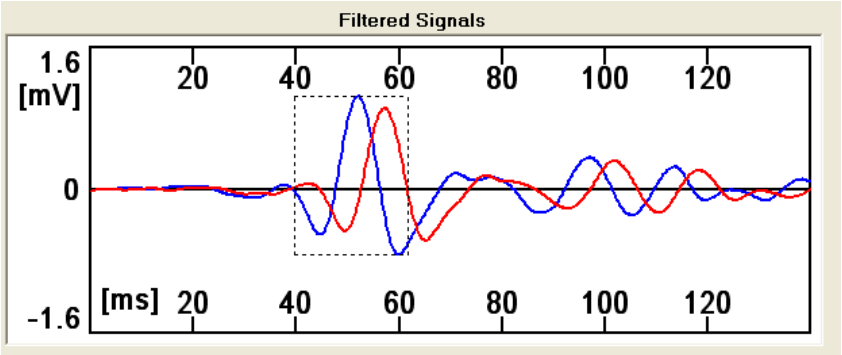

6: Cross correlation is performed and the filtered lower geophone signal replotted with the upper filtered geophone in order to review the V_S interpretation (a good match infers the wave travelling between the upper and lower geophone infers the assumptions used in cross correlation are reasonable (linear, single wave with minimal differences in dispersion/attenuation between the two devices)

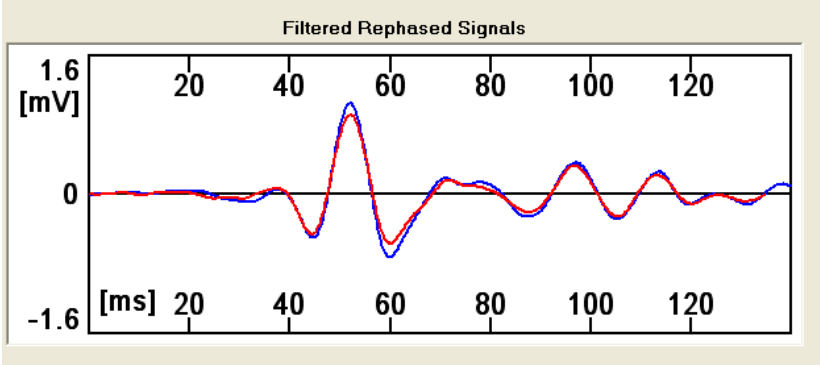

Appendix A4

7: Determination of wave travel distance L from verticality measurements and defined distance of source from the probe at surface level (L is defined as Ds in software).

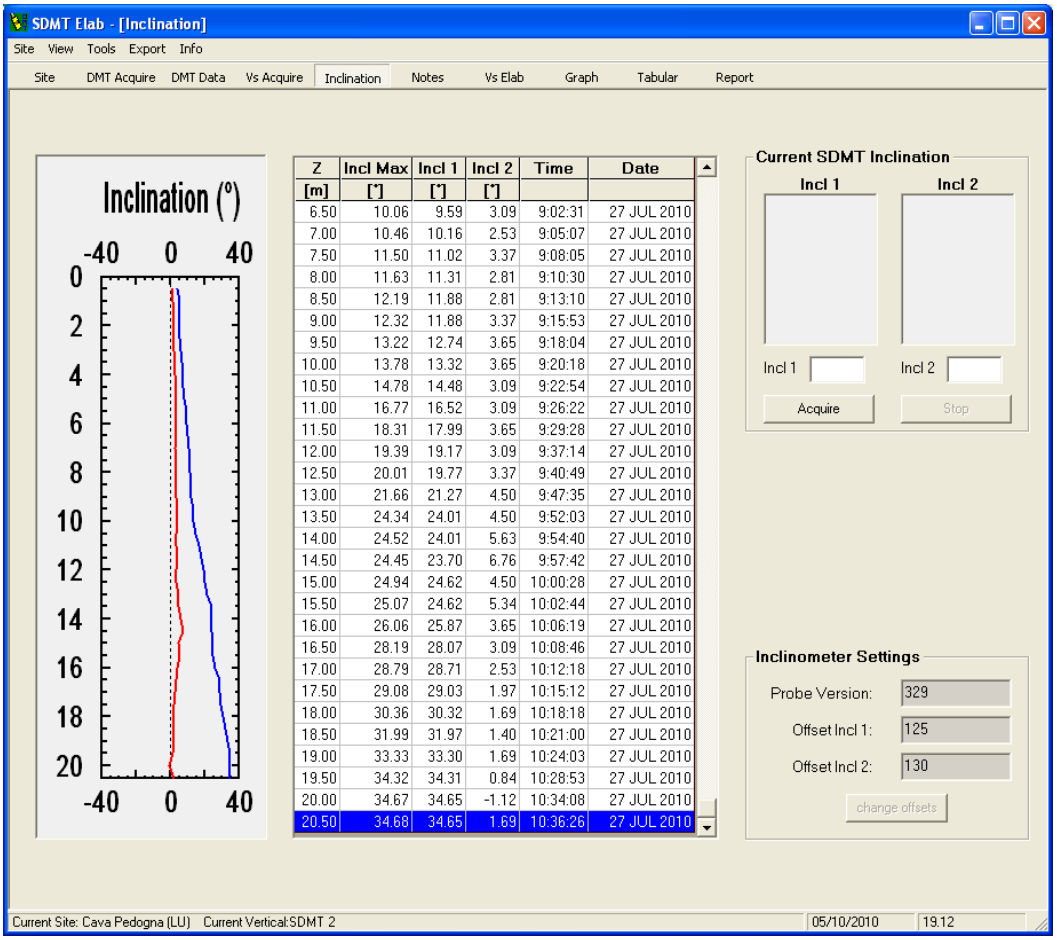

$$V_S = \frac{L}{t_{cc}}$$

8: Determination of V_S based on , from multiple shots saved at each test level is shown, together with variation coefficient for all tests at that level to enable quick review of the sensitivity in *Vs*.

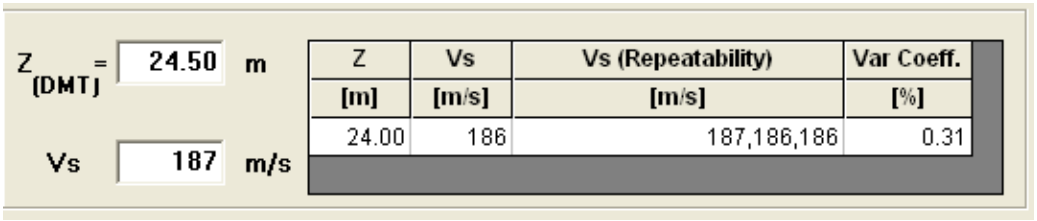

Appendix A4

9: Plot of V_S profile with depth is automatically generated and can be reviewed in the field along with other DMT empirically derived parameters.

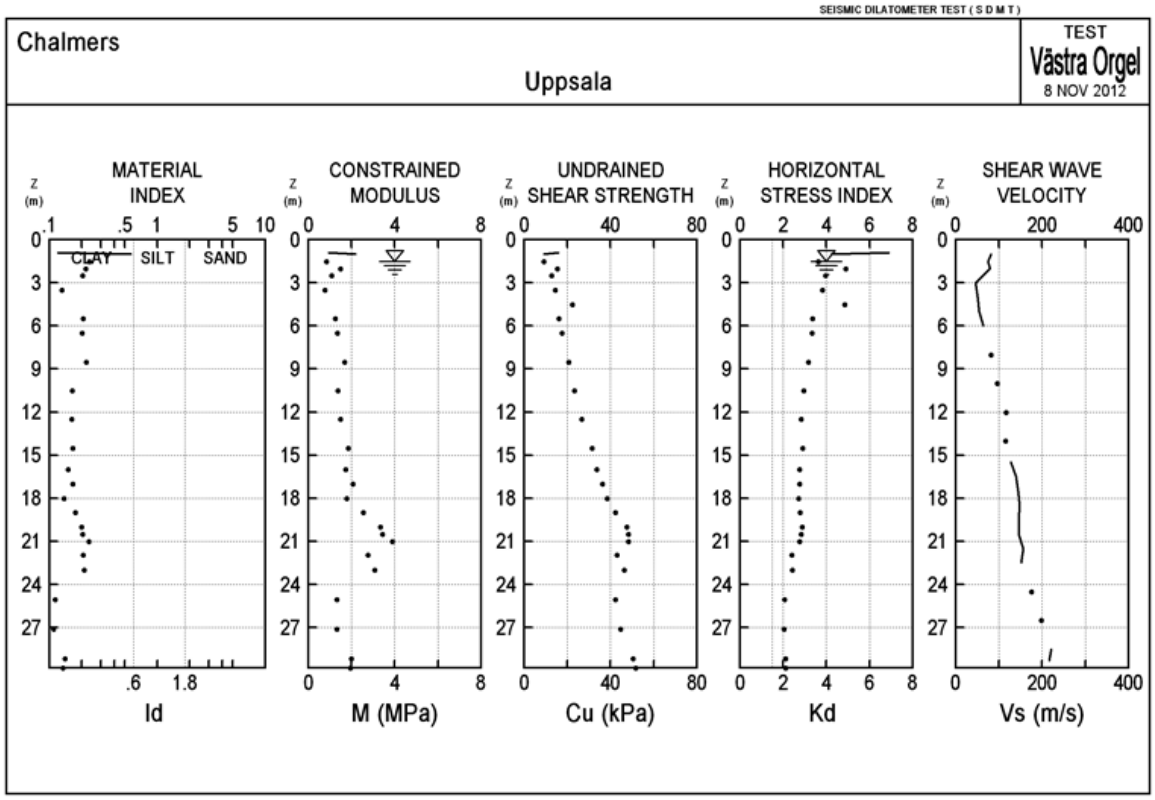

Appendix A5

Appendix A5: SGI BES setups used for validation of CTH and GDS BES system and bench marking results

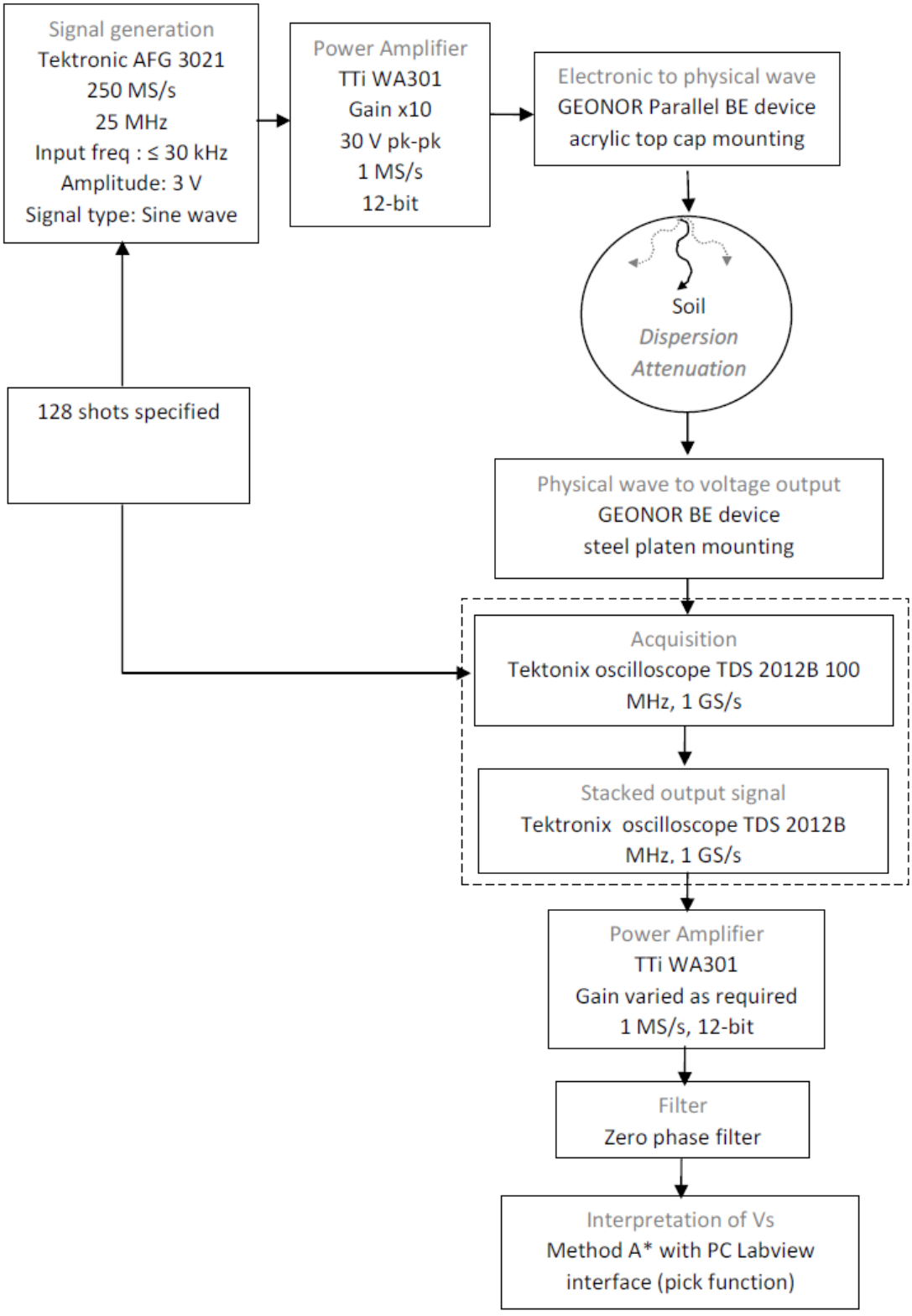

*Figure A5.1 SGI triaxial BES setup used for validation of CTH and GDS BES systems *refer to Figure 3.3.*

Appendix A5

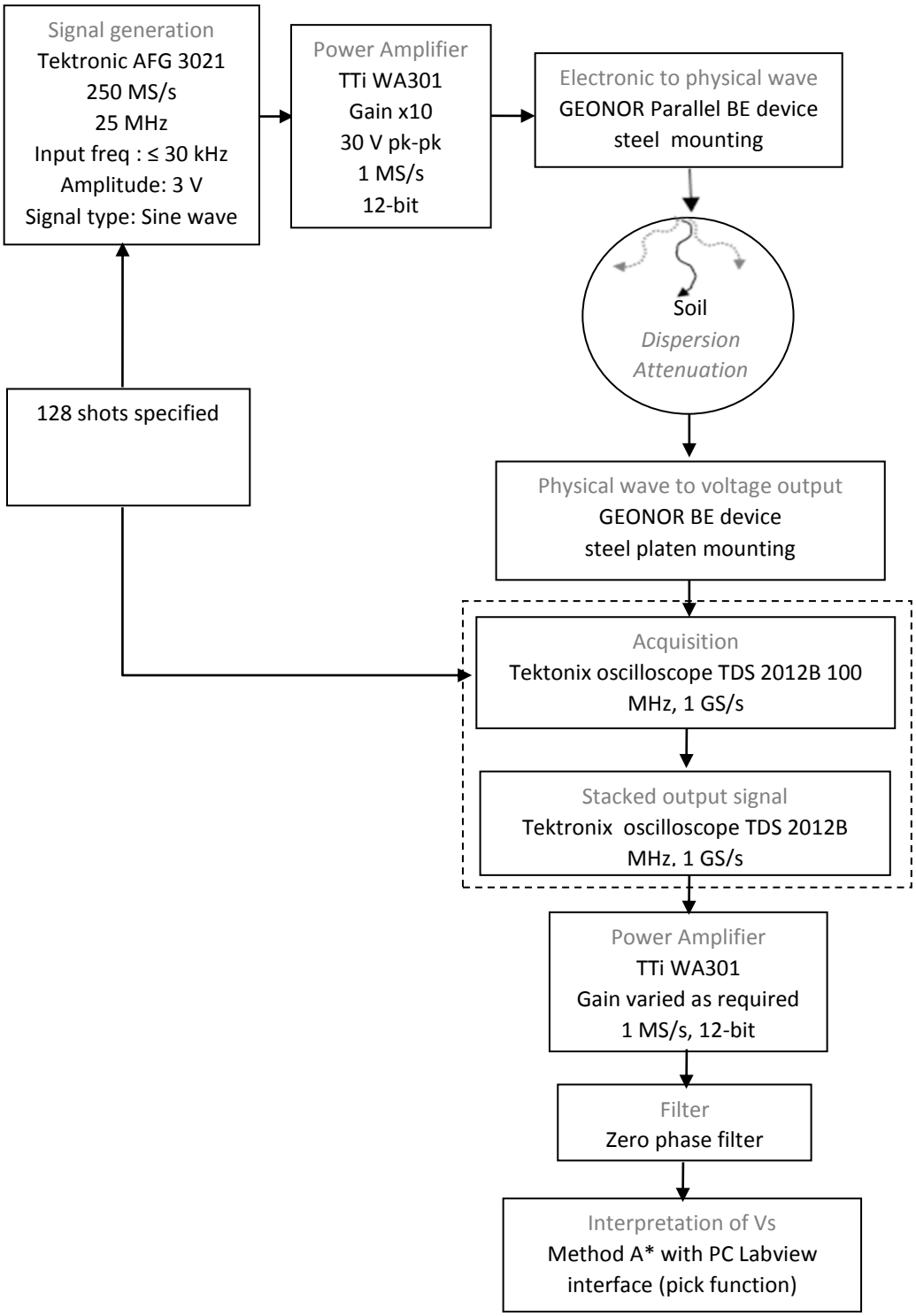

*Figure A5.2: SGI standalone BES setup used for validation of CTH/GDS BES systems, *refer to Figure 3.3.*

Appendix A5

Some results from the bench marking study

The impact of different BES systems on the determination of small strain stiffness using BE testing is exemplified by the results of a bench marking exercise conducted at the Swedish Geotechnical Institute (SGI) in which interpretation of V_{S0vh} using BES tests with 3 different systems in 4 different set ups (SGI systems only vary with respect to the material the BE devices are mounted in). All BES tests were interpreted in the same way using time domain position B. The same test specimen was used, a 3 week old $STII_{slow}$ sample from Site 7 (5 m). The results of the bench marking exercise are presented in Figure A5.3. At low excitation frequencies the differences in the interpreted values of V_{SOvh} are significant however for all but one of these systems the interpreted value of V_{S0vh} was around 42 m/s for high signal input frequencies when the influence of multimodal vibratation is minimised. This is consistent with Viggani and Atkinson (1991), Clayton (2010) and Yamashita *et al.* (2009) amoung others.

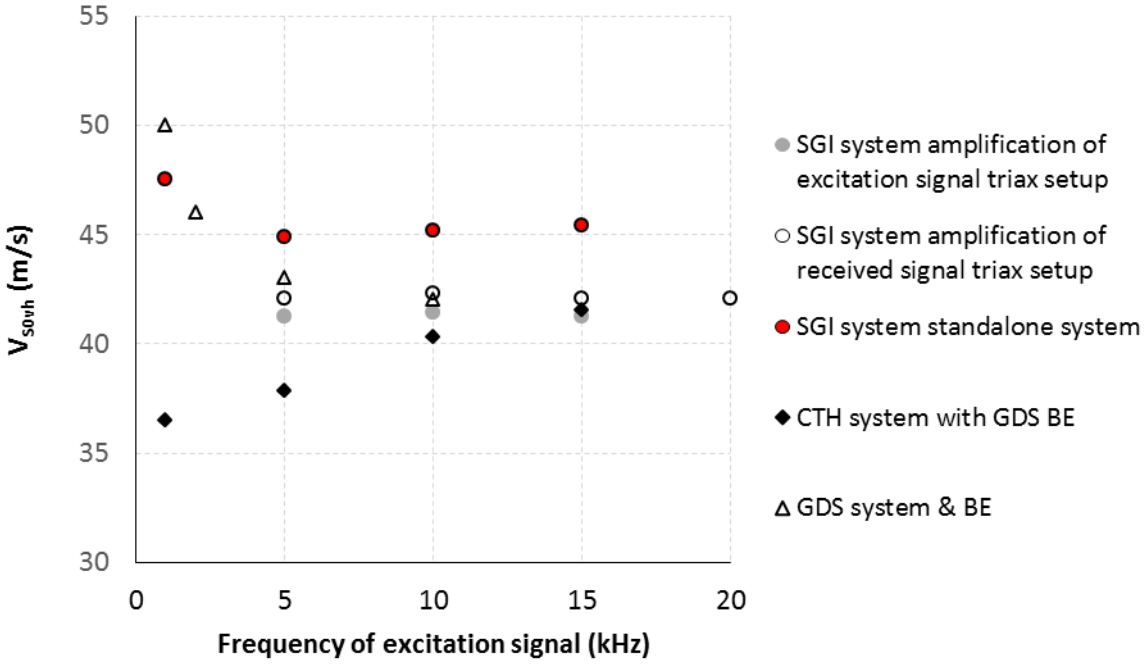

Figure A5.3 Bench marking study on influence on BES system on determination of V_{S0vh}

The CTH system applied signal amplification to the source (excitation) signal whereas the GDS system applied signal amplification to the received signal. When using the SGI triaxial system the effect of signal amplification before and after signal transmission was investigated and it was found that slightly more dispersion/attenuation occurred when the source signal was amplified. Which might partly explain the differences seen in the GDS and CTH systems

together with differences in resolution of these systems. Some form of stiffness non-compliance may exist when using the SGI standalone device in soft clays due to greater flexibility of the acrylic top cap in which the BE source device was embedded hence the slightly higher values of shear wave velocity a higher frequencies.

Appendix A6

Appendix A6: Validation of experimental procedures for stiffness degradation curves

The GDS hall-effect device as described by Clayton *et al.* (1989) was used for measurement of local horizontal deformation. The device was kept in place by use of an uneven spring force of the calliper hinge which sat on the sample using two radiused pads. According to Clayton *et al.* (1989) the repeatability of the device is of the order of 1/100 of a micrometre. Within this project the system (hall-effect transducer, GDS acquisition pad and GDS DCU) was insufficient and did not allow proper control of applied stresses. This is illustrated in Figure A6.1 which shows part of a K_0 triaxial unloading –reloading test conducted within this research. The Hall-effect device appeared to hop between two different values when the system was instructed to keep zero radial strains during drained unloading and reloading cycles and led to very unstable stress paths. For this reason the majority of tests within the research were conducted with the DVRT device which gave better control as shown in Figure A6.2 which is a comparable test (same soil and similar unload-reload loops applied).

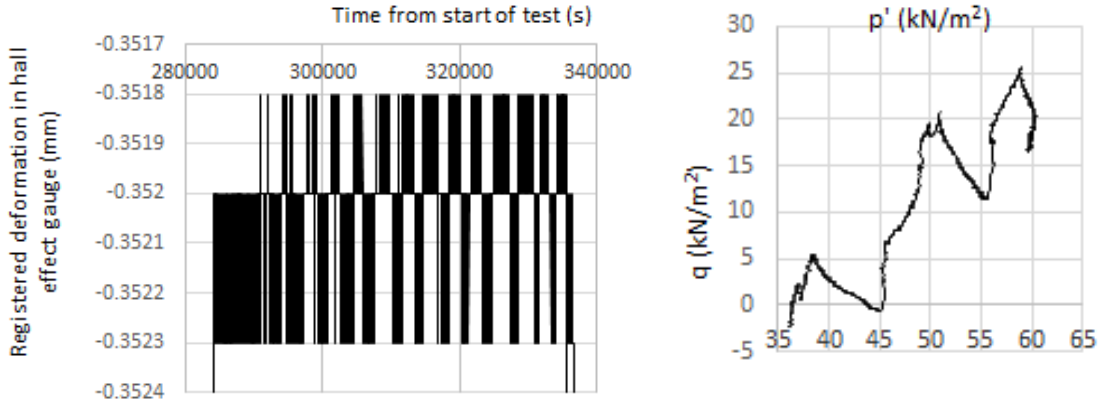

(a) (b)

Figure A6.1 (a) Horizontal deformation in Hall Effect transducer during K_0 reloading (b) ESP during K_0 unloading using automated stress control.

Appendix A6

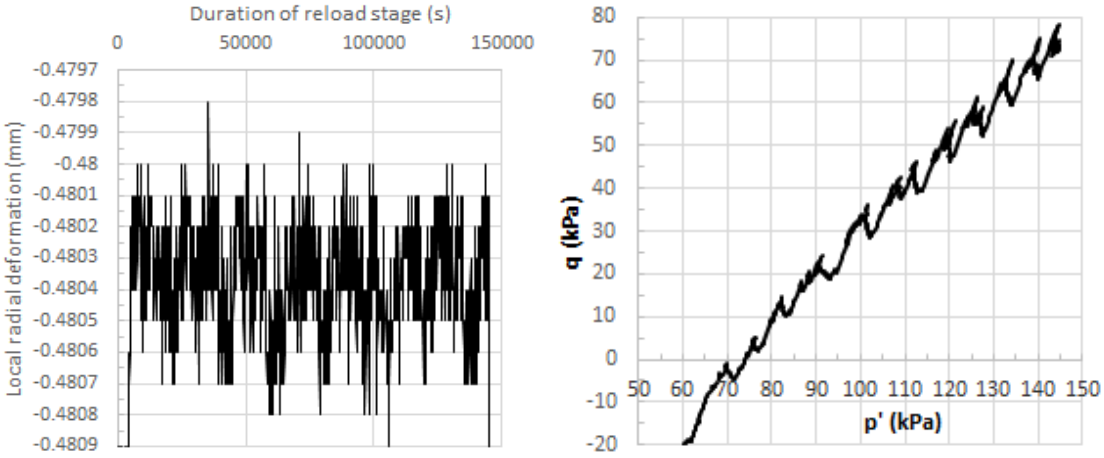

(a) (b)

Figure A6.2 (a) Horizontal deformation in DVRT transducer during K_0 reloading (b) ESP during K_0 reloading using automated stress control.

There is often much focus on the accuracy of strain measurements when discussing stiffness degradation. The magnitude of radial strains during shearing were often small compared to the axial strain for the soils tested so it was primarily the axial strain measurement that influenced the resolution of shear strains determined. A number of comparisons of local and external measurements of vertical strain have been made within this project in the range 0 to 2 % similar to Jardine *et al.* (1984), refer to Figure 2.7. These comparisons were done using two GDS Hall effect vertical strain gauges illustrated in Figure A6.3(b) for the local measurement of axial strain and a linear displacement potentiometer for the external strain measurement (on the upper surface of the top cap). However when comparisons were made between tests with local vertical and external vertical strain measurements and tests with only external measurement a number of issues became apparent and led to the decision not to use the Hall effect local vertical strain devices that were available for the tests in general, these were:

- Data obtained was erratic despite being averaged over the two vertical strain gauges; refer to Figure A6.3 (a).
- Placement of such a device on a soft clay sample appeared to affect the failure mechanism and may therefore effect the observed stiffness degradation.
- The length of the hall-effect device was too long for the 100 mm high samples tested thus measurement was not within the middle third but rather the middle two thirds.

Appendix A6

- The stroke length of the device used (± 3 mm) was less than the magnitude of the reconsolidation strains that could be expected for some samples.

- The general shape of the initial part of the stress strain curve from local and external measurement was fairly similar, particularly if a rolling average of 5 data points was used to smooth the local strain gauge readings. The disparity and shape of the external measurement curve shown by Jardine *et al*. (1984) was not observed.

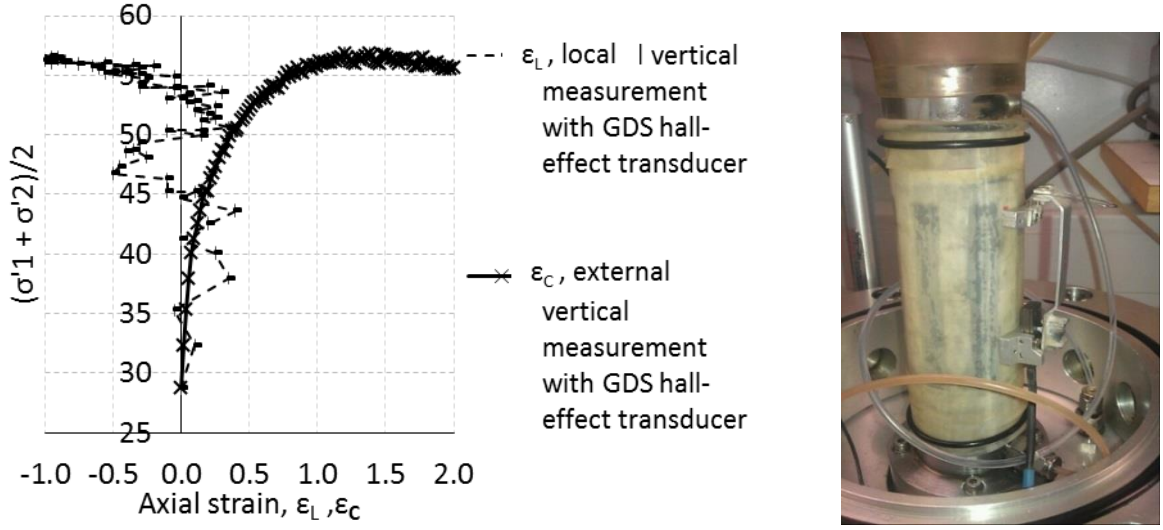

Figure A6.3 (a) Comparison of local vertical strains during shearing using the Hall effect device and external measurement using LVDT (b) 70 mm Hall effect gauge side view

The scatter of the data points in the hall-effect measurements in Figure A6.3 (a) is most likely due to a number of reasons: transducer resolution, resolution of the electrical A/D converter, performance of attachment method, slip and variations in elastic properties of the membrane as discussed by Goto *et al.* (1991) in addition to the device being at the limit of its linear range at the start of shear (deformation occurring during reconsolidation was 3.74 mm). The device is quite clearly designed for stiffer soils (smaller reconsolidation strains) and sample heights of 200 mm, as typical in the UK where the device was developed. Additional DVRT gauges were bought to attempt to create a new local vertical measurement device but a satisfactory way of measuring small strains (10^{-5}) in a sample that might undergo large deformation during reconsolidation (deformations up to 7 mm were observed within this work) with addition deformations of between 0.5 mm and 4 mm before failure could not be found without affecting the behaviour of the sample. It was felt that some form of optical

technique may be a better solution for local strain measurement but development of such a system lay outside the scope of this research.

The similarity of the external measurement curve in Figure A6.3 (a) to the local measurement curve presented by Jardine *et al.* (1984) and given in Figure 2.7(b) is striking. It was felt therefore that many of the issues that often cause differences between local and external measurements (system compliance, bedding errors, tilt of top cap etc.) in the 'relatively' small to medium strain range are not significant for the soils tested within this thesis. This may relate to the way samples were prepared and mounted and their low stiffness relative to the system stiffness. It was therefore decided to proceed with triaxial testing without local vertical strain measurement and accept the loss of data within the small strain range. The shape of the degradation curves obtained for the high quality glacio marine samples within this work compares well with similar tests reported by Long *et al.* (2003) on Onsøy clay which has very similar geological history and index properties to the Swedish west coast clays. Thus it was felt therefore that degradation curves produced during this work would give a reasonable indication of degradation curves for shear and axial strains from around 10^{-4}, despite a lack of vertical local strain measurement except for the few cases where the potential error in shear modulus measurement was high (very soft disturbed samples).

Appendix 7

Appendix A7: Non-destructive sample quality assessment methods

Suction measurements with the Tanaka assessment method

The potential advantage of assessment of sample quality using suction measurements is that these can be used to identify the best samples for more advanced testing, saving money, time and effort on unnecessary testing of disturbed specimens. Reliable suction measurements are difficult to achieve and large variations were noted between indirect measurements (filter paper) and direct methods (suction probe). An overview of all suction measurements can be found in Figure A7.1 (a) together with the "best" quality range given by Tanaka (1996). Many samples had higher relative suctions than typically reported in literature (20% of in-situ vertical stress) thus additional work is required to recalibrate the Tanaka method for these soils. The majority of suction measurements were on the glacio-marine clays. The lacustrine samples desaturated very quickly making the measurements of little value for quality assessment, although extremely high values were a good indicator of desaturation. In most cases the filter paper method gave higher assessments of suction. This may be due to spatial variations of suction within the samples. The probe measures suction at the sample surface, while the filter paper method is indicative of suctions within the sample as a whole.

There are difficulties with both suction measurement methods so no one method is preferred. Suction probe measurements could be used to quickly identify the best samples for testing (taking generally 10 to 20 minutes for equilibrium of the probe) even if this value was likely to be a lower bound for the sample as a whole. However, on the quick clay samples (Site 8) the clay in contact with the probe tended to collapse to a slurry thus only low suction readings were registered if at all. Thus for these samples the filter paper method was preferred even though it took around 14 days to get a result. Filter paper tests prepared in the field gave much lower suction assessments than repeated suction probe measurements at Site 7. It is thought that moisture in the mobile laboratory environment may have affected the filter papers thus are not thought to be indicative of actual matrix suctions. The suction probe was more flexible to use, however, a special lid had to be developed to limit moisture loss during equalisation of the probe. Without this desaturation of the sample occurred, making it difficult to identify the sample suction as opposed to surface desaturation. In Figure A7. 2 the results of suction tests on the glacio marine clays are presented where the marker size reflects the sample depth and the sample origin are indicated. The suctions measured in both block and STII piston samples

are similar. There were, however, consistent differences in the suctions measured in fresh samples at varying piston sample tube position with middle tubes having the greatest suctions. This indicates that middle samples are often the least disturbed, consistent with general assumptions. These differences were often small between middle and lower tube samples when tested quickly (< 2 days from extraction). In some cases suctions reduced with time; an example of which is indicated by the arrow in Figure A7. 2. However, in many cases only small variations with time were noted, this is thought to stem from inaccuracies of the suction measurement methods used. To conclude, the suction measurements were a useful indicator of sample quality, but are not assessed to be a good quantitative method for these clays. Further work specific to this end would be required to give increased confidence in this method, including a better understanding of the magnitude of the maximum relative suctions (u_r/σ'_{V0}) that can be maintained within these clays.

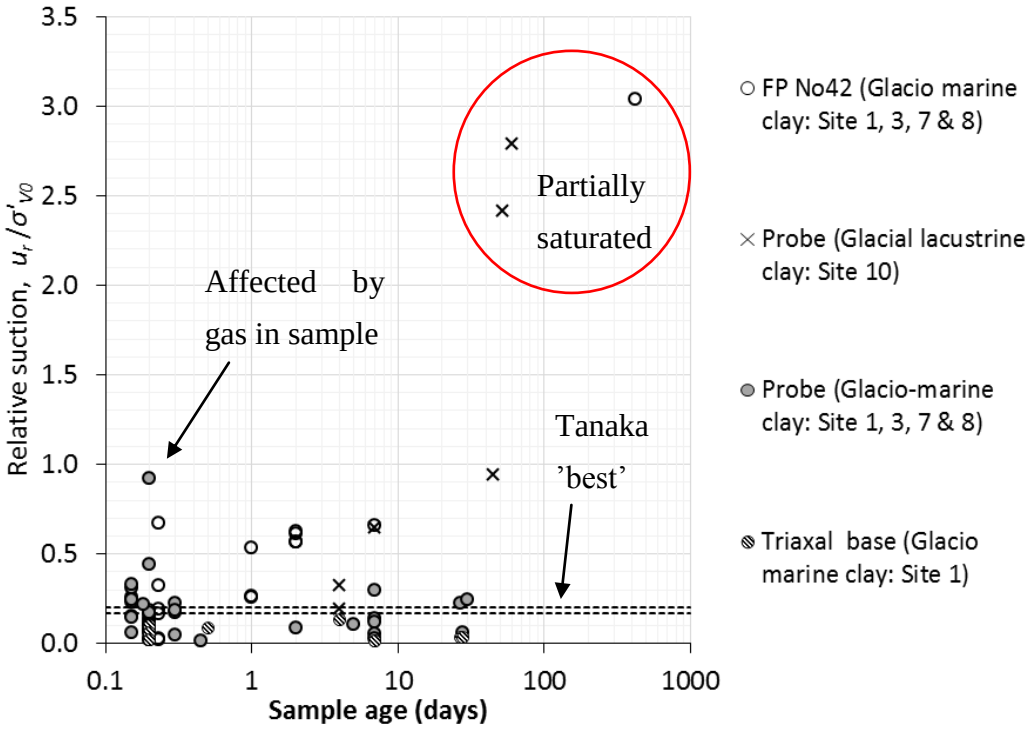

Figure A7. 1 Suction measurement of samples using different methods of measurement and different clays (FP No42 refers to Whatman's 42 filter paper method; Probe refers to high air entry suction probe).

Appendix 7

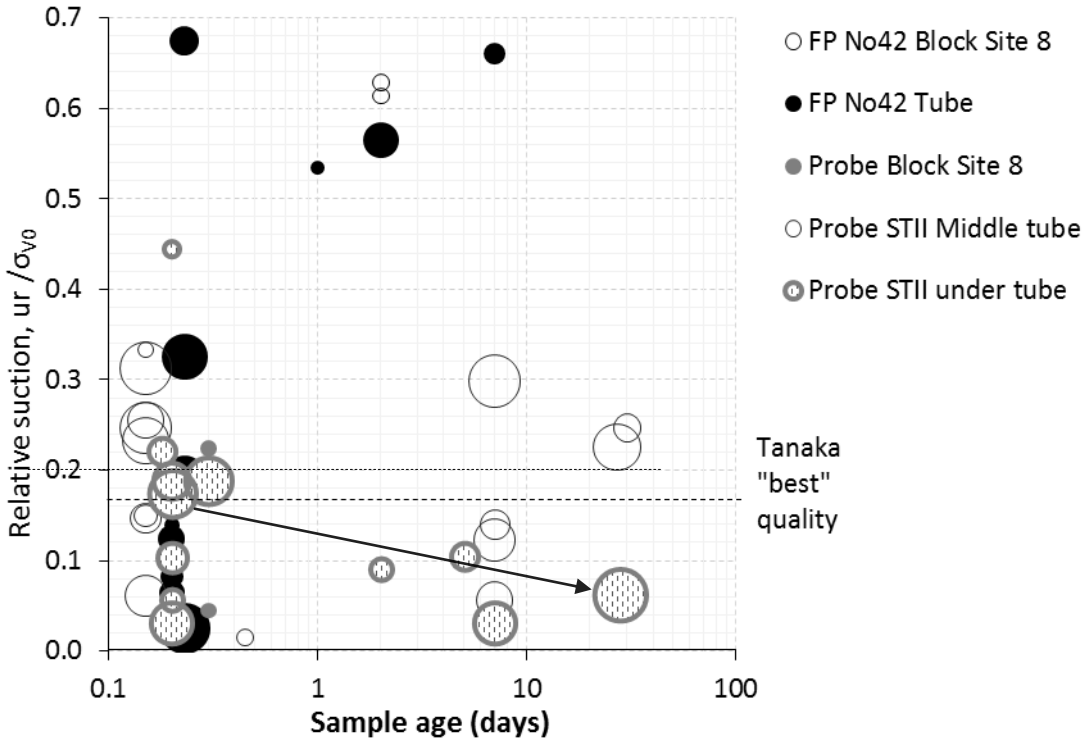

Figure A7. 2 Variation of suction measurements for different methods of sampling with storage time (FP No42 refers to Whatman's 42 filter paper method; Probe refers to high air entry suction probe).

Seismic methods to assess sample quality using the Landon criteria

Discussion on unconfined seismic measurements are covered more fully in Chapter 5, however, in order to assess the suitability of Landon *et al.* (2007) assessment criteria for identifying best sample quality Figure A7. 3 presents results using this method for samples from around the Gothenburg Central station area (Site 1, 2 and 3). There appears to be very little impact of storage time on the assessment of quality using this method. All samples are assessed to be of the highest quality except those from 35 m (where samples were mechanically disturbed during extraction due to a sand layer within the sampled soil profile, refer to also to Table 4.4. This method seems therefore useful in identifying highly disturbed samples but is not able to distinguish between samples of fair to excellent quality in these soils. As with the suction assessments of quality, this seismic method would need to be recalibrated, particularly at large depths where "higher quality" was indicated in conflict with the findings from pore volume change during reconsolidation.

Appendix 7

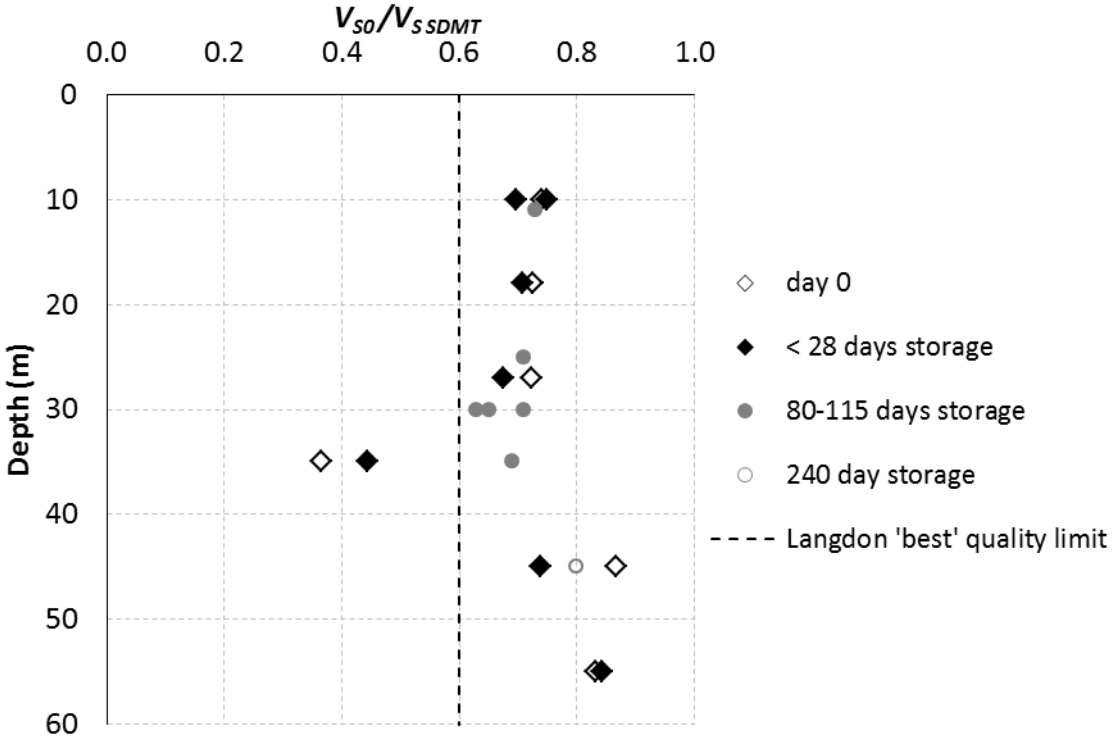

Figure A7. 3 Sample quality assessment using Landon criteria for piston samples from Central station area (Site 1, 2 and 3).

Combined seismic/suction assessment, Donohue & Long (2010) assessment criteria

This assessment method required the most effort, as it required 4 separate measurements, $V_{S\,field}$, V_{S0} and u_r in addition to the shear wave velocity of remoulded samples ($V_{S0\,remoulded}$) for each level that was to be assessed. The magnitude of $V_{S0\,remoulded}$ depends very much on the way the remoulded samples are created. For the clays tested it was not possible to merely remould the clay and then measure V_{S0} as the sample was essentially slurry at this point. Thus remoulded samples had to be allowed to consolidate in sedimentation tubes to a similar void ratio as the natural sample (not possible for highly structured clays, quick clays, varved clays), and to eliminate air, additional water had to be added. Depending on the amount of water added different values of $V_{S0\,remoulded}$ were obtained due to differences in the pore water chemistry (varied by 15% for 50% difference in initial water content of the slurry). The time taken for intrinsic samples to reach similar void ratios (assessed through volume change) to the natural samples was generally between 5 to 9 months but in one case (where the least amount of water had been added) even after 14 months void ratios were still 35% higher than the natural sample. In such cases it is impractical to wait for the correct void ratio of the intrinsic (remoulded) sample. At depth such issues had very little influence on the value of L_{VS}

Appendix 7

however for samples close to the surface (<20 m depth) such variations could easily influence the assessment of quality. The assessment of sample quality for samples extracted from Site 1 using the Donohue & Long (2010) method is presented in *Figure A7. 4* where L_u is based on suction probe measurements and has been normalized for suctions of 30% σ'_{V0} as use of the original 20% σ'_{V0} used by Donohue & Long (2010) leads to negative L_u values. The L_u quality boundaries have therefore been shifted to correspond to the same values of suction as the original calibration.

As to be expected similar trends (and limitations) discussed with the Tanaka and Landon methods are observed. The deepest samples obtained the "best" quality assessment and shallow samples were generally the worst except for the extreme case of the 35 m samples. Middle tube samples tended to be of better quality than lower tube samples consistent with expectations. Of note was the change in the quality of 55 m samples from excellent to poor over a period of storage of 28 days. While this may in part be related to difficulties in obtaining realistic sample suctions, this finding is consistent with other qualitative observations for this sample (touch, sound, sight).

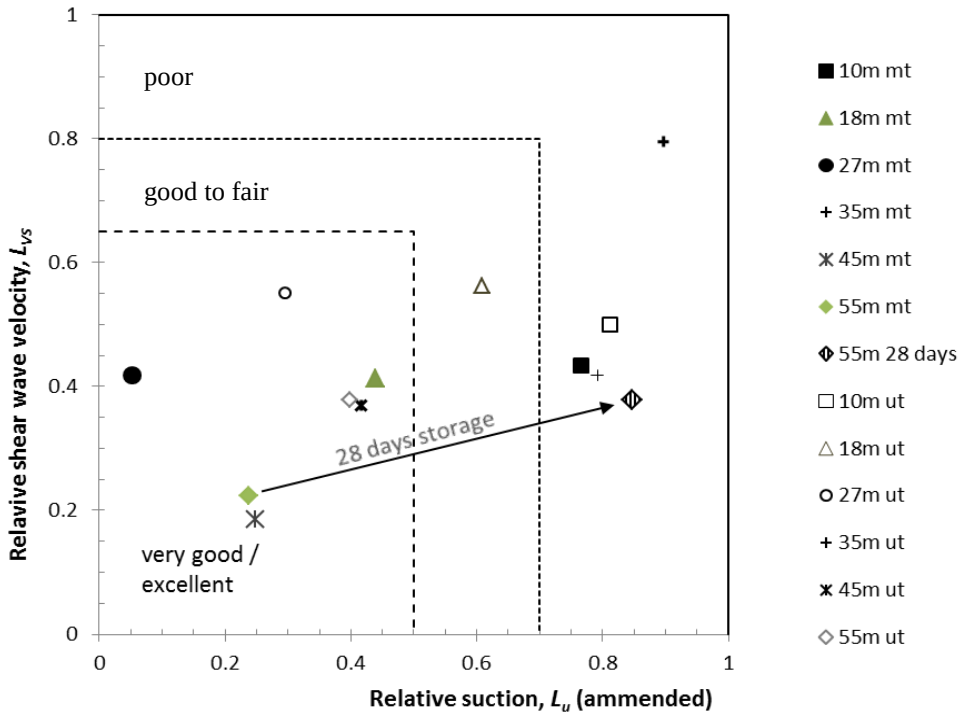

Figure A7. 4 Combined seismic/suction quality assessment of $STII_{slow}$ samples from Site 1, where mt denotes middle tube and ut denotes under tube, refer to Table 3-13 for definition of $L_{u,\ and}\ L_{VS}$.

Appendix A8

Appendix A8: Mechanical properties of the clays studied; Gothenburg Clays (Site 1 to 6)

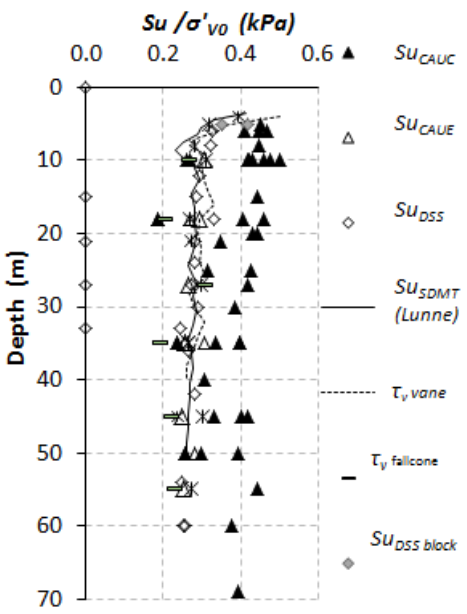

(a)

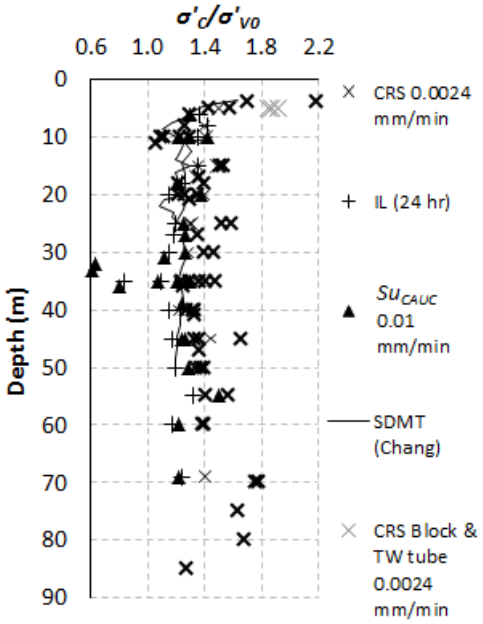

(b)

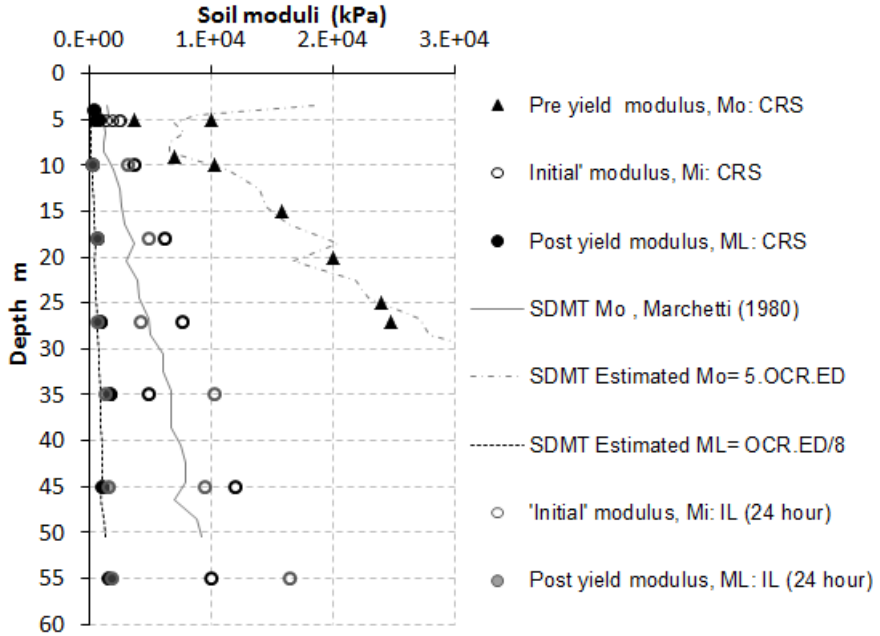

(c)

Figure A8.1 (a) Undrained strength for different modes of shear (normalised with σ'_{VC} (lab. based test) or σ'_{VO} (field based test), (b) Over-consolidation ratio assessed from different tests, (c) 1D moduli assessed from stepwise oedometer and CRS tests.

Appendix A8

Göta River valley: Nödinge site (Site 7)

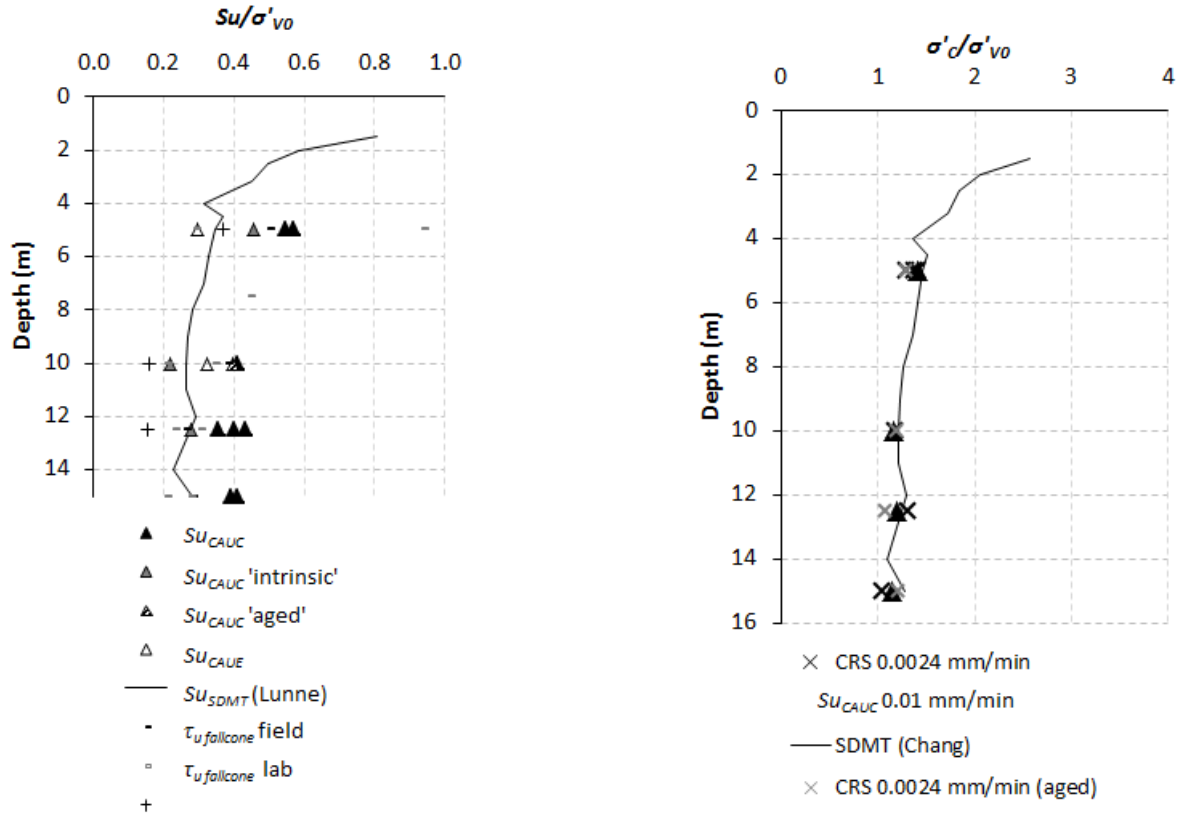

(a) (b)

Figure A8.2 Mechanical properties from testing at Site 7 (a) Undrained shear strength normalized by σ'_{VC} or σ'_{VO}, (b) Over-consolidation ratio,

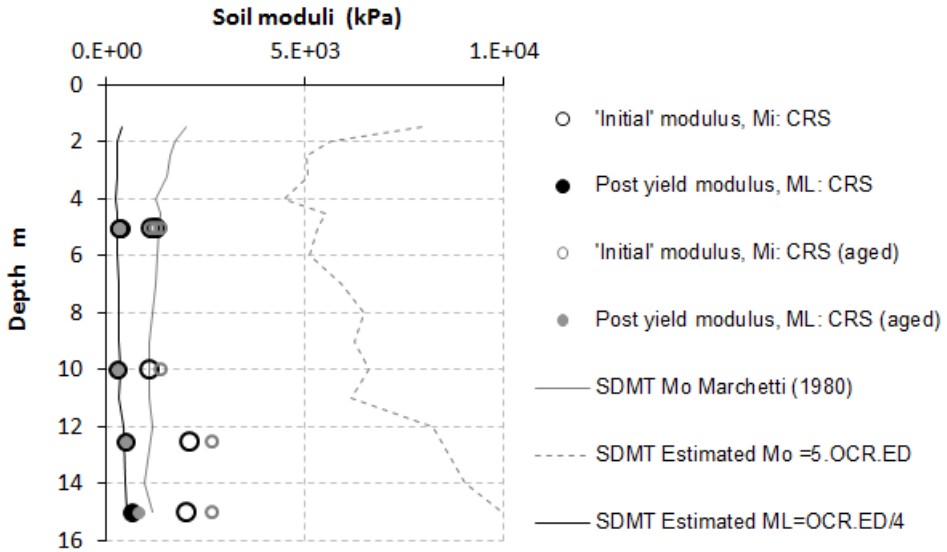

(c)

Figure A8.3 Drained 1D Moduli, M_0 ("elastic" modulus), M_i (initial "disturbed modulus), M_L (post yield "plastic"modulus) and empirical correlations from SDMT tests for Site 7.

Appendix A8

Göta River valley: Lödöse (Site 8)

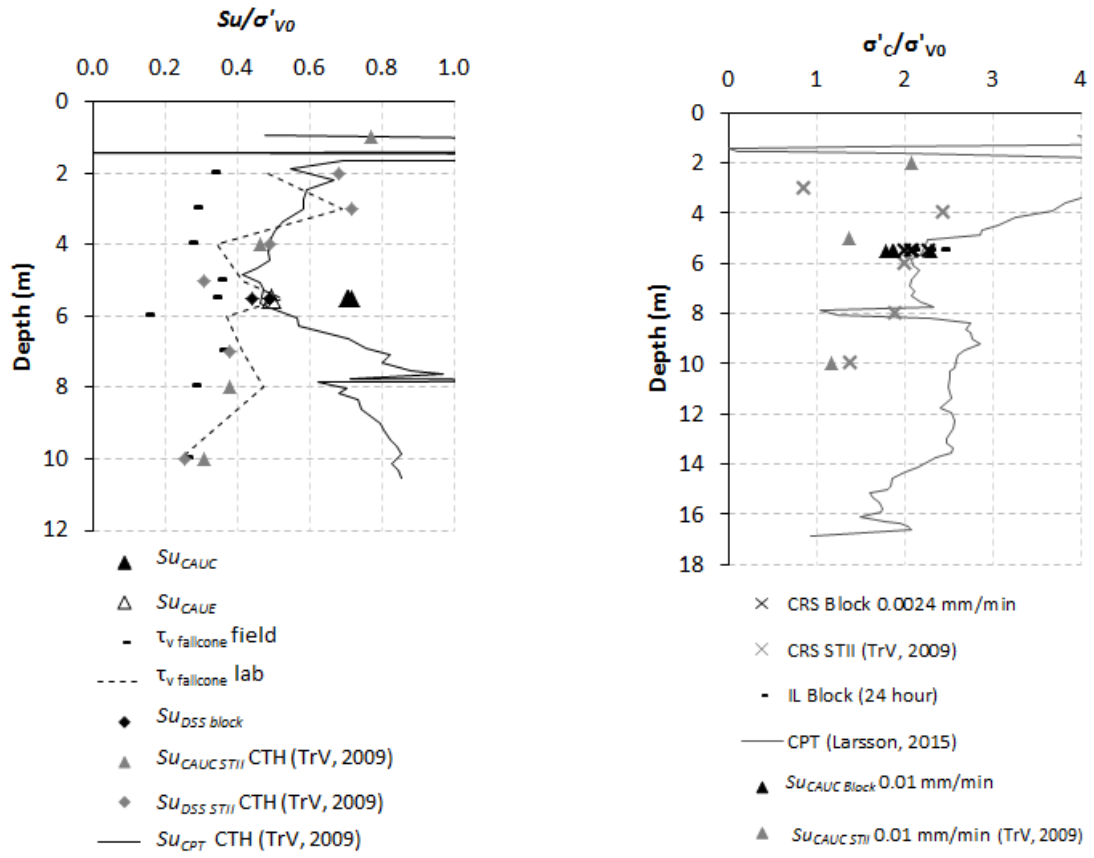

(a) (b)

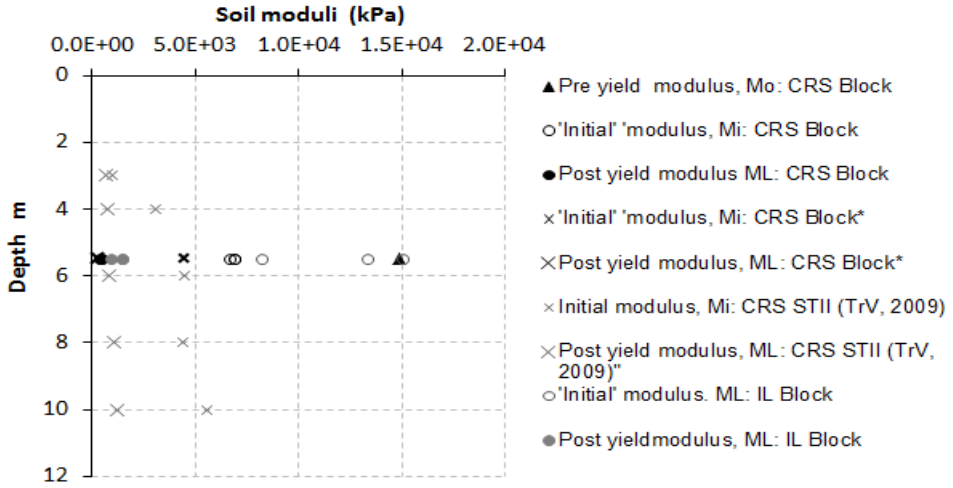

(c)

*Figure A8.4 Mechanical properties from testing at Site 8 (a) Undrained shear strength normalized by σ'_{VC} or $\sigma'_{VO,}$ (b) Over-consolidation ratio (c) Drained 1D Moduli, M_0 ("elastic" pre yield modulus), M_i (initial "disturbed" modulus), M_L (post yield "plastic" modulus), *denotes unconfined sample.*

Appendix A8

East coast, Uppsala: Västra Orgeln (Site 9)

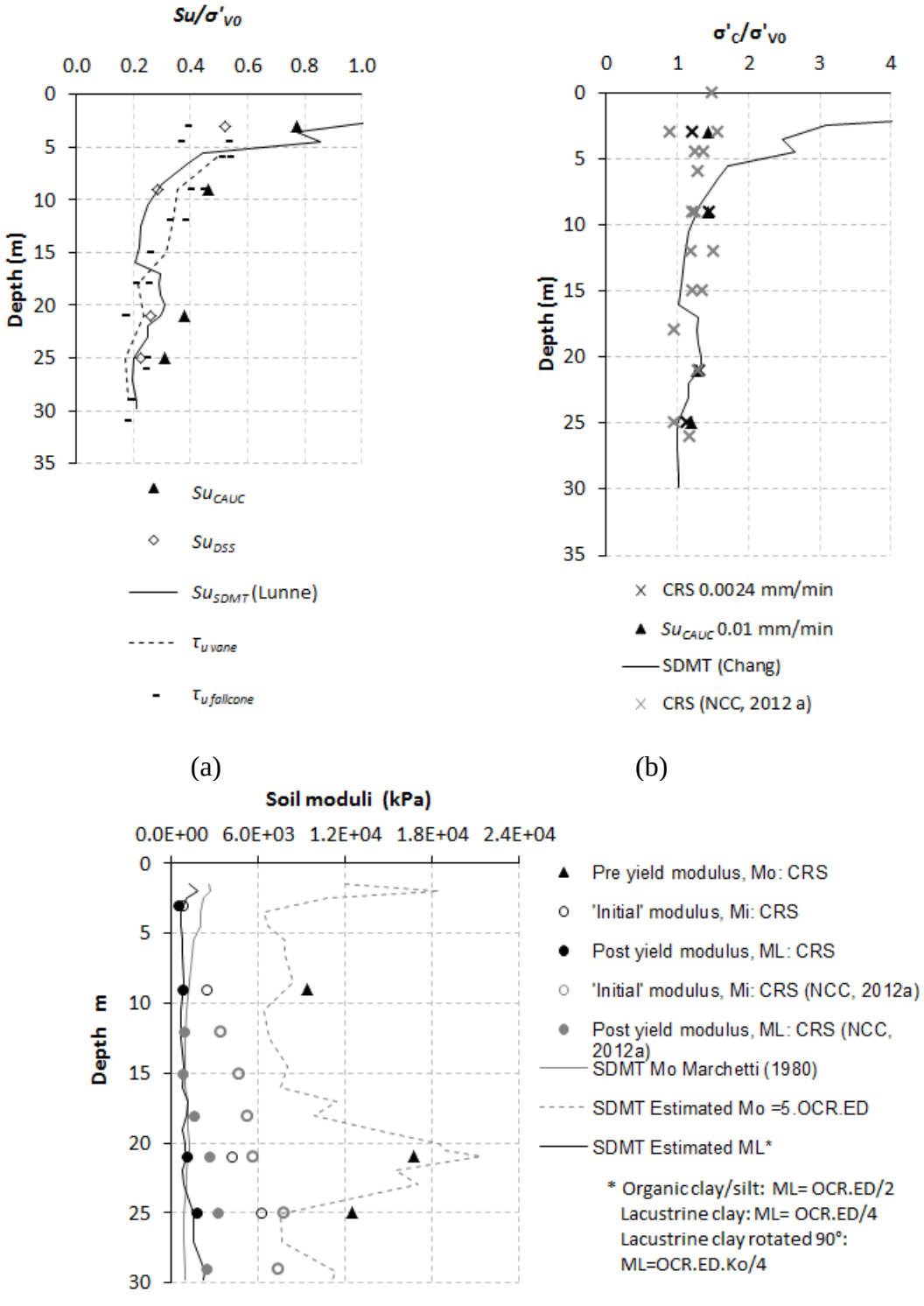

Figure A8.5 Mechanical properties from testing at Site 9 (a) Undrained shear strength normalized by σ'_{VC} or $\sigma'_{VO,}$ (b) Over-consolidation ratio, (c) Drained 1D Moduli, M_0 ("elastic" modulus), M_i (initial "disturbed modulus), M_L (post yield "plastic"modulus).

Appendix A8

East coast, Uppsala: Gränby (Site 10)

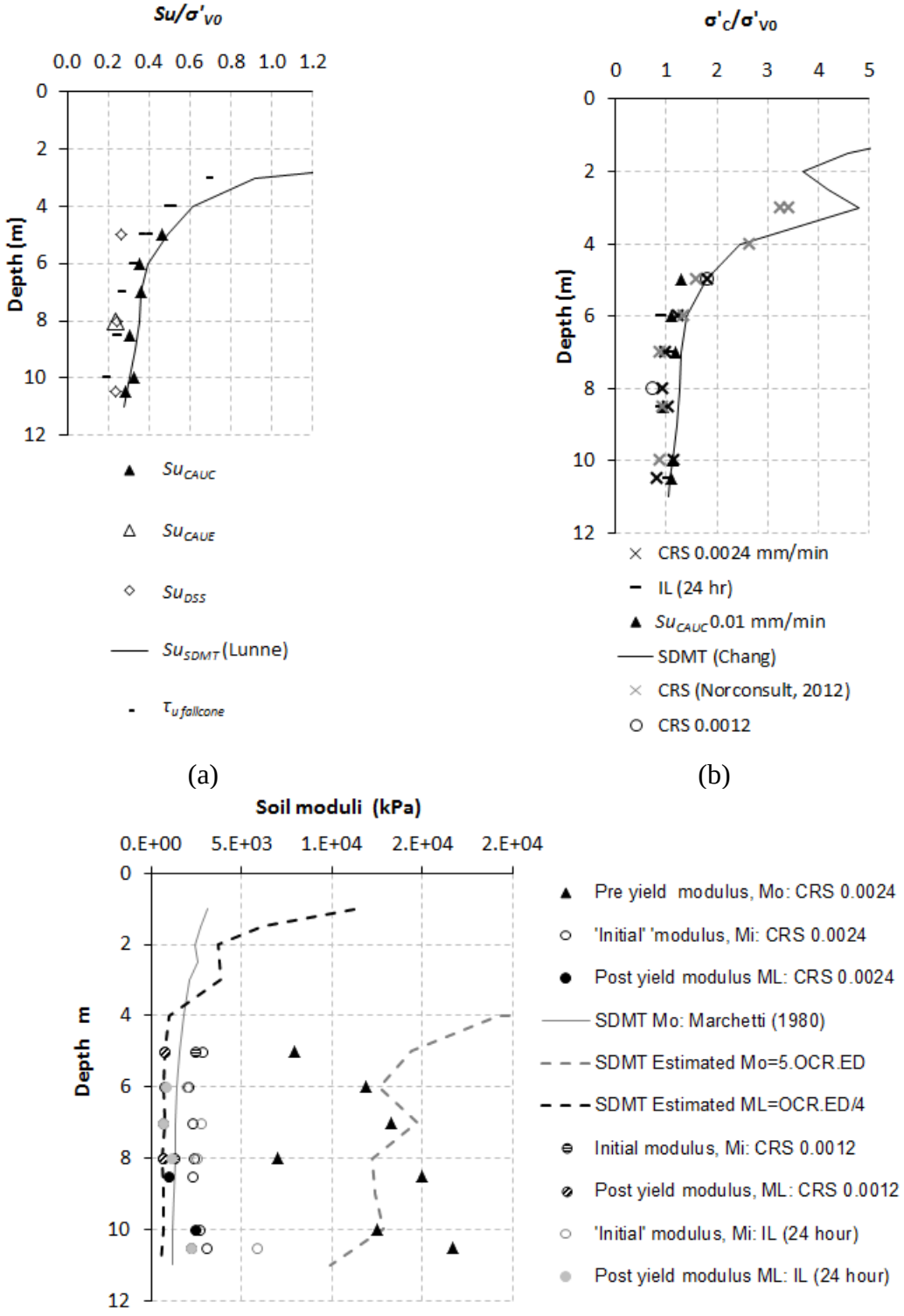

Figure A8.6 Mechanical properties from testing at Site 10 (a) Undrained shear strength normalized by σ'_{VC} or $\sigma'_{VO,}$ (b) Over-consolidation ratio, (c) Drained 1D Moduli, M_0 ("elastic" modulus), M_i (initial "disturbed modulus), M_L (post yield "plastic"modulus).

Appendix A8

East coast, Uppsala: Kvarntorget (Site 11)

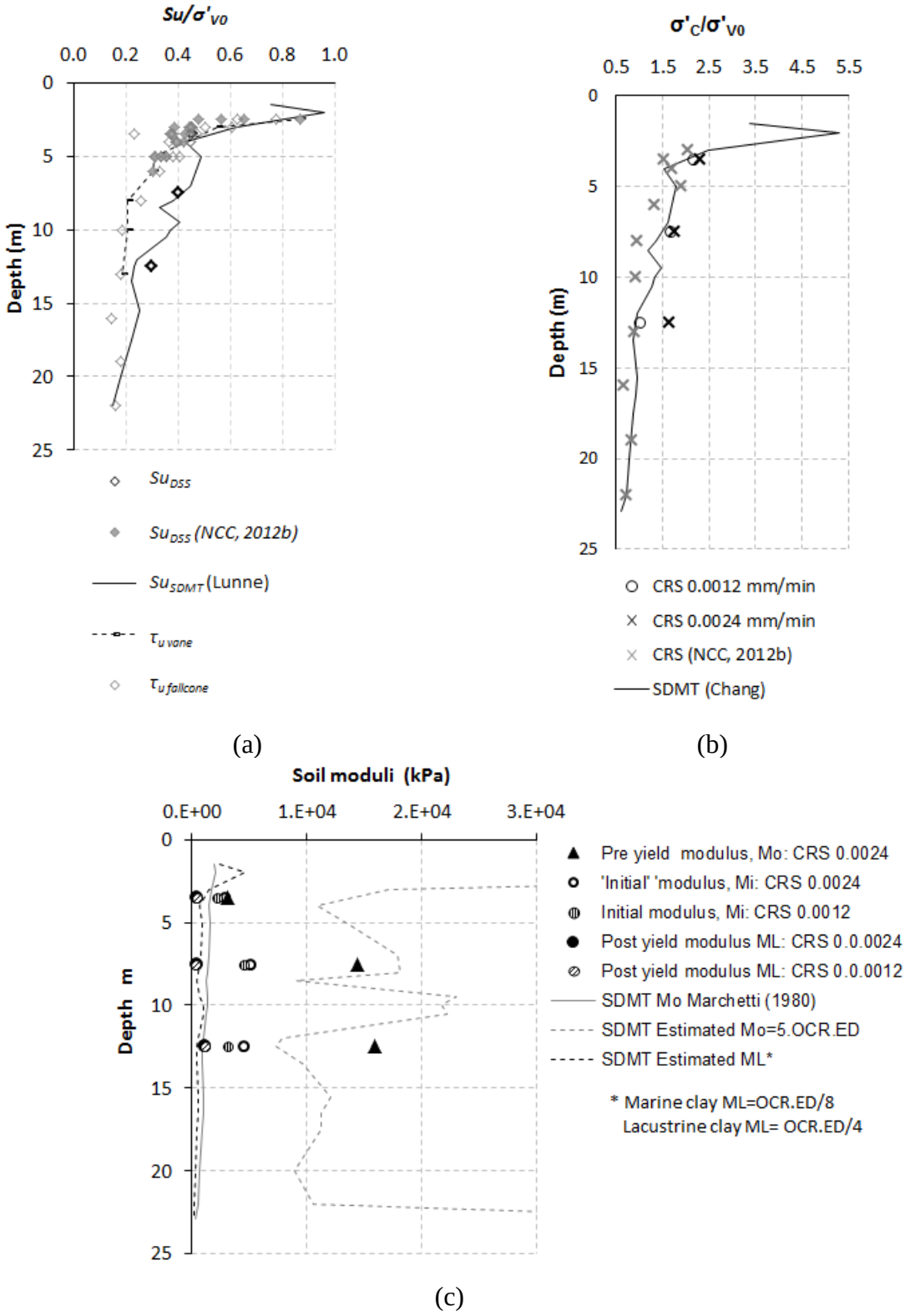

Figure A8.7 Mechanical properties from testing at Site 11 (a) Undrained shear strength normalized by σ'_{VC} or $\sigma'_{VO,}$ (b) Over-consolidation ratio, (c) Drained 1D Moduli, M_0 ("elastic" modulus), M_i (initial "disturbed modulus), M_L (post yield "plastic" modulus).

Appendix A8

Norwegian West Coast, Trondheim: Site 12A (non-quick sediments)

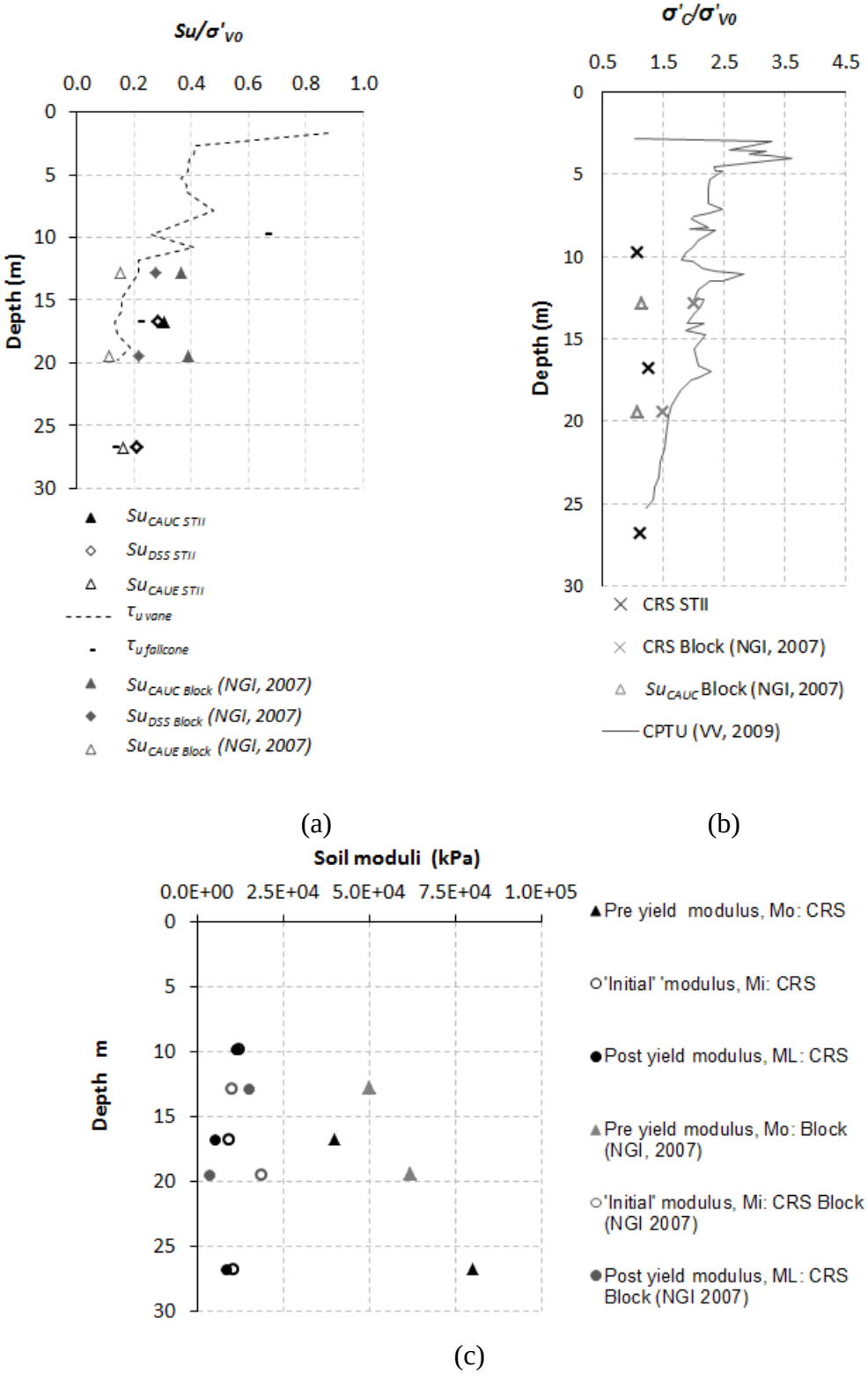

Figure A8.8 Mechanical properties from testing at Site 12a (a) Undrained shear strength normalized by σ'_{VC} or $\sigma'_{VO,}$ (b) Over-consolidation ratio, (c) Drained 1D Moduli, M_0 ("elastic" modulus), M_i (initial "disturbed modulus), M_L (post yield "plastic" modulus).

Appendix A8

Norwegian West Coast, Trondheim: Site 12B (quick sediments)

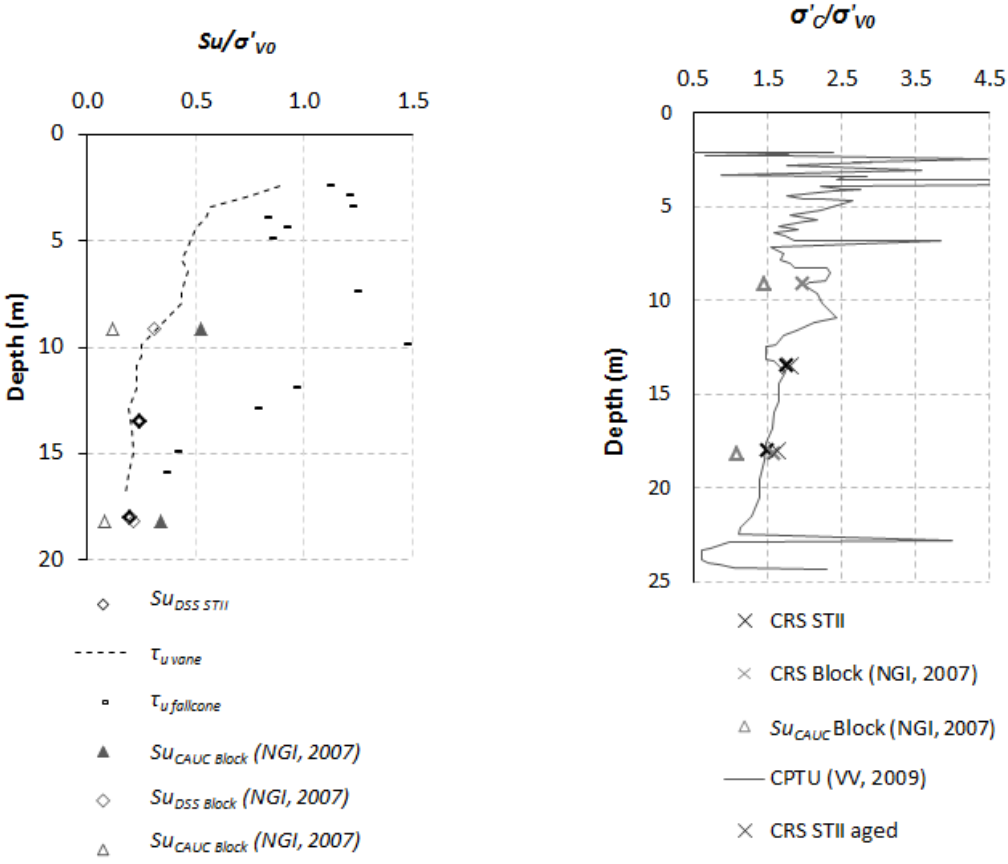

(a) (b)

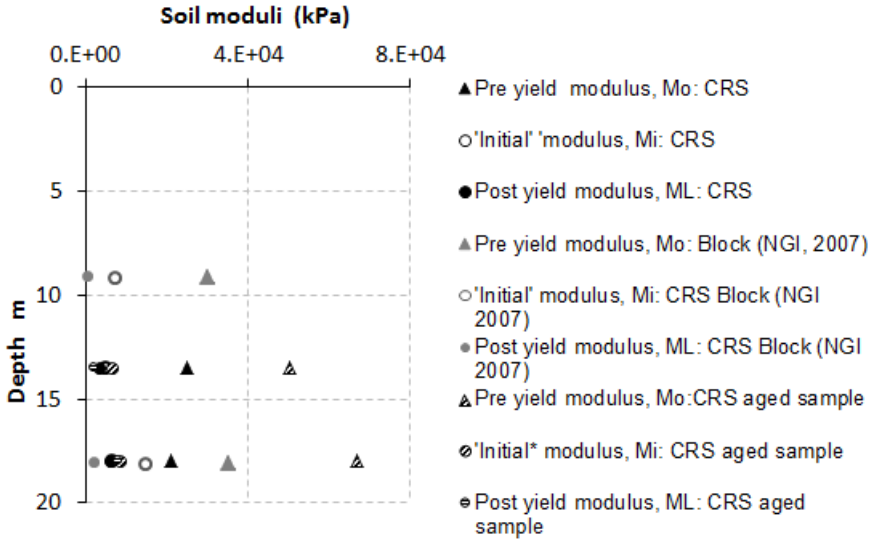

(c)

Figure A8.9 Mechanical properties from testing at Site 12:B (quick sediments) (a) Undrained shear strength normalized by σ'_{VC} or $\sigma'_{VO,}$ (b) Over-consolidation ratio, (c) Drained 1D Moduli, M_0 ("elastic" modulus), M_i (initial "disturbed modulus), M_L (post yield "plastic" modulus).

Appendix A9

Appendix 9: Assessment of strength parameters for Creep-SCLAY1S model

All tests used to determine model parameters from fresh piston samples with highest Lunne quality criteria, $\Delta e/e_0 < 0.04$ unless otherwise indicated.

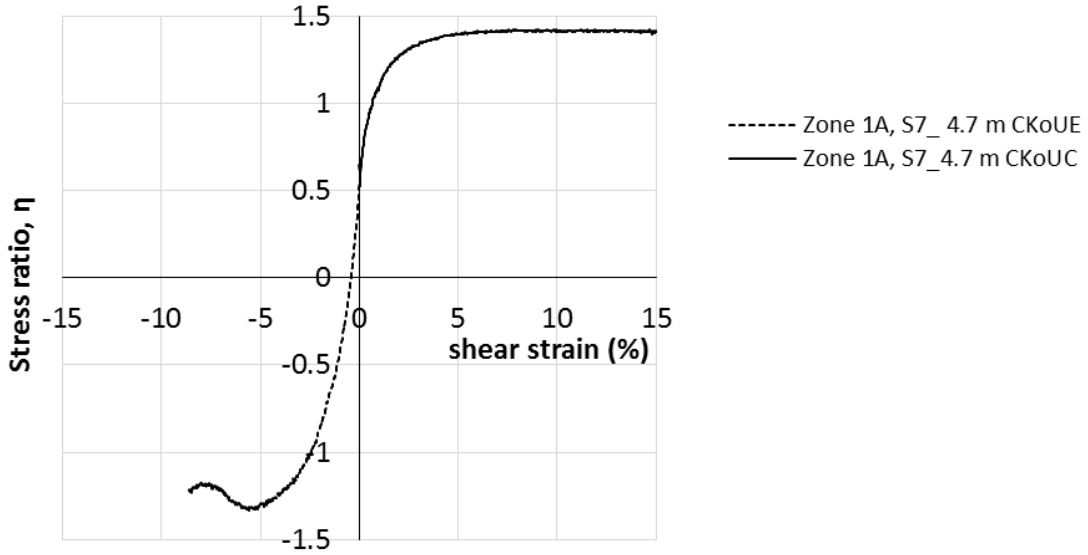

Figure A9.1: Shear strength parameters for Creep-SCLAY1S Zone 1A for West Coast glacio marine clays, M_c=1.4, M_e= 1.2.

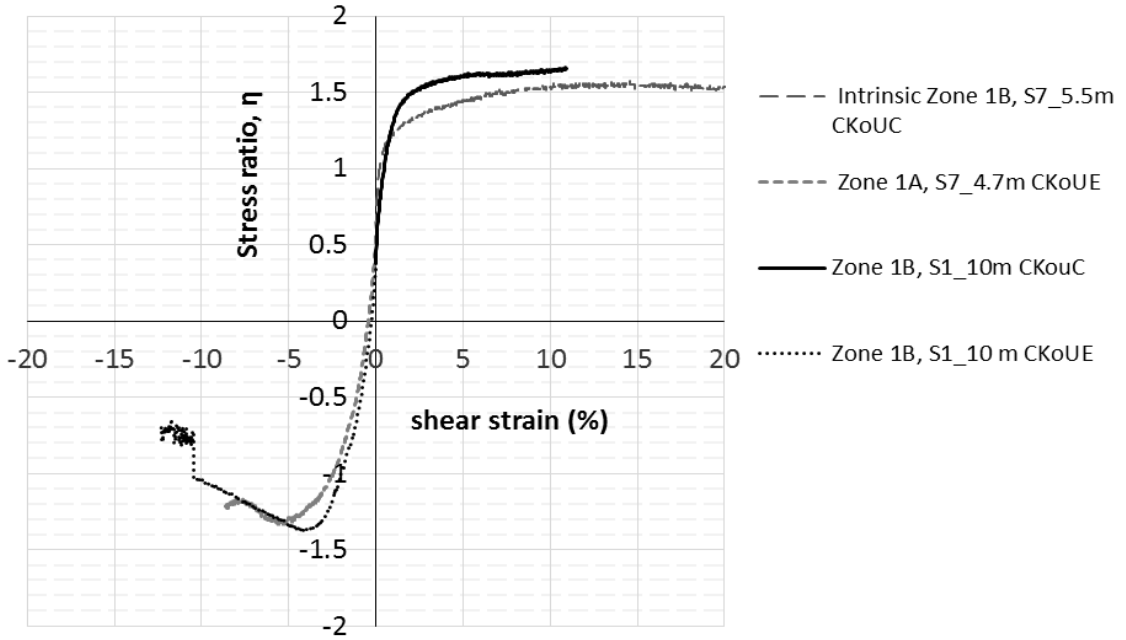

Figure A9.2: Shear strength parameters for Creep-SCLAY1S Zone 1B for West Coast glacio marine clays, M_c=1.55, M_e= 1.15.

Appendix A9

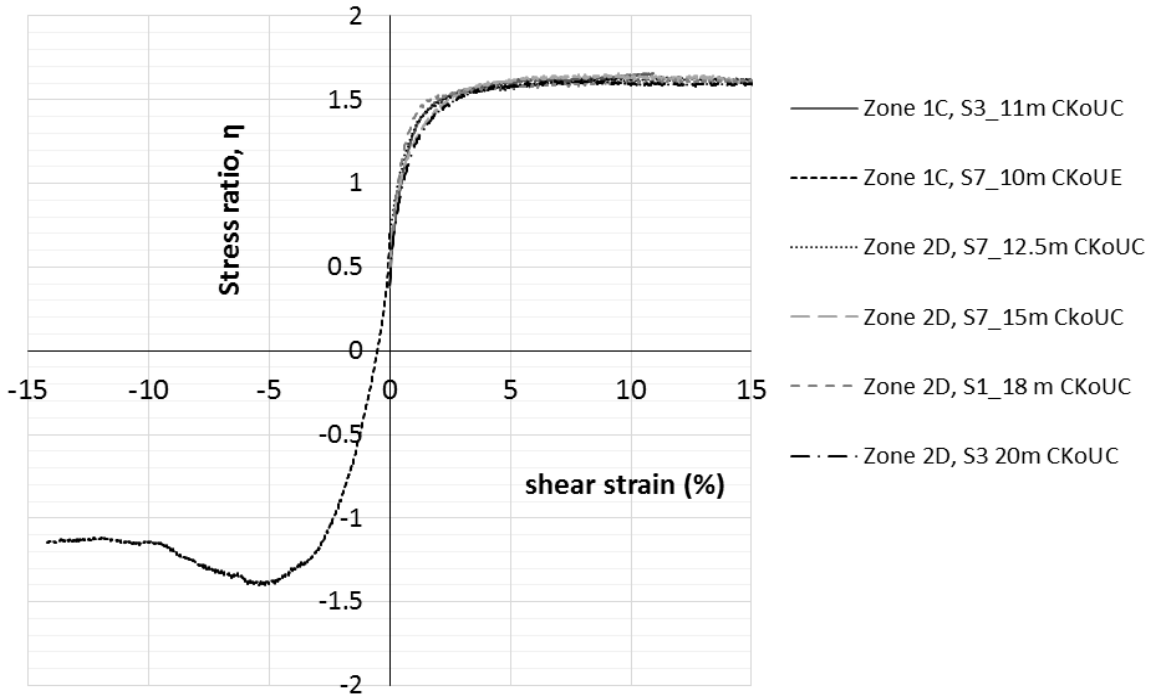

Figure A9.3: Shear strength parameters for Creep-SCLAY1S Zone 1C and 2D for West Coast glacio marine clays, M_c=1.6, M_e= 1.15.

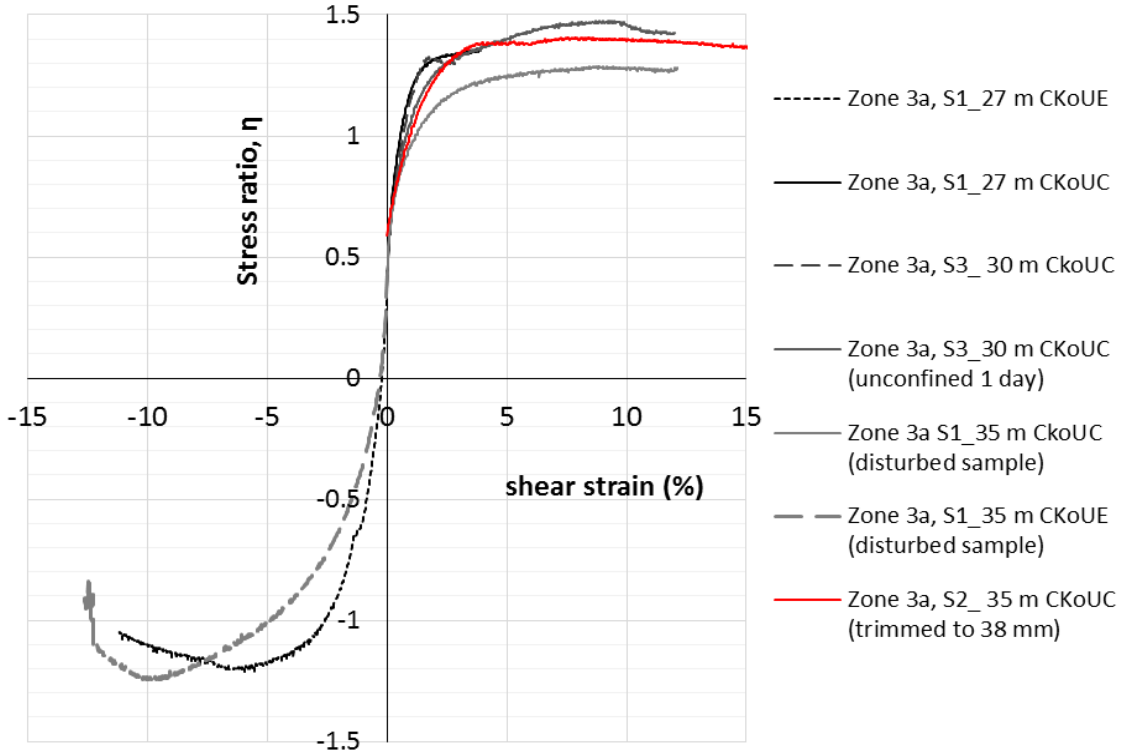

Figure A9.4: Shear strength parameters for Creep-SCLAY1S Zone 3a for West Coast glacio marine clays; clay 6: M_c=1.35, M_e= 1.1, clay 7: M_c=1.3, M_e= 1.1.

Appendix A9

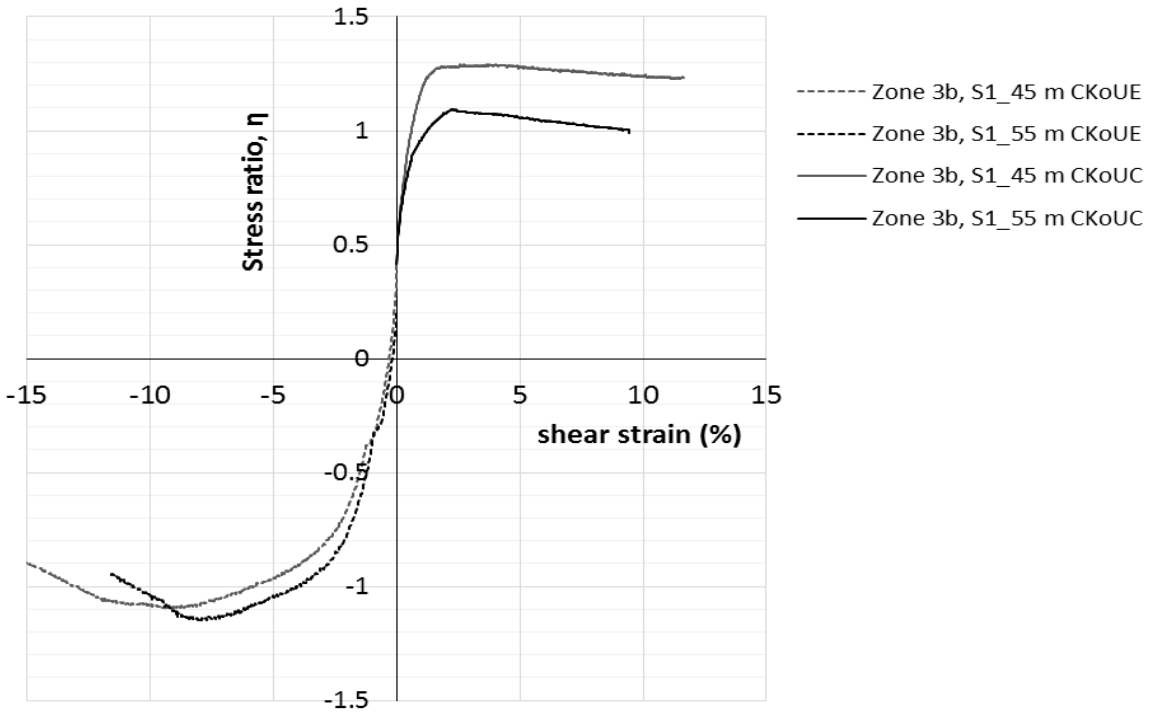

Figure A9.5: Shear strength parameters for Creep-SCLAY1S Zone 3b West Coast glacio marine clays; clay 8: M_c=1.23, M_e= 0.9, clay 9: M_c=1.0, M_e= 0.95.